frontiers | Research Topics

Advances in imaging and treatment of embolic stroke of undetermined source

Edited by
Bing Tian and Chengcheng Zhu

Published in
Frontiers in Neurology

ISSN 1664-8714
ISBN 978-2-83251-044-5
DOI 10.3389/978-2-83251-044-5

About Frontiers

Frontiers is more than just an open access publisher of scholarly articles: it is a pioneering approach to the world of academia, radically improving the way scholarly research is managed. The grand vision of Frontiers is a world where all people have an equal opportunity to seek, share and generate knowledge. Frontiers provides immediate and permanent online open access to all its publications, but this alone is not enough to realize our grand goals.

Frontiers journal series

The Frontiers journal series is a multi-tier and interdisciplinary set of open-access, online journals, promising a paradigm shift from the current review, selection and dissemination processes in academic publishing. All Frontiers journals are driven by researchers for researchers; therefore, they constitute a service to the scholarly community. At the same time, the *Frontiers journal series* operates on a revolutionary invention, the tiered publishing system, initially addressing specific communities of scholars, and gradually climbing up to broader public understanding, thus serving the interests of the lay society, too.

Dedication to quality

Each Frontiers article is a landmark of the highest quality, thanks to genuinely collaborative interactions between authors and review editors, who include some of the world's best academicians. Research must be certified by peers before entering a stream of knowledge that may eventually reach the public - and shape society; therefore, Frontiers only applies the most rigorous and unbiased reviews. Frontiers revolutionizes research publishing by freely delivering the most outstanding research, evaluated with no bias from both the academic and social point of view. By applying the most advanced information technologies, Frontiers is catapulting scholarly publishing into a new generation.

What are Frontiers Research Topics?

Frontiers Research Topics are very popular trademarks of the *Frontiers journals series*: they are collections of at least ten articles, all centered on a particular subject. With their unique mix of varied contributions from Original Research to Review Articles, Frontiers Research Topics unify the most influential researchers, the latest key findings and historical advances in a hot research area.

Find out more on how to host your own Frontiers Research Topic or contribute to one as an author by contacting the Frontiers editorial office: frontiersin.org/about/contact

Advances in imaging and treatment of embolic stroke of undetermined source

Topic editors

Bing Tian — Naval Medical University, China

Chengcheng Zhu — University of Washington, United States

Citation

Tian, B., Zhu, C., eds. (2023). *Advances in imaging and treatment of embolic stroke of undetermined source*. Lausanne: Frontiers Media SA.

doi: 10.3389/978-2-83251-044-5

Table of contents

05 Editorial: Advances in imaging and treatment of embolic stroke of undetermined source
Bing Tian, Xia Tian and Chengcheng Zhu

08 Extracranial Carotid Plaque Hemorrhage Is Independently Associated With Poor 3-month Functional Outcome After Acute Ischemic Stroke—A Prospective Cohort Study
Fengli Che, Yanfang Liu, Xiping Gong, Anxin Wang, Xiaoyan Bai, Yi Ju, Binbin Sui, Jing Jing, Xiaokun Geng and Xingquan Zhao

16 Atrial Cardiopathy and Cryptogenic Stroke
Yuji Kato and Shinichi Takahashi

24 Non-Coding RNA Regulatory Network in Ischemic Stroke
Zongyan Cai, Shuo Li, Tianci Yu, Jiahui Deng, Xinran Li and Jiaxin Jin

37 The Relationship Between Aortic Arch Calcification and Recurrent Stroke in Patients With Embolic Stroke of Undetermined Source—A Case-Control Study
Xiaofeng Cai, Yu Geng and Sheng Zhang

44 The Value of Contrast-Enhanced Ultrasound in the Evaluation of Carotid Web
Qingqing Zhou, Rui Li, Shuo Feng, Fengling Qu, Chunrong Tao, Wei Hu, Yuyou Zhu and Xinfeng Liu

52 Potential Embolic Sources Differ in Patients With Embolic Stroke of Undetermined Source According to Age: A 15-Year Study
Yan Hou, Ahmed Elmashad, Ilene Staff, Mark Alberts and Amre Nouh

58 Uncommon Female-Predominant Etiologies of Cryptogenic Stroke
Jing Dong and Xin Ma

66 A Cryptogenic Stroke Associated With Infective Endocarditis and Antiphospholipid Antibody Syndrome: Case Report and Literature Review
Lei Chen, Ping Zhang, Xuan Zhu, Minmin Zhang and Benqiang Deng

73 Vessel wall MR imaging of aortic arch, cervical carotid and intracranial arteries in patients with embolic stroke of undetermined source: A narrative review
Yu Sakai, Vance T. Lehman, Laura B. Eisenmenger, Emmanuel C. Obusez, G. Abbas Kharal, Jiayu Xiao, Grace J. Wang, Zhaoyang Fan, Brett L. Cucchiara and Jae W. Song

91 The role of cross-sectional imaging of the extracranial and intracranial vasculature in embolic stroke of undetermined source
Hediyeh Baradaran, Hooman Kamel and Ajay Gupta

98 Identification of magnetic resonance imaging features for the prediction of unrecognized atrial fibrillation in acute ischemic stroke
Chao-Hui Chen, Meng Lee, Hsu-Huei Weng, Jiann-Der Lee, Jen-Tsung Yang, Yuan-Hsiung Tsai and Yen-Chu Huang

108 Relationship between the stroke mechanism of symptomatic middle cerebral artery atherosclerotic diseases and culprit plaques based on high-resolution vessel wall imaging
Guo-hui Lin, Jian-xun Song, Teng-da Huang, Nian-xia Fu and Li-ling Zhong

frontiers | Frontiers in Neurology

TYPE Editorial
PUBLISHED 30 November 2022
DOI 10.3389/fneur.2022.1073545

OPEN ACCESS

EDITED AND REVIEWED BY
Sebastien Soize,
Centre Hospitalier Universitaire de Reims, France

*CORRESPONDENCE
Bing Tian
bing.tian@hotmail.com
Chengcheng Zhu
zhucheng043@gmail.com

†These authors have contributed equally to this work

SPECIALTY SECTION
This article was submitted to Applied Neuroimaging, a section of the journal Frontiers in Neurology

RECEIVED 18 October 2022
ACCEPTED 31 October 2022
PUBLISHED 30 November 2022

CITATION
Tian B, Tian X and Zhu C (2022) Editorial: Advances in imaging and treatment of embolic stroke of undetermined source. *Front. Neurol.* 13:1073545. doi: 10.3389/fneur.2022.1073545

Editorial: Advances in imaging and treatment of embolic stroke of undetermined source

Bing Tian[1*†], Xia Tian[1†] and Chengcheng Zhu[2*]

[1]Department of Radiology, Changhai Hospital of Shanghai, Shanghai, China, [2]Department of Radiology, University of Washington, Seattle, WA, United States

KEYWORDS

embolic stroke of undetermined source, embolic stroke, intracranial atherosclerotic plaque, imaging, antithrombotic, antiplatelets

Editorial on the Research Topic
Advances in imaging and treatment of embolic stroke of undetermined source

Determining the causes of acute ischemic stroke is crucial for patient management, particularly to prevent future strokes. Embolic stroke of undetermined source (ESUS) is a subtype of cryptogenic ischemic stroke and accounts for ∼20% of all ischemic stroke, and the average recurrence rate of 4.5% per year is relatively high, despite preventive treatment with antithrombotic agents (1). Recent studies have shown that novel clinical strategies and imaging techniques can improve the detection rate of the etiology of ESUS.

Atherosclerosis and ESUS

Non-stenotic atherosclerotic plaques are a major contributor to ESUS (2). Several previous studies revealed that certain morphological features of plaques on ultrasound, computed tomography (CTA), or high-resolution MRI vessel wall imaging (HR-VWI) are significantly more common in ESUS patients ipsilateral to the side of stroke than the contralateral side (3). High-risk culprit plaque can still present despite the stenosis degree being <50%, and the outward remodeling of the plaque is common. HR-VWI provides the opportunity to image the high-risk features of the plaques with <50% stenosis, including intraplaque hemorrhage, lipid-rich necrotic core, and thin or ruptured fibrous caps (4).

In this Research Topic, Che et al. concluded that extracranial carotid intra-plaque hemorrhage (IPH) on HR-VWI was significantly associated with poor 3-month outcomes after acute ischemic stroke and could predict a poor 3-month functional prognosis. Baradaran et al. discussed the role of cross-sectional imaging of the extracranial and intracranial arteries and how imaging might potentially uncover high-risk plaque features that may be contributing to ischemic strokes. They highlighted that, in the extracranial carotid artery, both MR and CTA could be used to identify certain plaque features which indicated more plaque vulnerability including IPH on MR

and increased soft plaque thickness on CTA. VW-MR can also be used as a powerful tool to identify active atherosclerotic plaque in the intracranial arteries with <50% stenosis by identifying an enhancing plaque with positive remodeling. Lin et al. found the culprit plaque characteristics of patients with symptomatic MCA atherosclerotic in different stroke mechanisms may be evaluated using HR-VWI. The plaque characteristics of different stroke mechanisms may have clinical value for the selection of treatment strategies to prevent stroke recurrence.

There has been increased attention given to decoding the contributory role of non-stenotic atherosclerosis in the carotid arteries, intracranial arteries, and the aortic arch in ESUS patients. Cai X. et al. found that aortic arch calcification, especially spotty calcification, had a good predictive value for stroke recurrence in patients with ESUS. Sakai et al. reviewed the use of VW-MRI in detecting and characterizing carotid, intracranial, and aortic arch atherosclerosis in ESUS patients. Besides high-risk feathers of carotid and intracranial atherosclerosis, HR-VWI also allows further characterization of aortic arch plaque compositions like that seen in carotid studies.

Cardioembolic and ESUS

Occult atrial fibrillation (AF) is a leading cause of stroke of unclear cause (5). Chen C.-H. et al. revealed that MRI at stroke onset provides critical clues for the prediction of newly detected AF, including single cortical infarcts, territorial infarcts, and early hemorrhage. Future studies are warranted to verify their new prediction model and to assess whether the identification of AF can be enhanced to improve outcomes after acute ischemic stroke. Hou et al. found that potential embolic sources (PES) differ in patients with ESUS according to age and differences in recurrence. PFO is the only common PES in young patients with ESUS. Future studies prospectively evaluating PES in both age groups are needed. Chen L. et al. provided a case of cryptogenic stroke associated with infective endocarditis (IE) and antiphospholipid antibody syndrome (APS). They pointed out that bicuspid aortic valve (BAV) vegetation-related cerebral embolism might present as cryptogenic and can be confusing in the acute phase, particularly when APS and IE were diagnosed simultaneously. Kato and Takahashi provided a review of atrial cardiopathy and cryptogenic stroke. They concluded that atrial cardiopathy should be considered as one of the mechanisms of ESUS. Abnormal atrial substrate (atrial cardiopathy) that leads to atrial fibrillation (AF) can result in embolic stroke before developing AF and may explain the source of cryptogenic stroke in some patients.

Other research in ESUS

There are many other biomarkers associated with ESUS. Cai Z. et al. outlined the current understanding of the regulatory network of non-coding RNAs (ncRNAs) and reviewed the recent evidence for the contribution of ncRNAs in the experimental ischemic stroke model. Zhou et al. pointed out that carotid web (CaW) was a risk factor in cryptogenic stroke because it could be detected in nearly 5% of young cryptogenic stroke patients. Contrast-enhanced ultrasound (CEUS) might have higher diagnostic accuracy for CaW with thrombosis, and it had a higher clinical application prospect. Dong and Ma reviewed advances in exploring uncommon female-predominant etiologies of cryptogenic stroke. This review provided novel clinical clues for the etiological diagnosis of cryptogenic stroke and will help to improve the management and secondary prevention of stroke in the female population.

Future directions

Though these studies can be helpful in determining the source of potential emboli for ESUS, further studies are needed to validate these imaging techniques and pave a path for their routine use in clinical practice. The use of VW-MRI to detect and characterize carotid, intracranial, and aortic arch atherosclerosis in ESUS patients is an exciting and rapidly evolving field. Additional efforts are warranted to elucidate the contributory role of these atherosclerotic plaques in ESUS. The ARCADIA trial is currently being performed to validate the diagnosis of atrial cardiopathy and to determine whether atrial cardiopathy can be a new therapeutic target for direct-acting oral anticoagulants (DOAC). It was also hypothesized that oral anticoagulation may decrease the risk of stroke recurrence in ESUS, which was tested in two large randomized controlled trials: the NAVIGATE ESUS and the RE-SPECT ESUS (6, 7). For ESUS patients without atherosclerotic lesions, it seems rational to hypothesize that oral anticoagulation could reduce the risk of stroke recurrence. But for ESUS patients with atherosclerosis, further research is needed to prove the combined use of low-dose anticoagulation with antiplatelets.

Author contributions

BT: writing—original draft and funding acquisition. XT: writing—original draft. CZ: writing—review and editing and funding acquisition.

Funding

This research activity is funded by the Medical Guidance Project of the Shanghai Science and Technology Commission (1941196500) and the Nature Science Foundation of Shanghai (21ZR1479300). CZ was supported by the US

National Institute of Health (NIH) Grants R01HL162743 and R00HL136883.

Conflict of interest

The authors declare that the research was conducted in the absence of any commercial or financial relationships that could be construed as a potential conflict of interest.

Publisher's note

References

1. Diener HC, Easton JD, Hart RG, Kasner S, Kamel H, Ntaios G. Review and update of the concept of embolic stroke of undetermined source. *Nat Rev Neurol.* (2022) 18:455–65. doi: 10.1038/s41582-022-00663-4

2. Goyal M, Singh N, Marko M, Hill MD, Menon BK, Demchuk A, et al. Embolic stroke of undetermined source and symptomatic nonstenotic carotid disease. *Stroke.* (2020) 51:1321–5. doi: 10.1161/STROKEAHA.119.028853

3. Tao L, Li XQ, Hou XW, Yang BQ, Xia C, Ntaios G, et al. Intracranial atherosclerotic plaque as a potential cause of embolic stroke of undetermined source. *J Am Coll Cardiol.* (2021) 77:680–91. doi: 10.1016/j.jacc.2020.12.015

4. Fakih R, Roa JA, Bathla G, Olalde H, Varon A, Ortega-Gutierrez S, et al. Detection and quantification of symptomatic atherosclerotic plaques with high-resolution imaging in cryptogenic stroke. *Stroke.* (2020) 51:3623–31. doi: 10.1161/STROKEAHA.120.031167

5. Hart RG, Catanese L, Perera KS, Ntaios G, Connolly SJ. Embolic stroke of undetermined source: a systematic review and clinical update. *Stroke.* (2017) 48:867–72. doi: 10.1161/STROKEAHA.116.016414

6. Harloff A, Schlachetzki F. Rivaroxaban for stroke prevention after embolic stroke of undetermined source. *N Engl J Med.* (2018) 379:986–7. doi: 10.1056/NEJMc1809065

7. Diener HC, Sacco RL, Easton JD, Granger CB, Bernstein RA, Uchiyama S, et al. Dabigatran for prevention of stroke after embolic stroke of undetermined source. *N Engl J Med.* (2019) 380:1906–17. doi: 10.1056/NEJMoa1813959

frontiers in Neurology

ORIGINAL RESEARCH
published: 14 December 2021
doi: 10.3389/fneur.2021.780436

Extracranial Carotid Plaque Hemorrhage Is Independently Associated With Poor 3-month Functional Outcome After Acute Ischemic Stroke—A Prospective Cohort Study

*Fengli Che[1,2], Yanfang Liu[1], Xiping Gong[1], Anxin Wang[3], Xiaoyan Bai[4], Yi Ju[1], Binbin Sui[3,4], Jing Jing[3], Xiaokun Geng[2,5] and Xingquan Zhao[1,3,6]**

[1] Department of Neurology, Beijing Tiantan Hospital, Capital Medical University, Beijing, China, [2] Department of Neurology, Beijing Luhe Hospital, Capital Medical University, Beijing, China, [3] Tiantan Neuroimaging Center for Excellence, Beijing Tiantan Hospital, Capital Medical University, Beijing, China, [4] Department of Neuroradiology, Beijing Tiantan Hospital, Capital Medical University, Beijing, China, [5] Department of Neurology, China-America Institute of Neuroscience, Beijing, China, [6] Research Unit of Artificial Intelligence in Cerebrovascular Disease, Chinese Academy of Medical Sciences, Beijing, China

OPEN ACCESS

Edited by:
Edgar A. Samaniego,
The University of Iowa, United States

Reviewed by:
Marialuisa Zedde,
Local Health Authority of Reggio Emilia, Italy
Danhong Wu,
Fudan University, China

***Correspondence:**
Xingquan Zhao
zxq@vip.163.com

Specialty section:
This article was submitted to Stroke, a section of the journal Frontiers in Neurology

Received: 21 September 2021
Accepted: 15 November 2021
Published: 14 December 2021

Citation:
Che F, Liu Y, Gong X, Wang A, Bai X, Ju Y, Sui B, Jing J, Geng X and Zhao X (2021) Extracranial Carotid Plaque Hemorrhage Is Independently Associated With Poor 3-month Functional Outcome After Acute Ischemic Stroke—A Prospective Cohort Study. Front. Neurol. 12:780436. doi: 10.3389/fneur.2021.780436

Background and Purpose: Carotid plaque hemorrhage (IPH) is a critical plaque vulnerable feature. We aim to elucidate the association between symptomatic extracranial carotid atherosclerotic IPH and poor 3-month functional outcome after acute ischemic stroke by high-resolution vessel wall MRI (HRVMRI).

Methods: We prospectively studied consecutive patients with a recent stroke or transient ischemic attack (TIA) of carotid atherosclerotic origin. All patients underwent a High-Resolution (HR) VWMRI scan of ipsilateral extracranial carotid within 1 week after admission. The patients recruited were interviewed by telephone after 3 months after stroke onset. The primary outcome was a 3-month functional prognosis of stroke, expressed as a modified Rankin Scale (mRS) score. A poor prognosis was defined as a 3-month modified Rankin Scale (mRS) score $\geq$ of 3. Univariate analysis was used to analyze the correlation between risk factors and IPH. The relation between IPH and 3-month functional outcome was analyzed by Logistic regression analysis.

Results: A total of 156 patients (mean age, 61.18 $\pm$ 10.12 years; 108 males) were included in the final analysis. There were significant differences in the age, gender, smoking history, national institutes of health stroke scale (NIHSS) on admission, and diastolic blood pressure (DBP) on admission between the IPH group and the non-IPH group (all $p < 0.05$). During the follow-up, 32 patients (20.5%) had a poor functional outcome. According to the prognosis analysis of poor functional recovery, there was a significant difference between the two groups [36.7 vs. 16.7%; unadjusted odds ratio (OR), 2.32, 95% confidence interval (CI), 1.12–4.81, $p = 0.024$). Even after adjusting for confounding factors [such as age, gender, smoking history, National Institutes of Health Stroke Scale (NIHSS) on admission, DBP on admission, stenosis rate of carotid artery (CA),

calcification, loose matrix, lipo-rich necrotic core (LRNC), and statins accepted at 3 months], IPH was still a strong predictor of poor 3-month outcome, and the adjusted OR was 3.66 (95% CI 1.68–7.94, $p = 0.001$).

Conclusions: Extracranial carotid IPH is significantly associated with poor 3-month outcome after acute ischemic stroke and can predict the poor 3-month functional prognosis.

Keywords: MRI, atherosclerosis, plaque, prognosis, acute ischemic stroke

INTRODUCTION

Atherosclerosis is the leading cause of ischemic stroke in the Chinese population (1). The Chinese Intracranial Atherosclerosis Study (CICAS) showed that 14% of patients with ischemic stroke had severe extracranial carotid atherosclerosis (> of 50%). Some studies have confirmed that carotid artery atherosclerotic stenosis is significantly associated with the onset and prognosis of acute ischemic stroke (2, 3). However, histopathological studies have demonstrated that the vulnerable features of carotid artery plaque are the underlying risk factors of most ischemic events (4–10). Therefore, identifying the vulnerable plaques based on advanced medical imaging technology and exploring the correlation between the vulnerability of the plaque and stroke recurrence has become research hotspots in recent years. Meanwhile, we still do not know whether the characteristics of carotid artery plaques in acute ischemic stroke are associated with the poor 3-month outcome of patients after stroke onset.

Our study aims to analyze the vulnerable characteristics of carotid plaque by high-resolution vessel wall magnetic resonance imaging (HR VWMRI) and find a relation between IPH and the early poor prognosis of acute ischemic stroke. With that in mind, we might identify the risk factors of poor 3-month outcome of stroke and take more effective individualized prevention strategies in the acute stage of ischemic stroke.

METHODS

Study Population

All patients were enrolled from a single-center prospective cohort study in Beijing Tiantan Hospital. We aimed to assess the characteristics of carotid atherosclerotic plaques and the relationship between IPH and poor 3-month outcome after stroke onset. All enrolled patients underwent an ultrasonographic screen and a HR VWMRI scan of the symptomatic extracranial carotid artery within 1 week after admission. They were followed up by telephone after 3 months (90 ± 7 days) after stroke onset. According to the latest international guidelines, we gave the enrolled patients standardized medical therapy and secondary prevention of stroke. In addition, the inclusion criteria and exclusion criteria of the study have been mentioned in the **Supplementary Material**. The Ethics Committee approved the study of Beijing Tiantan Hospital. All study subjects had signed written consent.

Carotid MR Imaging Protocol

All recruited subjects were scanned using 3.0 T MR scanners (Achieva TX; Philips Healthcare, Best, the Netherlands) with 8-channel head coils. A standardized multisequence protocol included three-dimensional time of flight (3D-TOF), T1-weighted quadruple inversion recovery, T2-weighted multislice double, and magnetization prepared gradient recalled echo (MPRAGE) imaging sequences. We used gadolinium diethylenetriamine pentametric acid (GD-DTPA) as the contrast medium, and the injection dose was 0.1 mmol/kg. We used spectral preservation attenuated inversion recovery (SPAIR) in the black blood technique. The study's imaging parameters of carotid atherosclerotic plaque MRI have also been mentioned in the **Supplementary Material**.

MRI Image Analysis

We used a standard workstation (ADW4.4, G.E. Medical System, USA) for imaging analysis. Two experienced senior neuroimaging physicians reviewed all slices of multi-contrast MR vessel wall images. They were both blinded to the diffusion-weighted images (DWI) and clinical information. The plaque was defined as a thickening of the focal wall relative to image slices beneath the T2 and T1-weighted imaging focal wall. We manually outlined the outer wall boundaries and lumen of carotid arteries at each slice. The parameters of plaque morphology and the stenosis ratio of the carotid were measured. According to the international criteria detailed previously, the plaque components such as carotid artery (CA), lipo-rich necrotic core (LRNC), IPH, and fibrous cap rupture (FCR) were detected by MRI (11). MR image quality was divided into a four-point grade (1 = poor; 2 = general; 3 = good; and 4 = excellent), and slices with image quality ≥ 3 were included in the statistical analysis. We would accept consensus interpretation as the final analysis if inconsistent in the two readers' interpretations. We randomly selected twenty patients from the study population every 2 months to test the consistency of inter-reader and intra-reader in measuring carotid plaque morphology and carotid plaque compositions.

Outcome Assessment

Patients were followed up at 3 months after stroke onset. The primary outcome was 3-month functional outcome, expressed as a modified Rankin Scale (mRS) score 3 months after discharge. A poor functional outcome was defined as mRS

score ≥of 3 at 3 months. The secondary outcomes were early stroke progression, early recurrent ischemic stroke, and hemorrhagic transformation at 3 months post-discharge. The recurrence of ischemic stroke was confirmed according to new neurological deficits documented in the medical records. Two experienced stroke neurologists reviewed patients' medical documents to ensure a reliable diagnosis of recurrent ischemic stroke. The early stroke progression was described as an incremental increase in the NIHSS score by ≥2 points in the total score or ≥1 point in motor power within 1 week after admission (excluding hemorrhage transformation of cerebral infarction and symptomatic intracranial hemorrhage), accompanied by the new ischemic signals on brain MRI or computed tomography (CT) (12). Early recurrent ischemic stroke (ERIS) was defined as the occurrence of an ischemic stroke in other independent arterial regions confirmed by clinical symptoms or by CT/MRI imaging techniques (13). Hemorrhagic transformation was defined as the hemorrhage in the infarct area or the corresponding vascular distribution area after acute cerebral infarction (14). Complications during hospitalization were defined as at least one syndrome, namely, urinary infection, pulmonary infection, gastrointestinal bleeding, deep vein thrombosis, other organ dysfunction, and/or acute coronary syndromes within 7 days. Patients or their authorized proxies were interviewed at 3 months by telephone by trained research coordinators. Two trained researchers in Beijing Tian Tan hospital completed all the telephone follow-ups of patients. Trained stroke neurologists assessed the NIHSS. The mRS at the 3-month time point was evaluated by trained and experienced neurologists by a telephone assessment using a standardized structured questionnaire. An experienced neurologist independently confirmed all the followed-up assessments. They were also blinded to imaging information of all patients.

Statistical Analysis

Continuous variables were described by means [standard deviations (SDs)] or medians [interquartile ranges (IQRs)], and categorical data were expressed as frequency and percentage. To analyze the difference between the IPH group and the non-IPH group, Student's *t*-test or Mann–Whitney *U*-test were used for continuous variables according to a normal distribution, and chi-squared test or Fisher exact test for categorical variables. Univariate and multivariable Cox regression analyses were

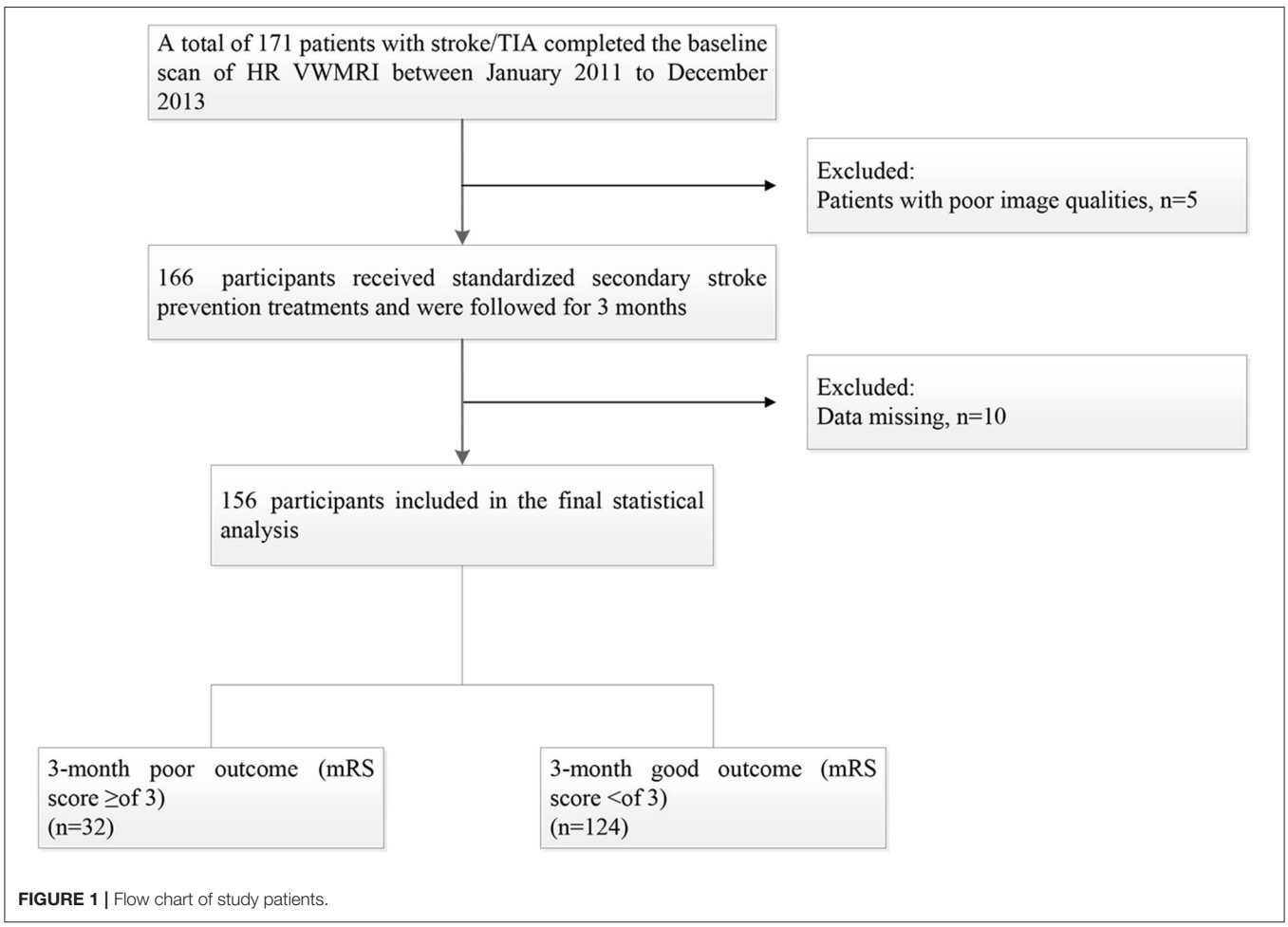

FIGURE 1 | Flow chart of study patients.

conducted to study predictors of poor prognosis of stroke by calculating odds ratio (OR) and 95% confidence interval. Statistical analyses were performed using SPSS version 22.0 (IBM, NY, USA). A two-sided $p < 0.05$ was considered statistically significant.

RESULTS

One hundred seventy-one patients were enrolled from January 2011 to December 2013, and 15 patients were excluded for the following reasons: (1) 10 patients were lost; and (2) the image quality of 5 patients was poor. Thus, a total of 156 patients were included in the final statistical analysis, including 108 males (69.2%) with a mean age of (61.18 ± 10.12, 33–85) years. The median day of follow-up time was [IQR, 93 (78–110)]. Thirty-two patients (20.5%) had a 3-month poor prognosis (**Figure 1**).

Intraplaque hemorrhage detected by HR VWMRI was found in 30 (20.5%) patients (**Figure 2**). There were significant differences in the age (mean, 66.30 ± 8.27 vs. 59.96 ± 10.16, $p = 0.002$), gender (male, 86.7 vs. 65.1%, $p = 0.021$), smoking history (60.0 vs. 31.7%, $p = 0.004$), NIHSS on admission [IQR, 3 (0–8) vs. 4 (2–12), $p = 0.031$], and DBP on admission (mean, 81.52 ± 11.40 vs. 86.94 ± 12.12 mmHg, $p = 0.037$) between the IPH group and the non-IPH group (**Table 1**).

Between the IPH group and the non-IPH group, there was no significant difference in the degree of stenosis ($p = 0.279$), lumen area (LA) ($p = 0.063$), and vessel area (VA) ($p = 0.269$). However, there were significant differences in the wall area (WA) [IQR, 34.56 (21.68–114.10) mm^2 vs. 29.61 (19.11–54.03) mm^2, $p < 0.001$], normalized wall index (NMI) [IQR, 0.46 (0.40–0.69) vs. 41 (0.28–0.63), $p < 0.001$], wall thickness (WI) [IQR, 1.33 (1.06–3.14) mm vs. 1.07 (0.81–1.80) mm, $p < 0.001$], plaque area (PA) [IQR, 38.32 (11.42–71.35) mm^2 vs. 22.22 (8.60–74.29) mm^2, $p < 0.001$], and remodeling index (RI) (mean, 0.68 ± 0.07 vs. 76 ± 0.07, $p < 0.001$) (**Table 1**).

During the follow-up, 32 patients (20.5%) had a poor functional outcome. The proportion of poor function outcome is 36.7% for the IPH group and 16.7% for the non-IPH group (crude OR 2.32; 95%CI 1.12–4.81; $p = 0.024$) (**Figure 3**). After adjusting the baseline variables as age, gender, smoking history, NIHSS on admission, DBP on admission, stenosis rate of CA, calcification, loose matrix, LRNC, and statins accepted at 3 months, there was still a statistical difference (adjusted OR 3.66; 95%CI 1.68–7.94; $p = 0.001$) between the two groups (**Table 2**). Regarding the second outcomes, the proportion of early stroke progression, early recurrent ischemic stroke, and hemorrhagic transformation in the IPH group was significantly higher (all $p < 0.05$, **Table 2**).

DISCUSSION

Our study investigated the association between IPH detected by HR VWMRI and functional outcome at 3 months after stroke onset. Our study found that the incidence of carotid plaque IPH in patients with acute ischemic stroke was

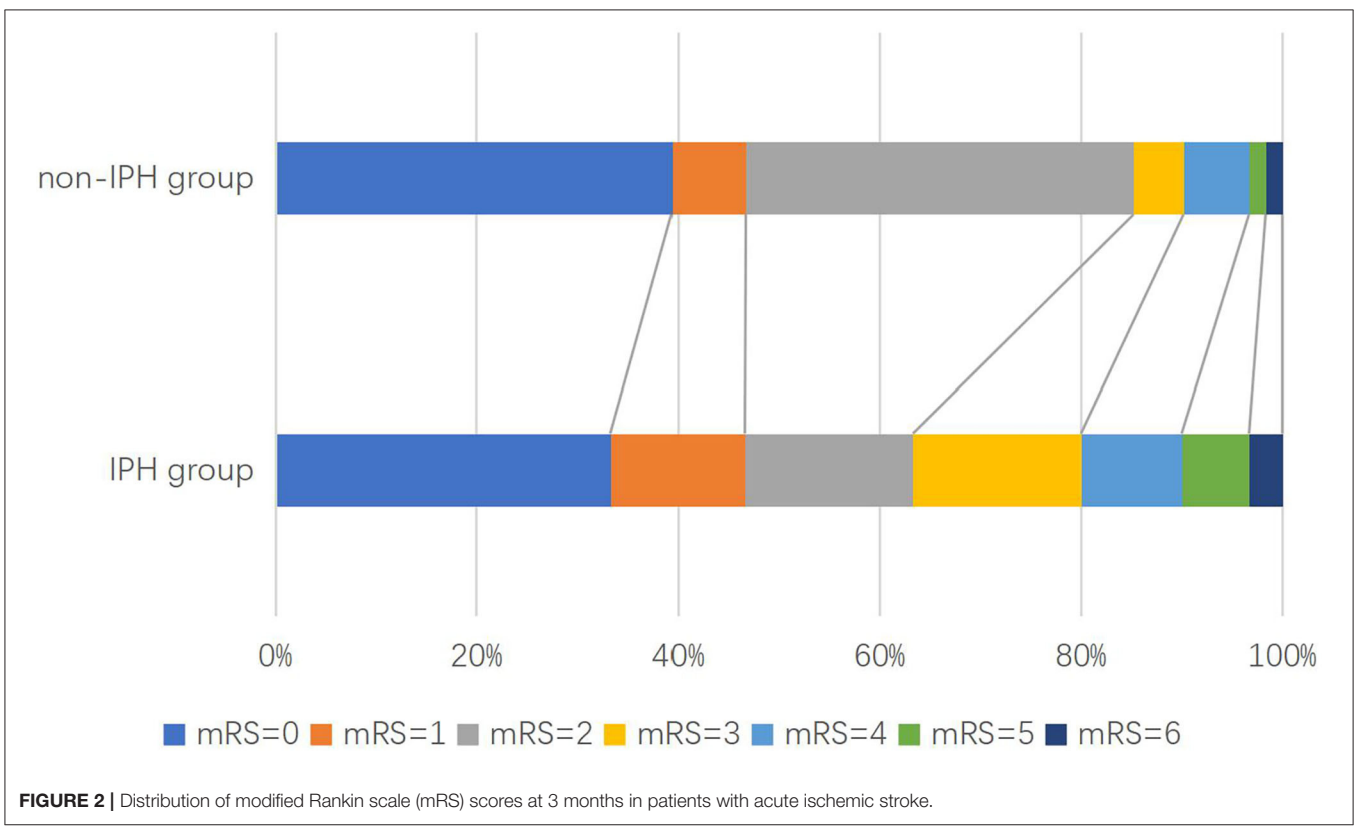

FIGURE 2 | Distribution of modified Rankin scale (mRS) scores at 3 months in patients with acute ischemic stroke.

TABLE 1 | Demographic and clinical characteristics in patients.

Variables	Total (n = 156)	IPH group (n = 30)	Non-IPH group (n = 126)	P-value
Gender, male, *n* (%)	108 (69.2)	26 (86.7)	82 (65.1)	**0.021**
Age, years	61.18 ± 10.12	66.30 ± 8.27	59.96 ± 10.16	**0.002**
Hypertension, *n* (%)	107 (68.6)	22 (73.7)	85 (67.5)	0.533
Diabetes mellitus, *n* (%)	50 (32.1)	13 (43.3)	37 (29.4)	0.141
Coronary heart disease, *n* (%)	18 (11.5)	2 (6.7)	16 (12.7)	0.528
Hyperlipidemia, *n* (%)	59 (37.8)	7 (23.3)	59 (37.8)	0.069
Prior stroke/TIA, *n* (%)	31 (19.9)	4 (13.3)	27 (21.4)	0.318
Smoking history, *n* (%)	58 (37.2)	18 (60.0)	40 (31.7)	**0.004**
Alcohol consuming, *n* (%)	51 (32.7)	9 (30.0)	42 (33.3)	0.726
Family history of stroke, *n* (%)	21 (13.5)	2 (6.7)	19 (15.1)	0.371
SBP on admission, mmHg	144.60 ± 21.75	143.15 ± 21.01	144.93 ± 21.99	0.702
DBP on admission, mmHg	85.92 ± 12.18	81.52 ± 11.40	86.94 ± 12.12	**0.037**
NIHSS on admission, IQR	4 (0–12)	3 (0–8)	4 (2–12)	**0.031**
Pre-admission mRS, IQR	1 (0–2)	1 (0–2)	1 (0–2)	0.059
hs-CRP, IQR, mg/L	2.60 (0.00–45.90)	3.30 (0.00–17.90)	2.50 (0.00–45.90)	0.617
TC, mmol/L	4.34 ± 1.07	4.25 ± 1.13	4.36 ± 1.06	0.634
TG, IQR, mmol/L	1.36 (0.50–8.44)	1.29 (0.67–3.89)	1.37 (0.50–8.44)	0.507
LDL-C, mmol/L	2.61 ± 0.96	2.39 ± 0.91	2.66 ± 0.96	0.184
HDL-C, mmol/L	1.07 ± 0.34	1.19 ± 0.56	1.05 ± 0.27	0.209
Hcy, IQR, umol/L	17.10 (6.60–75.00)	21.17 (10.50–51.20)	16.70 (6.60–75.00)	0.201
Stenosis rate of CA, %	62.77 ± 12.08	65.26 ± 14.32	62.18 ± 11.47	0.279
Stenotic degree of CA				**0.090**
Mild stenosis (<50%), *n* (%)	20 (12.8)	4 (13.3)	16 (12.7)	—
Moderate stenosis (50–69%), *n* (%)	92 (59.0)	13 (43.3)	79 (62.7)	—
Severe stenosis/occlusion (>70%), *n* (%)	44(28.2)	13 (43.3)	31 (24.6)	—
LA, mm^2	16.86 ± 6.99	14.73 ± 7.94	17.37 ± 6.67	**0.063**
WA, IQR, mm^2	30.65 (19.11–114.10)	34.56 (21.68–114.10)	29.61(19.11–54.03)	**<0.001**
VA, IQR, mm^2	74.45 (43.00–162.11)	73.22 (43.00–162.11)	74.45(45.01–133.74)	0.269
NWI, IQR	0.42 (0.28–0.69)	0.46 (0.40–0.69)	0.41(0.28–0.63)	**<0.001**
WT, IQR, mm	1.11 (0.81–3.14)	1.33 (1.06–3.14)	1.07(0.81–1.80)	**<0.001**
PA, IQR, mm^2	24.42 (8.60–74.29)	38.32 (11.42–71.35)	22.22 (8.60–74.29)	**<0.001**
RI	0.75 ± 0.08	0.68 ± 0.07	0.76 ± 0.07	**<0.001**
Calcification, *n* (%)	85 (54.5)	26 (86.7)	59 (46.8)	**<0.001**
Loose matrix, *n* (%)	74 (47.4)	24 (80.0)	50 (39.7)	**<0.001**
LRNC, *n* (%)	127 (81.4)	30 (100.0)	97 (77.7)	**0.004**
FCR, *n* (%)	4 (2.6)	4 (13.3)	0 (0.0)	**0.001**
Median on admission-to-following time, d (IQR)	93 (78–110)	93 (83–99)	93 (78–110)	0.750
mRS at 3 months, IQR	2 (0–5)	3 (0–5)	2 (0–5)	0.870
Medication at 3 months				
Aspirin, *n* (%)	89 (57.1)	19 (63.3)	70 (55.6)	0.439
Clopidogrel, *n* (%)	18 (11.5)	1 (3.3)	17 (13.5)	0.200
Statins, *n* (%)	68 (43.6)	8 (26.7)	60 (47.6)	0.038
Antihypertension, *n* (%)	49 (31.4)	9 (30.0)	40 (31.7)	0.853
Hypoglycemic, *n* (%)	47 (30.1)	11 (36.7)	36 (28.6)	0.385

IPH, intraplaque hemorrhage; TIA, transient ischemic attack; SBP, systolic blood pressure; DBP, diastolic blood pressure; hs-CRP, hypersensitive c-reactive protein; TC, cholesterol; TG, triglycerides; LDL-C, low-density lipoprotein cholesterol; HDL-C, high-density lipoprotein cholesterol; Hcy, homocysteine; CA, carotid artery; LA, lumen area; WA, wall area; VA, vessel area; NWI, normalized wall index; WT, wall thickness; PA, plaque area; RI, remodeling index; LRNC, lipo-rich necrotic core; FCR, fibrous cap rupture; NIHSS, national institutes of health stroke scale; mRS, modified Rankin scale; IQR, interquartile range.

19.27%. Meanwhile, the percentage of IPH was significantly higher than other plaque vulnerable features, which could reach 61.54%.

Our previous study has confirmed that IPH was associated with ipsilateral ischemic stroke recurrence, especially in the first 3 months after acute ischemic stroke. So, we hypothesized that IPH might be related to a 3-month poor prognosis. In our study, we found the proportion of patients with poor functional outcome in the IPH group is much higher than patients in the non-IPH group, which could be 3.66 times higher even after adjusting

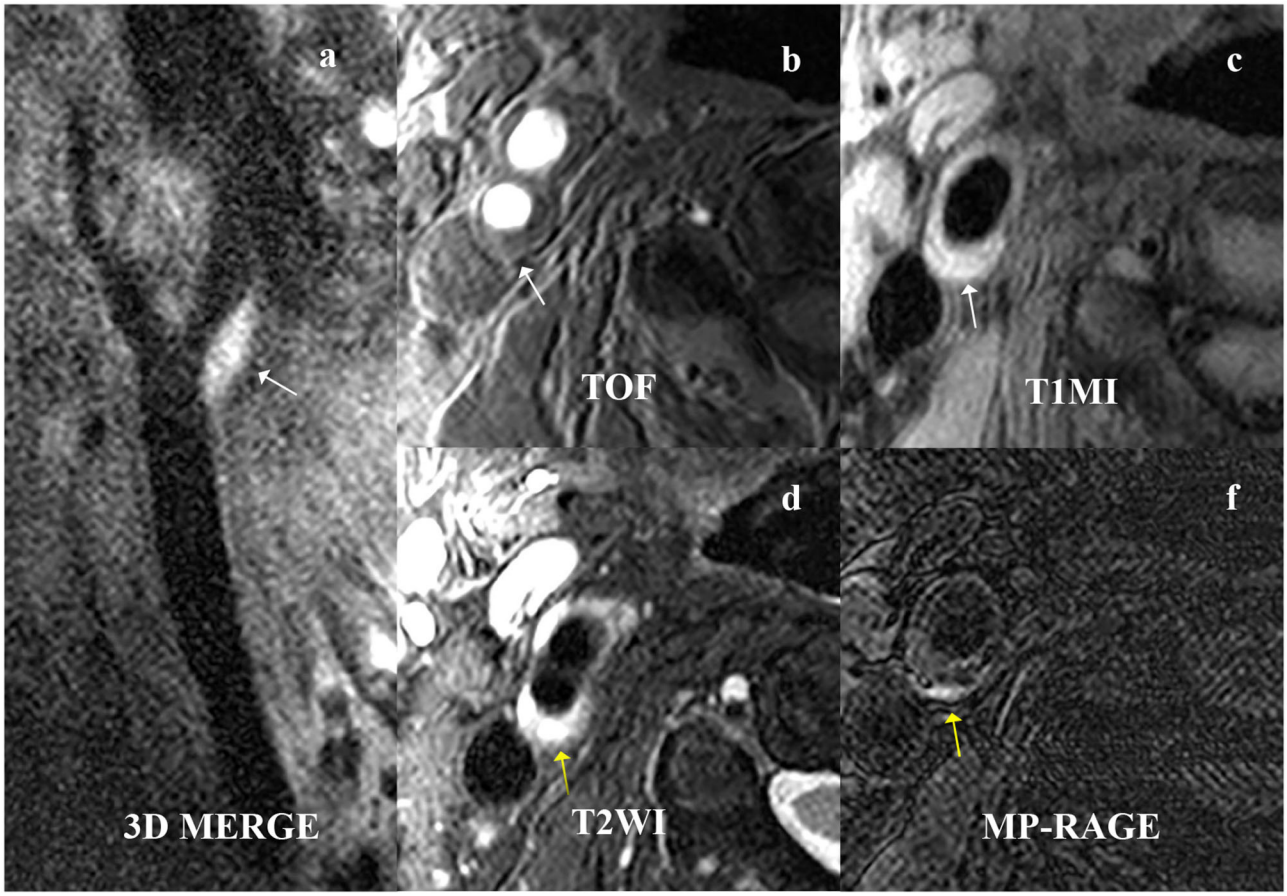

FIGURE 3 | A 61-year-old male patient presented with right ischemic stroke. The plaque is shown at the beginning of the right internal carotid artery on **(a)** 3D MERGE, **(b)** TOF, and **(c)** T1W (white arrow). The intraplaque hemorrhage (IPH) is characterized by hyperintensities on **(d)** T2WI and **(e)** MPRAGE (yellow arrow). 3D MERG, 3D multiple-echo recalled gradient-echo; 3D-TOF, three-dimensional time of flight; T1W, T1-weighted; T2W, T2-weighted; MPRAGE, magnetization-prepared rapid acquisition gradient-echo.

TABLE 2 | Outcomes at 3 months after stroke onset in carotid plaque hemorrhage (IPH) group vs. non-IPH group.

Outcome	No. (%) of patients		Unadjusted OR (95% CI)	*P*-value	Adjusted OR (95% CI)*	*P*-value
	IPH group ($n = 30$)	Non-IPH group ($n = 126$)				
Primary outcome						
mRS 3–6 at 3 months	11 (36.7)	21 (16.7)	2.32 (1.12–4.81)	0.024	3.66 (1.68–7.94)	**0.001**
Second outcomes						
Early stroke progression	5 (16.7)	4 (3.2)	5.25 (1.41–19.60)	0.014	5.43 (1.45–20.25)	**0.012**
Early recurrent ischemic stroke	15 (50.0)	14 (11.1)	4.90 (2.37–10.17)	0.000	7.49 (3.13–17.94)	**<0.001**
Hemorrhagic transformation	1 (3.3)	3 (2.4)	1.51 (0.16–14.53)	0.722	-	**0.010**

**Adjusted baseline variables: age, gender, smoking history, NIHSS on admission, DBP on admission, stenosis rate of CA, calcification, loose matrix, LRNC, and statins at 3 months. mRS, modified Rankin Scale; IPH, intraplaque hemorrhage; CA, carotid artery; LRNC, lipo-rich necrotic core. OR, odds ratio; CI, confidence interval; mRS, modified Rankin Scale; IPH, intraplaque hemorrhage; CA, carotid artery; LRNC, lipo-rich necrotic core.*

for confounding factors (including age, gender, smoking history, NIHSS on admission, DBP on admission, stenosis rate of CA, calcification, loose matrix, LRNC, and statins accepted at 3 months). However, we still wanted to know why the patients with IPH might be more prone to have a poor prognosis. So, we defined the early stroke progression, early recurrent ischemic stroke, and hemorrhagic transformation as the second outcomes. Our study found that patients with IPH might be more likely to occur early stroke progression, recurrent ischemic stroke, and hemorrhagic transformation.

Several studies have confirmed that IPH is associated with plaque progression (15, 16). Takaya et al. (17) followed the asymptomatic patients with carotid artery stenosis rate of 50–70% for 18 months. They found that the volume of the carotid artery wall and the percentage of lipid-rich necrotic core volume in the patients with IPH detected by MRI at baseline were significantly higher than in the control group. Meanwhile, the patients with IPH at baseline were also more likely to have new IPH at 18 months (43 vs. 0%; $p = 0.006$). According to the pathophysiological mechanism of plaque progression, some scholars believed that the hemoglobin would be released extracellularly after red blood cells are phagocytosed by macrophage. The free hemoglobin would increase inflammation, lipid core expansion, and oxidative stress, leading to plaque progression. IPH also carried proteolytic enzyme, leading to the degradation and destruction of the fibrous cap, and, finally, to the plaque rupture (18–20). Due to the limitations of this study, we did not study the pathophysiological process of IPH leading to the secondary outcomes, though it might be the research direction and hot spot in the future.

Our study still has some shortcomings. Firstly, because it is a single-center study with small sample size, the statistical results might be biased. Secondly, we did not make further study on the dynamic evolution of IPH, so we still do not know the pathophysiological mechanism of PH leading to poor functional outcome. Thirdly, our study did not exclude other risk factors affecting the prognosis of stroke, such as intracranial vascular artery disease, collateral circulation, and cerebral blood flow reserve capacity, which may be some errors in the results. Fourthly, we did not register the TOAST subtypes in our study, and it is a pity of the study. However, we have tried our best to rule out cardiogenic sources. We also hope to see the results of a large sample and more rigorous research in the future.

CONCLUSION

Compared with patients without IPH, patients with IPH have a higher risk of poor 3-month outcome after stroke onset. Based on this, we should not overlook the potential risk of IPH. It might be essential to understand the underlying pathophysiological mechanism of plaque vulnerability and the molecular biomarkers combined with neuroimaging markers.

DATA AVAILABILITY STATEMENT

The original contributions presented in the study are included in the article/**Supplementary Material**, further inquiries can be directed to the corresponding author/s.

ETHICS STATEMENT

The studies involving human participants were reviewed and approved by the Ethics Committee of Beijing Tiantan Hospital. Written informed consent to participate in this study was provided by the patient/participants or patient/participants' legal guardian/next of kin.

AUTHOR CONTRIBUTIONS

FC, XZ, XGo, BS, and YJ: concept and design. FC, YL, and XGe: drafting of the manuscript. XB and JJ: critical revision of the manuscript for important intellectual content. YL, BS, and YJ: provision of study material or patients. FC, YL, JJ, AW, XB, BS, YJ, and XGo: collection and assembly of data. XZ and BS: check and approve of clinical definition and supervision. FC and AW: data analysis. FC, AW, XB, BS, JJ, and XGe: data interpretation. XZ, BS, and YJ: administrative, and technical or material support. All authors: final approval of manuscript.

FUNDING

The study was supported by grants from the Beijing Natural Science Foundation (Z200016).

ACKNOWLEDGMENTS

Thanks were due to Professor Xihai Zhao from Tsinghua University for his selfless assistance with the experiment and Dr. Donghua Mi from Beijing Tiantan Hospital for her valuable discussion.

SUPPLEMENTARY MATERIAL

The Supplementary Material for this article can be found online at: https://www.frontiersin.org/articles/10.3389/fneur.2021.780436/full#supplementary-material

REFERENCES

1. Liu L, Wang D, Wong KS, Wang Y. Stroke and stroke care in China: huge burden, significant workload, and a national priority. *Stroke.* (2011) 42:3651–4. doi: 10.1161/STROKEAHA.111.635755
2. Dharmakidari S, Bhattacharya P, Chaturvedi S. Carotid artery stenosis: medical therapy, surgery, and stenting. *Curr Neurol Neurosci Rep.* (2017) 17:77. doi: 10.1007/s11910-017-0786-2
3. Al-Khaled M, Scheef B. Symptomatic carotid stenosis and stroke risk in patients with transient ischemic attack according to the tissue-based definition. *Int J Neurosci.* (2016) 126:888–92. doi: 10.3109/00207454.2015.1077834
4. Zhao X, Li R, Hippe DS, Hatsukami TS, Yuan C, Investigators C-I. Chinese Atherosclerosis Risk Evaluation (CARE II) study: a novel cross-sectional, multicentre study of the prevalence of high-risk atherosclerotic carotid plaque in Chinese patients with ischaemic cerebrovascular events-design and rationale. *Stroke Vasc Neurol.* (2017) 2:15–20. doi: 10.1136/svn-2016-000053
5. Jiang P, Chen Z, Hippe DS, Watase H, Sun B, Lin R, et al. Association between carotid bifurcation geometry and atherosclerotic plaque vulnerability: a Chinese atherosclerosis risk evaluation study. *Arterioscler Thromb Vasc Biol.* (2020) 40:1383–91. doi: 10.1161/ATVBAHA.119.313830
6. Yang D, Ji Y, Wang D, Watase H, Hippe DS, Zhao X, et al. Comparison of carotid atherosclerotic plaques between subjects in Northern and Southern

China: a Chinese atherosclerosis risk evaluation study. *Stroke Vasc Neurol.* (2020) 5:138–45. doi: 10.1136/svn-2019-000288
7. Finn AV, Nakano M, Narula J, Kolodgie FD, Virmani R. Concept of vulnerable/unstable plaque. *Arterioscler Thromb Vasc Biol.* (2010) 30:1282–92. doi: 10.1161/ATVBAHA.108.179739
8. Naghavi M, Libby P, Falk E, Casscells SW, Litovsky S, Rumberger J, et al. From vulnerable plaque to vulnerable patient: a call for new definitions and risk assessment strategies: part I. *Circulation.* (2003) 108:1664–72. doi: 10.1161/01.CIR.0000087480.94275.97
9. Naghavi M, Libby P, Falk E, Casscells SW, Litovsky S, Rumberger J, et al. From vulnerable plaque to vulnerable patient: a call for new definitions and risk assessment strategies: Part II. *Circulation.* (2003) 108:1772–8. doi: 10.1161/01.CIR.0000087481.55887.C9
10. Saam T, Underhill HR, Chu B, Takaya N, Cai J, Polissar NL, et al. Prevalence of American Heart Association type VI carotid atherosclerotic lesions identified by magnetic resonance imaging for different levels of stenosis as measured by duplex ultrasound. *J Am Coll Cardiol.* (2008) 51:1014–21. doi: 10.1016/j.jacc.2007.10.054
11. Kwee RM, van Oostenbrugge RJ, Mess WH, Prins MH, van der Geest RJ, ter Berg JWM, et al. MRI of carotid atherosclerosis to identify TIA and stroke patients who are at risk of a recurrence. *J Magn Reson Imaging.* (2013) 37:1189–94. doi: 10.1002/jmri.23918
12. Seners P, Baron JC. Revisiting "progressive stroke": incidence, predictors, pathophysiology, and management of unexplained early neurological deterioration following acute ischemic stroke. *J Neurol.* (2018) 265:216–25. doi: 10.1007/s00415-017-8490-3
13. Rothwell PM, Algra A, Chen Z, Diener HC, Norrving B, Mehta Z. Effects of aspirin on risk and severity of early recurrent stroke after transient ischaemic attack and ischaemic stroke: time-course analysis of randomised trials. *Lancet.* (2016) 388:365–75. doi: 10.1016/S0140-6736(16)30468-8
14. Alvarez-Sabin J, Maisterra O, Santamarina E, Kase CS. Factors influencing haemorrhagic transformation in ischaemic stroke. *Lancet Neurol.* (2013) 12:689–705. doi: 10.1016/S1474-4422(13)70055-3
15. Sun J, Underhill HR, Hippe DS, Xue Y, Yuan C, Hatsukami TS. Sustained acceleration in carotid atherosclerotic plaque progression with intraplaque hemorrhage: a long-term time course study. *JACC Cardiovasc Imaging.* (2012) 5:798–804. doi: 10.1016/j.jcmg.2012.03.014
16. Sun J, Balu N, Hippe DS, Xue Y, Dong L, Zhao X, et al. Subclinical carotid atherosclerosis: short-term natural history of lipid-rich necrotic core–a multicenter study with MR imaging. *Radiology.* (2013) 268:61–8. doi: 10.1148/radiol.13121702
17. Takaya N, Yuan C, Chu B, Saam T, Polissar NL, Jarvik GP, et al. Presence of intraplaque hemorrhage stimulates progression of carotid atherosclerotic plaques: a high-resolution magnetic resonance imaging study. *Circulation.* (2005) 111:2768–75. doi: 10.1161/CIRCULATIONAHA.104.504167
18. Moreno PR, Purushothaman M, Purushothaman KR. Plaque neovascularization: defense mechanisms, betrayal, or a war in progress. *Ann N Y Acad Sci.* (2012) 1254:7–17. doi: 10.1111/j.1749-6632.2012.06497.x
19. Michel JB, Delbosc S, Ho-Tin-Noé B, Leseche G, Nicoletti A, Meilhac O, et al. From intraplaque haemorrhages to plaque vulnerability: biological consequences of intraplaque haemorrhages. *J Cardiovasc Med.* (2012) 13:628–34. doi: 10.2459/JCM.0b013e328357face
20. Teng Z, Sadat U, Brown AJ, Gillard JH. Plaque hemorrhage in carotid artery disease: pathogenesis, clinical and biomechanical considerations. *J Biomech.* (2014) 47:847–58. doi: 10.1016/j.jbiomech.2014.01.013

Conflict of Interest: The authors declare that the research was conducted in the absence of any commercial or financial relationships that could be construed as a potential conflict of interest.

Publisher's Note: All claims expressed in this article are solely those of the authors and do not necessarily represent those of their affiliated organizations, or those of the publisher, the editors and the reviewers. Any product that may be evaluated in this article, or claim that may be made by its manufacturer, is not guaranteed or endorsed by the publisher.

frontiers in Neurology

REVIEW
published: 22 February 2022
doi: 10.3389/fneur.2022.839398

Atrial Cardiopathy and Cryptogenic Stroke

Yuji Kato and Shinichi Takahashi*

Department of Neurology and Cerebrovascular Medicine, Saitama Medical University International Medical Center, Hidaka, Japan

Recent advances in pathophysiology suggest that a pathological atrial substrate can cause embolic stroke even in patients without atrial fibrillation (AF). This pathological condition is called "atrial cardiopathy", which indicates atrial structural and functional disorders that can precede AF. The objective of this narrative review was to provide a current overview of atrial cardiopathy and cryptogenic stroke. We searched the PubMed database and summarized the recent findings of the identified studies, including the pathogenesis of atrial cardiopathy, biomarkers of atrial cardiopathy, relationship between atrial cardiopathy and cryptogenic stroke, and therapeutic interventions for atrial cardiopathy. Abnormal atrial substrate (atrial cardiopathy) that leads to AF can result in embolic stroke before developing AF, and may explain the source of cryptogenic stroke in some patients. Although there are several potential biomarkers indicative of atrial cardiopathy, P-wave terminal force in lead V1 (>5,000 μV* ms), N-terminal pro-brain natriuretic peptide (>250 pg/ml), and left atrial enlargement are currently promising biomarkers for the diagnosis of atrial cardiopathy. Because the optimal combination and thresholds of biomarkers for diagnosing atrial cardiopathy remain uncertain, atrial cardiopathy represents a spectrum disorder. The concept of atrial cardiopathy appears to be most valuable as a starting point for therapeutic intervention to prevent stroke. Validation of the diagnosis of atrial cardiopathy and whether it can be used as a new therapeutic target for direct oral anticoagulants are currently being covered in the ARCADIA trial.

Keywords: atrial cardiopathy, atrial dysfunction, atrial fibrillation, cardioembolic stroke subtype, embolic stroke of undetermined source

OPEN ACCESS

Edited by:
Bing Tian,
Naval Medical University, China

Reviewed by:
Raffaele Ornello,
University of L'Aquila, Italy
Arturo Tamayo,
University of Manitoba, Canada

****Correspondence:***
Yuji Kato
yujik@saitama-med.ac.jp

Specialty section:
This article was submitted to Stroke, a section of the journal Frontiers in Neurology

Received: *19 December 2021*
Accepted: *26 January 2022*
Published: *22 February 2022*

Citation:
Kato Y and Takahashi S (2022) Atrial Cardiopathy and Cryptogenic Stroke. Front. Neurol. 13:839398. doi: 10.3389/fneur.2022.839398

INTRODUCTION

Approximately one fourth of all ischemic stroke patients are classified as cryptogenic strokes, most of which are caused by an embolic mechanism (1). Cryptogenic strokes have usually meant a non-lacunar infarction without proximal arterial stenosis or cardioembolic sources; however, there is neither a widely accepted definition nor a required diagnostic assessment. This has inhibited clinical research into optimal preventive therapy for cryptogenic strokes. In 2014, the Cryptogenic Stroke/ESUS International Working Group proposed the classification of a new subgroup of cryptogenic stroke: embolic stroke of undetermined source (ESUS) (1). The definition of ESUS is as follows: (1) detection of a non-lacunar infarct on brain computed tomography/magnetic resonance imaging; (2) exclusion of ≥50% atherosclerotic stenosis proximal to the infarct with any imaging modality (catheter, magnetic resonance, computed tomography angiography, or ultrasonography); (3) exclusion of a major-risk cardioembolic source with echocardiography and cardiac monitoring

for ≥24 h; and (4) no other specific causes (e.g., arteritis, dissection, migraine, and drug misuse) (1). The concept of ESUS has contributed to facilitating clinical trials testing direct-acting oral anticoagulants (DOAC) for the secondary prevention of ESUS.

Although ESUS represents a heterogeneous clinical entity, the hypothesis that covert paroxysmal AF is the primary cause of ESUS is widely affirmed and has contributed to the current practice of performing long-term cardiac rhythm monitoring after ESUS. However, an implantable cardiac monitor detected AF in only 30% of patients during a 3-year period (2). This implies that AF may not be a necessary condition for cardioembolism.

Recent advances in pathophysiology have suggested that left atrial degeneration, including chamber dilation, remodeling, fibrosis, and damage to endothelial cells and cardiomyocytes, can induce thrombus generation and cause embolism, even in patients without AF (3, 4). This condition was defined as atrial cardiopathy, a term used to describe atrial structural and functional disorders that can precede AF (5). Atrial cardiopathy increases the stroke risk in patients with AF and is likely to also increase the stroke risk in patients without AF. In this article, we review the pathogenesis of atrial cardiopathy, its biomarkers, its association with stroke, and the potential for therapeutic intervention.

PATHOGENESIS OF ATRIAL CARDIOPATHY

The mechanism of thrombosis has long been recognized as Virchow's triad, summarized as stasis, hypercoagulability, and endothelial damage. In the case of AF, thrombus formation is induced by decreased left atrial appendage (LAA) flow velocity, activation of the coagulation cascade, and left atrial enlargement (LAE) and fibrosis. Recent findings suggest that the causal association between AF and stroke is not simple and still not fully understood.

Figure 1 shows the relationship between atrial cardiopathy and thromboembolic stroke. Aging and lifestyle-related diseases promote atrial damage, including stretching and enlargement of the left atrium. Over time, this causes increased fibrosis of the left atrial myocardium under a process modulated by genetic predisposition. The resulting fibrotic changes promote left atrial remodeling, including structural and electrical changes

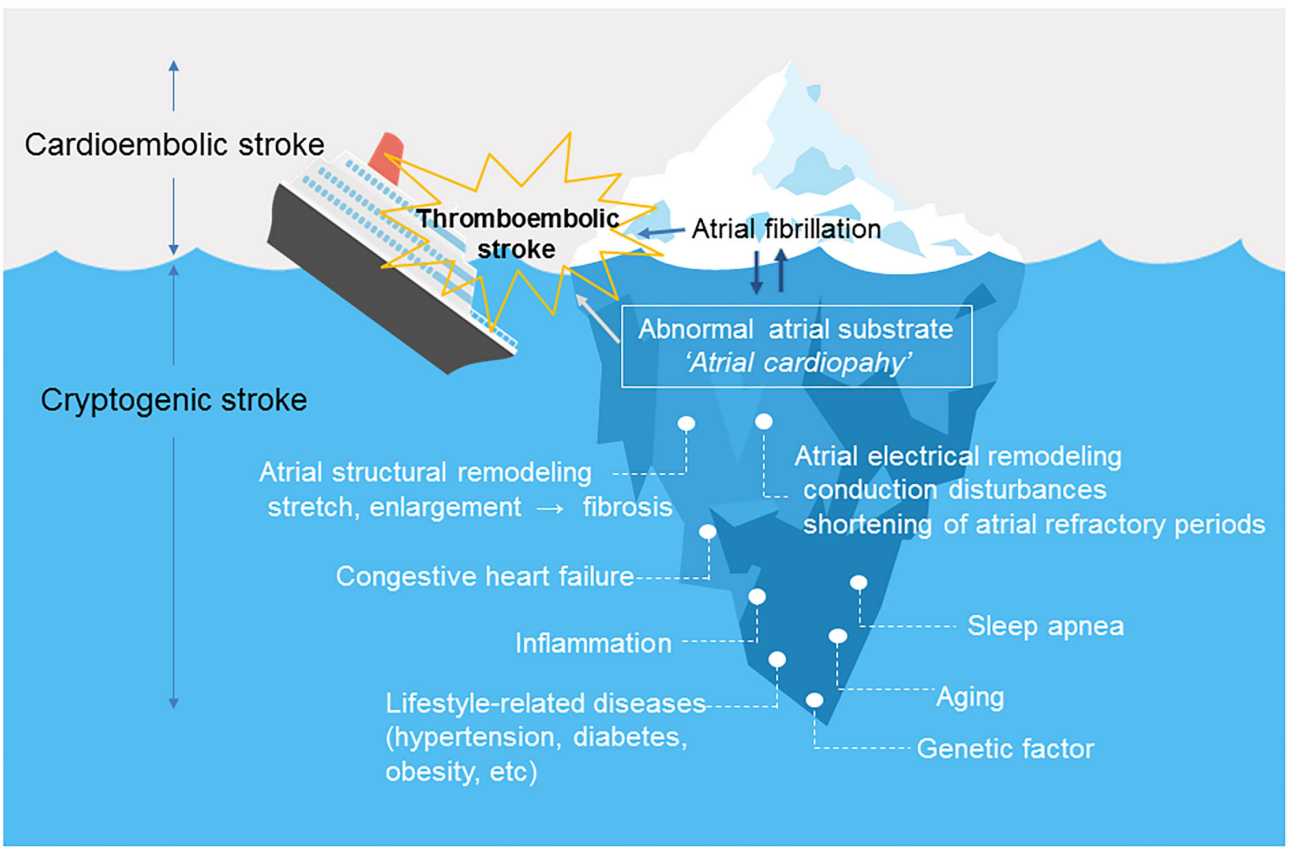

FIGURE 1 | Atrial cardiopathy as a cause of thromboembolic stroke. Atrial fibrillation is likely only a marker (tip of the iceberg) for underlying abnormal atrial substrate or "atrial cardiopathy". Underlying atrial cardiopathy can cause stroke, even in patients without atrial fibrillation. Once atrial fibrillation develops, the dysrhythmia causes structural and electrical remodeling, which further increases the risk of thromboembolism.

(6), which forms abnormal atrial substrate (atrial cardiopathy) that can lead to the occurrence of AF and embolic stroke (3, 7). AF leads to further atrial remodeling. It is important to note that atrial cardiopathy can predispose to embolic stroke even in patients without AF.

BIOMARKERS OF ATRIAL CARDIOPATHY

There are still no established criteria for the diagnosis of atrial cardiopathy. However, researchers have attempted to identify atrial cardiopathy biomarkers associated with stroke risk factors found in ESUS patients. **Table 1** shows the potential biomarkers of atrial cardiopathy associated with the risk of stroke. These biomarkers are classified as electrophysiological, structural, hemodynamic, serological, and genetic markers.

ELECTROPHYSIOLOGICAL MARKERS

Symptomatic stroke may be an initial clinical manifestation of underlying AF. Two randomized trials have found that prolonged rhythm monitoring of outpatients after ESUS results in a higher detection rate of AF than with standard monitoring (2, 8). Although even brief subclinical episodes of AF are associated with the occurrence of stroke (9), the causal association between ischemic stroke and AF remains circumstantial (3). Both the ASSERT and TRENDS studies reported that in only 8–28% of patients, subclinical AF was detected within 30 days before stroke or systemic embolism (10, 11). The absence of temporality implies that AF itself may not be the direct cause of stroke in patients with short-term AF. Instead, AF may be a risk indicator for embolic stroke associated with underlying atrial dysfunction.

The *P*-wave terminal force in lead V1 (PTFV1) (**Figure 2**) becomes prolonged with left atrial hypertrophy, fibrosis, and increased filling pressure, and is thought to reflect structural and functional impairment of the left atrium (12, 13). In the Multi-Ethnic Study of Atherosclerosis, which included 6,741 participants aged 45–85 years without a history of cardiovascular disease, stroke, or AF, PTFV1 was associated with a higher incidence of ischemic stroke [hazard ratio (HR) per standard deviation 1.21, 95% confidence interval (CI) 1.02–1.44] than AF (HR per standard deviation 1.11, 95% CI 1.03–1.21) after a mean of 8.5 years of observation (14). In the Atherosclerosis Risk in Communities study of 14,542 AF-free participants observed for a median of 22 years, ischemic stroke occurred more frequently in those with abnormal PTFV1 (>4,000 μV* ms) than in those without (6.3 vs. 2.9 per 1,000 person-years, respectively, $p < 0.001$; **Figure 3**). Abnormal PTFV1 was associated with ischemic stroke (HR 1.33, 95% CI 1.11–1.59) and non-lacunar infarction (HR 1.49, 95% CI 1.07–2.07) but not with lacunar infarction (HR 0.89, 95% CI 0.57–1.40) (15).

Paroxysmal supraventricular tachycardia (PSVT) is a benign rhythm disorder that has been associated with palpitations but that does not increase the risk of stroke. However, a follow-up of 169 patients with PSVT revealed that 12% developed AF within 1 year and 19% developed AF within a mean of 31 months (16). In addition, a large cohort study conducted in California found that PSVT was associated with ischemic stroke even in the absence of AF (adjusted HR 2.10, 95% CI 1.69–2.62) (17).

An ectopic atrial rhythm is also considered a risk factor for ischemic stroke. In the Copenhagen Holter Study, 678 patients aged 55–75 years without a history of cardiovascular disease, stroke, or AF underwent 48 hours of mobile electrocardiography (ECG) and were followed-up for 15 years (18). Excessive

TABLE 1 | Potential biomarkers associated with atrial cardiopathy and stroke risk.

Biomarkers classified into categories	Specific examples
Electrophysiological	
Atrial fibrillation	Subclinical atrial fibrillation
P-wave morphology	*P*-wave terminal force in lead V1
Paroxysmal supraventricular tachycardia	
Atrial ectopy	Excessive supraventricular ectopic activity
Structural	
Left atrial size	Left atrial enlargement, left atrial volume index
LAA morphology	Non-chicken wing type
Myocardial fibrosis	Regions of delayed gadolinium enhancement on cardiac MRI
Hemodynamic	
LAA flow velocity	Low flow velocity
Serological	
NT-proBNP, BNP	
Hs-cTnT	
Genetic	
Polymorphisms	rs2200733, rs10033464

LAA, left atrial appendage; MRI, magnetic resonance imaging; NT-proBNP, N-terminal pro-brain natriuretic peptide; BNP: brain natriuretic peptide; Hs-cTnT, high-sensitivity cardiac troponin T.

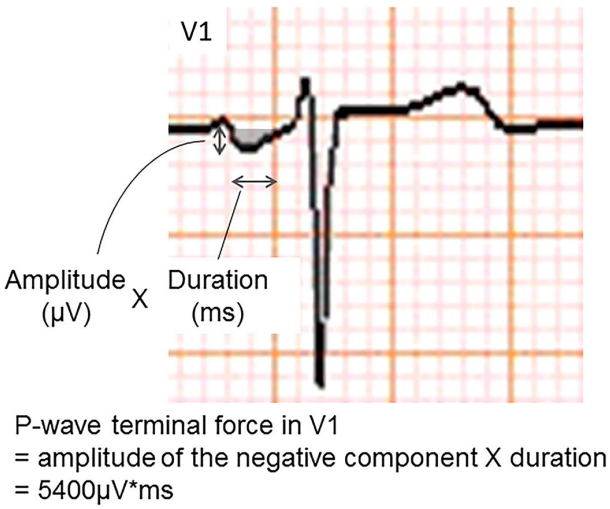

FIGURE 2 | An example of abnormal *P*-wave terminal force in lead V1. The *P*-wave terminal force in lead V1 was calculated as multiplying the amplitude and duration of the terminal negative part of the *P*-wave in lead V1.

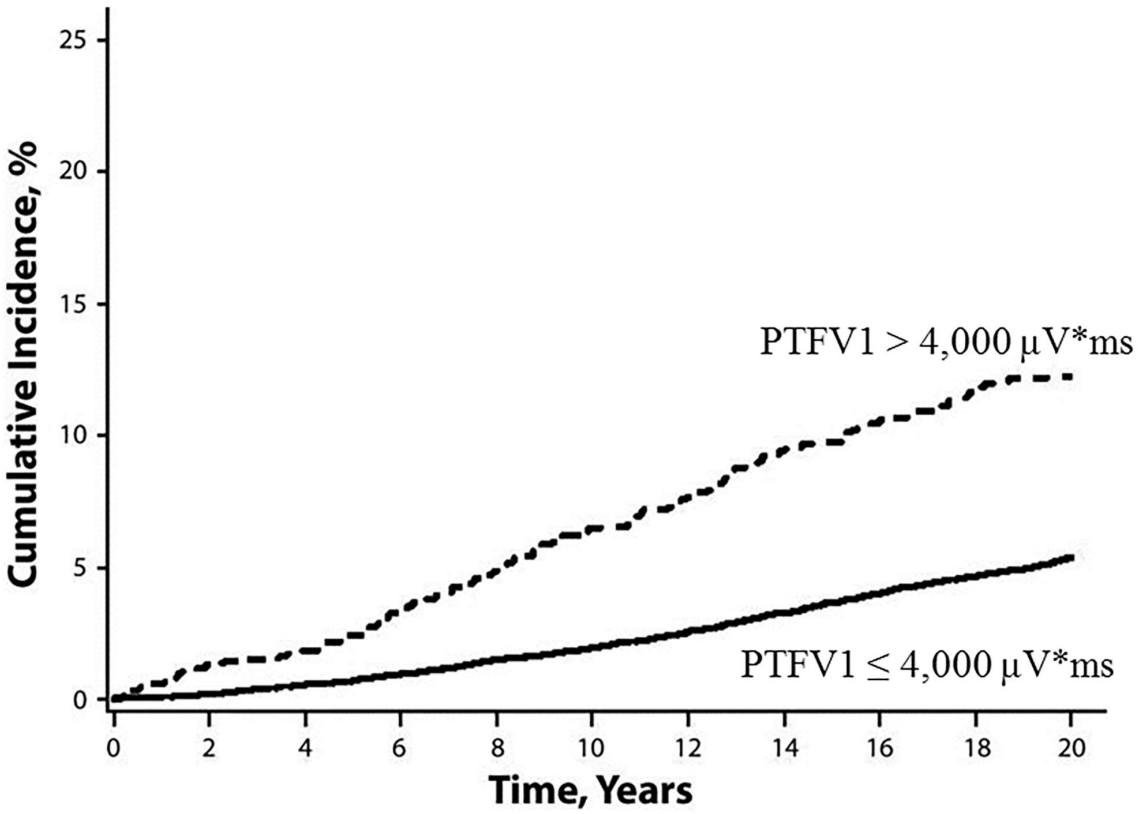

FIGURE 3 | Cumulative incidence of ischemic stroke, stratified by baseline PTFV1 (15). Ischemic stroke occurred more frequently in those with abnormal PTFV1 (>4,000 μV* ms) than in those without (log-rank test $p < 0.001$). PTFV1, *P*-wave terminal force in lead V1.

supraventricular ectopic activity (ESVEA) was defined as the presence of either ≥30 premature atrial contractions/hour or any runs that lasted for ≥1 h. Ninety-nine patients (15%) had ESVEA during follow-up. The incidence of stroke was higher in patients with ESVEA than those without in >65 years of age (38.5 vs. 13.6 per 1,000 person-years, respectively, $p = 0.0007$), but not in ≤65 years of age (8.9 vs. 5.0 per 1,000 person-years, respectively, $p = 0.2086$) (**Figure 4**). After adjusting for risk factors and censoring for the development of AF, the risk of stroke in patients with ESVEA was nearly twice as great as in those without ESVEA (HR 1.96, 95% CI 1.10–3.49). Of the patients with ESVEA who had cerebral infarction, 14.3% developed AF before their stroke. The incidence of cerebral infarction in patients with ESVEA and a CHA2DS2-VASc score of ≥2 points was 2.4%/year, indicating a risk similar to that of AF.

STRUCTURAL MARKERS

Structural abnormality of the left atrium indicates the need to search for findings of atrial cardiopathy. Population-based studies have shown that LAE is associated with developing AF (19) and incident ischemic stroke after multivariable adjustment including AF. The Framingham study reported that LAE is a significant predictor of stroke in men (adjusted HR per 10 mm increase 2.4, 95% CI 1.6–3.7) and women (adjusted HR per 10 mm increase 1.4, 95% CI 0.9–2.1) (20). In the Northern Manhattan Stroke Study of 655 patients with previous ischemic stroke, moderate to severe LAE (≥47 mm in men and ≥43 mm in women) was significantly associated with recurrent cardioembolic/cryptogenic stroke compared with normal LAE (adjusted HR 2.83, 95% 1.03–7.81) (21). However, one limitation of these studies is that they used left atrial diameter, which does not fully represent the true three-dimensional size of the left atrium. It has recently been shown that the left atrial volume index to the subject's body surface area is a superior indicator of left atrial size in terms of predicting cardiovascular outcomes (22). Furthermore, a recent study revealed that the left atrial volume index to the subject's body surface area is independently associated with the development of AF in ESUS patients (adjusted odds ratio per mL/m^2 1.09, 95% CI 1.02–1.15, $p = 0.007$) (23).

The fundamental cause of AF is thought to be atrial fibrosis (24, 25). On cardiac magnetic resonance imaging, fibrotic areas are visualized as areas of delayed gadolinium enhancement (26). The presence of left atrial fibrosis on cardiac magnetic resonance imaging appears to correlate with stroke risk. A cross-sectional analysis of 387 AF patients revealed that patients with previous strokes had significantly higher levels of fibrosis than those who had not experienced a stroke (27). In a multivariate analysis, the presence of fibrosis was a better predictor of stroke risk than the CHADS2 score. A recent study revealed that the prevalence of left

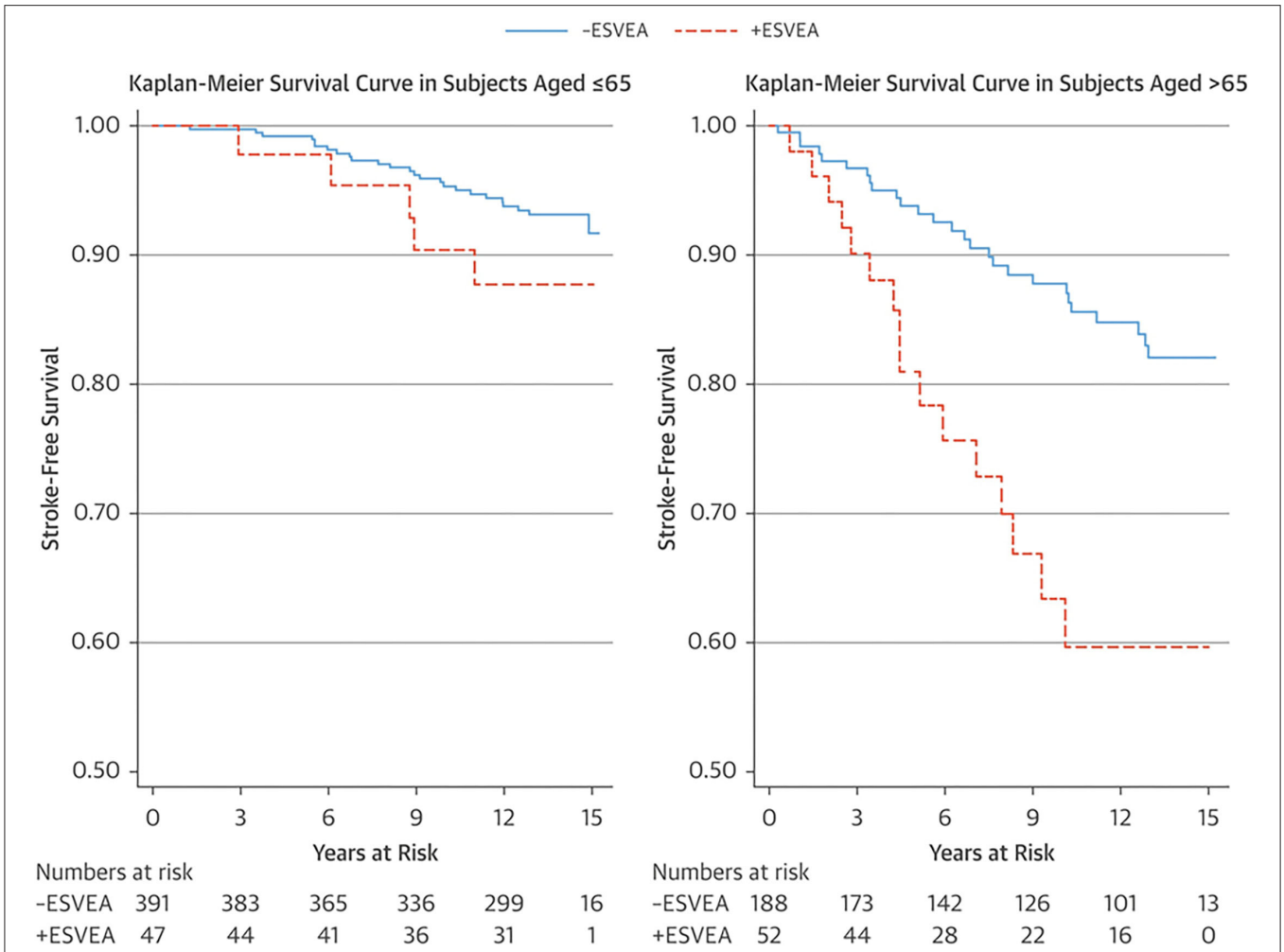

FIGURE 4 | Kaplan–Meier survival estimate of stroke-free survival stratified by age group and ESVEA (18). The incidence of stroke associated with ESVEA was higher in patients >65 years of age ($p = 0.0007$), but not in patients ≤65 years of age ($p = 0.2086$). ESVEA, excessive supraventricular ectopic activity.

atrial fibrosis in ESUS patients was higher than that in patients with stroke due to other causes ($p = 0.03$) and similar to that in stroke patients with AF ($p = 0.22$) (28).

The risk of stroke may also be associated with the morphological features of the LAA (29). In a previous study of AF patients, a non-chicken wing LAA morphology was more likely to be associated with ischemic stroke (30). In a retrospective study of 172 stroke patients, the prevalence of non-chicken wing LAA morphology on chest computed tomography tended to be higher in patients with cardioembolic stroke (58.7%) and ESUS (58.8%) than in those with noncardioembolic stroke (46.3%); however, the difference did not achieve statistical significance (31).

HEMODYNAMIC MARKERS

The LAA appears to play an important role in intracardiac thrombus generation in AF patients. More than 90% of intracardiac thrombi in AF patients are identified in the LAA (32), and a decreased LAA flow velocity is thought to be associated with the generation of stasis (33). Among 721 patients who underwent transesophageal echocardiography in a *post hoc* analysis of the Stroke Prevention in Atrial Fibrillation-III trial, reduced LAA flow velocity (<20 cm/s) was associated with thrombus formation and subsequent cardioembolic stroke (33). Similarly, a cross-sectional study of 909 stroke patients with or without AF found that decreased LAA flow velocity (<60 cm/s) was associated with clinically elevated stroke severity (34), and an observational study of 786 patients with cryptogenic stroke found that decreased LAA flow velocity on transesophageal echocardiography was associated with multiple infarcts (35). These results indicate that decreased flow velocity in the LAA is an additional risk factor for cardioembolic stroke, regardless of whether AF exists.

SEROLOGICAL MARKERS

Serum biomarkers could be informative to detect a high risk of paroxysmal AF in patients with stroke and to preselect

patients who require long-term cardiac monitoring after stroke. For example, B-type natriuretic peptide (BNP) and N-terminal pro-brain natriuretic peptide (NT-proBNP) are released by the cardiac myocytes in response to stretch and are therefore increased in patients with heart failure, AF, and ventricular strain. Thus, BNP and NT-proBNP levels have been proposed as indicators of cardioembolic origin in stroke of unknown cause (36).

In a case-cohort analysis of the Reasons for Geographic and Racial Differences in Stroke cohort (n = 1,502, mean follow-up 5.4 years), patients in the highest quartile of serum NT-proBNP concentration had a 3-fold higher stroke risk than those in the lowest quartile (HR 2.9, 95% CI 1.9–4.5); the association was strongest for cardioembolic subtypes (HR 9.1, 95% CI 2.9–29.2), suggesting that the stroke risk was due to embolism (37). A subanalysis of the Find-$AF_{RANDOMISED}$ trial of 398 stroke patients without AF showed that the median BNP level was higher in patients with paroxysmal AF detected by frequent and longer Holter ECG monitoring than in patients without AF (57.8 vs. 28.3 pg/mL, respectively, p = 0.0003) (38). A BNP cutoff value of ≥100 pg/mL was useful to preselect stroke patients who required frequent and longer Holter ECG monitoring.

Cardiac troponin (cTnT) is a biomarker of myocardial damage often used to detect myocardial ischemia. Highly sensitive assays can determine cTnT concentrations of less than one-tenth that detected in conventional assays used for the identification of acute myocardial ischemia. In the ARIC study of 10,902 stroke-free patients observed for a mean of 11.3 years, a highly sensitive assay concentration of cTnT in the highest quintile was significantly associated with cardioembolic stroke (HR 2.63, 95% CI 1.28–5.37, p = 0.003) compared with the lowest quintile, but not with lacunar infarction (39).

GENETIC MARKERS

Recently, a genome-wide association study found a haplotype block on chromosome 4q25 associated with AF (40). In addition, two single nucleotide polymorphisms (rs2200733 and rs10033464) have been reported to be associated with the development of AF (41) and ischemic stroke, especially the cardioembolic subtype, even in patients in whom active AF has not been detected (42). While paroxysmal AF may be underdiagnosed in these patients, their genetic predisposition may involve potential left atrial abnormalities that lead independently to both AF and stroke.

ATRIAL CARDIOPATHY AND CRYPTOGENIC STROKE

Although specific diagnostic criteria for atrial cardiopathy and the thresholds indicative of increased stroke risk are still being developed, it appears that atrial cardiopathy can be provisionally diagnosed by the presence of one or a few of the biomarkers of atrial dysfunction discussed above. In the Cardiovascular Health Study, among 3,723 participants without stroke and AF at baseline, 585 participants developed an incident ischemic stroke during a median 12.9 years of follow-up (43). PTFV1 (HR per 1,000 μV* ms 1.04, 95% CI 1.001–1.08), NT-proBNP (HR per doubling of NT-proBNP 1.09, 95% CI 1.03–1.16), and incident AF (HR 2.04, 95% CI 1.67–2.48) were each independently associated with incident ischemic stroke, but not the left atrial diameter (>4.3 cm in women, >4.7 cm in men).

In a cross-sectional study of 846 stroke patients, the prevalence of atrial cardiopathy (defined as PTFV1 >5,000 μV* ms or severe LAE) was higher in ESUS patients than in patients with noncardioembolic stroke (26.6 vs. 12.1%, respectively, in large artery atherosclerosis vs. 16.9% in small artery disease; p = 0.001) (44).

In a subanalysis of 3,983 eligible patients from the New Approach Rivaroxaban Inhibition of Factor Xa in a Global Trial vs. ASA to Prevent Embolism in Embolic Stroke of Undetermined Source (NAVIGATE ESUS), 235 (5.9%) patients had LAE, 939 (23.6%) had ipsilateral carotid plaque to ischemic stroke, and 94 (2.4%) had both (45). Although the common risk factors were male sex, Caucasian ethnicity, hypertension, tobacco use, and coronary artery disease, increasing atrial diameter was not associated with carotid plaque after adjustment (odds ratio per cm, 1.1, 95% CI 1.0–1.2, p = 0.08). There was also no association between line of atrial cardiopathy (premature atrial contractions on Holter ECG, new onset of AF) and carotid plaque formation. These results suggest that atrial cardiopathy and carotid plaque are likely separate and nonoverlapping risk factors in patients with ESUS.

THERAPEUTIC INTERVENTIONS FOR ATRIAL CARDIOPATHY

Current knowledge suggests that atrial cardiopathy is likely to be the stroke etiologic subtype most similar to AF and may benefit from anticoagulation, particularly DOAC therapy. In fact, secondary analyses of the NAVIGATE ESUS trial found that rivaroxaban was superior to aspirin in the subset of patients with LAE (>4.6 cm) (HR 0.26, 95% CI 0.07–0.94, p = 0.02) (46), but not in the subset of patients with ipsilateral nonstenosing plaque (47).

The AtRial Cardiopathy and Antithrombotic Drugs In prevention After cryptogenic stroke (ARCADIA) trial is currently underway (48), with the primary objective to validate the hypothesis that a DOAC (apixaban) is more effective than aspirin for stroke prevention in cryptogenic stroke patients with atrial cardiopathy. In the ARCADIA trial, atrial cardiopathy was defined as the presence of one or more of the following: PTFV1 >5,000 μV* ms, NT-proBNP >250 pg/ml, and left atrial diameter index ≥ 3 cm/m^2.

CONCLUSION

Atrial cardiopathy should be considered one of the mechanisms of ESUS. Although there are several potential biomarkers

indicative of atrial cardiopathy, PTFV1 (>5,000 μV* ms), NT-proBNP (>250 pg/ml), and left atrial enlargement are currently promising biomarkers for the diagnosis of atrial cardiopathy. Because the best combination and thresholds of biomarkers for diagnosing atrial cardiopathy remain uncertain, atrial cardiopathy represents a spectrum disorder. The concept of atrial cardiopathy is useful as a starting point for therapeutic intervention to prevent stroke. The ARCADIA trial is currently being performed to validate the diagnosis of atrial cardiopathy and to determine whether atrial cardiopathy can be a new therapeutic target for DOAC.

AUTHOR CONTRIBUTIONS

YK performed the literature review and drafted the manuscript. ST performed critical revision of the manuscript. All authors contributed to the article and approved the submitted version.

REFERENCES

1. Hart RG, Diener HC, Coutts SB, Easton JD, Granger CB, O'Donnell MJ, et al. Embolic strokes of undetermined source: the case for a new clinical construct. *Lancet Neurol*. (2014) 13:429–38. doi: 10.1016/S1474-4422(13)70310-7
2. Sanna T, Diener HC, Passman RS, Di Lazzaro V, Bernstein RA, Morillo CA, et al. Cryptogenic stroke and underlying atrial fibrillation. *N Engl J Med*. (2014) 370:2478–86. doi: 10.1056/NEJMoa1313600
3. Kamel H, Okin PM, Elkind MS, Iadecola C. Atrial fibrillation and mechanisms of stroke: time for a new model. *Stroke*. (2016) 47:895–900. doi: 10.1161/STROKEAHA.115.012004
4. Kamel H, Healey JS. Cardioembolic stroke. *Circ Res*. (2017) 120:514–26. doi: 10.1161/CIRCRESAHA.116.308407
5. Kamel H, Okin PM, Longstreth WT Jr, Elkind MS, Soliman EZ. Atrial cardiopathy: a broadened concept of left atrial thromboembolism beyond atrial fibrillation. *Future Cardiol*. (2015) 11:323–31. doi: 10.2217/fca.15.22
6. Jalife J. Mechanisms of persistent atrial fibrillation. *Curr Opin Cardiol*. (2014) 29:20–7. doi: 10.1097/HCO.0000000000000027
7. Elkind MSV. Atrial cardiopathy and stroke prevention. *Curr Cardiol Rep*. (2018) 20:103. doi: 10.1007/s11886-018-1053-0
8. Gladstone DJ, Spring M, Dorian P, Panzov V, Thorpe KE, Hall J, et al. Atrial fibrillation in patients with cryptogenic stroke. *N Engl J Med*. (2014) 370:2467–77. doi: 10.1056/NEJMoa1311376
9. Healey JS, Connolly SJ, Gold MR, Israel CW, van Gelder IC, Capucci A, et al. Subclinical atrial fibrillation and the risk of stroke. *N Engl J Med*. (2012) 366:120–9. doi: 10.1056/NEJMoa1105575
10. Daoud EG, Glotzer TV, Wyse DG, Ezekowitz MD, Hilker C, Koehler J, et al. Temporal relationship of atrial tachyarrhythmias, cerebrovascular events, and systemic emboli based on stored device data: a subgroup analysis of TRENDS. *Heart Rhythm*. (2011) 8:1416–23. doi: 10.1016/j.hrthm.2011.04.022
11. Brambatti M, Connolly SJ, Gold MR, Morillo CA, Capucci A, Muto C, et al. Temporal relationship between subclinical atrial fibrillation and embolic events. *Circulation*. (2014) 129:2094–9. doi: 10.1161/CIRCULATIONAHA.113.007825
12. Jin L, Weisse AB, Hernandez F, Jordan T. Significance of electrocardiographic isolated abnormal terminal *P*-wave force (left atrial abnormality). An echocardiographic and clinical correlation. *Arch Intern Med*. (1988) 148:1545–9. doi: 10.1001/archinte.148.7.1545
13. Tiffany Win T, Ambale Venkatesh B, Volpe GJ, Mewton N, Rizzi P, Sharma RK, et al. Associations of electrocardiographic *P*-wave characteristics with left atrial function, and diffuse left ventricular fibrosis defined by cardiac magnetic resonance: the PRIMERI Study. *Heart Rhythm*. (2015) 12:155–2. doi: 10.1016/j.hrthm.2014.09.044
14. Kamel H, Soliman EZ, Heckbert SR, Kronmal RA, Longstreth WT Jr, Nazarian S, et al. *P*-wave morphology and the risk of incident ischemic stroke in the multi-ethnic study of atherosclerosis. *Stroke*. (2014) 45:2786–8. doi: 10.1161/STROKEAHA.114.006364
15. Kamel H, O'Neal WT, Okin PM, Loehr LR, Alonso A, Soliman EZ. Electrocardiographic left atrial abnormality and stroke subtype in the atherosclerosis risk in communities study. *Ann Neurol*. (2015) 78:670–8. doi: 10.1002/ana.24482
16. Hamer ME, Wilkinson WE, Clair WK, Page RL, McCarthy EA, Pritchett EL. Incidence of symptomatic atrial fibrillation in patients with paroxysmal supraventricular tachycardia. *J Am Coll Cardiol*. (1995) 25:984–8. doi: 10.1016/0735-1097(94)00512-O
17. Kamel H, Elkind MS, Bhave PD, Navi BB, Okin PM, Iadecola C, et al. Paroxysmal supraventricular tachycardia and the risk of ischemic stroke. *Stroke*. (2013) 44:1550–4. doi: 10.1161/STROKEAHA.113.001118
18. Larsen BS, Kumarathurai P, Falkenberg J, Nielsen OW, Sajadieh A. Excessive atrial ectopy and short atrial runs increase the risk of stroke beyond incident atrial fibrillation. *J Am Coll Cardiol*. (2015) 66:232–41. doi: 10.1016/j.jacc.2015.05.018
19. Psaty BM, Manolio TA, Kuller LH, Kronmal RA, Cushman M, Fried LP, et al. Incidence of and risk factors for atrial fibrillation in older adults. *Circulation*. (1997) 96:2455–61. doi: 10.1161/01.CIR.96.7.2455
20. Benjamin EJ, D'Agostino RB, Belanger AJ, Wolf PA, Levy D. Left atrial size and the risk of stroke and death. The Framingham heart study. *Circulation*. (1995) 92:835–41. doi: 10.1161/01.CIR.92.4.835
21. Yaghi S, Moon YP, Mora-McLaughlin C, Willey JZ, Cheung K, Di Tullio MR, et al. Left atrial enlargement and stroke recurrence: the Northern Manhattan stroke study. *Stroke*. (2015) 46:1488–93. doi: 10.1161/STROKEAHA.115.008711
22. Tsang TS, Abhayaratna WP, Barnes ME, Miyasaka Y, Gersh BJ, Bailey KR, et al. Prediction of cardiovascular outcomes with left atrial size: is volume superior to area or diameter? *J Am Coll Cardiol*. (2006) 47:1018–23. doi: 10.1016/j.jacc.2005.08.077
23. Jordan K, Yaghi S, Poppas A, Chang AD, Mac Grory B, Cutting S, et al. Left atrial volume index is associated with cardioembolic stroke and atrial fibrillation detection after embolic stroke of undetermined source. *Stroke*. (2019) 50:1997–2001. doi: 10.1161/STROKEAHA.119.025384
24. Goldberger JJ, Arora R, Green D, Greenland P, Lee DC, Lloyd-Jones DM, et al. Evaluating the atrial myopathy underlying atrial fibrillation: identifying the arrhythmogenic and thrombogenic substrate. *Circulation*. (2015) 132:278–91. doi: 10.1161/CIRCULATIONAHA.115.016795
25. Dzeshka MS, Lip GY, Snezhitskiy V, Shantsila E. Cardiac fibrosis in patients with atrial fibrillation: mechanisms and clinical implications. *J Am Coll Cardiol*. (2015) 66:943–59. doi: 10.1016/j.jacc.2015.06.1313
26. Yaghi S, Liberman AL, Atalay M, Song C, Furie KL, Kamel H, et al. Cardiac magnetic resonance imaging: a new tool to identify cardioaortic sources in ischaemic stroke. *J Neurol Neurosurg Psychiatry*. (2017) 88:31–7. doi: 10.1136/jnnp-2016-314023
27. Daccarett M, Badger TJ, Akoum N, Burgon NS, Mahnkopf C, Vergara G, et al. Association of left atrial fibrosis detected by delayed-enhancement magnetic resonance imaging and the risk of stroke in patients with atrial fibrillation. *J Am Coll Cardiol*. (2011) 57:831–8. doi: 10.1016/j.jacc.2010.09.049
28. Fonseca AC, Alves P, Inácio N, Marto JP, Viana-Baptista M, Pinho-E-Melo T, et al. Patients with undetermined stroke have increased atrial fibrosis: a cardiac magnetic resonance imaging study. *Stroke*. (2018) 49:734–7. doi: 10.1161/STROKEAHA.117.019641
29. Petersen M, Roehrich A, Balzer J, Shin DI, Meyer C, Kelm M, et al. Left atrial appendage morphology is closely associated with specific echocardiographic flow pattern in patients with atrial fibrillation. *Europace*. (2015) 17:539–45. doi: 10.1093/europace/euu347
30. Di Biase L, Santangeli P, Anselmino M, Mohanty P, Salvetti I, Gili S, et al. Does the left atrial appendage morphology correlate with the risk of stroke in patients with atrial fibrillation? Results from a multicenter study. *J Am Coll Cardiol*. (2012) 60:531–8. doi: 10.1016/j.jacc.2012.04.032

31. Yaghi S, Chang AD, Hung P, Mac Grory B, Collins S, Gupta A, et al. Left atrial appendage morphology and embolic stroke of undetermined source: a cross-sectional multicenter pilot study. *J Stroke Cerebrovasc Dis*. (2018) 27:1497–1501. doi: 10.1016/j.jstrokecerebrovasdis.2017.12.036
32. Blackshear JL, Odell, JA. Appendage obliteration to reduce stroke in cardiac surgical patients with atrial fibrillation. *Ann Thorac Surg*. (1996) 61:755–9. doi: 10.1016/0003-4975(95)00887-X
33. Goldman ME, Pearce LA, Hart RG, Zabalgoitia M, Asinger RW, Safford R, et al. Pathophysiologic correlates of thromboembolism in nonvalvular atrial fibrillation: I. Reduced flow velocity in the left atrial appendage (The Stroke Prevention in Atrial Fibrillation [SPAF-III] study). *J Am Soc Echocardiogr*. (1999) 12:1080–7. doi: 10.1016/S0894-7317(99)70105-7
34. Schnieder M, Siddiqui T, Karch A, Bähr M, Hasenfuß G, Schroeter MR, et al. Low flow in the left atrial appendage assessed by transesophageal echocardiography is associated with increased stroke severity: results of a single-center cross-sectional study. *Int J Stroke*. (2019) 14:423–9. doi: 10.1177/1747493018816511
35. Tokunaga K, Hashimoto G, Mizoguchi T, Mori K, Shijo M, Jinnouchi J, et al. Left atrial appendage flow velocity and multiple infarcts in cryptogenic stroke. *Cerebrovasc Dis*. (2021) 50:429–34. doi: 10.1159/000514672
36. Llombart V, Antolin-Fontes A, Bustamante A, Giralt D, Rost NS, Furie K, et al. B-type natriuretic peptides help in cardioembolic stroke diagnosis: pooled data meta-analysis. *Stroke*. (2015) 46:1187–95. doi: 10.1161/STROKEAHA.114.008311
37. Cushman M, Judd SE, Howard VJ, Kissela B, Gutiérrez OM, Jenny NS, et al. N-terminal pro-B-type natriuretic peptide and stroke risk: the reasons for geographic and racial differences in stroke cohort. *Stroke*. (2014) 45:1646–50. doi: 10.1161/STROKEAHA.114.004712
38. Wasser K, Weber-Krüger M, Gröschel S, Uphaus T, Liman J, Hamann GF, et al. Brain natriuretic peptide and discovery of atrial fibrillation after stroke: a subanalysis of the Find-$AF_{RANDOMISED}$ Trial. *Stroke*. (2020) 51:395–401. doi: 10.1161/STROKEAHA.119.026496
39. Folsom AR, Nambi V, Bell EJ, Oluleye OW, Gottesman RF, Lutsey PL, et al. Troponin T, N-terminal pro-B-type natriuretic peptide, and incidence of stroke: the atherosclerosis risk in communities study. *Stroke*. (2013) 44:961–7. doi: 10.1161/STROKEAHA.111.000173
40. Gudbjartsson DF, Arnar DO, Helgadottir A, Gretarsdottir S, Holm H, Sigurdsson A, et al. Variants conferring risk of atrial fibrillation on chromosome 4q25. *Nature*. (2007) 448:353–7. doi: 10.1038/nature 06007
41. Kääb S, Darbar D, van Noord C, Dupuis J, Pfeufer A, Newton-Cheh C, et al. Large scale replication and meta-analysis of variants on chromosome 4q25 associated with atrial fibrillation. *Eur Heart J*. (2009) 30:813–9. doi: 10.1093/eurheartj/ehn578
42. Gretarsdottir S, Thorleifsson G, Manolescu A, Styrkarsdottir U, Helgadottir A, Gschwendtner A, et al. Risk variants for atrial fibrillation on chromosome 4q25 associate with ischemic stroke. *Ann Neurol*. (2008) 64:402–9. doi: 10.1002/ana.21480
43. Kamel H, Bartz TM, Elkind MSV, Okin PM, Thacker EL, Patton KK, et al. Atrial cardiopathy and the risk of ischemic stroke in the CHS (Cardiovascular Health Study). *Stroke*. (2018) 49:980–6. doi: 10.1161/STROKEAHA.117.020059
44. Jalini S, Rajalingam R, Nisenbaum R, Javier AD, Woo A, Pikula A. Atrial cardiopathy in patients with embolic strokes of unknown source and other stroke etiologies. *Neurology*. (2019) 92:e288–94. doi: 10.1212/WNL.0000000000006748
45. Kamel H, Pearce LA, Ntaios G, Gladstone DJ, Perera K, Roine RO, et al. Atrial cardiopathy and nonstenosing large artery plaque in patients with embolic stroke of undetermined source. *Stroke*. (2020) 51:938–3. doi: 10.1161/STROKEAHA.119.028154
46. Healey JS, Gladstone DJ, Swaminathan B, Eckstein J, Mundl H, Epstein AE, et al. Recurrent stroke with rivaroxaban compared with aspirin according to predictors of atrial fibrillation: secondary analysis of the NAVIGATE ESUS randomized clinical trial. *JAMA Neurol*. (2019) 76:764–73. doi: 10.1001/jamaneurol.2019.0617
47. Ntaios G, Swaminathan B, Berkowitz SD, Gagliardi RJ, Lang W, Siegler JE, et al. Efficacy and safety of rivaroxaban versus aspirin in embolic stroke of undetermined source and carotid atherosclerosis. *Stroke*. (2019) 50:2477–85. doi: 10.1161/STROKEAHA.119.025168
48. Kamel H, Longstreth WT Jr, Tirschwell DL, Kronmal RA, Broderick JP, Palesch YY, et al. The AtRial cardiopathy and antithrombotic drugs in prevention after cryptogenic stroke randomized trial: rationale and methods. *Int J Stroke*. (2019) 14:207–14. doi: 10.1177/1747493018799981

Conflict of Interest: The authors declare that the research was conducted in the absence of any commercial or financial relationships that could be construed as a potential conflict of interest.

frontiers in Neurology

REVIEW
published: 03 March 2022
doi: 10.3389/fneur.2022.820858

Non-Coding RNA Regulatory Network in Ischemic Stroke

Zongyan Cai[1†], Shuo Li[1†], Tianci Yu[1], Jiahui Deng[1], Xinran Li[1] and Jiaxin Jin[1,2]*

[1] The Second Clinical Medical College, Lanzhou University, Lanzhou, China, [2] Department of Orthopedics, The Second Hospital of Lanzhou University, Lanzhou, China

Stroke is a worldwide public health problem that has caused a substantial economic burden to families and society. Despite recent major advances, there is still a need for more timely, effective diagnosis and treatment methods for acute ischemic stroke. Non-coding RNAs (ncRNAs), which widely exist in the human body, do not encode proteins. Instead, these mediate various cellular processes as functional regulatory molecules from the RNA level. Each ncRNA node in organisms is not isolated but constitutes a complex regulatory network, regulating multiple molecular targets and triggering specific physiological or pathological reactions, leading to different outcomes. Abundant studies have proclaimed the impact of ncRNAs in ischemic stroke, which may enlighten new inspirations for diagnosing and treating ischemic stroke. This paper outlines the current understanding of the ncRNA regulatory network and reviews the recent evidence for the contribution of ncRNAs in the experimental ischemic stroke model.

Keywords: non-coding RNA, ischemic stroke, regulating network, lncRNA, circRNA

OPEN ACCESS

Edited by:
Bing Tian,
Naval Medical University, China

Reviewed by:
Feifei Ma,
Vall d'Hebron Research Institute (VHIR), Spain
Anatol Manaenko,
Innsbruck Medical University, Austria

***Correspondence:**
Jiaxin Jin
king1304288849@163.com

[†] These authors have contributed equally to this work and share first authorship

Specialty section:
This article was submitted to Neurological Biomarkers, a section of the journal Frontiers in Neurology

Received: *23 November 2021*
Accepted: *27 January 2022*
Published: *03 March 2022*

Citation:
Cai Z, Li S, Yu T, Deng J, Li X and Jin J (2022) Non-Coding RNA Regulatory Network in Ischemic Stroke. Front. Neurol. 13:820858. doi: 10.3389/fneur.2022.820858

INTRODUCTION

Stroke is a severe life-threatening acute cerebrovascular disease, which is mainly divided into ischemic stroke (IS) and hemorrhagic stroke. Furthermore, a proportion of hemorrhagic strokes can be secondary to IS. This is called the hemorrhagic transformation of brain infarction and is a complication of IS (1). Ischemic stroke, which accounts for the majority of strokes, is caused by a sharp decrease in cerebral blood flow, which will further cause hypoxia and tissue damage. The subsequent mechanism involves many pathological processes, such as energy failure, acidosis, calcium overload, excitotoxicity, mitochondrial damage, oxidative stress, inflammatory reaction, etc. (2). IS can ultimately cause cell necrosis or apoptosis, leading to a neurological deficit of the corresponding cerebral area and resulting in adverse outcomes. In terms of diagnosis, due to the rapid onset and few precursor symptoms, the diagnosis of IS is often based on the clinical and imaging manifestations after the disease onset. Hence, there is still a lack of sensitive early biomarkers. The key principle of IS treatment is "time is brain," which means that early recanalization of blood supply to the ischemic area is very important to improve the prognosis. At present, the standard treatment of IS is intravenous injection of recombinant tissue plasminogen activator (rtPA) and mechanical treatment to remove the clot to achieve vascular recanalization (3). However, the indications, complications, and possible ischemia-reperfusion injury of thrombolytic therapy limit its universal application in clinics. Therefore, it is essential to explore the molecular mechanisms underlying IS's pathogenesis to improve the diagnosis and treatment of the disease.

Non-coding RNA (ncRNA) widely exists in organisms. It does not encode proteins but serves as functional RNA which mainly regulates post-transcriptional gene expression. In the narrow sense, non-coding RNAs mainly include microRNA (miRNA), circular RNA (circRNA), and long

non-coding RNA (lncRNA). miRNA is a small molecule with a length of about 21 nucleotides. It can cause silencing or degradation of target messenger RNA (mRNA) by binding to the 3′-untranslated region (3′-UTR) of mRNA, regulating gene expression at the post-transcriptional level. miRNAs are expressed in all human tissues and are tissue- and time-specific. The relationship between miRNA and mRNA is not one-to-one. miRNAs can be divided into hundreds of families. Different members of the same miRNA family can target multiple genes and jointly regulate specific physiological processes. The same mRNA molecule can be regulated by multiple upstream miRNAs as well, and it can subsequently participate in multiple downstream pathways. Multiple nodes are interconnected to form a very complex and precise regulation network. Studies have shown that miRNA is involved in regulating almost all cell biological processes, and its expression changes are related to a variety of pathological processes (4). It has become a critical factor in the post-transcriptional regulation of gene expression. lncRNA is a non-coding RNA with a length >200 nucleotides. It possesses a wide range of functions and complex mechanisms to regulate the body's growth and development. For example, post-transcriptional regulation is one of the functions that can be achieved in various ways. lncRNA can directly interact with proteins, bind specific transcription factors as molecular bait to prevent it from binding with DNA, and regulate miRNA expression as a miRNA sponge or enhancer (5). circRNA is a circular single-stranded RNA molecule, which can be covalently closed by reverse splicing of mRNA precursor transcripts in eukaryotic cells. Unlike linear molecules, their 5′ and 3′ ends are directly connected to form a circular closed structure without free ends. At present, it has been found that circRNA can regulate transcription, splicing, and chromatin interactions. Moreover, it could directly bind to proteins and enter the cytoplasm to serve as endogenous competitive RNA (ceRNA) to prevent the binding of miRNAs to target mRNAs (6). The expression level of circRNAs in cells is generally low, and its expression is also tissue-specific. Significant enrichment of circRNAs can be observed in the brain, and they can participate in the disease progression (7). However, hitherto, the research on its function is not sufficient.

Non-coding RNAs (ncRNAs) are abundant in the brain. The level of ncRNAs in the brain can change to varying degrees at the time of the onset of neurovascular disease, forming a characteristic ncRNA expression profile. The change of ncRNA expression level after IS is the response of the body toward injury factors. Its follow-up effect has advantages and disadvantages for the progress and prognosis of the disease. Current studies have identified the role of ncRNAs' imbalance in the onset and development of IS and proposed the potential of ncRNAs to be novel biomarkers applied in clinical diagnosis and treatment. However, due to the complexity and multi-targeting of the ncRNA regulation mechanism, the relationship between different ncRNA nodes and between ncRNAs and downstream molecules remain unexplored. So, there are significant limitations in the clinical transformation of basic research. In this review, we innovatively classified the miRNAs involved in the stroke process into protective and damaging miRNAs according to their post-disease expression levels and relationships with prognosis to analyze their functions and effects in the disease progression or deterioration. Meanwhile, we preliminarily explored the potential molecular mechanism and regulatory network of ncRNAs in IS, forming various lncRNA/circRNA-miRNA-downstream molecular axes and constructing a primary regulatory network of ncRNAs, discussed ncRNA's significance as a biomarker and therapeutic target, and prospected the research prospect of ncRNA.

ALTERATIONS IN NCRNA EXPRESSION FOLLOWING ISCHEMIC STROKE

At present, many ncRNAs with abnormal expression in the occurrence and development of IS have been found, and many studies have explored the regulatory relationship of ncRNAs under the guidance of miRNAs. So far, miRNA has been proved to be involved in neuroprotection and repair, brain injury and cell death, changes in neuronal excitability, glial scar formation, and so forth (8). Therefore, we will describe the ncRNA expression profile of IS based on the expression change of miRNAs.

The expression level of miRNAs changes rapidly after ischemia, presenting diverse expression patterns in different periods. Jeyaseelan et al. analyzed the expression level of miRNAs in brain tissue and blood in 24–48 h after middle cerebral artery occlusion reperfusion and confirmed the abnormal expression of miRNAs of IS and firstly reported the role and molecular mechanism of miRNAs in the middle cerebral artery occlusion-related diseases (9). This part will classify the miRNAs related to the IS into protective and damaging types based on the expression alteration of miRNAs detected after the onset of IS, the effects of alteration, and the impact of the use of antagonists or agonists on the prognosis. The presence of protective miRNAs means that the alteration of miRNAs expression level after IS is advantageous to the prognosis, and reversing its expression has an opposite effect (**Table 1**). On the other hand, damaging miRNAs refer to miRNAs which expression level alteration after IS is unfavorable to prognosis, and reversing its expression level can reduce pathological damage (**Table 2**). In the existing research data, the expression of some miRNAs changes over time, making it difficult to define the benefits or harm of their function. Hence, they are not within the scope of discussion.

Neuronal apoptosis and necrosis are the most severe and common pathological changes of IS. This process is mediated by a variety of mechanisms, including but not limited to excitotoxicity, oxidative stress, inflammation, ion imbalance and secondary edema, transcription factor failure, endoplasmic reticulum stress, mitochondrial dysfunction, and abnormal methylation (56). The neurons' regeneration potentiality of the central nervous system is low (57). Once dead, the neuron will be phagocytosed by microglia and replaced by a glial scar, leaving neurological defects. Yin et al. found that miRNA-497 increased significantly within 24 h after middle cerebral artery embolization and verified it with the glucose oxygen deprivation model (OGD) (16). The results showed that the high expression of miR-497 would aggravate neuronal damage. miR-497 directly

TABLE 1 | Protective microRNA (miRNA) and its upstream and downstream molecules and main functions.

miRNAs	Up/ down	Target molecule/pathway	Affected pathological processes	Influence on pathological processes	Upstream molecules	Up/down
miR-26a (10)	Up	PI3K/AKT MAPK/ERK VEGF	cell proliferation Angiogenesis	Alleviated	-	-
miR-128 (11)	Up	MAPK	-	Alleviated	-	-
miR-146a (12)	Up	IRAK1	oligodendrogenesis	Alleviated	-	-
miR-124 (13)	Up	PI3K/AKT/mTOR caspase-3 Bcl-2 Bcl-xl	Apoptosis Autophagy	Alleviated	-	-
miR-199a (14)	Down	SIRT1 MAPK	cell proliferation	Alleviated	lncRNA-SNHG12	Up
miR-130a-5p (15)	Down	VEGF-A	Angiogenesis	Alleviated	lncRNA-MEG8	Up

binds to the predicted 3′-UTR target sites of bcl-2/-w genes and downregulates its expression level. Knockout of miR-497 can increase the level of Bcl-2/-w protein in the ischemic area, reducing the area of cerebral infarction and improving neurological function. Aquaporin 4 (AQP4), a protein on the cell membrane, can control the water molecules moving in and out of cells and help water molecules pass through the blood-brain barrier (BBB). The high abnormal expression of AQP4 can aggravate the cell damage caused by IS, leading to a poor prognosis. miR-145 has been proved to regulate AQP4 (24, 25). After IS, the expression level of miR-145 decreased, but AQP4 increased, showing a higher level of apoptosis. Accordingly, the use of miR-145 siRNA (small interfering RNA, which can lead to the silencing of target miRNAs complementary to it) reduced the damage and produced a protective effect.

Cysteine proteases (caspases) are a highly conserved family of cysteine proteases. There are many family members. Among them, hitherto 11 family members have been found. The imbalance of caspase activation plays an essential role in inflammation and tumorigenesis. At present, many studies have shown that caspase is abnormally expressed in IS and regulated by multiple miRNAs (58). For example, miR-let-tc-3p, miR-195, miR-24, miR-233, miR-503, etc., have been proved to be related to this process (17, 26–28, 59). miR-130a was upregulated in brain tissue of MCAO rats (60) and X-Linked Inhibitor Of Apoptosis (XIAP) was identified as its target molecule. XIAP is an inhibitor of caspase 3/7/9 and belongs to the inhibitor of the apoptosis protein family. It can be observed that the level of XIAP was upregulated when the expression of miR-130a was inhibited. Correspondingly, apoptosis reduced and angiogenesis increased to improve the neural function of rats. Other studies have shown that the high expression of miR-130a in serum is related to the adverse consequences of acute intracerebral hemorrhage and perihematomal edema, which can increase BBB permeability and aggravate inflammatory reaction during cerebral ischemia (61). Interestingly, the expression of miR-130a in neurons of MCAO rats is low, while upregulating miR-130a can inhibit phosphatase and tensin homolog (PTEN) expression and enhance PI3K/AKT pathway activity from preventing ischemia-reperfusion injury. The phenomenon suggests that the expression of miRNA is different inside and outside the cell. Some miRNAs can be induced to a high expression level and then released out of the cells in certain forms, resulting in the rise of miRNA expression in the tissue (2). The effect of miR-191 is similar to miR-130a (18). It was overexpressed in acute ischemic stroke brain tissue and preferentially expressed in endothelial cells. Its effects lie in anti-angiogenesis and inhibit endothelial cell proliferation and migration. miR-191 can inhibit the expression of Vascular Endothelial Zinc Finger 1 (VEZF1), thus inhibiting angiogenesis and promoting ischemia-reperfusion injury.

The inflammatory response is an adaptive response secondary to infection and tissue injury. Typically, the BBB limits the circulating immune cells and molecules to enter the brain. When the brain injury occurs, the BBB is damaged and demonstrates an increased permeability. Peripheral immune cells can pass through the BBB together with the innate immune cells and inflammatory mediators of brain tissue, which triggers the post-injury inflammatory response. Brain inflammation after IS is characterized by microglial activation and circulating inflammatory cell infiltration (62). Hypoxia due to ischemia is the main pathogenic factor of IS. Hypoxia is accompanied by the rapid increase of inflammatory mediators. The inflammatory response can cause irreversible damage to neurons in the ischemic area and lead to neurological dysfunction. The expression of miR-92b decreases in brain microvascular endothelial cells (BMECs) after IS, which is suppressed by upstream molecular transcription factor Forkhead Box O1 (FOXO1) that is induced to be highly expressed by IS. The promotion of the low expression of miR-92b is associated with lower BBB permeability, which was originally induced to elevate by the OGD. Intracerebroventricular injection of miR-92b adenovirus vector can improve the survival rate of BMECs and inhibit the expression of downstream nicotinamide adenine dinucleotide phosphate (NADPH) oxidase 4 (NOX4) to improve the stability of the BBB (29).

TABLE 2 | Damaging miRNA and its upstream and downstream molecules and main functions.

miRNAs	Up/ down	Target molecule/pathway	Affected pathological processes	Influence on pathological processes	Upstream molecules	Up/ down
miR-497 (16)	Up	Bcl-2/Bcl-w	Apoptosis	Aggravated	-	-
miR-503 (17)	Up	PI3K/Akt/eNOS Bcl-2, caspsase-3	Apoptosis Oxidative stress	Aggravated	-	-
miR-191 (18)	Up	VEZF1	Angiogenesis	Aggravated	-	-
miR-210 (19)	Up	TNF-α/IL-1β/IL-6	Inflammation	Aggravated	-	-
miR-449c-5p (20)	Up	STAT6	Neuroinflammation	Aggravated	lncRNA-SHNG4	Down
miR-186-5p (21)	Up	CTRP3	inflammation of microglia/macrophage Oxidative stress	Aggravated	lncRNA-OIP5-AS1	Down
miR-125b-5p (22)	Up	GDF11	Apoptosis	Aggravated	circRNA-UCK2	Down
miR-582-3p (23)	Up	NOS3	Neuroinflammation Apoptosis oxidative stress	Aggravated	lncRNA-ZFAS1	Down
miR-145 (24, 25)	Down	AQP4	apoptosis	Aggravated	lncRNA-TUG1 lncRNA-MALAT1	Up
miR-195 (26)	Down	Bcl-2/JNK/KLF5	Neuroinflammation Apoptosis	Aggravated	-	-
miR-let-7c-5p (27)	Down	Caspase-3	Apoptosis	Aggravated	-	-
miR-24 (28)	Down	Caspase-3	Apoptosis	Aggravated	-	-
miR-92b (29)	Down	NOX4	BBB damage	Aggravated	FOXO1	Up
miR-375 (30)	Down	PDE4D	Apoptosis neuroinflammation	Aggravated	lncRNA-MALAT1	Up
miR-30a (31)	Down	Beclin1	Autophagy	Aggravated	lncRNA-MALAT1	Up
miR-181b (32)	Down	12/15-LOX/HSPA5/UCHL1	Apoptosis	Aggravated	lncRNA-MEG3	Up
miR-424-5p (33)	Down	Sema3A	apoptosis	Aggravated	lncRNA-MEG3	Up
miR-147 (34)	Down	SOX2/NF-kB/ Wnt/β-catenin	Apoptosis	Aggravated	lncRNA-MEG3	Up
miR-21 (35)	Down	PTEN/PI3K/AKT/PDCD4	Apoptosis	Aggravated	lncRNA-Gas5 lncRNA-MEG3	Up
miR-181c-5p (36–38)	Down	HMGB1/BIM/BMF	Apoptosis	Aggravated	lncRNA-SNHG6 lncRNA-MALAT1 lncRNA-SNHG14	Up
miR-136-5p (39)	Down	ROCK1	Neuroinflammation	Aggravated	lncRNA-SNHG14	Up
miR-30b-5p (40)	Down	Atg5/Beciln1	Autophagy	Aggravated	lncRNA-SNHG14	Up
miR-199b (41)	Down	MAPK/ERK/Egr1/AQP4	macrophages apoptosis cell proliferation	Aggravated	lncRNA-SNHG14	Up
miR-183-5p	Down	FOXO1/PI3K/Akt	apoptosis	Aggravated	lncRNA-SNHG15	Up
miR-19a-3p	Down	PTEN/PI3K/AKT	Apoptosis oxidative stress	Aggravated	lncRNA-H19	Up
miR-153-3p (42)	Down	FOXO3	-	Aggravated	lncRNA-KCNQ1OT1	Up
miR-142 (43)	Down	Beclin1/TIPARP	Autophagy	Aggravated	circRNA-HECTD1	Up
miR-335-3p (44)	Down	TIPARP	apoptosis	Aggravated	circRNA-TLK1	Up
miR-133b (45)	Down	TRAF1 NF-κB	Apoptosis	Aggravated	circRNA-HECTD1	Up
miR-204-5p (46)	Down	HMGB1	Angiogenesis Inflammation	Aggravated	lncRNA-MIAT	Up
miR-130a-3p (47)	Down	DAPK1	Apoptosis	Aggravated	lncRNA-H19	Up
miR-24-3p (48)	Down	Nrp1/NF-κB	Apoptosis	Aggravated	lncRNA-THRIL	Up
miR-214 (49)	Down	PI3K/AKT VEGF	Apoptosis angiogenesis	Aggravated	lncRNA-NEAT1	Up
miR-26a-5p (50)	Down	DAPK1	apoptosis	Aggravated	lncRNA-AK038897	Up
miR-335 (51)	Down	ROCK1/AKT/GSK-3β	apoptosis	Aggravated	lncRNA-Gas5	Up
miR-455-5p (52)	Down	PTEN	Apoptosis oxidative stress	Aggravated	lncRNA-Gas5	Up
miR-19a (53)	Down	Id2	apoptosis	Aggravated	lncRNA-H19	Up

(Continued)

TABLE 2 | Continued

miRNAs	Up/ down	Target molecule/pathway	Affected pathological processes	Influence on pathological processes	Upstream molecules	Up/ down
miR-200a-3p (54)	Down	NLPR3	Neuroinflammation	Aggravated	lncRNA-TUG1	Up
miR-874-3p (55)	Down	IL1B	Apoptosis neuroinflammation	Aggravated	lncRNA-MIAT	Up

Some miRNA expressions can be induced by hypoxia. These miRNAs, such as miR-199a, miR-107, miR-210, and so on, are called hypoxia-induced miRNAs (hypoximiRs) (63, 64). As master hypoxamiR, miR-210 plays an essential role in fine-tuning the adaptive response of cells toward hypoxia and can be strongly induced by hypoxia (65). Many studies have proved that miR-210 is induced to be highly expressed in MCAO, and the application of miR-210-locking nucleotide (LNA, a kind of miRNA inhibitor) can reduce TNF-α level immediately after IS and completely block IL-1β, and the expression of pro-inflammatory factor IL-6 is blocked 12 h after IS, but the expression of anti-inflammatory factor such as TGF-β and IL-10 is insusceptible. At the same time, it can also inhibit the expression of chemokines CCL2 and CCL3. These two chemokines are excreted by activated microglia and injured endothelial cells after IS to recruit inflammatory cells to pass through the BBB and trigger ischemic inflammation, suggesting that miR-210-LNA plays a neuroprotective role by antagonizing pro-inflammatory factors and inhibiting inflammatory infiltration (19). However, some studies have found that exosomes containing miR-210 can induce angiogenesis after injection into the cerebral ventricle of MCAO mice (66). It can directly target cytokine Suppressor Of Cytokine Signaling 1 (SOCS1) and increase the expression of STAT3 and VEGF-C to promote angiogenesis around ischemic foci and the aggregation of neural precursor cells (NPCs), which is good for IS prognosis (67).

NCRNA REGULATORY NETWORK IN ISCHEMIC STROKE

It has been previously described that both lncRNAs and circRNAs act as miRNA sponges. Therefore, a large number of lncRNAs and circRNAs together with their regulated miRNAs and miRNAs targeting molecules constitute the lncRNA/circRNA-miRNA-mRNA axis, and interconnection of each axis ultimately forms a complicated ncRNA regulatory network of IS (**Figure 1**).

Long Non-Coding RNAs and MicroRNAs

A large number of studies have demonstrated that the pathology of the central nervous system is concerned with the abnormal expression of lncRNA. A variety of lncRNAs have been found to be involved in the onset and development of IS for several years. In addition, lncRNA can also be utilized as a potential new biomarker for disease diagnosis, treatment, and prognosis.

In recent years, lncRNA-MALAT1 has been observed to express abnormally in IS and participate in some pathological processes. The expression of MALAT1, the function of which refers to inflammatory and apoptosis pathways, was significantly upregulated in patients' microglia and neurons. miR-375 is one of the target molecules of MALAT1. The decrease causes high expression of Phosphodiesterase 4D (PDE4D) through the miR-375/PDE4D axis, promoting inflammation and apoptosis (30). MALAT1 can also target miR-181c-5p and upregulate the expression of High Mobility Group Box 1 (HMGB1), a pro-inflammatory factor (36), aggravating the degree of inflammation. Jin et al. found that the expression levels of MALAT1 and AQP4 were consistent (68). Relevant studies have shown that MALAT1 can increase the level of AQP4 and cause a larger infarct area by inhibiting miR-145 (24). Autophagy is a necessary evolutionarily conserved process of substance turnover within eukaryotic cells, also reflected in neural injury. In IS, autophagy can be activated under excitotoxic conditions, and autophagy activated by neurons under cerebral ischemia is adverse (69). MALAT1 can upregulate the expression of Beclin1 by inhibiting miR-30a (31). High levels of Beclin-1 will increase autophagy and deteriorate neuronal damage.

To sum up, the high expression of lncRNA-MALAT1 is related to more severe inflammation and autophagy, and it also spawns larger infarct size, which is unfavorable to the prognosis of IS. However, some studies have found that high expression of MALAT1 can improve the prognosis in IS. Zhang et al. found that the decrease of MALAT1 expression would increase ischemia-induced endothelial cell loss, apoptosis, and inflammation (70). Silencing MALAT1 provoked the expression of pro-apoptotic factor Bcl-2 interacting mediator of cell death (BIM), pro-inflammatory factor Monocyte Chemoattractant Protein-1 (MCP-1), IL-6, and E-selectin, significantly increasing caspase-3 activity and inducing BMECs' death.

As with MALAT1, the expression level of lncRNA-MEG3 also increased after IS. It can directly target miR-181b (32). The inhibitory effect of miR-181b on 12/15-lipoxygenase (LOX) was relieved, which exacerbated hypoxia-induced neuronal apoptosis. MEG3 can also target miR-424-5p, resulting in increased expression of downstream semaphorin 3A (Sema3A) (33), thereby activating the MAPK signal pathway associated with Sema3A and hampering the axon growth. Similarly, other studies have proved that Sema3A inhibitors can activate the Akt pathway and phosphorylate Glycogen synthase kinase-3β (GSK-3β). The phosphorylation of GSK-3β suppresses astrocyte activation and promotes axon regeneration after ischemia (71). GSK-3 is a highly conserved serine-threonine kinase that was

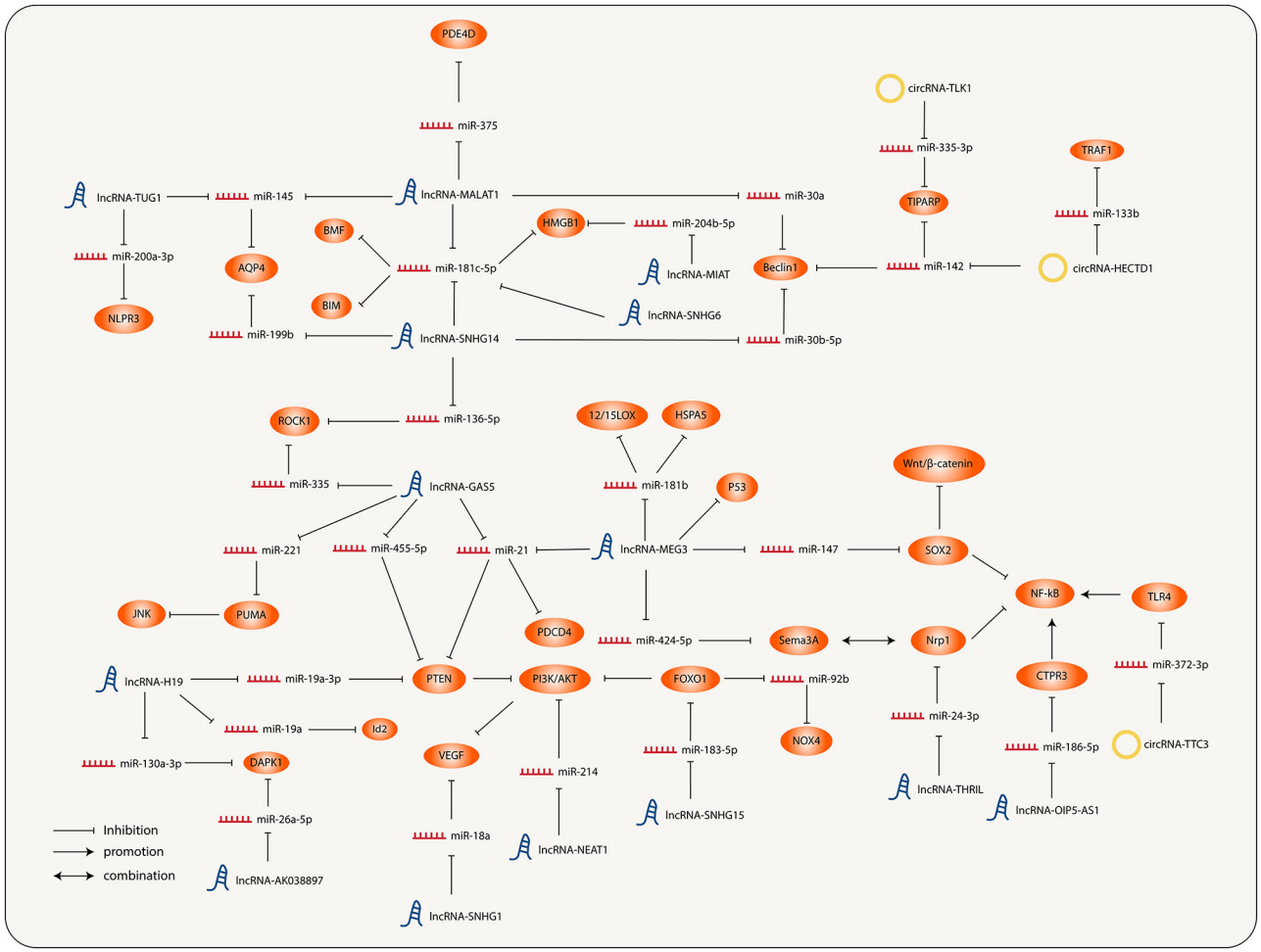

FIGURE 1 | Interconnection and regulation of the different molecular nodes involved in the progression of ischemic stroke (IS).

initially identified as phosphorylation and inactivator of glycogen synthase. It has two isoforms, α and β. GSK-3β is confirmed to participate in energy metabolism, inflammation, endoplasmic reticulum stress, mitochondrial dysfunction, apoptosis, etc., making it possible to become a new therapeutic target of IS (72). At the same time, Sema3A can also competitively bind Neuropilin 1 (NRP-1) and antagonize VEGF to prevent angiogenesis. In addition, MEG3 could target miR-21, increasing the expression of Programmed Cell Death 4 (PDCD4), a pro-apoptotic protein, and hindering the neuron-protective effect of miR-21. Inhibiting MEG3's expression level can boost nerve growth and reduce nerve injury led by ischemia-reperfusion (73). Furthermore, MEG3 was found to act on the Notch pathway and Wnt/β-catenin pathway, causing inhibition of angiogenesis and simultaneously increasing neuronal apoptosis (74). This finding was supplemented by Han et al. who argued that miR-147 and downstream molecule SRY-Box Transcription Factor 2 (SOX2) were involved in the effect of MEG3 on the regulation of Wnt/β-Catenin pathway and NF- κB pathway (34), and that the high level of SOX2 will activate the above pathways and cause more severe hypoxia injury.

Studies have confirmed that lncRNA-GAS5 negatively regulates multiple miRNAs. High expression of GAS5 in the brain after IS can block the cell cycle and increase apoptosis (75). Firstly, the GAS5 expression level was observed to be consistent with PTEN expression. Relevant studies pointed out that the effect could be mediated by miR-21 and miR-455-5p (35, 52). High levels of PTEN act as negative regulators to dephosphorylate AKT and reduce activation of which, inhibiting PI3K/AKT pathway, further affects neuronal survival, leading to cell apoptosis, oxidative damage, and mitochondrial damage, accelerating the progression of ischemic brain injury. In addition, Zhou et al. predicted and verified the accurate binding site between GAS5 and miR-221 (76). The rise of GAS5 level leads to the upregulation of p53 upregulated modulator of apoptosis (PUMA), further resulting in dephosphorylation and inactivation of histone H2AX through the JNK pathway and causing more severe cell apoptosis. On the contrary, the expression of miR-221 increased after the knockout of GAS5.

Consequently, the expression of PUMA decreased, and the apoptosis decreased correspondingly.

Small nucleolar RNA host genes (SNHGs) are a group of lncRNAs that have been proved to be oncogenes of many cancers. Recent studies have found that abnormal expression of SNHG1/4/6/12/14/15 exists in the process of IS. SNHG1 expressed significantly high in the MCAO mouse model and OGD-cultured microvascular endothelial cells, which function as a protective role. Knockdown of SNHG1 was correlated with higher caspase-3 activity and more severe apoptosis (77). Moreover, SNHG1 also acts as a ceRNA for miR-18a, resulting in elevated downstream HIF-1α expression and pro-proliferation of vascular endothelial cells *via* the HIF-1α/VEGF axis. It was also shown that SNHG4 has a regulatory effect on the severity of microglia inflammation (20) by comparing the content of lncRNA in serum and cerebrospinal fluid samples of MCAO model mice, patients with acute cerebral infarction, and ordinary people. Zhang et al. found that the expression of SNHG4 in microglia of patients and MCAO mice was significantly lower than the normal level. When increasing the expression level of SNHG4 and STAT6, the target molecule of miR-449c-5p was upregulated, which could inhibit the inflammatory response after cerebral ischemia-reperfusion injury.

The SNHG6 expression level was significantly upregulated after IS (37). It can act as the ceRNA of miR-181c-5p, relieving the transcriptional inhibition of miRNA on the downstream target gene BIM and causing more severe apoptosis. Knockout of SNHG6 can improve cell survival, suppress caspase-3 activity, and alleviate nerve injury. SNHG12 level was also notably raised after ischemia or reperfusion injury treatment (14, 78). Overexpressed SNHG12 targets miR-199a, promotes the expression of NAD-Dependent Protein Deacetylase Sirtuin-1(SIRT1), and further activates AMPK pathway and boosts cell proliferation, while inhibition of SNHG12 can reverse this effect. ncRNA-SNHG14 is a lncRNA that is widely upregulated in a variety of diseases (38). At present, many pathways that involve SNHG14 in IS have been found. The expression of SNHG14 increases in the brain of ischemia-reperfusion mice, which combines with miR-136-5p and stimulates the expression of downstream molecule ROCK1 and promotes inflammatory response (39). miR-181c-5p is also one of the downstream molecules of SNHG14 (38). BCL2 modifying factor (BMF) is a member of the Bcl-2 homologous domain 3 (BH3) protein family. As a pro-apoptotic protein, it was found to be negatively regulated by miR-181c-5p. SNHG14 positively regulates BMF expression and aggravates neuronal injury. The knockdown of SNHG14 can significantly promote OGD-induced neuronal proliferation, inhibit apoptosis, and play an anti-inflammatory role. Previously, miR-181c-5p has also been proved to be regulated by lncRNA MALAT1 (46), which suggests that miRNA itself is regulated in many aspects.

It is worth noting that some studies have pointed out that the expression of miR-181c-5p is upregulated in myocardial cells after ischemia-reperfusion and can aggravate the level of apoptosis and inflammation (79). This is opposite to the effect of miR-181c-5p in the brain, suggesting that the regulatory effects of ncRNAs vary in different cell types. Sun et al. argued that SNHG14 can target miR-30b-5p to promote the expression of Autophagy Related 5 (ATG5) and Beclin1 to activate autophagy and enhance brain inflammation level (40). They also found that transcription factor SP1 directly interacted with the promoter of SNHG14 and thus upregulated the expression of SNHG14. Meanwhile, SP1 itself was also regulated by P38/MAPK pathway, indicating that lncRNA itself was also regulated by upstream pathways and molecules. Otherwise, studies have demonstrated that it is through miR-199b/AQP4 axis that SNHG14 can promote inflammation and oxidative stress (41, 80). SNHG15 is highly expressed in MCAO rats according to the research of Wen et al., which can act as the ceRNA of miR-183-5p, upregulating the expression of FOXO1 and cyclin-dependent kinase inhibitor 1B ($P27^{Kip1}$) and resulting in cell cycle block and apoptosis.

The expression of lncRNA-H19 was upregulated in MCAO mice (81). It mediates the expression of PTEN through the downstream molecule miR-19a-3p. The upregulation of the PTEN level causes the inactivation of the PI3K/AKT pathway and aggravates oxidative stress and apoptosis. Knockout of H19 can alleviate the damage. The expression of lncRNA-KCNQ1OT1 was significantly increased in neurons of MCAO mice. Studies showed that its role in promoting neuronal injury was achieved by regulating the expression of FOXO3 as a ceRNA of miR-153-3p (42). OPA-interacting protein 5 antisense RNA1 (OIP5-AS1) is a recently discovered long non-coding RNA (21). It was downregulated in microglia of ischemic brain tissue, resulting in low expression of C1q/TNF-Related Protein 3 (CTRP3) by targeting miR-186-5p, thereby activating Nrf2 and NF-κB pathway, significantly promoting inflammation and oxidative stress response, and showing greater infarct size. At the same time, it has been proved that there is cross-talk between Nrf2 and NF-κB pathways. The interaction between Nrf2 and NF-κB pathways can make cells regulate their response more finely to stressors and improve their adaptability to environmental changes. Upregulation of OIP5-AS1 can increase the expression of CTPR3 and reduce the damage response induced by microglia and macrophages.

It should be noted that lncRNA acts in a wide range of ways *in vivo*. In addition to inhibiting the expression of miRNA through the molecular sponge, it can also directly interact with proteins and participate in pathophysiological processes. As Yan et al. (56) found the $DBD^{270-281}$ region of P53 is responsible for the direct association between MEG3 and P53. MEG3 can positively regulate P53 and activate its transcriptional activity, mediating neuronal death after IS.

Circular RNA and MicroRNAs

Many studies have shown that the imbalance of circRNA expression is one of the characteristics of IS (82). However, the research on the role of circRNA in IS is not sufficient. Dong et al. compared the circRNA expression profiles of monocytes from ordinary people and patients with IS (83). Bioinformatics analysis showed that abnormally expressed circRNA was involved

in multiple pathophysiological processes, such as inflammation and immune processes. Therefore, it is of positive significance to study the role of circRNA in IS (**Figure 2**).

Han et al. found that the expression of circRNA-HECTD1 was significantly increased in ischemic brain tissue of MCAO mice and plasma of patients with acute ischemic stroke (AIS) (43). It can be used as ceRNA of miR-142 to inhibit the translation inhibition of TCDD inducible poly (ADP ribose) polymerase (TIPARP) by miR-142. The highly expressed TIPARP can increase the activation of astrocytes and promote inflammation and apoptosis. Knockout of HECTD1 can significantly reduce infarct size and regulate astrocyte autophagy and activation. Similarly, the expression of circRNA-TLK1 increased in ischemic brain tissue (44). By inhibiting miR-335-3p, it leads to the decrease of TIPARP expression, which aggravates the neuronal injury. Neural stem cells (NSCs) are a kind of cells with self-renewal ability and multi-differentiation potential. After brain injury, endogenous static NSCs are activated. These then participate in the process of brain repair and play an essential role in IS (84). Yang et al. explored the effects of circRNA-TTC3 on ischemia-reperfusion injury and NSCs (85). TTC3 expression was significantly increased in hypoxic astrocytes, and its target was miR-372-3p. TTC3 depletion could lead to high expression of Toll-like receptor 4 (TLR4), inhibiting the activation of the OGD-induced apoptosis pathway and promoting the proliferation of NSCs. Zhang et al. found that highly expressed circRNA-camk4 after IS can significantly increase the cell mortality after ischemia-reperfusion in MCAO rats (82). In addition, they predicted and confirmed that miR-27a-3p, miR-324-3p, and miR-212-3p were the target molecules of camk4. The regulation of miRNA by camk4 involves the glutamatergic synaptic pathway, MAPK pathway, and apoptosis pathway.

The expression level of circRNA-UCK2 significantly decreased in the brain tissue of the ischemia-reperfusion mouse model (22). In contrast, increasing its expression can significantly reduce the size of the infarct area and improve the neurological deficit. It can inhibit the expression of miR-125b-5p and increase the expression of growth differentiation factor-11 (GDF11) and bind TGF-β Receptor to activate the downstream Smad3 signaling pathway, resulting in anti-apoptotic and anti-inflammatory effects. GDF11 is a member of the activin subfamily and TGF-β superfamily that binds two types of TGF- β receptors (TβRI and TβRII) to form an active signal transduction complex. TβRII activates TβRI kinase activity by phosphorylating TβRI before transmitting signals intracellularly *via* phosphorylating transcription factor Smad by TβRI. Smads mainly accumulate in the nucleus and regulate the expression of target genes by combining DNA and other transcription mechanisms. circRNA can also participate in the regulation of autophagy (86). circRNA-SHOC2 is highly expressed in ischemic-preconditioned astrocyte-derived exosomes (IPAS-EXOs). SHOC2 can target miR-7670-3p, increase the expression of downstream molecule SIRT1, and inhibit neuronal apoptosis. At the same time, SHOC2 can also reduce neuronal damage by regulating autophagy.

Circular RNA (circRNA) can directly function with targeted protein molecules. Yang et al. screened circRNA-SCMH1 from the plasma of patients with IS and found that its expression level significantly decreased after IS (87). After treating brain tissue with SCMH1 analogs, the functional recovery after IS was improved while enhancing neuronal plasticity and inhibiting glial cell activation and peripheral immune cell infiltration. The downstream target search results show that it could directly bind to the transcription factor Methyl-CpG Binding Protein 2 (MeCP2) and attenuate the transcriptional repression of MeCP2 on the target genes Myelin Associated Oligodendrocyte BasicProtein (Mobp), Insulin-Like Growth Factor Binding Protein 3 (Igfbp3), FXYD Domain Containing Ion Transport Regulator 1 (Fxyd1), and Proline Dehydrogenase 1(Prodh), all of which play an important role in maintaining brain function.

CLINICAL SIGNIFICANCE

A large number of studies have confirmed that ncRNAs can be utilized as new biomarkers and therapeutic targets. More and more pieces of evidence accumulated over the years show that miRNA can exist in tissues and various biological fluids, such as blood, urine, saliva, and so on (88). miRNA circulates in a highly stable acellular form in peripheral blood and can be detected in plasma or serum (64). Many studies have shown that nerve cells can somehow secrete miRNA after IS, providing a theoretical basis for ncRNA expression profile as a biomarker in IS. Zuo et al. identified the differentially expressed circRNA in IS patients' blood (89) before isolating platelets, lymphocytes, and granulocytes from the blood to identify the source of circRNA. It was identified that the expression of circFUNDC1, circPDS5B, and circCDC14A in plasma was higher than in the standard control group and positively correlated with infarct volume. PDS5B and CDC14A may come from lymphocytes and granulocytes. When three circRNAs were utilized in combination to detect IS, they showed high sensitivity and specificity. However, the limitation is that there is no sufficient research evidence based on lncRNA and circRNA targeted therapy after IS, but these ncRNAs involved in the pathological process of IS have the potential to become therapeutic targets.

As mentioned earlier, miRNA expression is disordered after IS, and abnormal expression of some miRNAs is related to poor prognosis. To improve the prognosis of patients, ncRNA antagonists or analogs can be applied to reverse the expression of ncRNAs at the pathological level to play a protective role. Liu et al. injected a miR-21/miR-24 inhibitor into the cerebral ventricle of MCAO rats and found that it can significantly reduce the apoptosis of hippocampal and cortical neurons (90). Early intraventricular injection of miR-124 has been shown to significantly improve neuronal survival and microglia M2-like polarization (91) and plays a neuroprotective and anti-inflammatory role. After the NSCs transduced by circRNA-HIPK2-siRNA were injected into the lateral ventricle of MCAO mice, NSCs were observed to migrate and differentiate into the ischemic hemisphere, representing a neuroprotective effect which not only increased the plasticity of neurons after ischemia but also significantly reduced functional defects (92). The application of extracellular vesicles is helpful to deliver ncRNA-related preparations into the brain, which is one of the

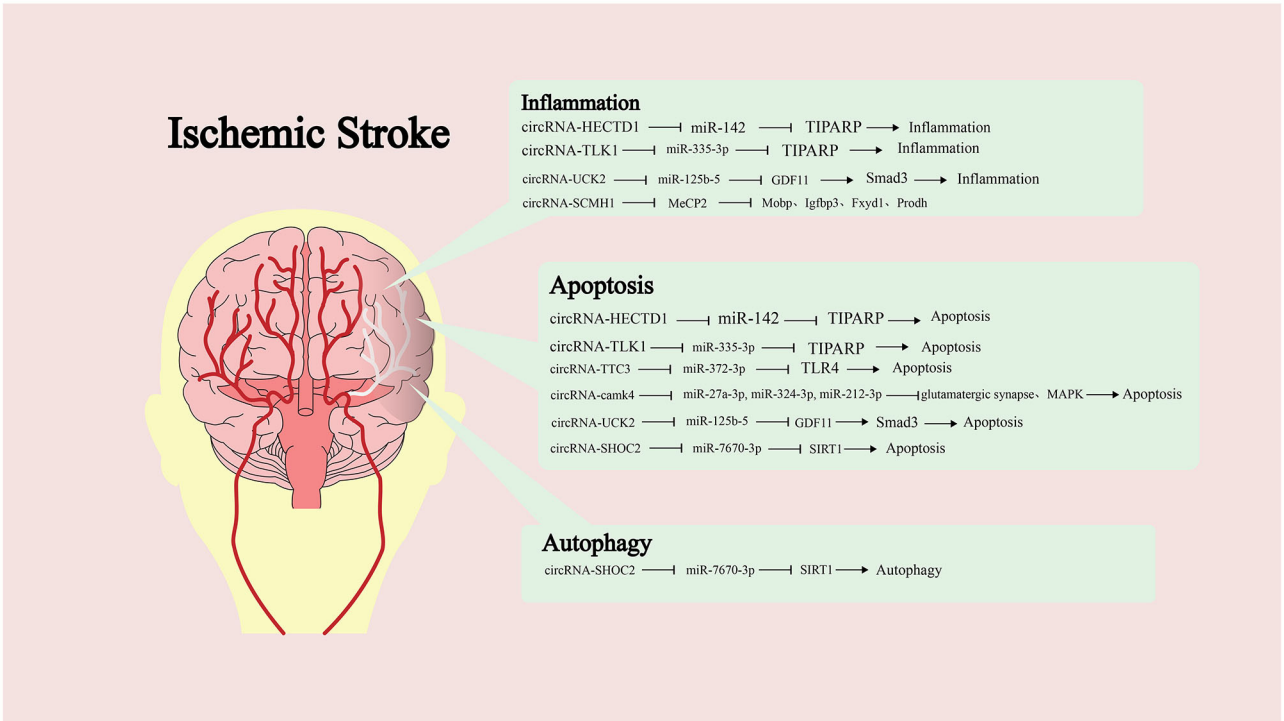

FIGURE 2 | Targeting of downstream microRNAs (miRNAs) by different circular RNAs (circRNAs) and the molecules or pathways are ultimately affected, along with the impact on pathological processes.

research hotspots of targeted therapy. In animal experiments, intraventricular injection of bone marrow mesenchymal cell exosomes overexpressing miR-223-3p can reduce the size of the infarct area caused by MCAO (93). The exosomes loaded with miR-210 could target the necrotic area after intravenous injection. After 2 weeks, the expressions of VEGF and CD34 were significantly upregulated, and the survival rate of animals was also improved. Yang et al. used engineered rabies virus glycoprotein-circSCMH1-extracellular vesicles to transport circRNA-SCMH1 into the brain (87) and found that the functional recovery after IS was promoted significantly. After transnasal administration of RVG29-modified microRNA-loaded nanoparticles (94), it was seen that cerebral ischemia-reperfusion injury was reduced. RVG29 is derived from the rabies virus glycoprotein and has shown efficient brain-targeted drug delivery and a good safety profile during its use. Transnasal delivery of targeted drugs is expected to be an effective treatment for neurological disorders.

Some drugs have also been found to cause changes in the expression of ncRNAs during the application with potential therapeutic effect on IS. Dexmedetomidine (DEX) is a good anesthetic sedative. At present, some studies have found that the application of DEX seems to be beneficial to the prognosis of IS (95). After DEX application, the low expression of miR-381 was reversed. Accordingly, the expression of miR-381 downstream molecules IRF4 and IL-9 decreased, showing smaller infarct foci. Sevoflurane (SEVO) is considered a neuroprotective agent for cerebral ischemia-reperfusion injury (96). After treatment with SEVO, the expression of miR-181a decreased in MCAO rats, increasing the expression of XIAP in cortical neurons and decreasing the release of Lactate Dehydrogenase (LDH), thereby showing better cell survival. Cao et al. showed that the expression of lncRNA-MALAT1 and downstream molecule HMGB1 decreased after preventive treatment with berberine (BBR) in MCAO mice (36), suggesting that BBR may be involved in the anti-inflammatory effect after inducing IS. Notably, these drugs are not directly targeting agents of ncRNAs. Relevant studies can only hint that the drug effect is related to the ncRNA regulatory network, but this may provide information for studying drug mechanisms and the development of targeted drugs.

CHALLENGES AND PERSPECTIVES

Even from the incomplete understanding of the role of ncRNAs in IS, ncRNAs are widely involved in the gene regulatory network, particularly in regulating the critical process of disease onset and development. However, most studies start with a single molecule to explore its upstream or downstream molecules to construct a single pathway that is scattered. Future studies should focus more on the relationship between ncRNAs to form a complete ncRNA regulatory network. Research shows that ncRNA after IS can be detected in serum and possess disease specificity, conveying the

potential to be used as early biomarkers of IS. However, whether ncRNAs are abnormally expressed before the onset of IS remains to be researched to help therapists identify and intervene early to prevent serious consequences. A comprehensive understanding of the interaction between ncRNA nodes, such as feedback loop and antagonism, is vital for applying the research results to clinical treatment. This is because single-dose targeted therapy can sometimes prove to be insufficient and combination therapy requires consideration of the interactions between drug pathways of action (97). Hence, the multi-temporal changes of molecular and cellular state changes after IS, targeting, and safety of ncRNAs agents are issues that need to be addressed by researchers.

More work is still demanded to describe ncRNA regulatory networks to help understand the onset of IS and provide information for selecting better therapeutic targets. The application of bioinformatics has dramatically promoted the interpretation of the interaction between ncRNA nodes and other signal pathway members, presenting great benefits to the study of complex ncRNA regulatory networks. With the help of computers, unlocking this complex network may just be around the corner. It is inevitable for ncRNA to become a hotspot with good prospects in basic and clinical research because of its significant role. The identification and development of the ncRNA regulatory network may change our understanding and treatment of diseases.

AUTHOR CONTRIBUTIONS

ZC and SL contributed to the investigation and wrote the original draft of the manuscript. TY and JD contributed to the revised version of our manuscript. XL contributed to the methodology. JJ contributed to the conceptualization. All authors read and approved the final manuscript.

FUNDING

This work was supported by the Cuiying Scientific and Technological Innovation Program of Lanzhou University Second Hospital (CY2018-QN17), Fundamental Research Funds for the Central Universities (lzujbky-2019-sp04), Gansu Province Youth Science and Technology Fund Project (20JR5RA318), the National Natural Science Foundation of China Regional Foundation Project (82060400), and the Cuiying Scientific Training Program for Undergraduates of Lanzhou University Second Hospital (CYXZ2021-01).

REFERENCES

1. Paciaroni M, Agnelli G, Corea F, Ageno W, Alberti A, Lanari A, et al. Early hemorrhagic transformation of brain infarction: rate, predictive factors, and influence on clinical outcome: results of a prospective multicenter study. *Stroke.* (2008) 39:2249-56. doi: 10.1161/STROKEAHA.107.510321
2. Zheng T, Shi Y, Zhang J, Peng J, Zhang X, Chen K, et al. MiR-130a exerts neuroprotective effects against ischemic stroke through PTEN/PI3K/AKT pathway. *Biomed Pharmacother.* (2019) 117:109117. doi: 10.1016/j.biopha.2019.109117
3. Powers WJ, Rabinstein AA, Ackerson T, Adeoye OM, Bambakidis NC, Becker K, et al. Guidelines for the early management of patients with acute ischemic stroke: 2019 update to the 2018 guidelines for the early management of acute ischemic stroke: a guideline for healthcare professionals from the American Heart Association/American Stroke Association. *Stroke.* (2019) 50:e344-418. doi: 10.1161/STR.0000000000000211
4. Wienholds E, Plasterk RHA. MicroRNA function in animal development. *FEBS Lett.* (2005) 579:5911-22. doi: 10.1016/j.febslet.2005.07.070
5. Ferrè F, Colantoni A, Helmer-Citterich M. Revealing protein-lncRNA interaction. *Brief Bioinform.* (2016) 17:106-16. doi: 10.1093/bib/bbv031
6. Chen L-L. The expanding regulatory mechanisms and cellular functions of circular RNAs. *Nat Rev Mol Cell Biol.* (2020) 21:475-90. doi: 10.1038/s41580-020-0243-y
7. Chen Y, Li C, Tan C, Liu X. Circular RNAs: a new frontier in the study of human diseases. *J Med Genet.* (2016) 53:359-65. doi: 10.1136/jmedgenet-2016-103758
8. Gubern C, Camós S, Ballesteros I, Rodríguez R, Romera VG, Cañadas R, et al. miRNA expression is modulated over time after focal ischaemia: up-regulation of miR-347 promotes neuronal apoptosis. *FEBS J.* (2013) 280:6233-46. doi: 10.1111/febs.12546
9. Jeyaseelan K, Lim KY, Armugam A. MicroRNA expression in the blood and brain of rats subjected to transient focal ischemia by middle cerebral artery occlusion. *Stroke.* (2008) 39:959-66. doi: 10.1161/STROKEAHA.107.500736
10. Liang Z, Chi YJ, Lin GQ, Luo SH, Chen YK. MiRNA-26a promotes angiogenesis in a rat model of cerebral infarction *via* PI3K/AKT and MAPK/ERK pathway. *Eur Rev Med Pharmacol Sci.* (2018) 22:3485-92. doi: 10.26355/eurrev_201806_15175
11. Liu P, Han Z, Ma Q, Liu T, Wang R, Tao Z, et al. Upregulation of MicroRNA-128 in the peripheral blood of acute ischemic stroke patients is correlated with stroke severity partially through inhibition of neuronal cell cycle reentry. *Cell Transpl.* (2019) 28:839-50. doi: 10.1177/0963689719846848
12. Liu XS, Chopp M, Pan WL, Wang XL, Fan BY, Zhang Y, et al. MicroRNA-146a promotes oligodendrogenesis in stroke. *Mol Neurobiol.* (2017) 54:227-37. doi: 10.1007/s12035-015-9655-7
13. Sun Y, Gui H, Li Q, Luo Z-M, Zheng M-J, Duan J-L, et al. MicroRNA-124 protects neurons against apoptosis in cerebral ischemic stroke. *CNS Neurosci Ther.* (2013) 19:813-9. doi: 10.1111/cns.12142
14. Yin W-L, Yin W-G, Huang B-S, Wu L-X. LncRNA SNHG12 inhibits miR-199a to upregulate SIRT1 to attenuate cerebral ischemia/reperfusion injury through activating AMPK signaling pathway. *Neurosci Lett.* (2019) 690:188-95. doi: 10.1016/j.neulet.2018.08.026
15. Sui S, Sun L, Zhang W, Li J, Han J, Zheng J, et al. LncRNA MEG8 attenuates cerebral ischemia after ischemic stroke through targeting miR-130a-5p/VEGFA signaling. *Cell Mol Neurobiol.* (2021) 41:1311-24. doi: 10.1007/s10571-020-00904-4
16. Yin K-J, Deng Z, Huang H, Hamblin M, Xie C, Zhang J, et al. miR-497 regulates neuronal death in mouse brain after transient focal cerebral ischemia. *Neurobiol Dis.* (2010) 38:17-26. doi: 10.1016/j.nbd.2009.12.021
17. Zhang H, Pan Q, Xie Z, Chen Y, Wang J, Bihl J, et al. Implication of MicroRNA503 in brain endothelial cell function and ischemic stroke. *Transl Stroke Res.* (2020) 11:1148-64. doi: 10.1007/s12975-020-00794-0
18. Du K, Zhao C, Wang L, Wang Y, Zhang K-Z, Shen X-Y, et al. MiR-191 inhibit angiogenesis after acute ischemic stroke targeting VEZF1. *Aging.* (2019) 11:2762-86. doi: 10.18632/aging.101948
19. Huang L, Ma Q, Li Y, Li B, Zhang L. Inhibition of microRNA-210 suppresses pro-inflammatory response and reduces acute brain injury of ischemic stroke in mice. *Exp Neurol.* (2018) 300:41-50. doi: 10.1016/j.expneurol.2017.10.024
20. Zhang S, Sun W-C, Liang Z-d, Yin X-R, Ji Z-R, Chen X-H, et al. LncRNA SNHG4 attenuates inflammatory responses by sponging miR-449c-5p and up-regulating STAT6 in microglial during cerebral ischemia-reperfusion injury. *Drug Design Dev Ther.* (2020) 14:3683-95. doi: 10.2147/DDDT.S245445

21. Chen Y, Liu W, Chen M, Sun Q, Chen H, Li Y. Up-regulating lncRNA OIP5-AS1 protects neuron injury against cerebral hypoxia-ischemia induced inflammation and oxidative stress in microglia/macrophage through activating CTRP3 via sponging miR-186-5p. *Int Immunopharmacol.* (2021) 92:107339. doi: 10.1016/j.intimp.2020.107339
22. Chen W, Wang H, Feng J, Chen L. Overexpression of circRNA circUCK2 attenuates cell apoptosis in cerebral ischemia-reperfusion injury *via* miR-125b-5p/GDF11 signaling. *Mol Ther Nucleic Acids.* (2020) 22:673-83. doi: 10.1016/j.omtn.2020.09.032
23. Zhang Y, Zhang Y. lncRNA ZFAS1 improves neuronal injury and inhibits inflammation, oxidative stress, and apoptosis by sponging miR-582 and upregulating NOS3 expression in cerebral ischemia/reperfusion injury. *Inflammation.* (2020) 43:1337-50. doi: 10.1007/s10753-020-01212-1
24. Wang H, Zheng X, Jin J, Zheng L, Guan T, Huo Y, et al. LncRNA MALAT1 silencing protects against cerebral ischemia-reperfusion injury through miR-145 to regulate AQP4. *J Biomed Sci.* (2020) 27:40. doi: 10.1186/s12929-020-00635-0
25. Shan W, Chen W, Zhao X, Pei A, Chen M, Yu Y, et al. Long noncoding RNA TUG1 contributes to cerebral ischaemia/reperfusion injury by sponging mir-145 to up-regulate AQP4 expression. *J Cell Mol Med.* (2020) 24:250-9. doi: 10.1111/jcmm.14712
26. Chang L, Zhang W, Shi S, Peng Y, Wang D, Zhang L, et al. microRNA-195 attenuates neuronal apoptosis in rats with ischemic stroke through inhibiting KLF5-mediated activation of the JNK signaling pathway. *Mol Med.* (2020) 26:31. doi: 10.1186/s10020-020-00150-w
27. Ni J, Wang X, Chen S, Liu H, Wang Y, Xu X, et al. MicroRNA let-7c-5p protects against cerebral ischemia injury via mechanisms involving the inhibition of microglia activation. *Brain Behav Immunity.* (2015) 49:75-85. doi: 10.1016/j.bbi.2015.04.014
28. Jiang Q, Shen D, Wang Y, Huang D, Wang Z. miR-24 reduces serum lipid levels and inhibits brain tissue cells apoptosis of rats with cerebral infarction. Turkish Neurosurg. (2020) 30:483-90.
29. Shen J, Li G, Zhu Y, Xu Q, Zhou H, Xu K, et al. Foxo1-induced miR-92b down-regulation promotes blood-brain barrier damage after ischaemic stroke by targeting NOX4. *J Cell Mol Med.* (2021) 25:5269-82. doi: 10.1111/jcmm.16537
30. Zhang G, Wang Q, Su D, Xie Y. Long non-coding RNAMALAT1 knockdown alleviates cerebral ischemia/reperfusion injury of rats through regulating the miR-375/PDE4D axis. *Front Neurol.* (2020) 11:578765. doi: 10.3389/fneur.2020.578765
31. Guo D, Ma J, Yan L, Li T, Li Z, Han X, et al. Down-regulation of lncrna MALAT1 attenuates neuronal cell death through suppressing beclin1-dependent autophagy by regulating Mir-30a in cerebral ischemic stroke. *Cell Physiol Biochem.* (2017) 43:182-94. doi: 10.1159/000480337
32. Liu X, Hou L, Huang W, Gao Y, Lv X, Tang J. The mechanism of long non-coding RNA MEG3 for neurons apoptosis caused by hypoxia: mediated by miR-181b-12/15-LOX signaling pathway. *Front Cell Neurosci.* (2016) 10:201. doi: 10.3389/fncel.2016.00201
33. Xiang Y, Zhang Y, Xia Y, Zhao H, Liu A, Chen Y. LncRNA MEG3 targeting miR-424-5p *via* MAPK signaling pathway mediates neuronal apoptosis in ischemic stroke. *Aging.* (2020) 12:3156-74. doi: 10.18632/aging.102790
34. Han L, Dong Z, Liu N, Xie F, Wang N. Maternally expressed gene 3 (MEG3) enhances PC12 cell hypoxia injury by targeting MiR-147. *Cell Physiol Biochem.* (2017) 43:2457-69. doi: 10.1159/000484452
35. Li J, Lv H, Che Y-Q. Long non-coding RNA Gas5 potentiates the effects of microRNA-21 downregulation in response to ischaemic brain injury. *Neuroscience.* (2020) 437:87-97. doi: 10.1016/j.neuroscience.2020.01.014
36. Cao D-W, Liu M-M, Duan R, Tao Y-F, Zhou J-S, Fang W-R, et al. The lncRNA Malat1 functions as a ceRNA to contribute to berberine-mediated inhibition of HMGB1 by sponging miR-181c-5p in poststroke inflammation. *Acta pharmacologica Sinica.* (2020) 41:22-33. doi: 10.1038/s41401-019-0284-y
37. Zhang Xa, Liu Z, Shu Q, Yuan S, Xing Z, Song J. LncRNA SNHG6 functions as a ceRNA to regulate neuronal cell apoptosis by modulating miR-181c-5p/BIM signalling in ischaemic stroke. *J Cell Mol Med.* (2019) 23:6120-30. doi: 10.1111/jcmm.14480
38. Bu X, Zhao Y, Chang M, Ge X. Downregulation of lncRNA SNHG14 alleviates neurons injury by modulating the miR-181c-5p/BMF axis in ischemic stroke. *Brain Res Bull.* (2021) 174:379-88. doi: 10.1016/j.brainresbull.2021.06.026
39. Zhong Y, Yu C, Qin W. LncRNA SNHG14 promotes inflammatory response induced by cerebral ischemia/reperfusion injury through regulating miR-136-5p /ROCK1. *Cancer Gene Ther.* (2019) 26:234-47. doi: 10.1038/s41417-018-0067-5
40. Sun B, Ou H, Ren F, Guan Y, Huan Y, Cai H. Propofol protects against cerebral ischemia/reperfusion injury by down-regulating long noncoding RNA SNHG14. *ACS Chemical Neurosci.* (2021) 12:3002-14. doi: 10.1021/acschemneuro.1c00059
41. Zhang G, Li T, Chang X, Xing J. Long noncoding RNA SNHG14 promotes ischemic brain injury *via* regulating miR-199b/AQP4 Axis. *Neurochem Res.* (2021) 46:1280-90. doi: 10.1007/s11064-021-03265-6
42. Wang H-J, Tang X-L, Huang G, Li Y-B, Pan R-H, Zhan J, et al. Long non-coding KCNQ1OT1 promotes oxygen-glucose-deprivation/reoxygenation-induced neurons injury through regulating MIR-153-3p/FOXO3 axis. *J Stroke Cerebrovasc Dis.* (2020) 29:105126. doi: 10.1016/j.jstrokecerebrovasdis.2020.105126
43. Han B, Zhang Y, Zhang Y, Bai Y, Chen X, Huang R, et al. Novel insight into circular RNA HECTD1 in astrocyte activation *via* autophagy by targeting MIR142-TIPARP: implications for cerebral ischemic stroke. *Autophagy.* (2018) 14:1164-84. doi: 10.1080/15548627.2018.1458173
44. Wu F, Han B, Wu S, Yang L, Leng S, Li M, et al. Circular RNA TLK1 aggravates neuronal injury and neurological deficits after ischemic stroke *via* miR-335-3p/TIPARP. *J Neurosci.* (2019) 39:7369-93. doi: 10.1523/JNEUROSCI.0299-19.2019
45. Dai Q, Ma Y, Xu Z, Zhang L, Yang H, Liu Q, et al. Downregulation of circular RNA HECTD1 induces neuroprotection against ischemic stroke through the microRNA-133b/TRAF3 pathway. *Life Sci.* (2021) 264:118626. doi: 10.1016/j.lfs.2020.118626
46. Deng W, Fan C, Shen R, Wu Y, Du R, Teng J. Long noncoding MIAT acting as a ceRNA to sponge microRNA-204-5p to participate in cerebral microvascular endothelial cell injury after cerebral ischemia through regulating HMGB1. *J Cell Physiol.* (2020) 235:4571-86. doi: 10.1002/jcp.29334
47. Feng M, Zhu X, Zhuo C. H19/miR-130a-3p/DAPK1 axis regulates the pathophysiology of neonatal hypoxic-ischemia encephalopathy. *Neurosci Res.* (2021) 163:52-62. doi: 10.1016/j.neures.2020.03.005
48. Kuai F, Zhou L, Zhou J, Sun X, Dong W. Long non-coding RNA THRIL inhibits miRNA-24-3p to upregulate neuropilin-1 to aggravate cerebral ischemia-reperfusion injury through regulating the nuclear factor κB p65 signaling. *Aging.* (2021) 13:9071-84. doi: 10.18632/aging.202762
49. Shen S, Ma L, Shao F, Jin L, Bian Z. Long non-coding RNA (lncRNA) NEAT1 aggravates cerebral ischemia-reperfusion injury by suppressing the inhibitory effect of miR-214 on PTEN. *Med Sci Monitor Int Med J Exp Clin Res.* (2020) 26:e924781. doi: 10.12659/MSM.924781
50. Wei R, Zhang L, Hu W, Wu J, Zhang W. Long non-coding RNA AK038897 aggravates cerebral ischemia/reperfusion injury via acting as a ceRNA for miR-26a-5p to target DAPK1. *Exp Neurol.* (2019) 314:100-10. doi: 10.1016/j.expneurol.2019.01.009
51. Wu N, Zhang X, Bao Y, Yu H, Jia D, Ma C. Down-regulation of GAS5 ameliorates myocardial ischaemia/reperfusion injury via the miR-335/ROCK1/AKT/GSK-3β axis. *J Cell Mol Med.* (2019) 23:8420-31. doi: 10.1111/jcmm.14724
52. Wu R, Yun Q, Zhang J, Bao J. Long non-coding RNA GAS5 retards neural functional recovery in cerebral ischemic stroke through modulation of the microRNA-455-5p/PTEN axis. *Brain Res Bull.* (2021) 167:80-8. doi: 10.1016/j.brainresbull.2020.12.002
53. Xiao Z, Qiu Y, Lin Y, Medina R, Zhuang S, Rosenblum JS, et al. Blocking lncRNA H19-miR-19a-Id2 axis attenuates hypoxia/ischemia induced neuronal injury. *Aging.* (2019) 11:3585-600. doi: 10.18632/aging.101999
54. Yin M, Chen W-P, Yin X-P, Tu J-L, Hu N, Li Z-Y. LncRNA TUG1 demethylated by TET2 promotes NLRP3 expression, contributes to cerebral ischemia/reperfusion inflammatory injury. *ASN Neuro.* (2021) 13:17590914211003247. doi: 10.1177/17590914211003247
55. Zhang S, Zhang Y, Wang N, Wang Y, Nie H, Zhang Y, et al. Long non-coding RNA MIAT impairs neurological function in ischemic stroke *via* up-regulating microRNA-874-3p-targeted IL1B. *Brain Res Bull.* (2021) 175:81-9. doi: 10.1016/j.brainresbull.2021.07.005

56. Yan H, Yuan J, Gao L, Rao J, Hu J. Long noncoding RNA MEG3 activation of p53 mediates ischemic neuronal death in stroke. *Neuroscience.* (2016) 337:191-9. doi: 10.1016/j.neuroscience.2016.09.017
57. Mahar M, Cavalli V. Intrinsic mechanisms of neuronal axon regeneration. *Nat Rev Neurosci.* (2018) 19:323-37. doi: 10.1038/s41583-018-0001-8
58. van Opdenbosch N, Lamkanfi M. Caspases in cell death, inflammation, and disease. *Immunity.* (2019) 50:1352-64. doi: 10.1016/j.immuni.2019.05.020
59. Sha R, Zhang B, Han X, Peng J, Zheng C, Zhang F, et al. Electroacupuncture alleviates ischemic brain injury by inhibiting the miR-223/NLRP3 pathway. *Med Sci Monitor Int Med J Exp Clin Res.* (2019) 25:4723-33. doi: 10.12659/MSM.917213
60. Deng W, Fan C, Zhao Y, Mao Y, Li J, Zhang Y, et al. MicroRNA-130a regulates neurological deficit and angiogenesis in rats with ischaemic stroke by targeting XIAP. *J Cell Mol Med.* (2020) 24:10987-1000. doi: 10.1111/jcmm.15732
61. Wang M-D, Wang Y, Xia Y-P, Dai J-W, Gao L, Wang S-Q, et al. High serum MiR-130a levels are associated with severe perihematomal edema and predict adverse outcome in acute ICH. *Mol Neurobiol.* (2016) 53:1310-21. doi: 10.1007/s12035-015-9099-0
62. Tobin MK, Bonds JA, Minshall RD, Pelligrino DA, Testai FD, Lazarov O. Neurogenesis and inflammation after ischemic stroke: what is known and where we go from here. *J Cereb Blood Flow Metab.* (2014) 34:1573-84. doi: 10.1038/jcbfm.2014.130
63. Thomas B, Roger R, Nicolas P, Bernard M. Chapter three - impact of MicroRNAs in the cellular response to hypoxia. In: Lorenzo G, Ilio V, editors. *MiRNAs in Differentiation and Development.* Academic Press (2017). p. 91-158.
64. Greco S, Gaetano C, Martelli F. HypoxamiR regulation and function in ischemic cardiovascular diseases. *Antiox Redox Signaling.* (2014) 21:1202-19. doi: 10.1089/ars.2013.5403
65. Kulshreshtha R, Ferracin M, Wojcik SE, Garzon R, Alder H, Agosto-Perez FJ, et al. A microRNA signature of hypoxia. *Mol Cell Biol.* (2007) 27:1859-67. doi: 10.1128/MCB.01395-06
66. Zhang H, Wu J, Wu J, Fan Q, Zhou J, Wu J, et al. Exosome-mediated targeted delivery of miR-210 for angiogenic therapy after cerebral ischemia in mice. *J Nanobiotechnol.* (2019) 17:29. doi: 10.1186/s12951-019-0461-7
67. Meng Z-Y, Kang H-L, Duan W, Zheng J, Li Q-N, Zhou Z-J. MicroRNA-210 promotes accumulation of neural precursor cells around ischemic foci after cerebral ischemia by regulating the SOCS1-STAT3-VEGF-C pathway. *J Am Heart Assoc.* (2018) 7:e005052. doi: 10.1161/JAHA.116.005052
68. Jin J, Wang H, Zheng X, Xie S, Zheng L, Zhan R. Inhibition of LncRNA MALAT1 attenuates cerebral ischemic reperfusion injury *via* regulating AQP4 expression. *Eur Neurol.* (2020) 83:581-90. doi: 10.1159/000511238
69. Ginet V, Spiehlmann A, Rummel C, Rudinskiy N, Grishchuk Y, Luthi-Carter R, et al. Involvement of autophagy in hypoxic-excitotoxic neuronal death. *Autophagy.* (2014) 10:846-60. doi: 10.4161/auto.28264
70. Zhang X, Tang X, Liu K, Hamblin MH, Yin K-J. Long noncoding RNA Malat1 regulates cerebrovascular pathologies in ischemic stroke. *J Neurosci.* (2017) 37:1797-806. doi: 10.1523/JNEUROSCI.3389-16.2017
71. Hira K, Ueno Y, Tanaka R, Miyamoto N, Yamashiro K, Inaba T, et al. Astrocyte-derived exosomes treated with a semaphorin 3A inhibitor enhance stroke recovery *via* prostaglandin D(2) synthase. *Stroke.* (2018) 49:2483-94. doi: 10.1161/STROKEAHA.118.021272
72. Rana AK, Singh D. Targeting glycogen synthase kinase-3 for oxidative stress and neuroinflammation: Opportunities, challenges and future directions for cerebral stroke management. *Neuropharmacology.* (2018) 139:124-36. doi: 10.1016/j.neuropharm.2018.07.006
73. Yan H, Rao J, Yuan J, Gao L, Huang W, Zhao L, et al. Long non-coding RNA MEG3 functions as a competing endogenous RNA to regulate ischemic neuronal death by targeting miR-21/PDCD4 signaling pathway. *Cell Death Dis.* (2017) 8:3211. doi: 10.1038/s41419-017-0047-y
74. You D, You H. Repression of long non-coding RNA MEG3 restores nerve growth and alleviates neurological impairment after cerebral ischemia-reperfusion injury in a rat model. *Biomed Pharmacother.* (2019) 111:1447-57. doi: 10.1016/j.biopha.2018.12.067
75. Zhang L, Wang H. Long non-coding RNA in CNS injuries: a new target for therapeutic intervention. *Mol Ther Nucleic Acids.* (2019) 17:754-66. doi: 10.1016/j.omtn.2019.07.013
76. Zhou X-B, Lai L-F, Xie G-B, Ding C, Xu X, Wang Y. LncRNAGAS5 sponges miRNA-221 to promote neurons apoptosis by up-regulated PUMA under hypoxia condition. *Neurol Res.* (2020) 42:8-16. doi: 10.1080/01616412.2019.1672382
77. Zhang L, Luo X, Chen F, Yuan W, Xiao X, Zhang X, et al. LncRNA SNHG1 regulates cerebrovascular pathologies as a competing endogenous RNA through HIF-1α/VEGF signaling in ischemic stroke. *J Cell Biochem.* (2018) 119:5460-72. doi: 10.1002/jcb.26705
78. Li Y, Guo S, Liu W, Jin T, Li X, He X, et al. Silencing of SNHG12 enhanced the effectiveness of MSCs in alleviating ischemia/reperfusion injuries *via* the PI3K/AKT/mTOR signaling pathway. *Front Neurosci.* (2019) 13:645. doi: 10.3389/fnins.2019.00645
79. Wang S, Ge L, Zhang D, Wang L, Liu H, Ye X, et al. MiR-181c-5p promotes inflammatory response during hypoxia/reoxygenation injury by downregulating protein tyrosine phosphatase nonreceptor type 4 in H9C2 cardiomyocytes. *Oxidative Med Cell Longev.* (2020) 2020:7913418. doi: 10.1155/2020/7913418
80. Wen Y, Zhang X, Liu X, Huo Y, Gao Y, Yang Y. Suppression of lncRNA SNHG15 protects against cerebral ischemia-reperfusion injury by targeting miR-183-5p/FOXO1 axis. *Am J Transl Res.* (2020) 12:6250-63.
81. Gao N, Tang H, Gao L, Tu G-L, Luo H, Xia Y. LncRNA H19 aggravates cerebral ischemia/reperfusion injury by functioning as a ceRNA for miR-19a-3p to Target PTEN. *Neuroscience.* (2020) 437:117-29. doi: 10.1016/j.neuroscience.2020.04.020
82. Zhang Z-H, Wang Y-R, Li F, Liu X-L, Zhang H, Zhu Z-Z, et al. Circ-camk4 involved in cerebral ischemia/reperfusion induced neuronal injury. *Sci Rep.* (2020) 10:7012. doi: 10.1038/s41598-020-63686-1
83. Dong Z, Deng L, Peng Q, Pan J, Wang Y. CircRNA expression profiles and function prediction in peripheral blood mononuclear cells of patients with acute ischemic stroke. *J Cell Physiol.* (2020) 235:2609-18. doi: 10.1002/jcp.29165
84. Huang L, Zhang L. Neural stem cell therapies and hypoxic-ischemic brain injury. *Prog Neurobiol.* (2019) 173:1-17. doi: 10.1016/j.pneurobio.2018.05.004
85. Yang B, Zang Le, Cui J, Wei L. Circular RNA TTC3 regulates cerebral ischemia-reperfusion injury and neural stem cells by miR-372-3p/TLR4 axis in cerebral infarction. *Stem Cell Res Ther.* (2021) 12:125. doi: 10.1186/s13287-021-02187-y
86. Chen W, Wang H, Zhu Z, Feng J, Chen L. Exosome-shuttled circSHOC2 from IPASs regulates neuronal autophagy and ameliorates ischemic brain injury *via* the miR-7670-3p/SIRT1 axis. *Mol Ther Nucleic Acids.* (2020) 22:657-72. doi: 10.1016/j.omtn.2020.09.027
87. Yang L, Han B, Zhang Z, Wang S, Bai Y, Zhang Y, et al. Extracellular vesicle-mediated delivery of circular RNA SCMH1 promotes functional recovery in rodent and nonhuman primate ischemic stroke models. *Circulation.* (2020) 142:556-74. doi: 10.1161/CIRCULATIONAHA.120.045765
88. Tijsen AJ, Pinto YM, Creemers EE. Circulating microRNAs as diagnostic biomarkers for cardiovascular diseases. *Am J Physiol Heart Circ Physiol.* (2012) 303:H1085-95. doi: 10.1152/ajpheart.00191.2012
89. Zuo L, Zhang L, Zu J, Wang Z, Han B, Chen B, et al. Circulating circular RNAs as biomarkers for the diagnosis and prediction of outcomes in acute ischemic stroke. *Stroke.* (2020) 51:319-23. doi: 10.1161/STROKEAHA.119.027348
90. Liu W, Chen X, Zhang Y. Effects of microRNA-21 and microRNA-24 inhibitors on neuronal apoptosis in ischemic stroke. *Am J Transl Res.* (2016) 8:3179-87.
91. Hamzei Taj S, Kho W, Riou A, Wiedermann D, Hoehn M. MiRNA-124 induces neuroprotection and functional improvement after focal cerebral ischemia. *Biomaterials.* (2016) 91:151-65. doi: 10.1016/j.biomaterials.2016.03.025
92. Wang G, Han B, Shen L, Wu S, Yang L, Liao J, et al. Silencing of circular RNA HIPK2 in neural stem cells enhances functional recovery following ischaemic stroke. *EBioMedicine.* (2020) 52:102660. doi: 10.1016/j.ebiom.2020.102660
93. Zhao Y, Gan Y, Xu G, Hua K, Liu D. Exosomes from MSCs overexpressing microRNA-223-3p attenuate cerebral ischemia through inhibiting microglial M1 polarization mediated inflammation. *Life Sci.* (2020) 260:118403. doi: 10.1016/j.lfs.2020.118403
94. Hao R, Sun B, Yang L, Ma C, Li S. RVG29-modified microRNA-loaded nanoparticles improve ischemic brain injury by nasal delivery. *Drug Delivery.* (2020) 27:772-81. doi: 10.1080/10717544.2020.1760960

95. Fang H, Li H-F, Yan J-Y, Yang M, Zhang J-P. Dexmedetomidine-up-regulated microRNA-381 exerts anti-inflammatory effects in rats with cerebral ischaemic injury *via* the transcriptional factor IRF4. *J Cell Mol Med.* (2021) 25:2098-109. doi: 10.1111/jcmm.16153
96. Zhang Y, Shan Z, Zhao Y, Ai Y. Sevoflurane prevents miR-181a-induced cerebral ischemia/reperfusion injury. *Chem Biol Interact.* (2019) 308:332-8. doi: 10.1016/j.cbi.2019.06.008
97. Anastasiadou E, Jacob LS, Slack FJ. Non-coding RNA networks in cancer. *Nat Rev Cancer.* (2018) 18:5-18. doi: 10.1038/nrc.2017.99

Conflict of Interest: The authors declare that the research was conducted in the absence of any commercial or financial relationships that could be construed as a potential conflict of interest.

Publisher's Note: All claims expressed in this article are solely those of the authors and do not necessarily represent those of their affiliated organizations, or those of the publisher, the editors and the reviewers. Any product that may be evaluated in this article, or claim that may be made by its manufacturer, is not guaranteed or endorsed by the publisher.

frontiers | Frontiers in Neurology

BRIEF RESEARCH REPORT
published: 25 April 2022
doi: 10.3389/fneur.2022.863450

The Relationship Between Aortic Arch Calcification and Recurrent Stroke in Patients With Embolic Stroke of Undetermined Source—A Case-Control Study

*Xiaofeng Cai, Yu Geng and Sheng Zhang**

Center for Rehabilitation Medicine, Department of Neurology, Zhejiang Provincial People's Hospital, Affiliated People's Hospital, Hangzhou Medical College, Hangzhou, China

OPEN ACCESS

Edited by:
Bing Tian,
Naval Medical University, China

Reviewed by:
Ching-Hui Sia,
National University of Singapore, Singapore
Benjamin Y. Q. Tan,
National University Hospital, Singapore

****Correspondence:***
Sheng Zhang
zhangsheng@hmc.edu.cn

Specialty section:
This article was submitted to Stroke, a section of the journal Frontiers in Neurology

Received: *27 January 2022*
Accepted: *16 March 2022*
Published: *25 April 2022*

Citation:
Cai X, Geng Y and Zhang S (2022) The Relationship Between Aortic Arch Calcification and Recurrent Stroke in Patients With Embolic Stroke of Undetermined Source—A Case-Control Study. Front. Neurol. 13:863450. doi: 10.3389/fneur.2022.863450

Background: Aortic arch calcification (AoAC) is associated with plaque development and cardiovascular events. We aimed to estimate the predictive value of AoAC for stroke recurrence in patients with embolic stroke of undetermined source (ESUS).

Methods: Consecutive patients with ESUS who were admitted to our center between October 2019 and October 2020 and who had a 1-year follow-up of stroke recurrence were retrospectively reviewed. According to our AoAC grading scale (AGS), AoAC was classified into four grades based on chest computed tomography (CT) findings: no visible calcification (grade 0), spotty calcification (grade 1), lamellar calcification (grade 2), and circular calcification (grade 3).

Results: Of the 158 patients with ESUS (age, 62.1 ± 14.5 years; 120 men) enrolled, 24 (15.2%) had recurrent stroke within a 1-year follow-up. The Cox regression analysis showed that stroke history [hazard ratio (*HR*), 4.625; 95% confidence interval (*CI*), 1.828–11.700, $p = 0.001$] and AoAC (*HR*, 2.672; 95% *CI*, 1.129–6.319; $p = 0.025$) predicted recurrent stroke. AGS grade 1 was associated with a significantly higher risk of stroke recurrence than AGS grade 0 (*HR*, 5.033; 95% *CI*, 1.858–13.635, $p = 0.001$) and AGS grade 2 plus 3 (*HR*, 3.388; 95% *CI*, 1.124–10.206, $p = 0.030$). In patients with AoAC, receiver operating characteristic (ROC) analysis showed that AGS had a good value in predicting stroke recurrence in patients with ESUS, with an area under curve (AUC) of 0.735 (95% *CI* = 0.601–0.869, $p = 0.005$).

Conclusions: Aortic arch calcification, especially spotty calcification, had a good predictive value for stroke recurrence in patients with ESUS.

Keywords: aortic arch calcification, embolic stroke of undetermined source (ESUS), recurrent stroke, chest CT scan, AoAC grading scale

INTRODUCTION

Embolic stroke of undetermined source (ESUS) is a new clinical entity with specific diagnostic criteria, such as (1) non-lacunar stroke on neuroradiological imaging, (2) no arterial stenosis >50% or occlusion in a corresponding large artery, (3) lack of a major cardioembolic source, and (4) lack of other determined stroke causes (1). Two large randomized controlled trial studies on secondary prevention in ESUS, the NAVIGATE–ESUS trial on rivaroxaban and dabigatran, showed that the secondary prevention effect of anticoagulants was not superior to aspirin and was associated with a higher risk of bleeding in the investigated population (2, 3). These findings indicate that the etiology of ESUS is not necessarily due to an undetected cardiogenic stroke. Recent studies have shown that the stroke mechanism underlying ESUS includes low-embolic risk cardiac diseases, paradoxical brain embolisms, aortic lesions, and mild-to-moderate carotid arterial disease (4–7). Therefore, the mechanism of recurrent stroke in ESUS and its secondary prevention strategies remains controversial.

Arterial calcification has long been considered a complication of advanced atherosclerosis (8, 9). Aortic arch calcification (AoAC) is a predictor of systemic atherosclerosis, which has been shown to be associated with the occurrence of cardiovascular and cerebrovascular events, such as ischemic cerebral infarction (9, 10). In recent years, studies have reported that complex AoACs are common in patients with ESUS (10). This finding suggests that AoAC may be involved in the occurrence and recurrence of ESUS.

Previous studies based on X-rays, such as the aortic arch calcification (AAC) grading scale (8, 11), calcification in the aortic arch, age, and multiple infarction (CAM) score (11), showed that the severity of AoAC was related to the recurrence of vascular events in patients with ESUS. However, these methods have limitations in clinical applications. First, a precise evaluation of the extent of calcification seems impossible on radiography, and the relationship between the amount of calcium involvement and plaque vulnerability cannot be evaluated using X-rays (12). Second, the degree of calcification assessed by X-ray may not be consistent with the true pathological stages of calcification, and the relationship between each degree of AoAC and stroke recurrence on ESUS is not yet clear. Recently, a new pathological classification system was developed to assess the calcium burden from a healthy artery with no calcification to the advanced calcific deposits spread throughout the tunica media (13). To investigate the relationship of AoAC and its severity with stoke recurrence of ESUS, based on this pathologic classification system, we generated an AoAC grading scale (AGS) on chest computed tomography (CT), and we tested the predictive value of AGS for stroke recurrence in patients with ESUS.

METHODS

Ethics Statement

The local ethics committee approved the study protocol. All clinical investigations were conducted in accordance with the principles of the Declaration of Helsinki.

Patients

Between October 2019 and October 2020, we retrospectively reviewed consecutive patients who had been admitted for acute ischemic stroke within 7 days at Zhejiang Provincial People's Hospital, China. Patients were enrolled if (1) they met the ESUS diagnostic criteria adopted the criteria proposed by the ESUS International Organization (14) and (2) completed a 1-year follow-up of stroke recurrence. Patients were excluded if (1) clinical or imaging data were incomplete and (2) imaging data were not available due to motion artifacts.

Imaging Protocol

Baseline non-contrast CT was performed using a 64-slice CT scanner (15). During hospitalization, the patients were required to undergo cranial imaging within 3–5 days after admission. All cranial MRIs in our study were performed using a 3.0T MR scanner (16). The sequences of cranial MRIs were as follows: T1WI [repetition time (TR)/echo time (TE): 160/3.05 ms], T2WI (TR/TE: 6,000/100 ms), T2-fluid-attenuated inversion recovery (FLAIR) (TR/TE: 9,000/94.0 ms), and DWI (TR/TE: 6,400/86.0 ms, *b* value 0, and 1,000 s/mm^2). In all sequences, slice thickness and slice spacing were set as 5 and 1.5 mm, respectively. New ischemic brain lesions were defined as hyperintense lesions on postoperative brain DWI.

Aortic Arch Calcification Grading Scale (AGS)

Based on the pathological staging of calcification (13, 17), spotty calcification was defined as calcification with a diameter of $\leq$ 1 mm in one or more areas of the aortic intima. As CT scans are very sensitive to calcification, we applied this standard to CT and defined calcification with a diameter of no more than 1 mm as grade 1 on the AGS. Pathologically, calcification with a diameter of 1–3 mm was defined as fragment calcification, and calcification >3 mm was defined as sheet-like calcification. Therefore, on CT, we defined this type of calcification with a diameter >1 mm as grade 2 AGS. Finally, an entirely calcified artery or circular-like calcification was ascribed to an AGS grade 3. Examples of each AGS grade are shown in **Figure 1**.

Since this AGS is a grading of calcification severity, when multiple degrees of calcification occurred in one patient, the grade of the most serious calcification was considered as the group of that patient. For example, when patient A had both spotty and lamellar calcifications simultaneously, patient A should be ascribed to a group of lamellar calcifications.

Two raters (XFC and SZ), who jointly evaluated the AGS, were blinded to the imaging and clinical data of patients. A single trained observer (XFC) measured the AGS in all patients two times, at an interval of 1 month apart. The other observer (SZ) independently performed the same evaluation.

Other Imaging Analysis

The Distribution of Infarction

New ischemic brain lesions were defined as hyperintense lesions on postoperative brain diffusion-weighted imaging. According to

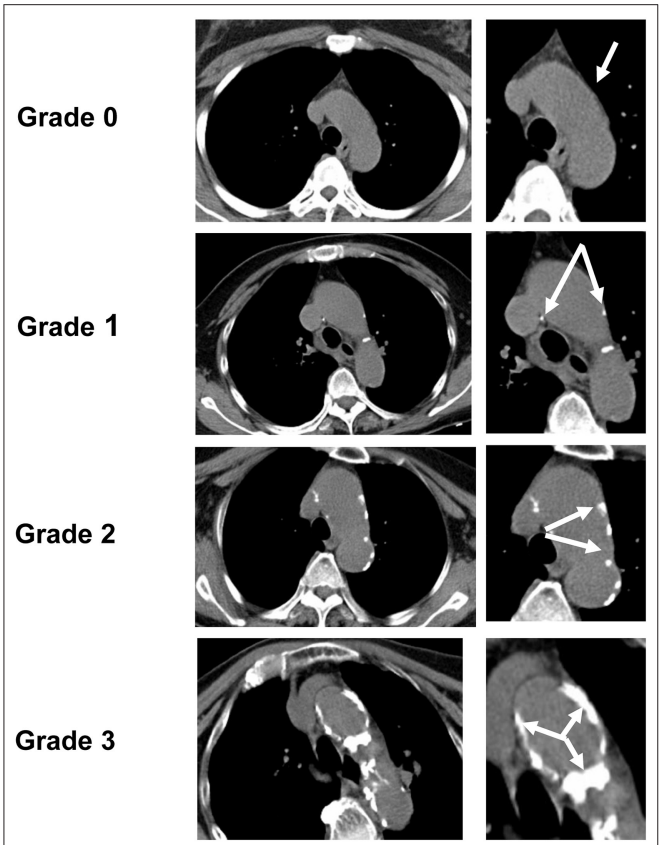

FIGURE 1 | Aortic arch calcification grading scale (AGS). According to AGS, the degree of aortic arch calcification (AoAC) detected by chest CT was divided into four grades (the white arrow points to the calcification area): grade 0, no visible calcification; grade 1, spotty calcification of the aortic arch ≤ 1 mm in diameter; grade 2, lamellar calcification > 1 mm in diameter; grade 3, circular calcification.

the distribution of infarctions, patients were divided into single territory and multiple territory infarctions.

Carotid Artery Ultrasound

Ipsilateral non-stenosing carotid plaque was defined using the site investigators' reports of cervical large-artery atherosclerotic plaques and infarct location. According to ultrasound echo, the characteristics of carotid plaques were defined as hypodense, hyperdense, or iso-dense.

Left Atrial Diameter (LAD) and Left Ventricular Ejection Fraction (LVEF)

All patients underwent transthoracic echocardiography (TTE) examination during hospitalization, and data, such as left atrial diameter (LAD), LAD/height (LAD/H), LAD/body surface area (LAD/BSA), and LVEF were recorded. LVEF estimation was based on TTE performed within 7 days after stroke. The LVEF was calculated using the Simpson biplane method (18).

Outcome

The primary outcome was recurrent strokes. If any of the following items of the Sacco criteria (19) were satisfied, stroke recurrence could be diagnosed.

All patients were evaluated through outpatient or telephone follow-up. The clinician (XF.C., 8-year experience of in stroke management) was responsible for determining recurrent stroke.

Statistical Analysis

Statistical analyses were performed using SPSS version 24.0. Kappa statistics were used to test inter- and intra-observer reliability for evaluating AGS. Excellent inter- and intra-observer reliabilities were observed in assessing the AGS score ($\kappa = 0.908$ and 0.867, respectively). Demographic and baseline characteristics and imaging features were reported using descriptive statistics. Numerical and nominal variables are expressed as mean standard deviation (SD) and frequency percentage, respectively. A *t*-test was used to compare the normally distributed data between groups, and the rank-sum test was used to compare the non-normally distributed data. Counting data are expressed as frequency and percentage, and chi-square analysis was used for comparison between groups. Multivariable logistic regression analysis was performed to identify risk factors for recurrent stroke in patients with ESUS. The Cox proportional hazards model was used to explore factors associated with recurrent stroke events, such as clinical characteristics and AoAC. After univariate analysis of all clinically relevant covariates, those with $p < 0.05$ were included in the multivariable Cox model. The Kaplan–Meier method and log-rank test were used to estimate the cumulative event rates of recurrent vascular events. Statistical significance was set at $p < 0.05$.

RESULTS

Clinical Characteristics of Patients With ESUS

In total, 158 patients were enrolled in this study. The median age of the patients was 62 years (interquartile range [IQR]: 53–73 years) and 75.9% were men. Of the 158 patients, 98.1% (155/158) were treated with statins, 96.8% (153/158) with antiplatelet therapy, and 7.8% (12/153) with dual antiplatelet therapy. Of the 153 patients who received antiplatelet therapy, 7.8% (12/153) were switched to anticoagulant therapy because of deep venous thrombosis ($n = 4$), pulmonary embolism ($n = 1$), vertebrobasilar dolichoectasia ($n = 1$), and atrial fibrillation ($n = 6$). Atrial fibrillation was found in four patients during follow-up and in two patients during hospitalization for recurrent stroke. Univariate Cox regression analysis showed that statin, antiplatelet, and anticoagulant therapies were not associated with stroke recurrence (all $p > 0.05$). This result has been added in **Table 1**. A flowchart of patient screening is shown in **Figure 1**. During the 1-year follow-up, 24 patients (15.2%) experienced recurrent stroke.

Univariate comparisons of baseline clinical characteristics are shown in **Supplementary Table 1**. Compared with patients

TABLE 1 | Univariate Cox regression analysis of baseline characteristics associated with stroke recurrence.

Variables	HR	95% CI	*P* value
Age, years	1.009	0.979–1.040	0.567
Male	1.88	0.823–4.295	0.134
Risk factors			
Hypertension	0.616	0.23–1.650	0.335
Diabetes mellitus	1.482	0.588–3.733	0.404
Dyslipidaemia	1.030	0.385–2.759	0.953
Stroke history	4.739	1.877–11.965	0.001
Chronic kidney disease	21.164	0.001–39.330	0.543
Tobacco use	0.999	0.428–2.335	0.999
Alcohol abuse	0.525	0.196–1.407	0.200
Medications			
Antiplatelet therapy	0.964	0.541–1.716	0.900
Duel antiplatelet therapy[a]	1.742	0.516–5.888	0.371
Anticoagulant therapy	1.948	0.581–6.533	0.280
Statin	0.455	0.117–1.771	0.256
BMI, kg/m^2	0.932	0.830–1.048	0.239
TCL, mmol/L	0.827	0.478–1.430	0.496
CHO, mmol/L	0.747	0.484–1.154	0.189
LDL, mmol/L	0.784	0.466–1.320	0.361
HDL, mmol/L	0.625	0.165–2.362	0.488
HbA1C, %	0.879	0.661–1.170	0.377
NIHSS score	0.981	0.882–1.090	0.721
TEE findings			
LAD, mm	1.020	0.948–1.096	0.600
LAD/H, mm/m	1.063	0.946–1.195	0.306
LAD/BSA, mm/m^2	1.105	0.988–1.236	0.080
LVEF %	0.974	0.930–1.020	0.266
PFO	1.552	0.463–5.202	0.477
Multiple territory infarcts	0.490	0.183–1.313	0.156
Carotid plaque features			
Ipsilateral non-stenosing carotid plaque	2.320	0.962–5.596	0.061
Grading of plaque density	1.252	0.866–1.809	0.233
Diameters of carotid artery plaque, mm	0.999	0.982–1.017	0.911
AoAC	2.819	1.206–6.590	0.017
AGS			
Grade 0	–	–	–
Grade 1	6.216	2.446–15.796	<0.001
Grade 2 plus 3*	1.922	0.667–5.539	0.226

[a]*indicates the aspirin combined with clopidogrel antiplatelet therapy.*

**As none of the patients with AGS grade 3 had recurrent stroke, patients with AGS grades 2 and 3, marked as grade 2 plus 3, were enrolled in the univariate Cox regression analysis. HR, hazard ratio; 95% CI, 95% confidence interval; AoAC, aortic arch calcification; AGS, aortic arch calcification grading scale; BMI, body mass index; NIHSS, National Institutes of Health Stroke Scale; LAD, left atrial diameter; LAD/H, left atrial diameter/height; BSA, body surface area; LEVF, left ventricular ejection fraction; PFO, patent foramen ovale. TCL, triglyceride, CHO, cholesterol, LDL, low-density lipoprotein, HDL, high-density lipoprotein, HbA1C, glycosylated hemoglobin.*

without recurrent stroke, patients with recurrent stroke were more likely to have a history of stroke (patients that had a history of stroke before enrolment in this study), left atrial diameter/height (LAD/H) enlargement, and AoAC (all $p < 0.001$). Stroke history, LAD/H, and AoAC were associated with stroke recurrence in the univariate Cox regression analysis ($p < 0.05$) (**Table 1**). These three factors were entered into multivariate Cox regression analysis as covariates to explore the predictors of stroke recurrence. AoAC use was significantly associated with stroke recurrence (hazard ratio [*HR*], 2.672; 95% confidence interval (*CI*), 1.129–6.319; $p = 0.025$). Stroke history was also predictive of recurrent stroke (*HR*, 4.625; 95% *CI*, 1.828–11.700, $p = 0.001$).

The Association Between AoAC and Stroke Recurrence

Among 158 patients with ESUS, 69 (43.7%) were identified as having AoAC. A comparison of the clinical characteristics of patients with and without AoAC is shown in **Supplementary Table 2**. In the AoAC subgroup ($n = 69$), 22 patients had spotty calcifications (grade 1), while 37 patients had lamellar calcification (grade 2) and 10 patients had circular calcification (grade 3), according to our AGS.

In patients with no AoAC on chest CT (AGS grade 0) ($n = 89$), only eight patients (9%) experienced stroke recurrence. In patients with AoAC ($n = 69$), the risk of stroke recurrence was reduced with an increase in AoAC severity. The rate of stroke recurrence was highest (45.5%) in patients with AGS grade 1, then followed by AGS grade 2 (16.2%). Of note, none (0%) of the patients with AGS grade 3 presented with stroke recurrence during the 1-year follow-up observation. Univariate comparison analysis showed that the rate of stroke recurrence was significantly higher in patients with AGS grade 1 than in those with any other AGS grade (all $p < 0.05$), while there was no significant difference in stroke recurrence among patients with AGS grades 0, 2, and 3 ($\chi^2 = 2.717$, $p = 0.257$).

After replacing AoAC with AGS in multivariate Cox regression analysis, AGS grade 1 (*HR*, 5.033; 95% *CI*, 1.858–13.635, $p = 0.001$) was associated with a significantly higher risk of stroke recurrence in comparison with AGS grade 0, while AGS grade 2 plus 3 (lamellar and circular calcification) showed no higher risk of stroke recurrence than AGS grade 0 (*HR*, 1.558; 95% *CI*, 0.539–4.509, $p = 0.413$).

In the AoAC subgroup ($n = 69$), multivariate Cox regression analysis showed that AGS grade 1 was associated with a significantly higher risk of stroke recurrence than AGS grade 2 plus 3 (*HR*, 3.388; 95% *CI*, 1.124–10.206, $p = 0.030$). An ROC analysis showed that AGS had a good value for predicting stroke recurrence with an AUC of 0.735 (95% *CI* = 0.601–0.869, $p = 0.005$).

Kaplan–Meier survival curves showed that the cumulative event (stroke recurrence) free rate was significantly lower in patients with a history of stroke than in those without a history of stroke (log-rank test, $p < 0.001$) and lower in patients with AoAC than in patients without AoAC (log-rank test, $p = 0.012$; **Figure 2A**). In the AoAC subgroup ($n = 69$), the Kaplan–Meier survival curves showed that the cumulative event-free rate was significantly lower in patients with AGS grade 1 than in patients with AGS grade 2 and 3 (log-rank test, $p = 0.008$; **Figure 2B**).

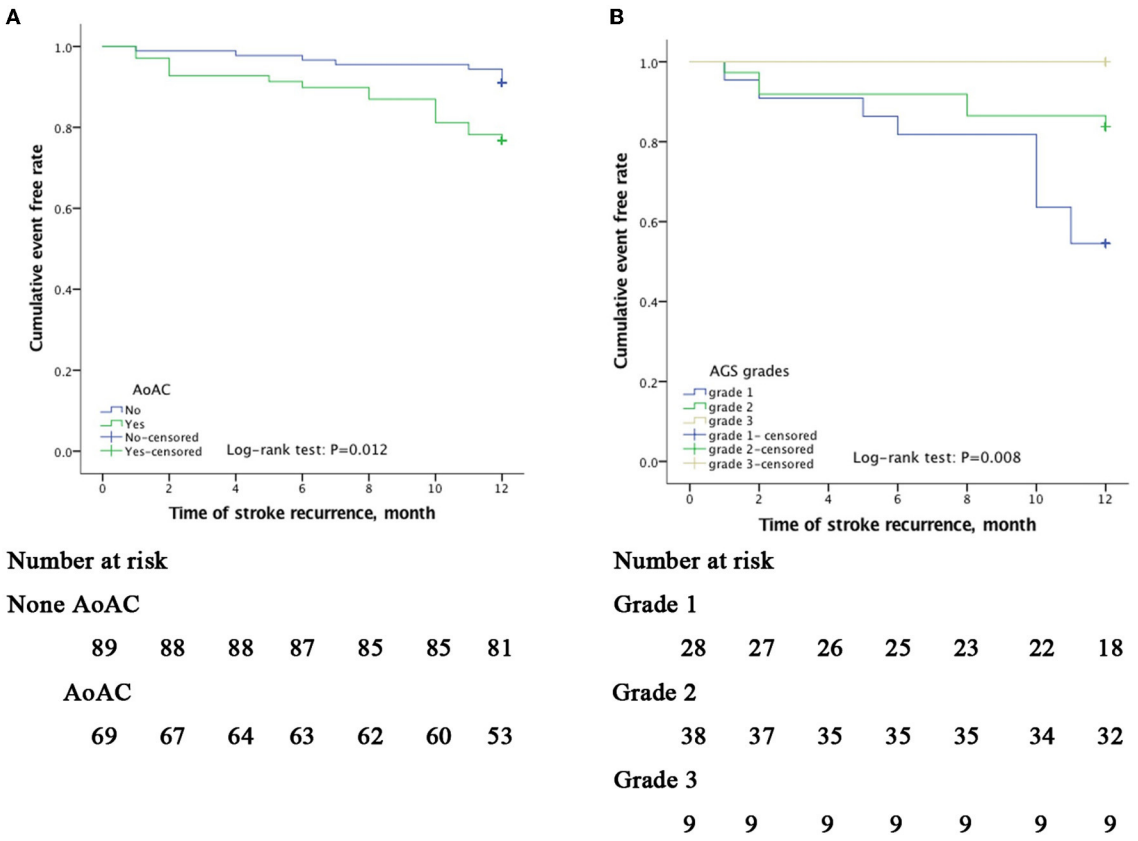

FIGURE 2 | Kaplan–Meier curves of freedom from recurrent stroke events during a 12-month follow-up. The *x*-axis indicates time in month since inclusion in the study. The *y*-axis indicates the proportion of patients with recurrence-free stroke. Cumulative event-free rates were compared based on the presence of AoAC **(A)** and among AGS grade 1(spotty calcification), 2 (lamellar calcification), and 3 (circular calcification); **(B)** showing $p = 0.012$ and $p = 0.008$ on the log-rank test, respectively.

DISCUSSION

In the present study, the 1-year stroke recurrence rate with ESUS was approximately 15%. A previous history of stroke and AoAC and its degree were demonstrated to be predictors for 1-year stroke recurrence in patients with ESUS. In contrast to the other subtypes of AoAC, spotty calcification (≤1 mm in diameter) was associated with a higher risk of stroke recurrence in our patients with ESUS.

First, the recurrence rate of ESUS in our study was higher than that in previous reports. In general, the prevalence of stroke recurrence in ESUS was annually approximately 2.3–13% (14, 20). We speculated that this gap was mainly caused by different study populations. It was reported that the stroke recurrence was more frequently seen in China than that in the West (21, 22). Data from the Chinese National Stroke Registry showed that the stroke recurrence rate in patients with ischemic stroke was 16% in the first year which was similar to our outcome (23, 24). According to data from the China National Stroke Screening and Prevention Project (CNSSPP), the standardized prevalence of AF among Chinese adults aged ≥40 years was 2.31%. Notably, the rate of stroke recurrence in our patients with ESUS was quite close to that reported in patients with large artery atherosclerosis (LAA) (25, 26), further supporting that large artery non-stenosing plaque might be the potential etiology of stroke and stroke recurrence in this ESUS population in China.

Second, we found that AoAC, especially spotty calcification, was a key factor in the high incidence of stroke recurrence in ESUS. Interestingly, the risk of recurrent stroke with spotty calcification is not only higher than that without calcification but also higher than that with lamellar and circular calcifications. This finding is very different from those of previous research. Some studies believe that the higher the severity of AoAC which is reflected by the AAC grade or CAM score, the higher the risk of stroke recurrence (11). However, some studies failed to find a strong correlation (27, 28). We speculated that the reasons why our results were different included (1) the study population was different and (2) the evaluation methods of calcification were different. Compared with AAC, our evaluation using CT is more objective and accurate than X-ray imaging (29). Compared with the CAM score, although our method was unable to quantify the degree of AoAC, our research method was simpler and might be easier to apply in other centers for patients with stroke. Although our results are in contrast to those of other studies, the mechanism of low-grade calcification in predicting stroke recurrence can still be logical. One important embolic source in

ESUS is atherosclerotic plaque in the carotid, vertebrobasilar, and intracranial arteries, or the aortic arch collectively described as supracardiac atherosclerosis (30). A previous research has shown that spotty calcification generally occurs in the aortic intima which increases the risk of plaque rupture. Macrocalcification, such as areas of calcification and circular calcification, is more common in the tunica media of the acral arteries and often leads to stenosis (10, 11). Moreover, this suggests that plaque size has certain limitations in evaluating stroke recurrence. In the future, plaque morphology or routine plaque vulnerability assessment for AoAC may better explain the relationship between AoAC and stroke recurrence. In addition, whether intensive statin treatment can better prevent stroke recurrence in patients with this type of spotty calcification is a problem that needs to be addressed in future research.

On chest CT, AoAC, a risk marker for cardiovascular disease, becomes available in subjects with no additional radiation burden to the patient and no additional work for the radiologist. Our AGS has proven to be a valuable evaluation tool for recurrent stroke risk for patients with ESUS. For AGS grade 0, the stroke recurrence rate was much lower than that of grade 1, but was close to the incidence in the severe calcification group (grades 2–3). We propose that patients without calcification should still be evaluated for cardiogenic stroke, such as recommending screening for 24 h or longer electrocardiograms (ECGs), and patent foramen ovale (PFO). For AGS grades 2–3, more serious calcification might be associated with a relatively low risk of recurrent stroke in patients with ESUS in comparison with spotty calcification (grade 1). Further assessment of atherosclerotic plaque stability upon cardiac imaging, such as computed tomography angiography (CTA) or digital subtraction angiography (DSA), might be beneficial as a secondary prevention strategy for ESUS stroke and calcification of ESUS etiology.

Furthermore, cardiovascular calcifications were associated with cardiovascular events and death (31, 32). They can involve the coronary arteries, cardiac valves, myocardium, pericardium, and aorta artery. Different location and the level of calcifications may be potential markers in identifying patients of a high-risk phenotype for developing recurrent stroke.

This study had several limitations. First, the study design was retrospective and selection bias could not be ruled out. Second, the data from the current study were derived from a single center and the number of patients with recurrent stroke was small. Third, we did not select the Agatston score to quantify the severity of AoAC on chest CT because we considered that the AGS might be more applicable and feasible in most centers. Moreover, with the advent of coronavirus disease 2019 (COVID-19), patients with stroke must undergo routine chest CT scans at admission, which provides convenience for further stroke recurrence risk assessment with a larger sample size in the future. At last, for technical and economic reasons, implantable loop recorder monitoring for atrial fibrillation has not been carried out in our hospital. Yushan et al. found that the rate of AF detection was much higher at 12% with insertable cardiac monitor (ICM) in patients with ESUS (33). Lack of ICM might influence the detection rate of AF in our research.

In conclusion, AoAC, particularly spotty calcification on chest CT, was effective in predicting future recurrent stroke in patients with ESUS. AGS might be a valuable evaluation tool for stroke recurrence risk in ESUS, which needs to be confirmed in prospective, large-sample-sized studies in the future.

DATA AVAILABILITY STATEMENT

The original contributions presented in the study are included in the article/**Supplementary Material**, further inquiries can be directed to the corresponding author/s.

ETHICS STATEMENT

The protocols of the study had been approved by the Local Ethics Committee. All clinical investigation has been conducted according to the principles expressed in the Declaration of Helsinki. The patients/participants provided their written informed consent to participate in this study.

AUTHOR CONTRIBUTIONS

XC and YG contributed to the conception and design of this study. XC contributed to the acquisition and analysis of the data and figures preparation. SZ contributed to the data analysis. XC and SZ contributed to drafting the manuscript. All authors contributed to the article and approved the submitted version.

SUPPLEMENTARY MATERIAL

The Supplementary Material for this article can be found online at: https://www.frontiersin.org/articles/10.3389/fneur.2022.863450/full#supplementary-material

REFERENCES

1. Hart RG, Diener HC, Coutts SB, Easton JD, Granger CB, O'Donnell MJ, et al. Embolic strokes of undetermined source: the case for a new clinical construct. *Lancet Neurol.* (2014) 13:429–38. doi: 10.1016/S1474-4422(13)70310-7
2. Diener HC, Sacco RL, Easton JD, Granger CB, Bernstein RA, Uchiyama S, et al. Dabigatran for prevention of stroke after embolic stroke of undetermined source. *N Engl J Med.* (2019) 380:1906–17. doi: 10.1056/NEJMoa1813959
3. Hart RG, Sharma M, Mundl H, Kasner SE, Bangdiwala SI, Berkowitz SD, et al. Rivaroxaban for stroke prevention after embolic stroke of undetermined source. *N Engl J Med.* (2018) 378:2191–201. doi: 10.1056/NEJMoa1802686
4. Komatsu T, Iguchi Y, Arai A, Sakuta K, Sakai K, Terasawa Y, et al. Large but nonstenotic carotid artery plaque in patients with a history of embolic stroke of undetermined source. *Stroke.* (2018) 49:3054–6. doi: 10.1161/STROKEAHA.118.022986
5. Kamel H, Pearce LA, Ntaios G, Gladstone DJ, Perera K, Roine RO, et al. Atrial cardiopathy and nonstenosing large artery plaque in patients

with embolic stroke of undetermined source. *Stroke.* (2020) 51:938–43. doi: 10.1161/STROKEAHA.119.028154
6. Ospel JM, Singh N, Marko M, Almekhlafi M, Dowlatshahi D, Puig J, et al. Prevalence of ipsilateral nonstenotic carotid plaques on computed tomography angiography in embolic stroke of undetermined source. *Stroke.* (2020) 51:1743–9. doi: 10.1161/STROKEAHA.120.029404
7. Kamtchum-Tatuene J, Nomani AZ, Falcione S, Munsterman D, Sykes G, Joy T, et al. Non-stenotic carotid plaques in embolic stroke of unknown source. *Front Neurol.* (2021) 12:719329. doi: 10.3389/fneur.2021.719329
8. Nicoll R, Henein M. Arterial calcification: a new perspective? *Int J Cardiol.* (2017) 228:11–22. doi: 10.1016/j.ijcard.2016.11.099
9. Yang TL, Huang CC, Huang SS, Chiu CC, Leu HB, Lin SJ. Aortic arch calcification associated with cardiovascular events and death among patients with acute coronary syndrome. *Acta Cardiol Sin.* (2017) 33:241–9. doi: 10.1016/j.jacc.2017.03.063
10. Ntaios G, Pearce LA, Meseguer E, Endres M, Amarenco P, Ozturk S, et al. Aortic arch atherosclerosis in patients with embolic stroke of undetermined source: An exploratory analysis of the navigate esus trial. *Stroke.* (2019) 50:3184–90. doi: 10.1161/STROKEAHA.119.025813
11. Ueno Y, Yamashiro K, Tanaka R, Kuroki T, Hira K, Kurita N, et al. Emerging risk factors for recurrent vascular events in patients with embolic stroke of undetermined source. *Stroke.* (2016) 47:2714–21. doi: 10.1161/STROKEAHA.116.013878
12. Kim HG, Lee SH, Nam TM, Jang JH, Kim YZ, Kim KH, et al. Association of aortic arch calcification on chest x-ray with procedural thromboembolism after mechanical thrombectomy for acute ischemic stroke. *Medicina (Kaunas).* (2021) 57:859. doi: 10.3390/medicina57090859
13. Kamenskiy A, Poulson W, Sim S, Reilly A, Luo J, MacTaggart J. Prevalence of calcification in human femoropopliteal arteries and its association with demographics, risk factors, and arterial stiffness. *Arterioscler Thromb Vasc Biol.* (2018) 38:e48–57. doi: 10.1161/ATVBAHA.117.310490
14. Hart RG, Catanese L, Perera KS, Ntaios G, Connolly SJ. Embolic stroke of undetermined source: A systematic review and clinical update. *Stroke.* (2017) 48:867–72. doi: 10.1161/STROKEAHA.116.016414
15. Yuyun X, Lexi Y, Haochu W, Zhenyu S, Xiangyang G. Early warning information for severe and critical patients with covid-19 based on quantitative ct analysis of lung segments. *Front Public Health.* (2021) 9:596938. doi: 10.3389/fpubh.2021.596938
16. Zhao H, Wang J, Lu Z, Wu Q, Lv H, Liu H, et al. Superficial siderosis of the central nervous system induced by a single-episode of traumatic subarachnoid hemorrhage: A study using mri-enhanced gradient echo t2 star-weighted angiography. *PLoS ONE.* (2015) 10:e0116632. doi: 10.1371/journal.pone.0116632
17. Mori H, Torii S, Kutyna M, Sakamoto A, Finn AV, Virmani R. Coronary artery calcification and its progression: what does it really mean? *JACC Cardiovasc Imaging.* (2018) 11:127–42. doi: 10.1016/j.jcmg.2017.10.012
18. Lang RM, Badano LP, Mor-Avi V, Afilalo J, Armstrong A, Ernande L, et al. Recommendations for cardiac chamber quantification by echocardiography in adults: An update from the american society of echocardiography and the european association of cardiovascular imaging. *Eur Heart J Cardiovasc Imaging.* (2015) 16:233–70. doi: 10.1093/ehjci/jev014
19. Lee JS, Hong JM, Moon GJ, Lee PH, Ahn YH, Bang OY, et al. A long-term follow-up study of intravenous autologous mesenchymal stem cell transplantation in patients with ischemic stroke. *Stem Cells.* (2010) 28:1099–106. doi: 10.1002/stem.430
20. Diener HC, Sacco RL, Easton JD, Granger CB, Bar M, Bernstein RA, et al. Antithrombotic treatment of embolic stroke of undetermined source: respect esus elderly and renally impaired subgroups. *Stroke.* (2020) 51:1758–65. doi: 10.1161/STROKEAHA.119.028643
21. Li S, Cui LY, Anderson C, Gao C, Yu C, Shan G, et al. Increased recurrent risk did not improve cerebrovascular disease survivors' response to stroke in china: A cross-sectional, community-based study. *BMC Neurol.* (2020) 20:147. doi: 10.1186/s12883-020-01724-1
22. Zhao W, Wu J, Liu J, Wu Y, Ni J, Gu H, et al. Trends in the incidence of recurrent stroke at 5 years after the first-ever stroke in rural china: a population-based stroke surveillance from 1992 to 2017. *Aging (Albany NY).* (2019) 11:1686–94. doi: 10.18632/aging.101862
23. Wang P, Wang Y, Zhao X, Du W, Wang A, Liu G, et al. In-hospital medical complications associated with stroke recurrence after initial ischemic stroke: A prospective cohort study from the china national stroke registry. *Medicine (Baltimore).* (2016) 95:e4929. doi: 10.1097/MD.0000000000004929
24. Wang Y, Cui L, Ji X, Dong Q, Zeng J, Wang Y, et al. The china national stroke registry for patients with acute cerebrovascular events: design, rationale, and baseline patient characteristics. *Int J Stroke.* (2011) 6:355–61. doi: 10.1111/j.1747-4949.2011.00584.x
25. Toi S, Shirai Y, Ishizuka K, Hosoya M, Seki M, Higuchi E, et al. Recurrent stroke incidence and etiology in patients with embolic stroke of undetermined source and other stroke subtypes. *J Atheroscler Thromb.* (2022) 29:393–402. doi: 10.5551/jat.61895
26. Wu Q, Cui J, Xie Y, Wang M, Zhang H, Hu X, et al. Outcomes of ischemic stroke and associated factors among elderly patients with large-artery atherosclerosis: A hospital-based follow-up study in china. *Front Neurol.* (2021) 12:642426. doi: 10.3389/fneur.2021.642426
27. Van der Linden J, Van der Linden W. How calcification in the atherosclerotic aorta can be associated with both a lower risk of recurrent stroke in clinical studies and an increased number of strokes in an autopsy study: Interpretation based on selection bias. *Ned Tijdschr Geneeskd.* (2008) 152:198–201.
28. van der Linden J, van der Linden W, Taube A. Berkson's fallacy: aortic arteriosclerosis and stroke as an example. Contradictory findings support the hypothesis of low risk of calcium plaque. *Lakartidningen.* (2007) 104:35—7.
29. Craiem D, Chironi G, Casciaro ME, Graf S, Simon A. Calcifications of the thoracic aorta on extended non-contrast-enhanced cardiac ct. *PLoS ONE.* (2014) 9:e109584. doi: 10.1371/journal.pone.0109584
30. Ntaios G, Wintermark M, Michel P. Supracardiac atherosclerosis in embolic stroke of undetermined source: the underestimated source. *Eur Heart J.* (2021) 42:1789–96. doi: 10.1093/eurheartj/ehaa218
31. Li TYW, Yeo LLL, Ho JSY, Leow AS, Chan MY, Dalakoti M, et al. Association of global cardiac calcification with atrial fibrillation and recurrent stroke in patients with embolic stroke of undetermined source. *J Am Soc Echocardiogr.* (2021) 34:1056–66. doi: 10.1016/j.echo.2021.04.008
32. Ahmed T, Ahmad M, Mungee S. Cardiac calcifications. Treasure Island (FL): Statpearls. (2022).
33. ushan B, Tan BYQ, Ngiam NJ, Chan BPL, Luen TH, Sharma VK, et al. Association between bilateral infarcts pattern and detection of occult atrial fibrillation in embolic stroke of undetermined source (esus) patients with insertable cardiac monitor (icm). *J Stroke Cerebrovasc Dis.* (2019) 28:2448–52. doi: 10.1016/j.jstrokecerebrovasdis.2019.06.025

Conflict of Interest: The authors declare that the research was conducted in the absence of any commercial or financial relationships that could be construed as a potential conflict of interest.

frontiers | Frontiers in Neurology

ORIGINAL RESEARCH
published: 27 April 2022
doi: 10.3389/fneur.2022.860979

The Value of Contrast-Enhanced Ultrasound in the Evaluation of Carotid Web

Qingqing Zhou†, Rui Li†, Shuo Feng, Fengling Qu, Chunrong Tao, Wei Hu, Yuyou Zhu and Xinfeng Liu**

Stroke Center & Department of Neurology, The First Affiliated Hospital of USTC, Division of Life Sciences and Medicine, University of Science and Technology of China, Hefei, China

OPEN ACCESS

Edited by:
Bing Tian,
Naval Medical University, China

Reviewed by:
Gador Canton,
University of Washington, United States
Anastasios Mpotsaris,
München Hospital, Germany

***Correspondence:**
Yuyou Zhu
zhuyuyou2020@126.com
Xinfeng Liu
xfliu2@vip.163.com

†These authors have contributed equally to this work and share first authorship

Specialty section:
This article was submitted to Stroke, a section of the journal Frontiers in Neurology

Received: *24 January 2022*
Accepted: *25 March 2022*
Published: *27 April 2022*

Citation:
Zhou Q, Li R, Feng S, Qu F, Tao C, Hu W, Zhu Y and Liu X (2022) The Value of Contrast-Enhanced Ultrasound in the Evaluation of Carotid Web. Front. Neurol. 13:860979. doi: 10.3389/fneur.2022.860979

Objectives: The purpose of this study was to investigate whether contrast-enhanced ultrasound (CEUS) is more advantageous than conventional ultrasound in the diagnosis of carotid web (CaW) and to compare the clinical characteristics of patients in different age groups.

Methods: Seventeen patients admitted to the hospital from October 2019 to December 2021 were included in our study. Patients were initially diagnosed with CaW using digital subtraction angiography (DSA), and conventional ultrasound and CEUS were completed. Baseline patient data were analyzed and compared between the <60 years old CaW group and the ≥60 years old CaW group to explore the differences between the two groups. Then, comparing the accuracy of conventional ultrasound and CEUS.

Results: A total of 17 CaW patients participated in this study, including 4 female patients (23.5%) and 13 male patients (76.5%), with an average age of 59.41 (±10.86) years. There were 9 patients (52.9%) with left CaW and 8 patients (47.1%) with right CaW. Acute ischemic stroke (AIS) occurred in 14 patients (82.4%). Thrombosis occurred in five of 17 patients (29.4%). There was a significant statistical difference about the thrombosis between the <60 years old CaW group and the ≥60 years old CaW group [<60 years group: 0 (0%), ≥60 years group: 5 (62.5%), $P = 0.005$]. Seven patients (41.2%) received medical management, nine patients (52.9%) had carotid artery stenting (CAS), and one patient (5.9%) had carotid endarterectomy (CEA). None of the patients had recurrent stroke during the follow-up period. The diagnostic rate of CaW and thrombus by CEUS was higher than that by conventional ultrasound, and there was a significant statistical difference in the diagnosis of thrombus between CEUS and conventional ultrasound ($\chi 2 = 4.286$, $P = 0.038$).

Conclusions: CEUS may have a higher diagnostic accuracy for CaW with thrombosis, and it has a higher clinical application prospect.

Keywords: carotid web, stroke, contrast-enhanced ultrasound, diagnosis, thrombus

INTRODUCTION

Stroke is a disease with high morbidity and disability rates (1) and is the second leading cause of death worldwide (2). Carotid web (CaW) can be detected in nearly 5% of young cryptogenic stroke patients (3). Therefore, CaW is a risk factor in cryptogenic stroke (4). CaW is a kind of endovascular variation caused by fibromuscular dysplasia (FMD) (5). It usually originates from the posterior wall of the carotid bulb and protrudes into the lumen, presenting a shelf-like structure in morphology (6). FMD was first proposed by Connett and Lansche (7), and the term "web" was first described in the literature by Momose and New (8). CaW is commonly associated with the occurrence of an ipsilateral cerebral infarction or transient ischemic attack (TIA) (9), suggesting its involvement in potential stroke mechanisms (3). CaW is prevalent in 1–7% of the population (10) and is more common in younger patients with cryptogenic stroke (3).

Although there are definite morphological characteristics of CaW, the diagnosis of CaW is clinically difficult and easily misdiagnosed or missed (11) because of its rarity, small size, and insufficient understanding (12). Conventional ultrasound is a non-invasive, rapid, and convenient method. It can be repeated many times and has a wide range of applicability (13). Contrast-enhanced ultrasound (CEUS) is a non-invasive method developed using conventional ultrasound technology as a foundation that provides more information, better image quality, and more quantitative data through intravenous injection of contrast agent as tracer (13). CEUS can clearly show conditions in the lumen, such as whether there is a contrast filling defect, and evaluate the degree of thrombus formation in the lumen. Therefore, CEUS is often used to display neovascularization in plaques in both symptomatic and asymptomatic patients, identify plaque vulnerability, and find the location of the thrombus and the site of involvement (14). CEUS is a more accurate method to measure the stenosis of lumen than conventional angiography and magnetic resonance angiography (MRA) (15).

Previous studies have explored the diagnosis of CaW using computed tomographic angiogram (CTA), high-resolution magnetic resonance imaging (MRI), and conventional ultrasound (16). However, few studies have explored the diagnostic value of CEUS for CaW. In particular, the diagnosis of superimposed thrombosis by CEUS has not yet been reported. Therefore, there is some confusion about the application value of CEUS in CaW and thrombosis. In addition, the incidence and severity of stroke is age-related and increases with age (17). The elderly patients with acute ischemic stroke (AIS) showed specific characteristics and epidemiology, with more baseline comorbidities, disability and higher NIHSS score at admission compared with younger patients (18). Moreover, the rate of thrombosis increases with age (19). To our knowledge, no studies have reported the characteristics of CaW in different age groups. Therefore, the purpose of this study was to identify different manifestations of CaW and thrombosis using CEUS and to explore the diagnostic value of CEUS. In addition, comparing the clinical characteristics of patients with CaWs in different age groups.

METHODS

Study Population and Design

Patients diagnosed with CaW at the First Affiliated Hospital of the University of Science and Technology of China from October 2019 to December 2021 were retrospectively analyzed. The inclusion criteria were as follows: (1) age older than 18 years; (2) digital subtraction angiography (DSA) used to diagnose CaW; (3) improved conventional ultrasound and CEUS examination. The exclusion criteria were as follows: (1) incomplete medical history; (2) severe infection, tumor, failure of the liver, kidney, or respiratory system; (3) no follow-up data. Baseline characteristics and associated risk factors were collected, including sex, age, hypertension, diabetes, hyperlipidemia, coronary heart disease, history of stroke, alcohol, and smoking. In addition, the low-density lipoprotein (LDL), high-density lipoprotein (HDL), glucose, total cholesterol (TC), and triglyceride (TG) levels of patients were also recorded. Moreover, the length, width, location of CaWs, and degree of carotid artery stenosis were measured.

Imaging Assessment and Analysis

The diagnosis of CaW was achieved with DSA, which was chosen for its high temporal and spatial resolution (20). DSA is considered the gold standard for CaW diagnosis (9). The CaW showed a contrast filling defect when assessed with DSA (21) (**Figure 1**). On conventional ultrasound, the CaW appears as a hypoechoic plaque with an axial shelf-like structure (16) (**Figure 2**). Upon assessment with CEUS, CaW showed delayed filling of contrast agent. Imaging examination results were read independently and blinded by two physicians in the department of neurology. If there were inconsistent judgments, they were determined after further discussion.

Statistical Analysis

Statistical analysis was performed in SPSS 22.0 software (IBM SPSS Statistics 22.0). Categorical variables are presented as numbers (%). Continuous variables that were normally distributed were described as the mean ± standard deviation. Continuous variables that were not normally distributed were presented as the median and quartile intervals. The Chi-square test was used when comparing categorical variables. Continuous variables were compared using the *t*-test or Mann-Whitney *U*-test. $P < 0.05$ indicated that there was statistical difference.

RESULTS

A total of 17 CaW patients were enrolled in this study, including 4 females (23.5%) and 13 males (76.5%), with an average age of 59.41 (±10.86) years (**Table 1**). All 17 patients had unilateral CaW, including nine patients (52.9%) with left CaW and eight patients (47.1%) with right CaW. AIS occurred in 14 patients (82.4%). Among the 17 patients, 13 patients (76.5%) had hypertension, one patient (5.9%) had hyperlipidemia, eight patients (47.1%) had diabetes, two patients (11.8%) had coronary heart disease, and six patients had (35.3%) a history of stroke. Thrombosis occurred in five of 17 patients (29.4%). The median

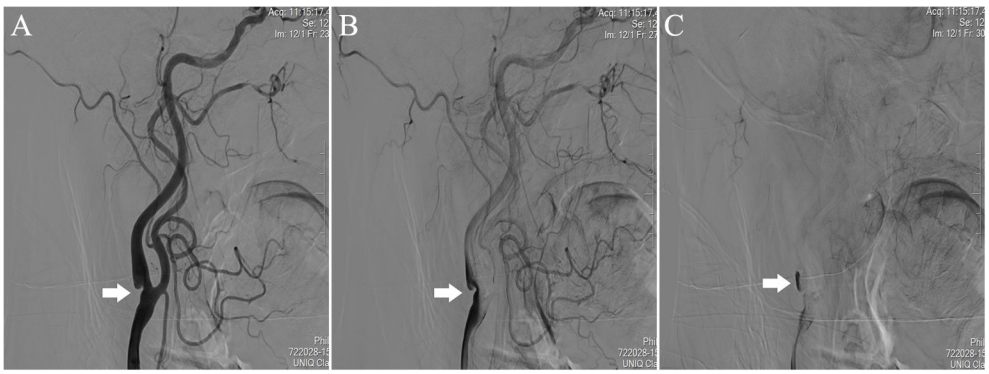

FIGURE 1 | Performance of CaW at the right internal carotid artery of the patient during DSA. Compared with **(A)** early-arterial phase, **(B)** mid-arterial phase, and **(C)** late-arterial phase showed significant contrast agent retention.

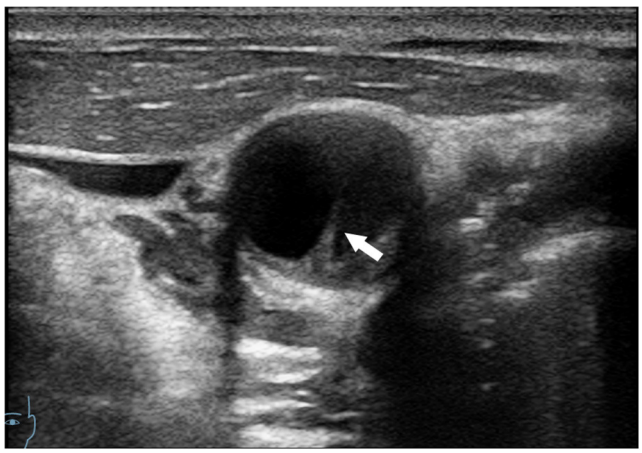

FIGURE 2 | Conventional ultrasound showing axial view of CaW (arrow indicates shelf-like CaW).

TABLE 1 | Clinical characteristics of CaW patients.

Characteristics	All patients (*N* = 17)
Age, yr, mean (±SD)	59.41 (±10.86)
Sex (male), *n* (%)	13 (76.5)
Hypertension, *n* (%)	13 (76.5)
Dyslipidemia, *n* (%)	1 (5.9)
Diabetes, *n* (%)	8 (47.1)
Coronary heart disease, *n* (%)	2 (11.8)
History of stroke, *n* (%)	6 (35.3)
SBP, mmHg, Median (IQR)	129 (118–143)
DBP, mmHg, Median (IQR)	77 (72–88)
Glucose, mmol/L, Median (IQR)	5.46 (4.89–6.08)
TG, mmol/L, Median (IQR)	1.17 (0.73–1.94)
TC, mmol/L, Median (IQR)	3.59 (2.91–4.88)
HDL, mmol/L, Median (IQR)	1.12 (0.90–1.38)
LDL, mmol/L, Median (IQR)	2.06 (1.23–3.00)
Stenosis (%), Median (IQR)	40 (30–50)
AIS, *n* (%)	14 (82.4)
Left CaW, *n* (%)	9 (52.9)
Thrombosis, *n* (%)	5 (29.4)
Smoking, *n* (%)	5 (29.4)
Alcohol, *n* (%)	3 (17.6)

AIS, acute ischemic stroke; CaW, carotid web; DBP, diastolic blood pressure; HDL, high-density lipoprotein; LDL, low-density lipoprotein; TC, total cholesterol; TG, triglyceride; SBP, systolic blood pressure; yr, year.

systolic blood pressure (SBP) value was 129 mmHg (IQR, 118–143 mmHg), the median diastolic blood pressure (DBP) value was 77 mmHg (IQR, 72–88 mmHg), and the median glucose value was 5.46 mmol/L (IQR, 4.89–6.08 mmol/L). The median TG value was 1.17 mmol/L (IQR, 0.73–1.94 mmol/L), the median TC value was 3.59 mmol/L (IQR, 2.91–4.88 mmol/L), the median HDL value was 1.12 mmol/L (IQR, 0.90–1.38 mmol/L), and the median LDL value was 2.06 mmol/L (IQR, 1.23–3.00 mmol/L).

The clinical difference between the <60 years old CaW group and the ≥60 years old CaW group was compared in **Table 2**. The median admission glucose level in the <60 years old CaW group was found to be higher than the ≥60 years old CaW group [<60 years: 5.47 mmol/L (IQR, 4.88–6.69 mmol/L), ≥60 years: 5.39 mmol/L (IQR, 4.84–5.39 mmol/L)]. In addition, the median TC and LDL levels of patients in the <60 years old CaW group were higher than that of patients in the ≥60 years old CaW group [TC: < 60 years 4.51 mmol/L (IQR, 2.91–5.47 mmol/L), ≥60 years old 3.28 mmol/L (IQR, 2.89–4.37 mmol/L); LDL: <60 years 2.84 mmol/L (IQR, 1.12–3.47 mmol/L), ≥60 years old 1.68 mmol/L (IQR, 1.28–2.27 mmol/L)]. Furthermore, there was a significant statistical difference about the thrombosis between the two groups [<60 years: 0 (0%), ≥60 years: 5 (62.5%), $P = 0.005$].

Seventeen patients received the corresponding treatment strategy after admission (**Table 3**), of whom seven patients (41.2%) received medical management, nine patients (52.9%) received carotid artery stenting (CAS), and one patient (5.9%) received carotid endarterectomy (CEA). Among patients who received medical management, there were five patients (71.4%) had right CaW, median length 7.1 mm (IQR, 4.5–13.0 mm),

TABLE 2 | Comparison of characteristics between the <60 years old CaW group and the ≥60 years old CaW group.

Characteristics	Age < 60 years (*N* = 9)	Age ≥ 60 years (*N* = 8)	*P*-value
Sex (male), *n* (%)	8 (88.9)	5 (62.5)	0.410
Hypertension, *n* (%)	6 (66.7)	7 (87.5)	0.312
Dyslipidemia, *n* (%)	1 (11.1)	0 (0)	0.331
Diabetes, *n* (%)	5 (55.6)	3 (37.5)	0.457
Coronary heart disease, *n* (%)	1 (11.1)	1 (12.5)	0.929
History of stroke, *n* (%)	3 (33.3)	3 (37.5)	0.858
SBP, mmHg, Median (IQR)	138 (120, 145)	126 (112, 138)	0.423
DBP, mmHg, Median (IQR)	77 (70, 88)	77 (71, 91)	1.000
Glucose, mmol/L, Median (IQR)	5.47 (4.88, 6.69)	5.39 (4.84, 5.39)	0.541
TG, mmol/L, Median (IQR)	1.17 (0.69, 2.44)	1.18 (0.81, 1.60)	0.606
TC, mmol/L, Median (IQR)	4.51 (2.91, 5.47)	3.28 (2.89, 4.37)	0.277
HDL, mmol/L, Median (IQR)	1.04 (0.83, 1.34)	1.24 (0.95, 1.41)	0.673
LDL, mmol/L, Median (IQR)	2.84 (1.12, 3.47)	1.68 (1.28, 2.27)	0.481
Stenosis (%), Median (IQR)	40.0 (30.0, 55.0)	35.0 (22.5, 47.5)	0.370
AIS, *n* (%)	7 (77.8)	7 (87.5)	0.600
Left CaW, *n* (%)	5 (55.6)	4 (50.0)	0.819
Thrombosis, *n* (%)	0 (0)	5 (62.5)	**0.005**
Smoking, *n* (%)	4 (44.4)	1 (12.5)	0.149
Alcohol, *n* (%)	3 (33.3)	0 (0)	0.072

AIS, acute ischemic stroke; CaW, carotid web; DBP, diastolic blood pressure; HDL, high-density lipoprotein; LDL, low-density lipoprotein; TC, total cholesterol; TG, triglyceride; SBP, systolic blood pressure; yr, year; The bold values means $p < 0.05$.

TABLE 3 | Treatment of patients with CaW.

Treatment	*N*	Age (yr), Median (IQR)	Sex (male), *n* (%)	Location (right), *n* (%)	Length (mm), Median (IQR)	Width (mm), Median (IQR)	Stenosis (%), Median (IQR)	Follow up (month), Median (IQR)	Recurrence, *n* (%)
Medical management	7	58 (53–64)	4 (57.1)	5 (71.4)	7.1 (4.5–13.0)	2.5 (1.6–2.9)	30 (25–50)	11 (4–13)	0
CAS	9	63 (49–72)	8 (88.9)	2 (22.2)	8.7 (5.1–11.4)	2.5 (1.6–4.1)	40 (30–55)	9 (6–20)	0
CEA	1	58	1 (100)	1 (100)	8.9	5.1	50	2	0

CAS, carotid artery stenting; CaW, carotid web; CEA, carotid endarterectomy; yr, year.

median width 2.5 mm (IQR, 1.6–2.9 mm), median stenosis rate 30% (IQR, 25–50%), and no recurrence at a median follow-up of 11 months (IQR, 4–13 months). Among patients who underwent CAS, seven patients (77.8%) had left CaW, with median length of 8.7 mm (IQR, 5.1–11.4 mm), a median width of 2.5 mm (IQR, 1.6–4.1 mm), a median stenosis rate of 40% (IQR, 30–55%), and no recurrence at a median follow up of 9 months (IQR, 6–20 months). Only 1 patient received CEA.

Upon conventional ultrasound, CaW appeared as a hypoechoic plaque that protrudes into the lumen. On CEUS, delayed infusion of the contrast agent was observed and a perfusion defect was revealed (**Figure 3**), where the web was located, to be protruding into the lumen after the injection of contrast agent. All 17 patients with CaW underwent conventional ultrasound and CEUS (**Table 4**). Among them, 16 patients (94.1%) with CaW were diagnosed by CEUS, and 1 patient was missed. Fourteen patients (82.4%) were diagnosed by conventional ultrasound, and three patients were missed. We found there was no statistical difference when comparing conventional ultrasound to CEUS in the diagnosis of CaW ($P = 0.287$). DSA confirmed thrombosis in five of 17 patients, five patients were diagnosed by CEUS (100%) and two patients were diagnosed by conventional ultrasound (40%), indicating that CEUS was statistically better than conventional ultrasound in the diagnosis of thrombosis ($\chi 2 = 4.286$, $P = 0.038$).

DISCUSSION

The pathological characteristics of CaW are intimal thickening of the carotid artery and proliferation of fibroblasts (22). Angiography showed that most of the shelf-like structures associated with CaW were convex into the lumen (20). However, the exact etiology of CaW is still unclear and could involve factors such as genetics, presence of chronic vascular injury, hormone levels, and trophoblast vascular abnormalities (23). Our results found that hypertension accounted for a higher proportion of risk factors (76.5%), followed by diabetes (47.1%) and then smoking history (29.4%). Hypertension is associated with the

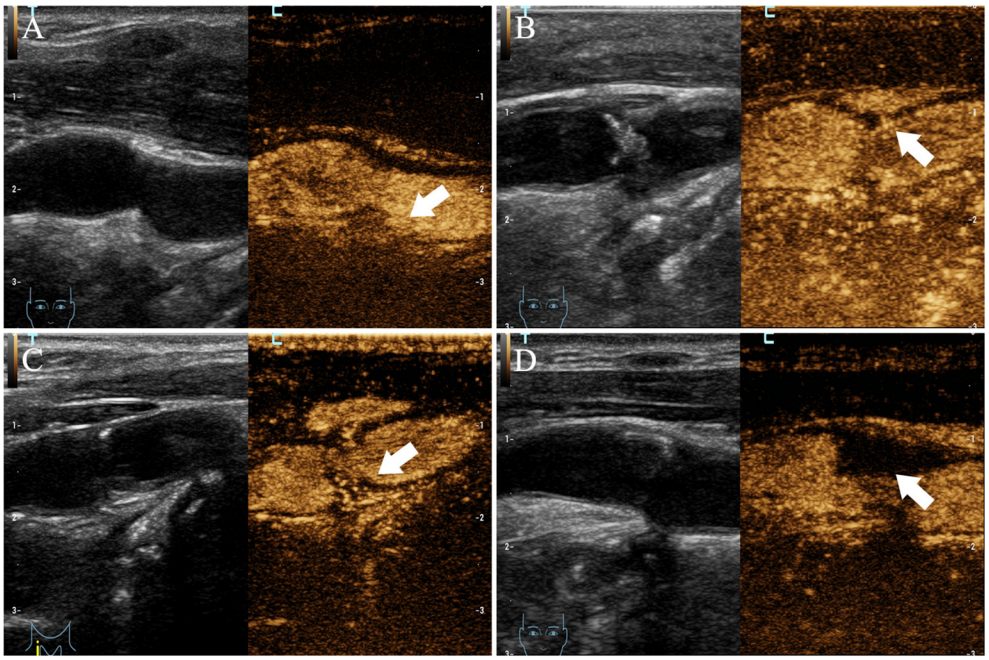

FIGURE 3 | Imaging manifestations of CaW using CEUS. **(A–D)** all have obvious contrast filling defects (arrows indicate filling defects).

onset of stroke and small-vessel disease (24). Therefore, it is very important for patients with CaW to control their blood pressure. In addition, fourteen patients (82.4%) experienced AIS. There was no significant difference when looking at the prevalence of the left CaW group and the right CaW group, which is consistent with previous study (25). Moreover, our results showed that there were statistical differences in the thrombosis between the <60 years old CaW group and the ≥60 years old CaW group ($P = 0.005$). However, there was no statistical difference in hematological indexes between the two groups. In this study, the proportion of male CaW patients was higher than that of female CaW patients, which contradicted the previous conclusion that there were more female patients than male patients (26, 27). This may be due to selection bias in the preponderance of male patients.

CaW leads to lumen stenosis and produces greater hemodynamic changes than atherosclerosis of a similar degree of lumen stenosis (10). The shelf-like structures of the CaW alter the distal hemodynamic pattern (22), resulting in the formation of a superimposed thrombus at the vortex (16). Superimposed thrombosis is associated with slow filling defects and turbulent blood flow (28). Thromboembolism can lead to stroke and neurological deterioration (29). Therefore, the examination of thrombosis is very important. Early detection of thrombi and taking corresponding treatment measures play an important role in saving patients' lives. In this study, the proportion of CaW patients with thrombosis reached 29.4%. Particularly, all patients with thrombosis were in the ≥60 years group, indicating that the incidence of CaW with thrombosis was higher in elderly patients. The risk of arterial and venous thrombosis increases with age (19, 30), which may be related to thrombin generation (31). The relationship and physiological mechanism between age and thrombosis in patients with CaW need to further study. Furthermore, the median stenosis rate of CaW patients was 40% (IQR, 30–50%). Patients with mild to moderate stenosis were at an increased risk of future vascular events (32).

TABLE 4 | Comparison of conventional ultrasound and CEUS in the diagnosis of CaW and thrombosis.

	Conventional ultrasound *n*(%)	CEUS *n*(%)	$\chi 2$	*P*-value
CaW ($n = 17$)	14 (82.4)	16 (94.1)	1.133	0.287
Thrombosis ($n = 5$)	2 (40.0)	5 (100)	4.286	**0.038**

CaW, carotid web; CEUS, contrast-enhanced ultrasound. The bold values means p < 0.05.

There are many diagnostic methods for identifying CaWs. DSA has high temporal and spatial resolution, it can provide dynamic information on regional blood flow, which is the gold standard for CaW diagnosis (9). However, DSA is invasive and expensive (33, 34). Therefore, it is not suitable for routine examinations. CTA can quickly obtain high-resolution imaging and reconstructed-imaging in multiple planes (24). It can provide detailed vascular morphology information, and can distinguish between CaW, atherosclerosis, and artery dissection (35). However, CTA does not provide information on hemodynamics and lesion composition, and it exposes patients to radiation and iodine contrast agents (36). Conventional ultrasound is a non-invasive, convenient, and rapid examination method (37). Nevertheless, conventional ultrasound has limited depth and is highly dependent on doctors' subjectivity. CEUS was based

on conventional ultrasound, and has more advantages (38). SonoVue was used as a contrast agent for CEUS, and there were no serious adverse reactions and no significant effects on liver and kidney function, so it was easily accepted by patients. Additionally, it can enhance the carotid lumen, allowing for a more in-depth assessment of arterial wall. CEUS can clearly show plaques in various parts of the vessel by signs of filling defects (39), provide higher image resolution and more quantitative data, such as quantitative plaque angiogenesis (13). Nevertheless, CEUS requires a high level of technical expertise from doctors because of the limited time-of-use of contrast agent. Conventional ultrasound and CEUS are important tools in the detection of carotid artery plaques, which indicates they have good diagnostic value for characterizing carotid artery plaques with cerebrovascular events (40). Some studies explored the diagnostic rate of atherosclerosis by CEUS and conventional ultrasound (41), and the results showed that CEUS could identify atherosclerotic plaques at a higher frequency ($P = 0.02$). Although CEUS does not show a high advantage in the diagnosis of CaW, it does show an advantage in the diagnosis of thrombus. The occurrence of AIS in CaW patients was associated with thrombus (34). Therefore, it is crucial to diagnose thrombosis timely for the treatment and medication of patients.

The treatment strategies for CaW mainly include medical management, CAS, and CEA. However, whether any of these treatment strategies are optimal remains unclear. Medical management alone has a higher recurrence rate (25). Although surgery is a first-line treatment strategy, patients may be at risk of vascular occlusion and more severe carotid stenosis (25, 42). CAS is the preferred treatment strategy because of its safety and effectiveness (43). Moreover, it has fewer perioperative complications (44). In this study, medical management, CAS, and CEA were used. The medical management in this study was antiplatelet therapy, including aspirin and cilostazol tablets. Antiplatelet therapy was chosen in most studies, and anticoagulant therapy was recommended by only few physicians (35). In a recent paper, Guglielmi et al. showed that 93% of ipsilateral CaW patients received drug therapy. Most of these patients were treated with antiplatelet therapy. However, the incidence of recurrent stroke was relatively higher in patients receiving anticoagulant therapy (27). Therefore, antiplatelet therapy is a reasonable treatment strategy in the patients with transient ischemic stroke or minor stroke (6). We suggested that antiplatelet therapy can be used in asymptomatic patients or patients with low stenosis rate of carotid artery, and surgical intervention is preferred for CaW patients with recurrent ischemic stroke. During the follow-up period, there was no recurrence of stroke in the CaW patients and the prognosis was good, indicating that these three methods are safe and effective. Due to the short follow-up period, long-term follow-up studies can be carried out in the future to explore the impact of different treatment strategies on the long-term prognosis of CaW patients.

CaW should be considered as a factor in patients with cryptogenic stroke. Doctors should improve their understanding of CaWs because CaW has a high risk of recurrence and early recognition and treatment are needed to help decrease the risk of additional strokes (3). This paper has several limitations. We only analyzed 17 CaW patients, which is a small sample size. The large sample size and multi-center studies are needed to verify our views in the future. The second limitation was the absence of histopathological verification. Finally, we did not compare the diagnostic rates of CaW between CTA and CEUS.

CONCLUSIONS

CEUS may have a higher diagnostic accuracy for CaW with thrombosis, and it has a higher clinical application prospect for CaW patients.

DATA AVAILABILITY STATEMENT

The raw data supporting the conclusions of this article will be made available by the authors, without undue reservation.

ETHICS STATEMENT

Ethical review and approval was not required for the study on human participants in accordance with the local legislation and institutional requirements. The patients/participants provided their written informed consent to participate in this study. Written informed consent was obtained from the individual(s) for the publication of any potentially identifiable images or data included in this article.

AUTHOR CONTRIBUTIONS

QZ and RL interpreted the data and drafted the manuscript. SF and FQ were responsible for the study coordination and implementation. WH and CT were responsible for design and organization. YZ acquired the data and designed the research. XL was responsible for funding and supervision. All authors contributed to the article and approved the submitted version.

FUNDING

This work was supported by the National Natural Science Foundation of China (U20A20357), the Fundamental Research Funds for the Central Universities (WK9110000056), and by Program for Innovative Research Team of the First Affiliated Hospital of USTC.

ACKNOWLEDGMENTS

We gratefully acknowledge the patients for their consent and all the participants for their work.

SUPPLEMENTARY MATERIAL

The Supplementary Material for this article can be found online at: https://www.frontiersin.org/articles/10.3389/fneur.2022.860979/full#supplementary-material

REFERENCES

1. Feigin VL, Krishnamurthi R. Stroke prevention in the developing world. *Stroke.* (2011) 42:3655–8. doi: 10.1161/STROKEAHA.110.596858
2. Wolosker N, Portugal MFC, da Silva MFA, Massaud R, Amaro E Jr., Jerussalmy C, et al. Epidemiological analysis of 37,424 carotid artery stenosis intervention procedures during 11 years in the public health system in brazil: stenting has been more common than endarterectomy. *Ann Vasc Surg.* (2021) 76:269–75. doi: 10.1016/j.avsg.2021.05.011
3. Mac Grory B, Nossek E, Reznik ME, Schrag M, Jayaraman M, McTaggart R, et al. Ipsilateral internal carotid artery web and acute ischemic stroke: a cohort study, systematic review and meta-analysis. *PLoS ONE.* (2021) 16:e0257697. doi: 10.1371/journal.pone.0257697
4. Rzepka M, Chmiela T, Bosowska J, Cebula M, Krzystanek E. Fibromuscular dysplasia/carotid web in angio-Ct imaging: a rare cause of ischemic stroke. *Medicina.* (2021) 57. doi: 10.3390/medicina57101112
5. Joux J, Chausson N, Jeannin S, Saint-Vil M, Mejdoubi M, Hennequin JL, et al. Carotid-bulb atypical fibromuscular dysplasia in young afro-caribbean patients with stroke. *Stroke.* (2014) 45:3711–3. doi: 10.1161/STROKEAHA.114.007313
6. Mac Grory B, Emmer BJ, Roosendaal SD, Zagzag D, Yaghi S, Nossek E. Carotid web: an occult mechanism of embolic stroke. *J Neurol Neurosurg Psychiatry.* (2020) 91:1283–9. doi: 10.1136/jnnp-2020-323938
7. Connett MC, Lansche JM. Fibromuscular hyperplasia of the internal carotid artery: Report of a case. *Ann Surg.* (1965) 162:59–62. doi: 10.1097/00000658-196507000-00010
8. Momose KJ, New PF. Non-atheromatous stenosis and occlusion of the internal carotid artery and its main branches. *Am J Roentgenol Radium Ther Nucl Med.* (1973) 118:550–66. doi: 10.2214/ajr.118.3.550
9. Olindo S, Marnat G, Chausson N, Turpinat C, Smadja D, Gaillard N. Carotid webs associated with ischemic stroke. Updated general review and research directions. *Rev Neurol.* (2021) 177:627–38. doi: 10.1016/j.neurol.2020.09.007
10. Park CC, El Sayed R, Risk BB, Haussen DC, Nogueira RG, Oshinski JN, et al. Carotid webs produce greater hemodynamic disturbances than atherosclerotic disease: a Dsa time-density curve study. *J Neurointerv Surg.* (2021). doi: 10.1136/neurintsurg-2021-017588
11. Osehobo EM, Nogueira RG, Koneru S, Al-Bayati AR, de Camara CP, Nahab F, et al. Carotid web: an under-recognized and misdiagnosed ischemic stroke etiology. *J Neurointerv Surg.* (2021). doi: 10.1136/neurintsurg-2021-017306
12. Mi X, Zhao Y, Shu J. A case of cryptogenic ischemic stroke caused by a carotid web. *Acta Neurol Belg.* (2021) 121:1847–9. doi: 10.1007/s13760-020-01326-1
13. Cismaru G, Serban T, Tirpe A. Ultrasound methods in the evaluation of atherosclerosis: from pathophysiology to clinic. *Biomedicines.* (2021) 9. doi: 10.3390/biomedicines9040418
14. Deyama J, Nakamura T, Takishima I, Fujioka D, Kawabata K, Obata JE, et al. Contrast-enhanced ultrasound imaging of carotid plaque neovascularization is useful for identifying high-risk patients with coronary artery disease. *Circ J.* (2013) 77:1499–507. doi: 10.1253/circj.CJ-12-1529
15. Kono Y, Pinnell SP, Sirlin CB, Sparks SR, Georgy B, Wong W, et al. Carotid arteries: contrast-enhanced us angiography–preliminary clinical experience. *Radiology.* (2004) 230:561–8. doi: 10.1148/radiol.2302020318
16. Zhu C, Li Z, Ju Y, Zhao X. Detection of carotid webs by Ct angiography, high-resolution Mri, and ultrasound. *J Neuroimaging.* (2021) 31:71–5. doi: 10.1111/jon.12784
17. Russo T, Felzani G, Marini C. Stroke in the very old: a systematic review of studies on incidence, outcome, and resource use. *J Aging Res.* (2011) 2011:108785. doi: 10.4061/2011/108785
18. Sudre J, Venditti L, Ancelet C, Chassin O, Sarov M, Smadja D, et al. Reperfusion therapy for acute ischemic stroke in older people: an observational real-life study. *J Am Geriatr Soc.* (2021) 69:3167–76. doi: 10.1111/jgs.17394
19. Mahe I, Caulin C, Bergmann JF. [Age, an independent risk factor for thrombosis. Epidemiologic Data]. *Presse Med.* (2005) 34:878–86. doi: 10.1016/s0755-4982(05)84068-0
20. Madaelil TP, Grossberg JA, Nogueira RG, Anderson A, Barreira C, Frankel M, et al. Multimodality imaging in carotid web. *Front Neurol.* (2019) 10:220. doi: 10.3389/fneur.2019.00220
21. Semerano A, Mamadou Z, Desilles JP, Sabben C, Bacigaluppi M, Piotin M, et al. Carotid webs in large vessel occlusion stroke: clinical, radiological and thrombus histopathological findings. *J Neurol Sci.* (2021) 427:117550. doi: 10.1016/j.jns.2021.117550
22. Ozaki D, Endo T, Suzuki H, Sugiyama SI, Endo K, Itabashi R, et al. Carotid web leads to new thrombus formation: computational fluid dynamic analysis coupled with histological evidence. *Acta Neurochir.* (2020) 162:2583–8. doi: 10.1007/s00701-020-04272-2
23. Gao M, Lei J. Image and clinical analysis of common carotid web: a case report. *BMC Med Imaging.* (2021) 21:1. doi: 10.1186/s12880-020-00536-6
24. Wang Y, Xu J, Zhao X, Wang D, Wang C, Liu L, et al. Association of hypertension with stroke recurrence depends on ischemic stroke subtype. *stroke.* (2013) 44:1232–7. doi: 10.1161/STROKEAHA.111.000302
25. Olindo S, Chausson N, Signate A, Mecharles S, Hennequin JL, Saint-Vil M, et al. Stroke recurrence in first-ever symptomatic carotid web: a cohort study. *J Stroke.* (2021) 23:253–62. doi: 10.5853/jos.2020.05225
26. Compagne KCJ, van Es A, Berkhemer OA, Borst J, Roos Y, van Oostenbrugge RJ, et al. Prevalence of carotid web in patients with acute intracranial stroke due to intracranial large vessel occlusion. *Radiology.* (2018) 286:1000–7. doi: 10.1148/radiol.2017170094
27. Guglielmi V, Compagne KCJ, Sarrami AH, Sluis WM, van den Berg LA, van der Sluijs PM, et al. Assessment of recurrent stroke risk in patients with a carotid web. *JAMA Neurol.* (2021) 78:826–33. doi: 10.1001/jamaneurol.2021.1101
28. Choi PM, Singh D, Trivedi A, Qazi E, George D, Wong J, et al. Carotid webs and recurrent ischemic strokes in the era of Ct angiography. *Am J Neuroradiol.* (2015) 36:2134–9. doi: 10.3174/ajnr.A4431
29. Koge J, Matsumoto S, Nakahara I, Ishii A, Hatano T, Tanaka Y, et al. Impact of thrombus migration on clinical outcomes in patients with internal carotid artery occlusions and patent middle cerebral artery. *J Neurol Sci.* (2020) 412:116737. doi: 10.1016/j.jns.2020.116737
30. Nurmohamed MT, Buller HR. ten Cate JW. Physiological changes due to age implications for the prevention and treatment of thrombosis in older patients. *Drugs Aging.* (1994) 5:20–33. doi: 10.2165/00002512-199405010-00003
31. Haidl H, Cimenti C, Leschnik B, Zach D, Muntean W. Age-dependency of thrombin generation measured by means of calibrated automated thrombography (cat). *Thromb Haemost.* (2006) 95:772–5. doi: 10.1160/TH05-10-0685
32. Cui L, Xing Y, Zhou Y, Wang L, Liu K, Zhang D, et al. Carotid intraplaque neovascularisation as a predictive factor for future vascular events in patients with mild and moderate carotid stenosis: an observational prospective study. *Ther Adv Neurol Disord.* (2021) 14. doi: 10.1177/17562864211023992
33. Lenck S, Labeyrie MA, Saint-Maurice JP, Tarlov N, Houdart E. Diaphragms of the carotid and vertebral arteries: an under-diagnosed cause of ischaemic stroke. *Eur J Neurol.* (2014) 21:586–93. doi: 10.1111/ene.12343
34. Ben Z, Wang J, Zhan J, Chen S. Ultrasonic characteristics of carotid webs. *Neuroradiology.* (2022) 64:95–8. doi: 10.1007/s00234-021-02757-0
35. Kim SJ, Nogueira RG, Haussen DC. Current understanding and gaps in research of carotid webs in ischemic strokes: a review. *JAMA Neurol.* (2019) 76:355–61. doi: 10.1001/jamaneurol.2018.3366
36. Krasteva MP, Diamantaras AA, Siller T, Mordasini P, Heldner MR. Symptomatic carotid web in a female patient. *SAGE Open Med Case Rep.* (2020) 8. doi: 10.1177/2050313X20940540
37. Sparchez Z. Interventional ultrasound beyond the classical abdominal applications. Are guidelines for other applications urgent needed? *Med Ultrason.* (2015) 17:271–2. doi: 10.11152/mu.2013.2066.173.zsp
38. Guang Y, He W, Ning B, Zhang H, Yin C, Zhao M, et al. Deep learning-based carotid plaque vulnerability classification with multicentre contrast-enhanced ultrasound video: a comparative diagnostic study. *BMJ Open.* (2021) 11:e047528. doi: 10.1136/bmjopen-2020-047528
39. Rafailidis V, Charitanti A, Tegos T, Destanis E, Chryssogonidis I. Contrast-enhanced ultrasound of the carotid system: a review of the current literature. *J Ultrasound.* (2017) 20:97–109. doi: 10.1007/s40477-017-0239-4
40. Wang Q, Huang Y, Zhang Y, Wang Y, Xie Y, Zhang L, et al. Carotid artery vulnerable plaque model for cerebrovascular events by conventional

ultrasound & contrast-enhanced ultrasound: a preliminary study. *Clin Hemorheol Microcirc.* (2021). doi: 10.3233/CH-211216
41. Shah BN, Chahal NS, Kooner JS, Senior R. Contrast-enhanced ultrasonography vs B-mode ultrasound for visualization of intima-media thickness and detection of plaques in human carotid arteries. *Echocardiography.* (2017) 34:723–30. doi: 10.1111/echo.13513
42. Multon S, Denier C, Charbonneau P, Sarov M, Boulate D, Mitilian D, et al. Carotid webs management in symptomatic patients. *J Vasc Surg.* (2021) 73:1290–7. doi: 10.1016/j.jvs.2020.08.035
43. Mathew S, Davidson DD, Tejada J, Martinez M, Kovoor J. Safety and feasibility of carotid revascularization in patients with cerebral embolic strokes associated with carotid webs and histopathology revisited. *Interv Neuroradiol.* (2021) 27:235–40. doi: 10.1177/1591019920980271
44. Haynes J, Raz E, Tanweer O, Shapiro M, Esparza R, Zagzag D, et al. Endarterectomy for symptomatic internal carotid artery web. *J Neurosurg.* 1–8. doi: 10.3171/2020.5

Conflict of Interest: The authors declare that the research was conducted in the absence of any commercial or financial relationships that could be construed as a potential conflict of interest.

frontiers | Frontiers in Neurology

ORIGINAL RESEARCH
published: 17 May 2022
doi: 10.3389/fneur.2022.860827

Potential Embolic Sources Differ in Patients With Embolic Stroke of Undetermined Source According to Age: A 15-Year Study

Yan Hou[1,2], *Ahmed Elmashad*[2], *Ilene Staff*[3], *Mark Alberts*[1,2] *and Amre Nouh*[1,2]*

[1] Department of Neurology, Hartford Hospital, Hartford, CT, United States, [2] Department of Neurology, University of Connecticut, Farmington, CT, United States, [3] Department of Research, Hartford Hospital, Hartford, CT, United States

Introduction: Understanding the potential embolic source in young patients with ESUS may improve the diagnosis and treatment of such patients.

Hypothesis: Potential embolic sources (PES) differ in young vs. older patients with ESUS, and, therefore, not all patients with ESUS have the same risk profile for stroke recurrence.

Methods: Young patients (age 18-49) with ESUS, who were admitted to our stroke center from 2006 to 2019, were identified retrospectively and matched with next consecutive older patients (age 50–99) with ESUS by admission date. PES were categorized as atrial cardiopathy, AFib diagnosed during follow-up, left ventricular disease (LVD), cardiac valvular disease (CVD), PFO or atrial septal aneurysm (ASA), and arterial disease. Patients, who had cancer or thrombophilia, were excluded. The type and number of PES and stroke recurrence rates were determined and compared between young and older patients.

Results: In young patients (55.3% women, median age 39 years), the most common PES was PFO/ASA, and the rate of other PES was low (2–7%). Half of the young patients (54.1%) had a single PES, only 10% had multiple PES, and 35.3% of young patients did not have any PES identified. In older patients (41.7% women, median age 74 years), the 3 most common PES were atrial cardiopathy (38.1%), LVD (35.7%), and arterial disease (23.8%). Nearly half of older patients (42.9%) had multiple PES. The rate of stroke recurrence tended to be lower in young patients as compared to older patients (4.9 vs. 11.4%, $p = 0.29$). During a median follow-up of 3 years, only 3 young patients (4.9%) had a recurrent stroke, and two of them had unclosed PFO. There were no recurrent strokes among young patients with no PES identified.

Conclusions: It was noted that PES differ in patients with ESUS according to age and differences in recurrence. PFO is the only common PES in young patients with ESUS. Future studies prospectively evaluating PES in both age groups are needed.

Keywords: ESUS, potential embolic source, PFO, ischemic stroke in young adults, AFib

OPEN ACCESS

Edited by:
Bing Tian,
Naval Medical University, China

Reviewed by:
Ching-Hui Sia,
National University of Singapore, Singapore
Simona Lattanzi,
Marche Polytechnic University, Italy

***Correspondence:**
Amre Nouh
amre.nouh@hhchealth.org

Specialty section:
This article was submitted to Stroke, a section of the journal Frontiers in Neurology

Received: *23 January 2022*
Accepted: *14 April 2022*
Published: *17 May 2022*

Citation:
Hou Y, Elmashad A, Staff I, Alberts M and Nouh A (2022) Potential Embolic Sources Differ in Patients With Embolic Stroke of Undetermined Source According to Age: A 15-Year Study. Front. Neurol. 13:860827. doi: 10.3389/fneur.2022.860827

INTRODUCTION

The concept of embolic stroke of undetermined source (ESUS) was introduced by the cryptogenic stroke/ESUS international working group in 2014 (1). In patients with ESUS, the causal etiology might not be identified, but there are many potential embolic sources, also referred to as potential embolic sources (PES) (2, 3). These underlying PES are heterogeneous, but it is hypothesized that emboli are either cardiogenic, arteriogenic, or paradoxical from the veins. At present, the main challenge in ESUS remains how to decide on optimal secondary stroke prevention in the absence of a known stroke mechanism. The efficacy of antithrombotic agents for secondary prevention in ESUS was tested in the NAVIGATE ESUS and RE-SPECT ESUS trials. Results showed that anticoagulation was not superior to aspirin for the prevention of stroke in patients with ESUS (4, 5). Ischemic stroke in young adults is usually defined clinically by an age threshold of <50 at stroke occurrence, based on different risk factors and clinical characteristics between young and older patients with stroke (6). Approximately 15–20% of patients with ESUS are young patients (7, 8). However, previous RCTs and studies included mainly older patients at a mean age of around 65 years (2–5). There is limited information about PES and the associated risk of recurrent stroke in young patients with ESUS. In this retrospective study, we evaluated the rate and overlap degree of previously reported PES and assessed the rate of stroke recurrence per PES in young patients with ESUS and compared them with older patients with ESUS.

MATERIALS AND METHODS

We retrospectively reviewed young patients (age 18–49) with ESUS who were admitted and followed at Hartford Hospital from 2006 to 2019. Each young patient was matched with the next consecutive older patient (age 50–99) with ESUS by admission date within the same period.

The ESUS was defined as non-lacunar brain infarct in the absence of extracranial or intracranial atherosclerosis causing ≥50% luminal stenosis in arteries supplying the area of infarcts, established major cardioembolic source, other specific cause (e.g., vasculitis/vasculopathy, dissection, vasospasm, or thrombophilia) according to the criteria proposed by the Cryptogenic Stroke/ESUS International Working Group and previous studies (1). The minimal standard evaluation was required for the diagnosis of ESUS, which included transthoracic or transesophageal echocardiography, CTA/MRA of head and neck, 12-lead EKG, at least 24 hours of continuous heart rhythm monitoring, and screening for inherited thrombophilia in patients younger than 50-year-old (1, 9). We did not include cancer as PES as hypercoagulability and embolism are both possible mechanisms of cancer-related stroke.

According to previous studies, we used the definitions of PES described in **Table 1**: categorized as atrial cardiopathy, AFib diagnosed during follow-up, left ventricular disease (LVD), cardiac valvular disease (CVD), PFO and/or Atrial septal aneurysm (ASA), and arterial disease (1–3). In a single patient, there may be none, single, or multiple PES. Atrial cardiopathy was defined as left atrial (LA) volume index >34 ml/m^2 according to American Society of Echocardiography guidelines (10). AFib was diagnosed by EKG, 30-day or implanted heart rhythm monitor during follow-up.

TABLE 1 | Definition of potential embolic sources (PES).

Atrial cardiopathy	Left atrium dilation on echo[a]
Afib/Aflutter at follow-up	Atrial Fib/flutter, detected by 30 day or implanted event monitor or by any EKG performed after discharge
Left ventricular dysfunction	heart failure history, or LV ejection fraction was <35%[b], LV hypertrophy, moderate diastolic dysfunction, global or regional wall motion abnormality
Cardiac valve disease	bioprosthetic valve, mitral valve prolapse, moderate to severe annular calcification, moderate stenosis or regurgitation of mitral or aortic valve
PFO	PFO and/or ASA detected on Echo
Arterial disease	ipsilateral atherosclerotic plaque causing luminal stenosis of <50% or complex aortic arch atherosclerotic plaque[c]

[a] *Left atrial dilation was defined according to Echo lab criteria based on LA volume index >34 ml/m^2.*
[b] *Patients with LVEF ≤25% was excluded.*
[c] *Complex aortic plaque defined as mobile, ulcerated, and/or size ≥4 mm on CTA or TEE.*

Baseline and clinical stroke characteristics were compared between young and older patients using proportions for categorical variables and medians with interquartile range for continuous variables. The rate of different types of PES and numbers of PES were determined and compared between young and older patients with ESUS. After discharge, patients were followed up at Hartford Healthcare for at least one year with the available medical record. Patients who did not follow with Hartford Healthcare for at least one year were considered as lost to follow-up and were not included in the study. The recurrent ischemic stroke was diagnosed by repeated brain MRI or head CT during follow-up. The rate of stroke recurrence during follow-up was assessed by different types of PES, numbers of PES, and comparison with young and older patients with ESUS. All comparisons were performed using the Pearson Chi-square test with SPSS and $p<0.05$ as the significance level.

RESULTS

A total of 85 young patients with ESUS (55.3% women, median age 39 years) were identified and matched with 84 older patients (41.7% women, median age 74 years). The baseline and clinical characteristics of patients are summarized in **Table 2**. Young patients with ESUS tended to be women and ethnic minorities as compared to older patients.

As expected, a lower proportion of young patients with ESUS had hypertension, hyperlipidemia, and diabetes, although both young and older patients with ESUS had a similar rate of active smoking. The initial NIHSS at admission as well as the rate of large vessel occlusion were similar in young and older patients with ESUS, with young patients tending to receive mechanical thrombectomy. Young

TABLE 2 | Baseline and clinical characteristics.

	Baseline and clinical characteristics		
	Young ESUS N = 85	**Older ESUS N = 84**	***P***
Age	39 (32–44)	74 (63–81)	<0.001
Female	55.3% (47/85)	41.7% (35/84)	0.08
Caucasian	62.4% (53/85)	77.4% (65/84)	0.07
Afr-Am	12.9% (11/85)	4.8% (4/84)	
Other race	24.7% (21/85)	17.9% (15/84)	
Hypertension	23.5% (20/85)	81.0% (68/84)	<0.001
Hyperlipidemia	24.7% (21/85)	61.9% (52/84)	<0.001
Diabetes	17.6% (15/85)	32.1% (27/84)	0.03
Active Smoking	20.0% (17/85)	14.1% (12/84)	0.33
NIHSS (0-5)	65.9% (54/82)	62.0% (49/79)	0.88
NIHSS (6–9)	14.6% (12/82)	16.5% (13/79)	
NIHSS (≥10)	19.5% (16/82)	21.5% (17/79)	
LVO	22.4% (19/85)	17.9% (15/84)	0.63
Thrombectomy	14.1% (12/85)	6.0% (5/84)	0.08
Discharge home	71.6% (58/81)	48.0% (36/75)	0.003
Discharge rehab	28.4% (23/81)	52.0% (39/75)	
Antiplatelet	87.8% (72/82)	79.8% (67/84)	0.16
Anticoagulation	12.2% (10/82)	20.2 (17/84)	
Recurrence after 1 year	2.6% (2/77)	6.3% (5/79)	0.26
Recurrence during follow-up	4.1% (3/74)	11.4% (9/79)	0.29

Data are given as a percentage (number). Age is presented as median (interquartile range).

patients were more likely to be discharged home compared to older patients. Most young (87.8%) and older (79.8%) patients with ESUS were treated with antiplatelet agents with lower rates of anticoagulation among younger patients. Young patients with ESUS tended to have a lower rate of recurrent embolic stroke during follow-up as compared to older patients.

The most common PES in young patients with ESUS was PFO, with or without an atrial septal defect (ASA) (42.4%). Other types of PES were only identified in 2–7% of young patients with ESUS (**Table 3**). About half of young patients (54.1%) with ESUS were found to have a single PES, only 10% had multiple PES and about one-third (35.3%) did not have any PES identified (**Table 3**). In older patients with ESUS, the 3 most common PES were atrial cardiopathy (38.1%), LVD (35.7%), and arterial disease (23.8%). wDuring follow up, AFib was detected in 17.9% of older patients (about 32% of older patients with ESUS had a 30-day monitor and 11% had implanted monitors) as compared to in 2.4% of young patients with ESUS (∼20% of young patients with ESUS had a 30-day monitor and 5% received implanted monitor). As compared to young patients, at least one PES was identified in 78.6% of older patients with ESUS. Nearly half (42.9%) of older patients had multiple PES (**Table 3**).

TABLE 3 | Rate of PES by types and numbers.

	Young ESUS *N* = 85	**Old ESUS *N* = 84**	***P***
Individual PES Atrial cardiopathy	2.4% (2)	38.1% (32)	<0.001
Afib	2.4% (2)	17.9% (15)	0.001
Left ventricular dysfunction	5.9% (5)	35.7% (30)	<0.001
Cardiac valve disease	5.9% (5)	16.7% (14)	0.026
PFO/ASA	42.4% (36)	9.5% (8)	<0.001
Arterial disease	7.1% (6)	23.8% (20)	0.003
Number of PES			
NO PES	35.3% (30)	21.4% (18)	<0.001
Single PES	54.1% (46)	35.7% (30)	
Multiple PES	10.6% (9)	42.9% (36)	

Data are given as percentages (numbers).

The rate of recurrent embolic stroke by PES is summarized in **Table 4**. During a median follow-up of 3 years, 13% of young patients with ESUS and 6% of older patients with ESUS were lost follow-up. About one out of 10 (11.4%) older patients with ESUS had a recurrent stroke. Older patients who were found to have A-fib during follow-up tended to have the highest rate of stroke recurrence (26.7%). Older patients who had multiple PES had a rate of 15.8% stroke recurrence compared to those who had single or no PES at 6.7% and 5.6%, respectively. Only one out of 25 young patients with ESUS (4.1%) had a recurrent stroke. Among the three young patients who had a recurrent stroke, two patients had PFO without closure and one patient

TABLE 4 | Recurrent embolic stroke by type and number of PES.

	Stroke recurrence	
PES	**Young ESUS**	**Old ESUS**
Atrial cardiopathy	0/2	18.8% (6/32)
Afib at F/U	0/2	26.7% (4/15)
Left ventricular dysfunction	0/5	13.3% (4/30)
Cardiac valve disease	20.0% (1/5)	14.2% (2/14)
PFO/ASA	5.6% (2/36)	12.5% (1/8)
Arterial disease	0/6	10% (2/20)
No PES	0/30	5.6% (1/18)
Single PES	6.5% (3/46)	6.7% (2/30)
Multiple PES	0/7	15.8% (6/38)
Total	4.1% (3/74)	11.4% (9/79)

Data are given as a percentage (number).

had cardiac valve disease. There were no recurrent strokes among young patients with no PES identified.

DISCUSSION

In this observational study, PFO and/or ASA were the only common PES in young patients with ESUS and found in nearly half (42%) of young patients. In contrast, PFO and/or ASA were detected in less than 10% of older patients, albeit many older patients who usually underwent transthoracic echocardiography without bubble study. Other PES, such as atrial cardiopathy, LVD, arterial disease, AFib, and cardiac valve disease, were frequently identified in about 15–40% of older patients, but they were uncommonly detected in less than 10% of young patients. Overall, young patients with ESUS had a lower burden and less overlap of PES than older patients. Half (54%) of young patients had single PES, and one-third of young patients did not have any PES identified, whereas nearly half of older patients had two or three PES. Our findings are consistent with a recent study that identified three main clusters of patients with ESUS according to clinical characteristics and cerebrovascular risk factors. Those clusters were correlated to the potential arteriogenic, cardiogenic, and paradoxical source of embolic stroke. One cluster was associated with PFO in patients at young ages (11).

According to a systemic review including most studies of older patients, ESUS is associated with a recurrent stroke rate of 4.5% per year (8). Among the young patients registered to the Helsinki Young Stroke Registry, young patients with ESUS had a relatively low cumulative risk of recurrent stroke that is about 1.95% annually over a median follow-up time of 10 years (7). Again, our study showed young patients with ESUS tended to have a lower rate of stroke recurrence as compared with older patients with ESUS. Only three young patients had a recurrent stroke, and two of them had PFO without closure. In recent years, emerging evidence indicates that paradoxical embolism through PFO is a potential causal mechanism of ESUS (12). PFO with large shunting and/or ASA was associated with a high risk for recurrent stroke (12, 13). Two recent RCTs found that percutaneous closure of PFO in appropriately selected patients decreases the risk of recurrent stroke in young patients with ESUS (14, 15). Only one patient with cardiac valve disease had a recurrent stroke for other PES. The rate of other PES-associated stroke recurrence is difficult to be interpreted in our study because of their low detection rate in young patients with ESUS. As compared to young patients, older patients who were found to have A-fib during follow-up tended to have the highest rate of stroke recurrence (26.7%). And all other PES-associated stroke recurrence rate was 10–20% in older patients with ESUS. However, given half of older patients had multiple PES, it is difficult to determine the PES that are potentially implicated in each patient. Previous studies found that older patients with multiple PES were not at increased risk of recurrent stroke as compared to patients who had single PES (2, 3). The finding may indicate high-risk PES, but not multiple low-risk PES, play the key role in stroke recurrence. Young patients with ESUS had less overlap of PES; our study showed that among 10% of young patients who had two PES identified, none of them had a recurrent stroke.

The low rate of PES in young patients with ESUS is partly explained by the low rate of traditional cerebrovascular risk factors. In addition, according to recommendations from the international ESUS working group, only minimal standard evaluation is required to rule out established etiology, other diagnostic tests such as malignancy screening, hypercoagulable testing, 30-day or implanted rhythm monitors, TEE, and special MRIs may be considered on a case-by-case basis (1). PES detection rate may be higher if all the young patients underwent TEE, prolonged cardiac monitoring, and more advanced diagnostic workup. It is important to note, however, that occult AFib was a rare finding in younger patients with ESUS in our study, and of low yield. High-resolution MRI had higher sensitivity and specificity in detecting vessel wall abnormality such as atheroma and dissection (16, 17). If high-resolution MRI can be used in routine practice, it may help to identify more PES in young patients. Furthermore, young stroke patients have unique risk factors such as migraines, the use of oral contraceptive pills, or illicit drugs (18–20). Mechanisms other than embolisms such as hypercoagulability, vasospasm, and *in-situ* thrombosis may be the cause of cryptogenic stroke in young patients. Cancer, especially active cancer is considered a risk factor for ischemic stroke in young adults (21, 22). The hypercoagulable state is the most important mechanism of malignancy-associated ischemic stroke and other potential mechanisms include marantic endocarditis, the effect of chemotherapy or radiotherapy, accelerated atherosclerosis, and intravascular disease (Lymphoma) (22). Inherited thrombophilia is a group of disorders including factor V Leiden or Prothrombin mutation, deficiency of Antithrombin, protein C and protein S, and hyperhomocysteinemia caused by mutations in methylenetetrahydrofolate reductase (23, 24). Studies have shown an inconsistent or weak association between inherited thrombophilia and ischemic stroke (23–25), although a moderately stronger risk was reported in a subgroup of younger patients (25, 26). Our study focused on ESUS with embolism as a likely cause of stroke and we did not include

patients with malignancy or inherited thrombophilia, in which a hypercoagulable state is a potential mechanism. However, malignancy and thrombophilia are important risk factors for cryptogenic stroke in young adults and they can cause imaging patterns similar as embolic stroke. Of note, our study shows PES was not identified in one-third of young patients with ESUS, and none of those patients had a recurrent stroke. Although the causal mechanism remains unknown, this finding is reassuring that stroke recurrence was rare in these young patients with ESUS without PES identified.

The findings of our study suggest young patients differ from older patients with ESUS. Although the two groups have similar stroke severity and rate of large vessel occlusion, they are different regarding risk factors, possible embolic source, and stroke recurrence. Current RCTs testing antithrombotics for stroke prevention in ESUS mainly focused on older patients and the finding would not be well-applicable to young patients (5, 6). Severe atrial cardiopathy was identified as an independent risk factor in the absence of AFib in patients with ESUS (27). However, due to the low prevalence of atrial cardiopathy in younger patients, the ongoing ARCADIA (Atrial Cardiopathy and Antithrombotic Drugs in Prevention after Cryptogenic Stroke) trial only enrolls patients with ESUS older than 45 years (28). PFO is the only common PES in young patients with ESUS. Given the low rate of other PES, their roles in stroke recurrence are less significant in young patients with ESUS. Future studies in young patients with ESUS should focus on PFO-related stroke to better define features of high-risk PFO and identify appropriate patients to benefit from PFO closure as it will further lower stroke recurrence.

Strengths and Limitations

Our study is the first study to assess PES and its associated rate of stroke recurrence in young patients with ESUS over 15 years. However, due to a single-center design, we were unable to estimate the risk of recurrent stroke by PES given the relatively small number of patients. One common limitation of all PES studies is that the rate and overlap of PES are usually underestimated. PES in our study was defined according to criteria used in NAVIGATE ESUS study and reviewed by an international ESUS working group (1, 2). Many recently identified PES such as new biomarkers of atrial cardiopathy, including NT-proBNP and ECG indexes (28–30), pulmonary arteriovenous fistula, and carotid web, were not included in the study (31, 32). Another common limitation in PES studies is that the criteria also likely include many low-risk PES. Those PES are usually associated with a very low rate of stroke and are often likely incidental without clinical significance. In the future, a prospective multi-center study better defined PES, with a sufficient sample size and completion of extensive diagnostic tests, is needed to assess the PES burden and associated risk of stroke recurrence in young patients with ESUS.

In conclusion, PES differs in patients with ESUS according to age. PFO is the only common PES in young patients with ESUS. Young patients have less burden and overlap with other PES that are commonly identified in older patients. Future research should continue to identify high-risk PES specific to young patients and verify features of high-risk PFO.

DATA AVAILABILITY STATEMENT

The raw data supporting the conclusions of this article will be made available by the authors, without undue reservation.

ETHICS STATEMENT

The studies involving human participants were reviewed and approved by IRB of Research Center at Hartford Hospital. Written informed consent for participation was not required for this study in accordance with the National Legislation and the Institutional Requirements.

AUTHOR CONTRIBUTIONS

YH: study design, data collection, and manuscript writing and revision. AN: study design and manuscript revision. MA: manuscript revision. IS: data analysis and manuscript revision. AE: data collection. All authors contributed to the article and approved the submitted version.

ACKNOWLEDGMENTS

The authors would like to thank Dr. Walter N. Kernan at Yale-New Haven Health for his suggestions on study design.

REFERENCES

1. Hart RG, Diener HC, Coutts SB, Easton JD, Granger CB, O'Donnell MJ, et al. Cryptogenic Stroke/ESUS international working group. embolic strokes of undetermined source: the case for a new clinical construct. *Lancet Neurol.* (2014) 13:429–38. doi: 10.1016/S1474-4422(13)70310-7
2. Ntaios G, Perlepe K, Lambrou D, Sirimarco G, Strambo D, Eskandari A, et al. Prevalence and overlap of potential embolic sources in patients with embolic stroke of undetermined source. *J Am Heart Assoc.* (2019) 8:e012858. doi: 10.1161/JAHA.119.012858
3. Ntaios G, Pearce LA, Veltkamp R, Sharma M, Kasner SE. Korompoki E et al. NAVIGATE ESUS investigators potential embolic sources and outcomes in embolic stroke of undetermined source in the NAVIGATE-ESUS trial. *Stroke.* (2020) 51:1797–804. doi: 10.1161/STROKEAHA.119.028669
4. Putaala J, Metso AJ, Metso TM, Konkola N, Kraemer Y, Haapaniemi E, et al. Analysis of 1008 consecutive patients aged 15 to 49 with first-ever ischemic stroke: the Helsinki young stroke registry. *Stroke.* (2009) 40:1195–203. doi: 10.1161/STROKEAHA.108.529883
5. Hart RG, Sharma M, Mundl H, Kasner SE, Bangdiwala SI, Berkowitz SD. el al. NAVIGATE ESUS Investigators. rivaroxaban for stroke prevention after embolic stroke of undetermined source. *N Engl J Med.* (2018) 378:2191–201.
6. Diener HC, Sacco RL, Easton JD, Granger CB, Bernstein RA, Uchiyama S, et al. RE-SPECT ESUS steering committee and investigators. dabigatran for prevention of stroke after embolic stroke of undetermined source. *N Engl J Med.* (2019) 380:1906–17. doi: 10.1056/NEJMoa1813959
7. Martinez-Majander N, Aarnio K, Pirinen J, Lumikari T, Nieminen T, Lehto M, et al. Embolic strokes of undetermined source in young adults:

baseline characteristics and long-term outcome. *Eur J Neurol.* (2018) 25:535–41. doi: 10.1111/ene.13540
8. Hart RG, Catanese L, Perera KS, Ntaios G, Connolly SJ. Embolic stroke of undetermined source: a systematic review and clinical update. *Stroke.* (2017) 48:867–72. doi: 10.1161/STROKEAHA.116.016414
9. Morris JG, Singh S, Fisher M. Testing for inherited thrombophilias in arterial stroke: can it cause more harm than good? *Stroke.* (2010) 41:2985–90. doi: 10.1161/STROKEAHA.110.595199
10. Tan BYQ, Ho JSY, Sia CH, Boi Y, Foo ASM, Dalakoti M, et al. Left atrial volume index predicts new-onset atrial fibrillation and stroke recurrence in patients with embolic stroke of undetermined source. *Cerebrovasc Dis.* (2020) 49:285–91. doi: 10.1159/000508211
11. Lattanzi S, Rinaldi C, Pulcini A, Corradetti T, Angelocola S, Zedde ML, et al. Clinical phenotypes of embolic strokes of undetermined source. *Neurol Sci.* (2021) 42:297–300. doi: 10.1007/s10072-020-04700-2
12. Goel SS, Tuzcu EM, Shishehbor MH, de Oliveira EI, Borek PP, Krasuski RA, et al. Morphology of the patent foramen ovale in asymptomatic versus symptomatic (stroke or transient ischemic attack) patients. *Am J Cardiol.* (2009) 103:124–9. doi: 10.1016/j.amjcard.2008.08.036
13. Mas JL, Arquizan C, Lamy C, Zuber M, Cabanes L, Derumeaux G, et al. Patent Foramen Ovale and Atrial Septal Aneurysm Study Group. Recurrent cerebrovascular events associated with patent foramen ovale, atrial septal aneurysm, or both. *N Engl J Med.* (2001) 345:1740–6. doi: 10.1056/NEJMoa011503
14. Søndergaard L, Kasner SE, Rhodes JF, Andersen G, Iversen HK, Nielsen-Kudsk JE, et al. Gore REDUCE clinical study investigators. patent foramen ovale closure or antiplatelet therapy for cryptogenic stroke. *N Engl J Med.* (2017) 377:1033–42. doi: 10.1056/NEJMoa1707404
15. Mas JL, Derumeaux G, Guillon B, Massardier E, Hosseini H, Mechtouff L, et al. CLOSE investigators. patent foramen ovale closure or anticoagulation vs. antiplatelets after stroke. *N Engl J Med.* (2017) 377:1011–21. doi: 10.1056/NEJMoa1705915
16. Yuan X, Cui X, Gu H, Wang M, Dong Y, Cai S, et al. Evaluating cervical artery dissections in young adults: a comparison study between high-resolution MRI and CT angiography. *Int J Cardiovasc Imaging.* (2020) 36:1113–9. doi: 10.1007/s10554-020-01799-4
17. Freilinger TM, Schindler A, Schmidt C, Grimm J, Cyran C, Schwarz F, et al. Prevalence of nonstenosing, complicated atherosclerotic plaques in cryptogenic stroke. *JACC Cardiovasc Imaging.* (2012) 5:397–405. doi: 10.1016/j.jcmg.2012.01.012
18. Bousser MG. Estrogens, migraine, and stroke. *Stroke.* (2004) 35:2652–6. doi: 10.1161/01.STR.0000143223.25843.36
19. Roach RE, Helmerhorst FM, Lijfering WM, Stijnen T, Algra A, Dekkers OM. Combined oral contraceptives: the risk of myocardial infarction and ischemic stroke. *Cochrane Database Syst Rev.* (2015) 2015:CD011054. doi: 10.1002/14651858.CD011054.pub2
20. Fonseca AC, Ferro JM. Drug abuse and stroke. *Curr Neurol Neurosci Rep.* (2013) 13:325. doi: 10.1007/s11910-012-0325-0
21. Aarnio K, Joensuu H, Haapaniemi E, Melkas S, Kaste M, Tatlisumak T, et al. Cancer in young adults with ischemic stroke. *Stroke.* (2015) 46:1601–6. doi: 10.1161/STROKEAHA.115.008694
22. Navi BB, Kasner SE, Elkind MSV, Cushman M, Bang OY, DeAngelis LM. Cancer and embolic stroke of undetermined source. *Stroke.* (2021) 52:1121–30. doi: 10.1161/STROKEAHA.120.032002
23. Chiasakul T, De Jesus E, Tong J, Chen Y, Crowther M, Garcia D, et al. Inherited thrombophilia and the risk of arterial ischemic stroke: a systematic review and meta-analysis. *J Am Heart Assoc.* (2019) 8:e012877. doi: 10.1161/JAHA.119.012877
24. Ho GY, Eikelboom JW, Hankey GJ, Wong CR, Tan SL, Chan JB, et al. Methylenetetrahydrofolate reductase polymorphisms and homocysteine-lowering effect of vitamin therapy in Singaporean stroke patients. *Stroke.* (2006) 37:456–60. doi: 10.1161/01.STR.0000199845.27512.84
25. Alhazzani AA, Kumar A, Selim M. Association between factor v gene polymorphism and risk of ischemic stroke: an updated meta-analysis. *J Stroke Cerebrovasc Dis.* (2018) 27:1252–61. doi: 10.1016/j.jstrokecerebrovasdis.2017.12.006
26. Jiang B, Ryan KA, Hamedani A, Cheng Y, Sparks MJ, Koontz D, et al. Prothrombin G20210A mutation is associated with young-onset stroke: the genetics of early-onset stroke study and meta-analysis. *Stroke.* (2014) 45:961–7. doi: 10.1161/STROKEAHA.113.004063
27. Kamel H, Okin PM, Elkind MS, Iadecola C. Atrial fibrillation and mechanisms of stroke: time for a new model. *Stroke.* (2016) 47:895–900. doi: 10.1161/STROKEAHA.115.012004
28. Kamel H, Longstreth WT Jr, Tirschwell DL, Kronmal RA, Broderick JP, Palesch YY, et al. The AtRial cardiopathy and antithrombotic drugs in prevention after cryptogenic stroke randomized trial: rationale and methods. *Int J Stroke.* (2019) 14:207–14. doi: 10.1177/1747493018799981
29. Bahit MC, Sacco RL, Easton JD, Meyerhoff J, Cronin L, Kleine E, et al. RE-SPECT ESUS Steering Committee and Investigators. predictors of atrial fibrillation development in patients with embolic stroke of undetermined source: an analysis of the RE-SPECT ESUS Trial. *Circulation.* (2021) 144:1738–46. doi: 10.1161/CIRCULATIONAHA.121.055176
30. Li TYW, Yeo LLL, Ho JSY, Leow AS, Chan MY, Dalakoti M, et al. Association of electrocardiographic p-wave markers and atrial fibrillation in embolic stroke of undetermined source. *Cerebrovasc Dis.* (2021) 50:46–53. doi: 10.1159/000512179
31. Sousa S, Vasco Costa N, Carmona C, Coimbra É, Pita F. Recurrent stroke in a young woman with a single pulmonary arteriovenous fistula: an unusual association. *Case Rep Neurol.* (2017) 9:293–8. doi: 10.1159/000484682
32. Mac Grory B, Cheng D, Doberstein C, Jayaraman MV, Yaghi S. Ischemic stroke and internal carotid artery web. *Stroke.* (2019) 50:e31–4. doi: 10.1161/STROKEAHA.118.024014

Conflict of Interest: The authors declare that the research was conducted in the absence of any commercial or financial relationships that could be construed as a potential conflict of interest.

frontiers | Frontiers in Neurology

MINI REVIEW
published: 24 June 2022
doi: 10.3389/fneur.2022.900991

Uncommon Female-Predominant Etiologies of Cryptogenic Stroke

Jing Dong[1] *and Xin Ma*[1,2,3]*

[1] Department of Neurology, Xuanwu Hospital, Capital Medical University, Beijing, China, [2] National Clinical Research Center for Geriatric Disorders, Beijing, China, [3] Clinical Center for Cardio-Cerebrovascular Disease of Capital Medical University, Beijing, China

The etiologies of cryptogenic stroke are complex and heterogeneous. A number of uncommon etiologies are not fully recognized, some of which predominantly affect females. Most of these etiologies are closely related to the hormonal level, reproductive factors, coagulation function, and medications of females. Moreover, once cryptogenic stroke is diagnosed, females tend to have worse outcomes. Therefore, prompt etiological recognition and treatment are crucial for good recovery. The aim of this article is to review advances in exploring uncommon female-predominant etiologies of cryptogenic stroke. These etiologies are categorized into arterial, cardiac, and venous sources. Arterial vasoconstrictive narrowing, intimal injury, and intimal developmental abnormality can cause brain ischemia or artery-to-artery cerebral embolism. Myocardial contraction dysfunction, cardiac wall injury, and developmental abnormality can induce intracardiac thrombosis and lead to cardiac embolism. In addition, cortical venous thrombosis and occult venous thromboembolism *via* intracardiac or extracardiac channels also account for cryptogenic stroke in females. Due to the lack of knowledge, in clinical practice, the above etiologies are seldom assessed. The low incidence rate of these etiologies can lead to missed diagnosis. This review will provide novel clinical clues for the etiological diagnosis of cryptogenic stroke and will help to improve the management and secondary prevention of stroke in the female population. In the future, more studies are needed to explore the etiology and prevention strategies of cryptogenic stroke.

Keywords: female, etiology, uncommon, stroke, cryptogenic

OPEN ACCESS

Edited by:
Bing Tian,
Naval Medical University, China

Reviewed by:
Cen Zhang,
New York University, United States

***Correspondence:**
Xin Ma
maxin@xwh.ccmu.edu.cn

Specialty section:
This article was submitted to Stroke, a section of the journal Frontiers in Neurology

Received: *21 March 2022*
Accepted: *16 May 2022*
Published: *24 June 2022*

Citation:
Dong J and Ma X (2022) Uncommon Female-Predominant Etiologies of Cryptogenic Stroke. Front. Neurol. 13:900991. doi: 10.3389/fneur.2022.900991

INTRODUCTION

The etiologies of cryptogenic stroke are complex and heterogeneous. A number of uncommon etiologies are not fully recognized, some of which predominantly affect females. Studies have shown that differences in hormonal factors, coagulation state, and immunity may predispose females to stroke at certain physiological periods, including pregnancy and the peripartum period (1, 2). Once cryptogenic stroke is diagnosed, females tend to have worse outcomes (1, 3), therefore prompt etiological recognition and treatment are crucial for good recovery. However, these potential etiologies are often undiagnosed in clinical practice due to the limitation of knowledge and examination technologies. In this article, we will review the advancement in exploring uncommon female-predominant etiologies of cryptogenic stroke, which will provide novel clinical clues for the etiological diagnosis of cryptogenic stroke and might be helpful in improving the diagnosis and secondary prevention of stroke as a whole.

ARTERIAL SOURCES OF CEREBRAL INFARCTION OR EMBOLISM

Vascular Sources of Cerebral Infarction or Embolism

Atherosclerotic arterial stenosis/occlusion and vulnerable plaque eruption are predominant pathogenic mechanisms of ischemic stroke (23). However, some uncommon conditions, including cerebral vasoconstrictive narrowing and thromboembolism caused by arterial intimal injury or intimal developmental abnormality, are unrecognized. These conditions are closely related to the hormonal level, gestational status, and medications of females, which deserve more attention from clinicians.

Reversible Cerebral Vasoconstriction Syndrome

Reversible cerebral vasoconstriction syndrome (RCVS) refers to a group of disorders characterized by reversible vasoconstriction of the cerebral vasculature, including uncommon conditions like drug-induced angiopathy and postpartum angiopathy… RCVS. should be highly suspected in patients with recurrent thunderclap headache, multifocal segmental cerebral artery narrowing typically showing a beaded appearance on angiography, and after exclusion of diseases with similar clinical manifestations including arterial dissection, aneurysm, and vasculitis. In addition, the arterial narrowing in RCVS is characteristically reversible within 3 months (4).

In previous studies, up to 64.2–85.6% of RCVS patients were female (4, 5), while only 14.4–35.8% were men. The predominance of females in RCVS might be associated with the use of vasoactive medications including triptans, selective serotonin reuptake inhibitors, or noradrenergic and selective serotonergic antidepressants, or with postpartum and eclampsia (6, 7). Vasoactive substances and surge of blood pressure can induce sympathetic overactivation and subsequently persistent vasoconstriction. Estrogen also participated in the deregulation of cerebral vascular tone (4). Further, placental growth factor, soluble fms-like tyrosine kinase-1, and transforming growth factor β might be implicated in developing postpartum RCVS (2, 4), the mechanism of which is still unclear.

It is usually thought that RCVS has a benign course, but in fact, around 6–39% of RCVS cases developed ischemic stroke (4). Particular attention should be paid to RCVS-related stroke in pregnancy and the postpartum periods. Recently, two retrospective studies have indicated that RCVS might be the most common cause of stroke during these periods. Moreover, the condition of RCVS-related stroke in these periods might continuously worsen and even lead to death (24–26). It should be noted that the prodromal headache symptom of RCVS-related stroke is sometimes atypical or even absent (27), which would lead to misdiagnosis of RCVS as atherosclerotic stenosis or aneurysm, or missed diagnosis. Thus, for females with cryptogenic stroke, particularly for those in pregnancy and the postpartum periods, not only should detailed history taking of prodromal headache symptom, precipitating factors, and medications be taken, but also dynamic observation of the reversible changes of cerebral vasculature should be highlighted, in order to clarify the diagnosis.

Pregnancy Associated Aortic Dissection

Aortic dissection is a known uncommon etiology of cryptogenic stroke, but surprisingly, for young and middle-aged female, over half of aortic dissections developed in pregnancy (8). Particularly, pregnant females with multiple gestation, connective tissue disorders, gestational diabetes, gestational hypertension and pre-eclampsia/eclampsia are more prone to pregnancy-associated aortic dissection (PAD) (28, 29). PAD might develop under the synergistic effect of various factors. The increase in heart rate, cardiac output, and abdominal pressure in pregnancy would add forces to the aortic wall. In addition, changes in estrogen level during pregnancy might be associated with the weakening of elastic fibers and medial degeneration of the aortic wall (28). These factors combined could increase the risk of aortic intimal laceration.

Studies have shown that up to 76% of PAD were Stanford type A, which means the dissection might involve the orifices and proximal segments of the three major branches of aorta and would lead to stroke and upper limb ischemia (30, 31). Moreover, PAD-related stroke is a rapidly progressive life-threatening condition with a high rate of maternal and fetal death, which requires urgent diagnosis and treatment. Patients with PAD might sometimes present with atypical chest pains. Moreover, the characteristic imaging features of dissection, including entrance and exit tears, true and false lumen, and intimal flap, are easily neglected in routine examinations for stroke, such as carotid ultrasonography and echocardiogram, which would delay or mislead the diagnosis of PAD-related stroke. Therefore, for pregnant females with cryptogenic stroke, clinicians should be highly alert to PAD even when encountering atypical manifestations.

Intracranial Arterial Dissection

Unlike vertebral and carotid artery dissections, fewer than 20% of stroke-related dissections involve intracranial arteries, including dissections of the basilar artery, posterior inferior cerebellar artery, and arteries around the circle of Willis, which are not fully recognized. The smaller diameters of these arteries limit the ability of routine vascular imaging examinations to detect characteristic imaging features of dissection, including true and false lumen and intimal flap; the dissection tends to be missed or misdiagnosed as aneurysm, vasculitis, or fibromuscular dysplasia, etc. (32, 33).

It is worth noting that among East Asian patients, up to 67–78% of cervicocranial arterial dissections are intracranial arterial dissection (IAD), and around half of IAD patients are female (9). In this regard, when east Asian females with cryptogenic stroke presented with dissection related factors, including prodromal headache and medical history of head trauma or violent movement, while no evidence of carotid or vertebral artery dissection was found, high resolution magnetic resonance imaging or thin slice spiral CT should be applied to detect IAD.

Carotid Web

Carotid web (CW) refers to a thin shelf-like projection developed from the posterior wall of the carotid bulb, which was

demonstrated to be the fibroelastic thickening of the intima in histopathological examinations (34). Researchers hypothesized that CW might be a rare and atypical subtype of fibromuscular hyperplasia with unknown pathogenesis (10).

In recent years, studies have found a close relationship between CW and the incidence and recurrence of cryptogenic stroke in young and middle-aged adults. CW has been detected in 9.4–37% of young and middle-aged cryptogenic stroke patients; the percentage was markedly higher than that of non-stroke controls (1–7%) (35). In addition, a cohort study of cryptogenic stroke patients has reported that 29% of CW ipsilateral to the infarction developed mural thrombi; during 1-year follow-up, 32% of stroke patients had recurring cerebral infarctions in brain regions ipsilateral to the CW (11). Researchers hypothesized that the pathogenic mechanism of CW-related stroke might be a cerebral embolism due to dislodgement of mural thrombus formed within CW.

Particularly, in recent meta-analyses and case control studies, up to 61–91% of CW-related stroke patients were female (10–13). The underlying mechanism of developing CW in females is still not clear, although genetic, hormonal factors, and vascular injury might play a role. When evaluating for cryptogenic stroke in young and middle-aged females, careful examination of the posterior wall for a protrusion along the carotid bulb should be done on computed tomography angiography or magnetic resonance angiography.

Aortic Mural Thrombus

While mural thrombus due to aortic atherosclerotic plaque rupture is a known source of cryptogenic stroke, less attention has been given to aortic mural thrombus (AMT) with no underlying aortic diseases. The pathogenesis of AMT is unclear, although coagulation disorders and malignancy have both been reported. The pathogenesis of this AMT is still unclear; some cases also have coagulation disorders, hematologic disorders, malignancy, inflammatory bowel disease, or are under chemotherapy or taking steroids or oral contraceptives (14), which suggests a possible link with hypercoagulable state. Intimal injuries secondary to smoking and trauma might also induce aortic thrombosis (36). Although only around 200 AMT cases were reported to date (14), over half of the patients were female, and about 88% of AMT were movable floating thrombus with potentially high risk of embolism. Moreover, about 4–14% of the embolic events were stroke (14, 37). Therefore, if the aortic origin of cryptogenic cerebral embolism was suspected, especially in females with hypercoagulation disorders and systemic embolism, the aorta should be examined for AMT by transesophageal echocardiogram or contrast enhanced computed tomography even when atherosclerosis was not evident.

Cardiac Thromboembolism

Cardiac thrombi secondary to atrial fibrillation, recent myocardial infarction, systolic heart failure, and prosthetic heart valves are common sources of cerebral embolism. In addition, infective endocarditis, papillary fibroelastoma, and myxoma are relatively uncommon but known sources of cardioembolism (15). Apart from these, some uncommon diseases compromising the structure and function of the heart can cause cardiac thrombi s as well. As most symptoms of these diseases are non-specific, they tend to be misdiagnosed or neglected, particularly when accompanied by common heart diseases. Moreover, this group of diseases are difficult to detect *via* routine transthoracic echocardiogram; transesophageal echocardiogram or other high-resolution imaging techniques are usually needed to clarify the diagnosis. In these situations, the etiology of stroke would be underdiagnosed. Several of these diseases are female-predominant, which call for special attention.

Takotsubo Syndrome

Takotsubo syndrome is an acute cardiac syndrome characterized by transient and reversible left ventricular contraction dysfunction affecting more than one coronary artery territory. The incidence of TTS was reported to be approximately 10/100,000. TTS patients frequently suffered from emotional or physical stress prior to symptom onset and have clinical and electrocardiographic manifestations similar to that of acute coronary syndrome; in a few cases, patients might present with a chronic course or remain asymptomatic. On left ventriculography, TTS characteristically shows an apical ballooning appearance due to dyskinetic apical contraction and compensatively enhanced basal wall contraction of the left ventricle. The ventricle configuration and function usually recovered spontaneously within days or months (16).

TTS is an uncommon etiology of stroke and could be the underlying etiology of cryptogenic stroke. According to previous studies, the incidence of stroke among TTS patients admitted to the hospital, 30 days and 1 year after disease onset, were 1–1.7, 2.8, and 4.2%, respectively (17). The pathogenic mechanism of TTS-related stroke might be cardioembolism secondary to ventricular thrombosis, as left ventricular thrombi were detected in about 1.3–5.3% of TTS cases (38). Once the ventricle function returned to normal, the thrombi might dislodge from the ventricle wall after myocardial contraction and cause cerebral embolism. Whereas, since the clinical manifestations of TTS mimics that of acute coronary syndrome, and sometimes even no obvious symptoms are presented, TTS tends to be misdiagnosed or missed in clinical practice.

Up to 70–90% of TTS patients and most of the recurring TTS cases were female (16, 18, 39); in addition, 10% of hospitalized female patients who initially presented with suspected acute coronary syndrome were ultimately diagnosed with TTS (16). It should be noted that most of the females with TTS were postmenopausal, which means TTS might be explained by the hormonal changes after menopause. Catecholamine cardiotoxicity plays a key role in the pathogenesis of TTS. Emotional and physical stressors can induce sympathetic hyperactivation and surge of circulating catecholamines, which would cause myocardial stunning and coronary spasm, and ultimately lead to ventricular contraction dysfunction. It is well-established that estrogen protects against the cardiotoxicity of catecholamine; as the estrogen level decreases after menopause, its protective effect attenuates, which would render the heart vulnerable to TTS in response to stress (16).

When diagnosing cryptogenic stroke in females, especially in postmenopausal females, detailed inquiry of predisposing stressful events would be helpful. If prodromal acute chest pain is presented, careful discrimination of TTS from acute coronary syndrome would be necessary.

Left Atrial Appendage Aneurysm

Left atrial appendage aneurysm (LAAA) refers to the abnormal aneurysmal enlargement of the left atrial appendage. The pathogenesis of LAAA is undetermined; 90% of LAAA cases were congenital, probably due to congenital dysplasia of the atrial pectinate muscles, others were secondary to mitral valve diseases, or other conditions leading to elevated left atrial pressure. Most LAAA patients were asymptomatic, while others presented with palpitation, dyspnea, or chest pain. In histopathological examinations, endocardium or myocardium fibrosis of left atrial appendage was demonstrated. The enlarged aneurysm might compress the left coronary artery and result in myocardial ischemia and atrial arrhythmia including atrial fibrillation/flutter (26.7%) and supraventricular tachycardia (9.9%) (40). Of the LAAA cases, 5.9% developed thromboembolic events (40), and mural thrombi were detected attaching to the wall of left atrial appendage in published LAAA-related stroke cases (19, 41). LAAA is rare, only around 100 cases were reported in literature, although 52.5% of patients were female. Thus, for females with cryptogenic stroke, particularly for those presenting with palpitation, dyspnea, or arrhythmia, echocardiogram should be performed to assess for LAAA.

Left Atrial Dissection

Left atrial dissection (LAD) refers to the blood-filling false cavity extending from the mitral annular area to the left atrium free wall or interatrial septum. Most LAD cases were reported after cardiac surgery, such as mitral valve replacement, radiofrequency ablation, coronary bypass surgery, or percutaneous coronary angioplasty, while no more 1/8 of cases were spontaneous. LAD tended to occur in the posterior atrial wall; the false cavity might gradually enlarge and grow into a hematoma, which would obstruct the mitral valve inflow or orifices of pulmonary veins and induce thrombosis. The clinical manifestations of LAD vary widely, including dyspnea, hemodynamically instable symptoms, chest pain, arrhythmia, dysphagia, and stroke (20, 42). In most cases, the symptom presented within hours or days post-surgery (73.3%), while a few presented after months or years. About half of LAD patients were hemodynamically instable and presented with congestive heart failure and low-output syndrome, while 15% were asymptomatic (42). Although no more than 100 LAD cases were reported, over half of patients were female. In this regard, LAD should be counted as another rare etiology of cardioembolism in females. Particularly for female patients who had a recent history of cardiac surgery prior to stroke onset and presented with hemodynamically unstable symptoms, LAD should be considered. The imaging features of LAD are not easily distinguishable from that of cardiac tumor or pericardial effusion in routine transthoracic echocardiogram and magnetic resonance imaging, when suspecting LAD, transesophageal echocardiogram is possibly needed to clarify the diagnosis (20).

VENOUS SOURCES OF CEREBRAL INFARCTION AND EMBOLISM

Venous thrombi cause stroke in two ways, either by direct occlusion of cerebral drainage veins or by indirect paroxysmal thromboembolism *via* intracardiac or extracardiac channels. Apart from cerebral venous sinuses and lower limb veins, some venous thrombi form in uncommon locations, which are almost undetectable by routine vascular examinations and are closely associated with a hypercoagulable state. Since females are prone to hypercoagulation disorders, it is necessary to screen for occult venous thrombi for females with cryptogenic stroke.

Isolated Cortical Venous Thrombosis

It is known that infarction due to cerebral venous sinus thrombosis is an uncommon type of stroke. Unexpectedly, stroke due to isolated cortical venous thrombosis (ICVT) is even more uncommon and unrecognized. In previous reports, only 6% of intracranial venous thrombosis were ICVT (43, 44). The clinical manifestations of ICVT were similar to that of cerebral venous sinus thrombosis, but intracranial hypertension was seldom presented (44). The diagnosis of ICVT-related stroke is often difficult, as the imaging features of ICVT are not evident in routine vascular imaging examinations due to the small diameter of involved cortical veins. Magnetic resonance venography, black-blood magnetic resonance imaging, or CT venography is always needed to clarify the diagnosis.

According to the meta-analysis conducted in 2014, up to 2/3 of ICVT patients were females (44). The development of ICVT in females might be associated with a hypercoagulable state. In this study, 21% of female had histories of taking contraceptives and 35% were pregnant or in the postpartum period (44), both conditions were closely related to hypercoagulation. In addition, intracranial hypotension might also be an inducing factor of ICVT in females. In a retrospective study recruiting 51 ICVT patients, 10 patients (23.3%) had intracranial hypotension, while intracranial hypotension was present in merely 2% of all patients with cerebral venous thrombosis. Among the 10 patients, seven patients were female while only three were men (21).

In clinical practice, when encountering a female stroke patient with a history of taking contraceptives, pregnant or in the postpartum period, or with intracranial hypotension, particularly those with isolated cortical lesion, ICVT should be suspected.

Paradoxical Emboli

May-Thurner Syndrome

May-Thurner syndrome (MTS) is characterized by the impairment of iliac venous return and obstruction of the iliac vein due to compression by the overlying iliac artery against the lumbar spine. Although the compression is a common anatomic variation found in 14–32% of cadavers (45), and most MTS patients were asymptomatic or with only insignificant presentations like mild lower limb edema and pigmentation, it still calls for attention. In a meta-analysis of 1,569 symptomatic MTS cases, 52.4% of patients had deep venous thrombosis and 7.8% had pulmonary embolism (46). A hypercoagulable state might be an inducing factor of MTS-related venous thrombosis.

TABLE 1 | Proportion of women vs. men and screening recommendations for uncommon female-predominant etiologies of cryptogenic stroke.

Etiology	Proportion of women vs. men	Clinical history clues	Diagnostic testing clues
Arterial sources			
Vascular sources			
Reversible cerebral vasoconstriction syndrome	64.2–85.6% vs. 14.4–35.8% (4, 5)	1. Prodromal thunderclap headache 2. Medical history of migraine, eclampsia 3. Postpartum or stage of pregnancy 4. Vasoactive medications including triptans, selective serotonin reuptake inhibitors, noradrenergic and selective serotonergic antidepressants, cannabis, binge drinking, etc. (6, 7)	1. Multifocal segmental cerebral artery narrowing with beaded appearance on DSA//MRA/CTA/contrast-enhanced vessel wall imaging 2. Complete or substantial resolution of vasoconstriction within 3 months of clinical onset
Pregnancy associated aortic dissection	100% (60% in pregnancy and peripartum) vs. 0 (8)	1. Chest pain or back pain, hemodynamically instable symptoms, asymmetric brachial arterial pressure 2. Medical history of multiple gestation, connective tissue disorders, gestational diabetes, gestational hypertension and pre-eclampsia/eclampsia 3. Stages of pregnancy or postpartum	1. Entrance and exit tears, true and false lumen, intimal flap on CTA/DSA/TEE
Intracranial arterial dissection	33–42% vs. 58–67% (9)	1. Age 2. Ethnicity 3. Prodromal headache 4. Recent medical history of head trauma, violent movement	1. True and false lumen, intimal flap on high resolution MRI/ thin- slice spiral CT
Carotid web	61–91% vs. 9–39% in carotid web related stroke patients (10–13)	1. Age	1. Thin shelf-like filling defect attached to the wall of carotid bulb on carotid ultrasonography/MRA/CTA
Aortic mural thrombus	53 vs. 47% (14)	1. Medical history of coagulation disorders, hematologic disorders, malignancy, inflammatory bowel disease 2. Medications including chemotherapy, steroids, oral contraceptives	1. Coagulation tests including protein c, protein S, factor V, anticardiolipin antibodies, etc. 2. Movable floating mass attached to the aortic wall on TEE/aortic CTA
Cardiac sources			
Takotsubo syndrome	70–90% vs. 10–30% (15–17)	1. Prodromal emotional or physical stressful events, chest pain or discomfort 2. Postmenopausal	1. Dyskinetic ventricle contraction, typically apical ballooning appearance on left ventriculography/echocardiogram 2. Resolution of configuration and function within months of clinical onset
Left atrial appendage aneurysm	52.5 vs. 47.5% (18)	1. Palpitation, dyspnea or arrhythmia	1. Aneurysmal enlargement of the left atrial appendage on echocardiogram/cardiac MRI
Left atrial dissection	55 vs. 45% (19)	1. Recent history of cardiac surgery or intervention 2. Hemodynamically instable symptoms	1. Resembling cardiac tumor or pericardial effusion on TEE/TTE/cardiac MRI
Venous sources			
Isolated cortical venous thrombosis	68 vs. 32% (20)	1. Headache, seizure 2. Medical history of coagulation disorders, intracranial hypotension 3. Pregnancy or postpartum 4. Taking oral estrogen containing contraceptives	1. Coagulation tests including protein c, protein S, factor V, anticardiolipin antibodies, etc. 2. Black-blood MRI/MRV/ CTV
May-Thurner syndrome	67 vs. 33% in symptomatic patients (21)	1. Asymmetric lower limb edema, pigmentation 2. Medical history of patent foramen ovale, pulmonary embolism, coagulation disorders 3. Pregnancy or postpartum 4. Taking oral estrogen containing contraceptives	1. Coagulation tests including protein c, protein S, factor V, anticardiolipin antibodies, etc. 2. Compression of iliac vein by the overlying iliac artery and thrombosis on contrast enhanced MRI /contrast enhanced CT of pelvic veins
Pulmonary arteriovenous malformation	60–64% vs. 36–40% (22)	1. Recurrent epistaxis, multifocal cutaneous telangiectasis 2. Medical history of hypoxemia, brain abscess, migraine, decompression illness, hemoptysis and hemothorax 3. Family history of hemorrhagic telangiectasis	1. Positive transcranial doppler bubble test, but no intracardiac shunting in TEE 2. DSA/contrast enhanced chest CT

CT, computed tomography; CTA, computed tomography angiography; CTV, computed tomography venography; DSA, digital subtraction angiography; MRA, magnetic resonance angiography; MRV, magnetic resonance venography; TEE, transesophageal echocardiogram; TTE, transthoracic echocardiogram.

In this study, 11.2% of MTS patients had malignant tumor, 16.9% had a history of recent surgery, 4.6% had trauma, and 9.6% had coagulation disorders including factor V Leiden thrombophilia, protein C, and protein S deficiency (46).

MTS tends to develop in females. In previous studies, about 2/3 of symptomatic MTS patients were female, which might be associated with pregnancy, taking contraceptives, or estrogen replacement therapy. Moreover, the condition of females with MTS tended to be more severe than men; it was reported that females had a higher percentage of severe iliac venous stenosis (19.5 vs. 11.1%) (47) and pulmonary embolism (9.9 vs. 1.6%) compared with men (46).

MTS might not only cause pulmonary embolism, but also lead to stroke. One of the recent studies utilizing magnetic resonance imaging to examine the pelvic veins of cryptogenic stroke patients has found that 31% of cryptogenic stroke patients had MTS, which was significantly higher than that of controls (10%). The compression degree of iliac veins in cryptogenic stroke patients with MTS was also higher than that of controls (32 vs. 13%) (22). Another study had retrospectively analyzed 50 cryptogenic stroke cases with patent foramen ovale (PFO) and found that 10% of patients had MTS and 8% had pelvic venous thrombosis, while none of the patients had lower limb venous thrombosis (48). It is known that the patent foramen ovale is the main conduit from which the venous thrombi crosses directly into the systemic circulation and causes cerebral embolism. This study indicated that pelvic venous thrombi secondary to MTS might be the origin of paraxysmal cerebral embolism apart from lower limb venous thrombi, and MTS might be the potential etiology of crytogenic stroke.

Therefore, for female patients with cryptogenic stroke with PFO, especially those with hypercoagulation disorders, pregnant, or taking oral contraceptives, the use of RoPE (Risk of Paradoxical Embolism) score and PASCAL (PFO-Associated Stroke Causal Likelihood) classification system to evaluate the association between stroke and PFO and the screening for MTS by contrast enhanced magnetic resonance imaging or contrast enhanced computed tomography of pelvic venous thrombi would be necessary.

Pulmonary Arteriovenous Malformation

Apart from patent foramen ovale, which is the most common etiology of paraxysmal cerebral embolism, in a few conditions, venous thrombi can flow through the vascular bed of pulmonary arteriovenous malformation (PAVM) into systemic circulation. The incidence of PAVM was reported to be 2–3/100,000; female patients outnumber male with a female to male ratio of 1.5–1.8:1, and more than half of PAVM patients had hereditary hemorrhagic telangiectasis (49). While most PAVM patients were asymptomatic, 30% developed hypoxemia, stroke, brain abscess, migraine, decompression illness, hemoptysis, or hemothorax. In previous studies, about 3.2–55% of PAVM patients developed stroke (49, 50). The pathogenic mechanism of stroke might be paraxysmal cerebral embolism caused by venous thrombi passing through the abnormal communication between pulmonary artery and veins and ultimately into the left heart chamber and arterial system.

Special attention should be paid to PAVM in pregnancy. Studies have observed that, in pregnancy, PAVM tended to increase in volume and number (49, 51), which might be related to the elevation of cardiac output in this period (52).

Therefore, for female patients with cryptogenic stroke, when paraxysmal cerebral embolism was suspected but no intracardiac shunting was demonstrated, for instance, when the transcranial doppler bubble test was positive but no patent foramen ovale was found in transesophageal echocardiogram, PAVM should be screened. Particularly for female patients with a family history of hemorrhagic telangiectasis or with recurrent epistaxis or multifocal cutaneous telangiectasis, pre-pregnancy screening for PAVM would be helpful in preventing severe complications like stroke in pregnancy.

DISCUSSION

Various uncommon stroke etiologies exist in the female population that still remain unrecognized. The incidence rates of these etiologies are generally low, for instance, the incidence of TTS and PAVM are 10/100,000 and 2–3/100,000, respectively, and no more than 200 cases of AMT, LAAA, and LAD were reported in the literature. The development of these etiologies are closely related to the hormonal profiles in different physiological stages of female life, coagulation function, and medications. In pregnancy and postpartum, the changes of estrogen and placental-related hormones might influence the regulation of cerebral vascular tone, and induce aortic wall degeneration, which would predispose females to RCVS and PAD. In addition, the hormonal changes might promote hypercoagulability, and subsequently induce thrombosis in uncommon locations as seen in AMT, ICVT, and MTS. In post menopause, the decrease in estrogen level attenuates its protective effect against the cardiotoxicity of catecholamine, which would render the heart more vulnerable to stress and predispose females to TTS. In clinical practice, for females with cryptogenic stroke, detailed medical history taking, comprehensive coagulation tests, and special imaging applications are vital for detecting occult thrombi, dissection, and vascular/cardiac developmental abnormalities that might be easily missed in routine examinations (the screening recommendations for uncommon female-predominant etiologies of cryptogenic stroke are listed in **Table 1**). Currently, etiological studies focusing on females with cryptogenic stroke are scarce. In the future, greater efforts should be made to explore the etiology and prevention strategies of cryptogenic stroke in the female population, so as to improve the diagnosis and treatment of stroke.

AUTHOR CONTRIBUTIONS

All authors contributed to the article and approved the submitted version.

REFERENCES

1. Bushnell C, McCullough LD, Awad IA, Chireau MV, Fedder WN, Furie KL, et al. Guidelines for the prevention of stroke in women: a statement for healthcare professionals from the American Heart Association/American Stroke Association. *Stroke.* (2014) 45:1545–88. doi: 10.1161/01.str.0000442009.06663.48
2. Wang N, Shen X, Zhang G, Gao B, Lerner A. Cerebrovascular disease in pregnancy and puerperium: perspectives from neuroradiologists. *Quant Imaging Med Surg.* (2021) 11:838–51. doi: 10.21037/qims-20-830
3. Ntaios G, Lip G, Vemmos K, Koroboki E, Manios E, Vemmou A, et al. Age- and sex-specific analysis of patients with embolic stroke of undetermined source. *Neurology.* (2017) 89:532–9. doi: 10.1212/WNL.0000000000004199
4. Miller TR, Shivashankar R, Mossa-Basha M, Gandhi D. Reversible cerebral vasoconstriction syndrome, part 1: epidemiology, pathogenesis, and clinical course. *Am J Neuroradiol.* (2015) 36:1392–9. doi: 10.3174/ajnr.A4214
5. Choi HA, Lee MJ, Choi H, Chung CS. Characteristics and demographics of reversible cerebral vasoconstriction syndrome: a large prospective series of Korean patients. *Cephalalgia.* (2018) 38:765–75. doi: 10.1177/0333102417715223
6. Burton TM, Bushnell CD. Reversible cerebral vasoconstriction syndrome. *Stroke.* (2019) 50:2253–8. doi: 10.1161/STROKEAHA.119.024416
7. Ducros A. Reversible cerebral vasoconstriction syndrome. *Lancet Neurol.* (2012) 11:906–17. doi: 10.1016/S1474-4422(12)70135-7
8. Rommens KL, Sandhu HK, Miller CR, Cecchi AC, Prakash SK, Saqib NU, et al. In-hospital outcomes and long-term survival of women of childbearing age with aortic dissection. *J Vasc Surg.* (2021) 74:1135–42. doi: 10.1016/j.jvs.2021.03.028
9. Debette S, Compter A, Labeyrie MA, Uyttenboogaart M, Metso TM, Majersik JJ, et al. Epidemiology, pathophysiology, diagnosis, and management of intracranial artery dissection. *Lancet Neurol.* (2015) 14:640–54. doi: 10.1016/S1474-4422(15)00009-5
10. Wirth FP, Miller WA, Russell AP. Atypical fibromuscular hyperplasia. Report of two cases. *J Neurosurg.* (1981) 54:685–9. doi: 10.3171/jns.1981.54.5.0685
11. Haussen DC, Grossberg JA, Bouslama M, Pradilla G, Belagaje S, Bianchi N, et al. Carotid web (Intimal fibromuscular dysplasia) has high stroke recurrence risk and is amenable to stenting. *Stroke.* (2017) 48:3134–7. doi: 10.1161/STROKEAHA.117.019020
12. Compagne K, van Es A, Berkhemer OA, Borst J, Roos Y, van Oostenbrugge RJ, et al. Prevalence of carotid web in patients with acute intracranial stroke due to intracranial large vessel occlusion. *Radiology.* (2018) 286:1000–7. doi: 10.1148/radiol.2017170094
13. Olindo S, Marnat G, Chausson N, Turpinat C, Smadja D, Gaillard N. Carotid webs associated with ischemic stroke. Updated general review and research directions. *Rev Neurol.* (2021) 177:627–38. doi: 10.1016/j.neurol.2020.09.007
14. Fayad ZY, Semaan E, Fahoum B, Briggs M, Tortolani A, D'Ayala M. Aortic mural thrombus in the normal or minimally atherosclerotic aorta. *Ann Vasc Surg.* (2013) 27:282–90. doi: 10.1016/j.avsg.2012.03.011
15. Kamel H, Healey JS. Cardioembolic stroke. *Circ Res.* (2017) 120:514–26. doi: 10.1161/CIRCRESAHA.116.308407
16. Akashi YJ, Nef HM, Lyon AR. Epidemiology and pathophysiology of Takotsubo syndrome. *Nat Rev Cardiol.* (2015) 12:387–97. doi: 10.1038/nrcardio.2015.39
17. Abanador-Kamper N, Kamper L, Wolfertz J, Vorpahl M, Haage P, Seyfarth M. Temporarily increased stroke rate after Takotsubo syndrome: need for an anticoagulation? *BMC Cardiovasc Disord.* (2018) 18:117. doi: 10.1186/s12872-018-0842-0
18. Singh K, Carson K, Usmani Z, Sawhney G, Shah R, Horowitz J. Systematic review and meta-analysis of incidence and correlates of recurrence of takotsubo cardiomyopathy. *Int J Cardiol.* (2014) 174:696–701. doi: 10.1016/j.ijcard.2014.04.221
19. Kwan CM, Tsai LM, Lin LJ, Yang YJ, Chen JH. Congenital left atrial appendage aneurysm with thrombus formation: diagnosis by transesophageal echocardiography. *J Clin Ultrasound.* (1993) 21:480–3. doi: 10.1002/jcu.1870210715
20. Mohan JC, Shukla M, Mohan V, Sethi A. Spontaneous dissecting aneurysm of the left atrium complicated by cerebral embolism: a report of two cases with review of literature. *Indian Heart J.* (2016) 68(Suppl. 2):S140–5. doi: 10.1016/j.ihj.2015.12.020
21. Kitamura Y, Hara K, Tsunematsu K. Isolated superficial sylvian vein thrombosis with long cord sign: case report and review of the literature. *Neurol Med Chir.* (2014) 54:253–9. doi: 10.2176/nmc.cr2012-0220
22. Prabhakar AM, Misono AS, Brinegar KN, Khademhosseini A, Oklu R. Use of magnetic resonance venography in screening patients with cryptogenic stroke for May-Thurner syndrome. *Curr Probl Diagn Radiol.* (2016) 45:370–2. doi: 10.1067/j.cpradiol.2016.04.006
23. Wong KS, Caplan LR, Kim JS. Stroke mechanisms. *Front Neurol Neurosci.* (2016) 40:58–71. doi: 10.1159/000448302
24. Miller EC, Yaghi S, Boehme AK, Willey JZ, Elkind MS, Marshall RS. Mechanisms and outcomes of stroke during pregnancy and the postpartum period: a cross-sectional study. *Neurol Clin Pract.* (2016) 6:29–39. doi: 10.1212/CPJ.0000000000000214
25. Yoshida K, Takahashi JC, Takenobu Y, Suzuki N, Ogawa A, Miyamoto S. Strokes associated with pregnancy and puerperium: a nationwide study by the japan stroke society. *Stroke.* (2017) 48:276–82. doi: 10.1161/STROKEAHA.116.014406
26. Katz BS, Fugate JE, Ameriso SF, Pujol-Lereis VA, Mandrekar J, Flemming KD, et al. Clinical worsening in reversible cerebral vasoconstriction syndrome. *JAMA Neurol.* (2014) 71:68–73. doi: 10.1001/jamaneurol.2013.4639
27. Wolff V, Ducros A. Reversible cerebral vasoconstriction syndrome without typical thunderclap headache. *Headache.* (2016) 56:674–87. doi: 10.1111/head.12794
28. Kamel H, Roman MJ, Pitcher A, Devereux RB. Pregnancy and the risk of aortic dissection or rupture: a cohort-crossover analysis. *Circulation.* (2016) 134:527–33. doi: 10.1161/CIRCULATIONAHA.116.021594
29. Beyer SE, Dicks AB, Shainker SA, Feinberg L, Schermerhorn ML, Secemsky EA, et al. Pregnancy-associated arterial dissections: a nationwide cohort study. *Eur Heart J.* (2020) 41:4234–42. doi: 10.1093/eurheartj/ehaa497
30. Balbay E, Basci S, Bozkurt I, Ozkok A, Dogruyol S, Sirkeci EE, et al. Postpartum stanford type a aortic dissection: a case report and review of the literature. *Cardiol Res.* (2013) 4:129–32. doi: 10.4021/cr276w
31. De Martino A, Morganti R, Falcetta G, Scioti G, Milano AD, Pucci A, et al. Acute aortic dissection and pregnancy: review and meta-analysis of incidence, presentation, and pathologic substrates. *J Card Surg.* (2019) 34:1591–7. doi: 10.1111/jocs.14305
32. Shi Z, Tian X, Tian B, Meddings Z, Zhang X, Li J, et al. Identification of high risk clinical and imaging features for intracranial artery dissection using high-resolution cardiovascular magnetic resonance. *J Cardiovasc Magn Reson.* (2021) 23:74. doi: 10.1186/s12968-021-00766-9
33. Yoshioka K, Mori T. Clinical and radiological difficulties to detect isolated MCA dissection before intravenous tPA therapy. *J Stroke Cerebrovasc Dis.* (2019) 28:104365. doi: 10.1016/j.jstrokecerebrovasdis.2019.104365
34. Choi PM, Singh D, Trivedi A, Qazi E, George D, Wong J, et al. Carotid webs and recurrent ischemic strokes in the era of CT angiography. *AJNR Am J Neuroradiol.* (2015) 36:2134–9. doi: 10.3174/ajnr.A4431
35. Kyaw K, Htun L, Sammy S, Jay B, Rajesh R. Rare case of carotid web presenting with ischemic stroke in a young woman and a brief review of the literature. *Case Rep Med.* (2018) 2018:3195679. doi: 10.1155/2018/3195679
36. Yang S, Yu J, Zeng W, Yang L, Teng L, Cui Y, et al. Aortic floating thrombus detected by computed tomography angiography incidentally: five cases and a literature review. *J Thorac Cardiovasc Surg.* (2017) 153:791–803. doi: 10.1016/j.jtcvs.2016.12.015
37. Meyermann K, Trani J, Caputo FJ, Lombardi JV. Descending thoracic aortic mural thrombus presentation and treatment strategies. *J Vasc Surg.* (2017) 66:931–6. doi: 10.1016/j.jvs.2017.05.109
38. Stollberger C, Finsterer J, Schneider B. Left ventricular thrombi and embolic events in takotsubo syndrome despite therapeutic anticoagulation. *Cardiology.* (2020) 145:504–10. doi: 10.1159/000506925
39. Deshmukh A, Kumar G, Pant S, Rihal C, Murugiah K, Mehta JL. Prevalence of Takotsubo cardiomyopathy in the United States. *Am Heart J.* (2012) 164:66–71. doi: 10.1016/j.ahj.2012.03.020
40. Wang B, Li H, Zhang L, He L, Zhang J, Liu C, et al. Congenital left atrial appendage aneurysm: a rare case report and literature review. *Medicine.* (2018) 97:e9344. doi: 10.1097/MD.0000000000009344

41. Jiang B, Wang X, Liu F, Song L. Left atrial appendage aneurysm. *Interact Cardiovasc Thorac Surg.* (2020) 30:495–6. doi: 10.1093/icvts/ivz283
42. Fukuhara S, Dimitrova KR, Geller CM, Hoffman DM, Tranbaugh RF. Left atrial dissection: An almost unknown entity. *Interact Cardiovasc Thorac Surg.* (2015) 20:96–100. doi: 10.1093/icvts/ivu317
43. Croci DM, Michael D, Kahles T, Fathi AR, Fandino J, Marbacher S. Ipsilateral dural thickening and enhancement: a sign of isolated cortical vein thrombosis? A case report and review of the literature. *World Neurosurg.* (2016) 90:706–11. doi: 10.1016/j.wneu.2016.03.026
44. Coutinho JM, Gerritsma JJ, Zuurbier SM, Stam J. Isolated cortical vein thrombosis: systematic review of case reports and case series. *Stroke.* (2014) 45:1836–8. doi: 10.1161/STROKEAHA.113.004414
45. Harbin MM, Lutsey PL. May-Thurner syndrome: History of understanding and need for defining population prevalence. *J Thromb Haemost.* (2020) 18:534–42. doi: 10.1111/jth.14707
46. Kaltenmeier CT, Erben Y, Indes J, Lee A, Dardik A, Sarac T, et al. Systematic review of May-Thurner syndrome with emphasis on gender differences. *J Vasc Surg Venous Lymphat Disord.* (2018) 6:399–407. doi: 10.1016/j.jvsv.2017.11.006
47. Nazzal M, El-Fedaly M, Kazan V, Qu W, Renno AW, Al-Natour M, et al. Incidence and clinical significance of iliac vein compression. *Vascular.* (2015) 23:337–43. doi: 10.1177/1708538114551194
48. Osgood M, Budman E, Carandang R, Goddeau RJ, Henninger N. Prevalence of pelvic vein pathology in patients with cryptogenic stroke and patent foramen ovale undergoing MRV pelvis. *Cerebrovasc Dis.* (2015) 39:216–23. doi: 10.1159/000376613
49. Cartin-Ceba R, Swanson KL, Krowka MJ. Pulmonary arteriovenous malformations. *Chest.* (2013) 144:1033–44. doi: 10.1378/chest.12-0924
50. Baby N, Kunnathuparambil SG, Varghese P, Kuriakose AM. Paradoxical embolism in a case of hereditary hemorrhagic telangiectasia: case report with literature review. *Neurol India.* (2020) 68:665–8. doi: 10.4103/0028-3886.288990
51. Swinburne AJ, Fedullo AJ, Gangemi R, Mijangos JA. Hereditary telangiectasia and multiple pulmonary arteriovenous fistulas. Clinical deterioration during pregnancy. *Chest.* (1986) 89:459–60. doi: 10.1378/chest.89.3.459
52. Dupuis O, Delagrange L, Dupuis-Girod S. Hereditary haemorrhagic telangiectasia and pregnancy: a review of the literature. *Orphanet J Rare Dis.* (2020) 15:5. doi: 10.1186/s13023-019-1286-z

Conflict of Interest: The authors declare that the research was conducted in the absence of any commercial or financial relationships that could be construed as a potential conflict of interest.

frontiers | Frontiers in Neurology

CASE REPORT
published: 25 July 2022
doi: 10.3389/fneur.2022.872279

A Cryptogenic Stroke Associated With Infective Endocarditis and Antiphospholipid Antibody Syndrome: Case Report and Literature Review

Lei Chen†, *Ping Zhang*†, *Xuan Zhu, Minmin Zhang and Benqiang Deng**

Department of Neurovascular Center, Changhai Hospital, Naval Medical University, Shanghai, China

OPEN ACCESS

Edited by:
Chengcheng Zhu,
University of Washington,
United States

Reviewed by:
Sonu M. M. Bhaskar,
South West Sydney Local Health District (SWSLHD), Australia
Qin Hu,
Shanghai Jiao Tong University, China
Li Gao,
Shanghai Jiao Tong University, China

***Correspondence:**
Benqiang Deng
chnxgnk@163.com

†*These authors have contributed equally to this work and share first authorship*

Specialty section:
This article was submitted to Applied Neuroimaging, a section of the journal Frontiers in Neurology

Received: *09 February 2022*
Accepted: *22 June 2022*
Published: *25 July 2022*

Citation:
Chen L, Zhang P, Zhu X, Zhang M and Deng B (2022) A Cryptogenic Stroke Associated With Infective Endocarditis and Antiphospholipid Antibody Syndrome: Case Report and Literature Review. Front. Neurol. 13:872279. doi: 10.3389/fneur.2022.872279

Introduction: Accurate definition of stroke etiology is crucial, as this will guide effective targets for treatment. Both antiphospholipid antibody syndrome (APS) and infective endocarditis (IE) can be independent risk factors for ischemic stroke in young adults. When an embolic stroke occurs with IE and APS simultaneously, the origin of the embolic source is difficult to identify.

Case Report: A 19-year-old man was admitted to the hospital for the onset of stroke. A diagnosis of APS accompanied by IE was made after a series of examinations. We identified aortic valve vegetation as the embolic source. Although both APS and IE can induce valve vegetation, we considered IE to be the primary cause according to the infective clues. Despite treatment with ampicillin, the patient's fever persisted, and surgical aortic valve replacement was performed urgently. The patient recovered without recurrence of stroke during the 1-year follow-up.

Conclusion: A considerable challenge for physicians is evaluating all the signs suggestive of embolic sources in acute stroke and identifying the primary etiology when there are multiple causes. Early diagnosis and surgical intervention for bicuspid aortic valve (BAV) vegetation complicated by acute stroke may yield favorable clinical results.

Keywords: antiphospholipid antibody syndrome (APS), infective endocarditis, embolic, cryptogenic stroke, surgery

INTRODUCTION

Approximately 35% of non-lacunar stroke cases occur due to cardioembolic sources (1). Intracardiac thrombi can indicate various common diseases, such as atrial fibrillation, patent foramen ovale (PFO), papillary fibroelastoma, myxoma, and infective endocarditis (IE) (1). Native valve disease, such as a bicuspid aortic valve (BAV) vegetation-induced septic embolic cerebrovascular accident, is even less common (2). Although rare, antiphospholipid antibody syndrome (APS) can develop into cardiac valvular lesions and produce intracardiac thrombi (3, 4). While cardioembolic stroke is often a severe condition and the etiology is various, diagnosis is challenging for physicians, particularly given the time pressure (5). We report a rare case of stroke in a young patient with BAV vegetation who did not present with any clinical features referable to the cardiovascular system before this attack.

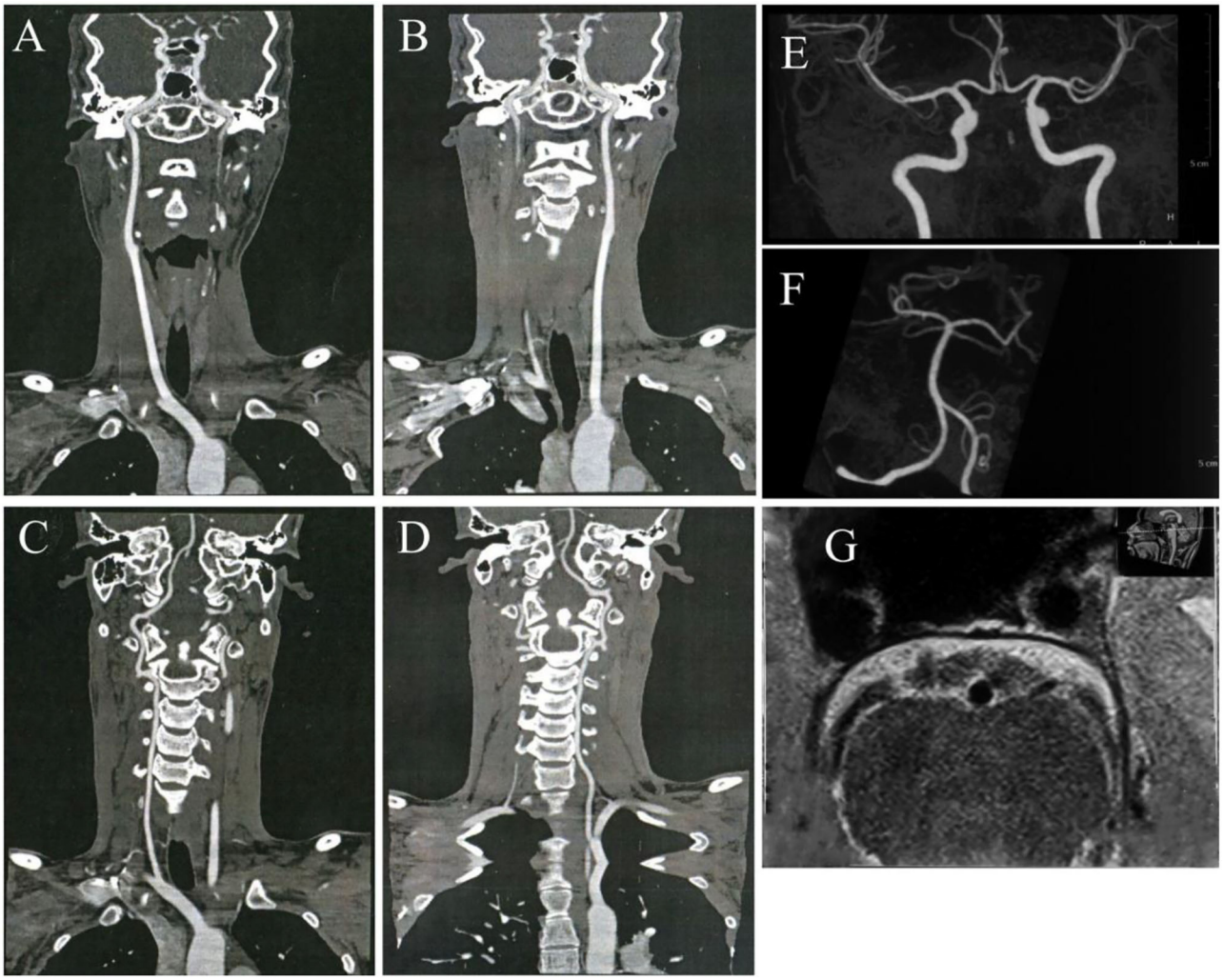

FIGURE 1 | No arterial occlusion, stenosis, or plaque was discovered in bilateral carotid arteries **(A,B)**, vertebral arteries **(C,D)**, and all the intracranial arteries **(E,F)**. The high-resolution vessel wall magnetic resonance imaging (MRI) of the basilar artery shows no occlusion or stenosis **(G)**.

This stroke was thought to be cryptogenic because it could be associated with IE and APS at the same time.

CASE DESCRIPTION

An 18-year-old man was referred to the ER for sudden onset of left hemiplegia, vomiting, and disturbance of consciousness. He was a healthy college student who had never taken any medication before for any disease or illness. There was no exposure to toxins or history of alcohol intake. The patient's family history was significant only for hypertension in his grandmother. A complete system review was negative. His vital signs on admission were as follows: blood pressure, 105/63 mmHg; pulse, 84 beats/min; respiration, 18 breaths/min; and temperature, 36.5°C. Neurological investigation revealed somnolence, global aphasia, gaze palsy, and right-sided hemiplegia. The National Institutes of Health Stroke Scale (NIHSS) score was 15. The patient was transferred to our neurovascular center after 5 h of onset, so thrombolysis with alteplase was not administered. He was not a candidate for acute intervention because multimodal computed tomography revealed no arterial occlusion or perfusion defect (**Figure 1**), and after this examination, the patient had significant recovery of his consciousness. His power improved to 4/5 in the affected limbs, bringing his NIHSS score to 1. Treatment of aspirin, clopidogrel, and atorvastatin was administrated. Laboratory parameters on admission indicated an acute bacterial infection with a C-reactive protein (CRP) level of 38.21 mg/L and leukocytosis of 12.71×10^9/L.

Neuroimaging with brain magnetic resonance imaging (MRI) showed foci of restricted diffusion in the left thalamus and the right brain stem suggestive of an embolic stroke (**Figure 2**). Blood work showed an erythrocyte sedimentation rate (ESR) of 38 mm/h and an antistreptolysin O (ASO) concentration of

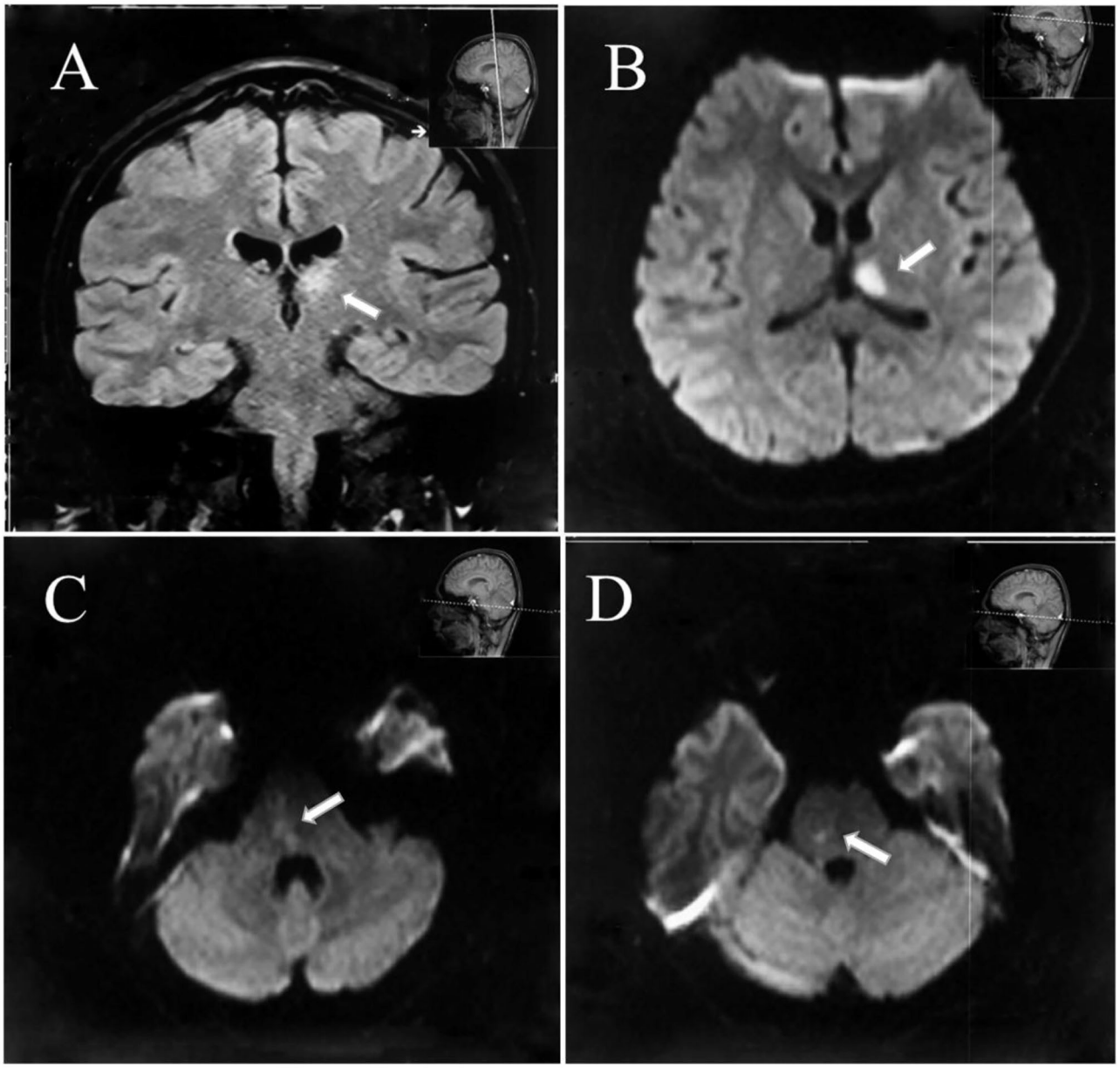

FIGURE 2 | Diffusion restriction of the left thalamus **(A,B)** and the right brain stem as demonstrated on diffusion-weighted magnetic resonance imaging consistent with acute ischemic infarction **(C,D)**.

290.01 IU/ml. The patient tested positive for antiphospholipid (aPL) antibodies, including antibodies against anticardiolipin (aCL) antibodies, lupus anticoagulant (LA), and β2-glycoprotein-1 (β2GP-1). The β2GP-1 (133 relative unit (RU)/ml) level was elevated in high titers. Hence, a diagnosis of APS was considered. At the same time, a transthoracic echocardiogram (TTE) revealed a BAV with moderate regurgitation and vegetation. The vegetation was attached to the anterior commissure, and the longest oscillating mass was 8 mm. Supported by the infection evidence, we believed septic emboli due to IE should be the primary etiology despite APS. However, the patient developed an increasing fever with shivering after 5 days of antibiotic therapy with high-dose penicillin. Further etiological workup on blood cultures demonstrated the growth of oral *Streptococcus*, and the patient was transferred to thoracic surgery for aortic valve replacement. Seven weeks after successful mechanical aortic valve replacement, the patient was discharged with only mild unsteadiness. He received a total 6-week course of IV penicillin in the hospital and was advised to continue a long-term warfarin treatment. The patient did not receive any immunotherapy and his aCL, LA, and β2GP-1 tests were still positive in other hospitals in half a year. He had no residual neurological deficits

TABLE 1 | The clinical features and treatment of the patient according to the timeline.

Clinical features	Time	Treatment
Left hemiplegia and left facial numbness	2018-11-17 14:00	
Left hemiplegia, vomiting, and disturbance of consciousness	2018-11-17 17:00	
The patient arrived at the emergency room and presented somnolence, global aphasia, left hemiplegia, gaze palsy, and emesis. (NHISS 15)	2018-11-17 19:00	
Returned consciousness and left hemiparesis (NHISS 1)	2018-11-17 19:30	Aspirin, clopidogrel, and atrovastatin
Antiphospholipid antibodies (+)	2018-11-21	
Transthoracic echocardiogram (TTE) revealed bicuspid aortic valve (BAV) vegetation	2018-11-22	Penicillin and nadroparin calcium (stop aspirin and clopidogrel)
Fever and chills	2018-11-27	
Blood cultures demonstrated the growth of oral *Streptococcus*.	2018-11-28	
There are no additional focal neurological deficits (NIHSS 1). His temperature was normal for 10 days and the repeated brain MRI did not show any new infarct lesions	2018-12-10	Stopped nadroparin calcium 2 days ago, and aortic valve replacement was performed
	2018-12-16	Penicillin and warfarin (add warfarin)
Discharge	2019-01-22	The patient finished 6-week course of penicillin injection and continued warfarin treatment
No residual neurological deficits and no recurrence of stoke	2020-01-31	Warfarin

or recurrence of stoke when evaluated 1 year later. The patient had returned to the college and felt that he can live and study as before.

The timeline of the case is summarized in (**Table 1**).

DISCUSSION

According to the episode, this patient suffered from acute stroke due to basilar artery occlusion and was soon self-recanalized. Following the assessment, large-artery atherosclerosis and small-vessel occlusion, two of the most common stroke etiologies, were excluded first. The cardioembolic stroke had been considered in the presence of BAV vegetation with multiple bilateral lesions on MRI. BAV is a congenital heart abnormality that may involve endocarditis, which is the most severe comorbidity with significant morbidity (6). Two types of endocarditis, infective and non-infective, can both cause stroke (5). Cardiac embolism due to IE is an extraordinary stroke etiology, accounting for nearly 30% of all patients with IE (7). Non-infective endocarditis can complicate APS, which is a systemic autoimmune disease characterized by thrombotic complications in patients positive for aPL (5, 8, 9). The APS-associated non-infective endocarditis was reported to be Libman–Sacks (LS) endocarditis (10). LS endocarditis can be quite difficult to diagnose and often mimics the presentation of bacterial endocarditis. In this case, IE and APS were found to coexist, but which disease was accountable for the aortic valve vegetation was ambiguous. Treatments of APS-induced stroke are antithrombotic medications and modulation of the immune response with immunotherapy, while IE requires antibiotics or even emergency surgery. The radical etiology of this cardioembolic stroke needed to be identified to inform the treatment.

Management decisions for patients with complicated cardioembolic stroke should be discussed and decided by a multidisciplinary team comprised of cardiologists, infectious diseases specialists, and cardiothoracic surgeons with a major contribution from neurologists. We consulted all the specialists and deemed IE to be the primary cause of the cardiac embolism in terms of the patient's elevated leukocytosis and CRP level as well as the positive blood cultures. In APS, valvular vegetations are often non-bacterial with negative blood cultures (11). These findings were consistent with the evaluation of helpful markers in distinguishing IE from LS endocarditis in the previous literature (10).

In ∼15–20% of patients with IE, clinical features referable to the cardiovascular system, such as clubbing, splinter hemorrhages, and hematuria, may be absent (12). Furthermore, if fever is not present during the initial evaluation, a rapid and accurate diagnosis of IE complicated by stroke is difficult during the rapid intravenous thrombolysis (IVT) treatment process in the emergency department. IVT and endovascular therapy (EVT) are the standard of care in selected patients for acute ischemic stroke, but their use in patients with stroke secondary to IE is controversial (13, 14). IVT is contraindicated because of the increased risk of intracranial hemorrhage and worse outcomes (15, 16). We found 10 cases of IE-related acute ischemic stroke who received IVT, and IE was suspected post-thrombolysis in all these cases (17–22). Nine of them were identified with sufficient clinical outcome data (17–19, 21, 22) (**Table 2**). Among the nine cases, the median age was 56 years (range 25–75 years); four were women and five were men. Vegetations affected the

TABLE 2 | Summary of clinical characteristics in reported case series of IE presenting as AIS treated with IVT.

Reference	Age/Sex	Affected valve	Acute treatment	NIHSS (initial)	NIHSS (follow up)	mRS	sICH	Mortality
Ashkanani et al. (17)	65/M	Mitral valve	IVT	18	ND	3 (8 weeks)	No	No
Brownlee et al. (18)	27/F	Mitral valve	IVT	15	20	1 (6 months)	Yes	No
Gopal et al. (19)	44/F	Mitral valve	IVT	4	ND	6 (3 months)	No	Yes
Gopal et al. (19)	56/F	Mitral valve	IVT	2	ND	6 (3 months)	No	Yes
Gopal et al. (19)	74/F	Mitral valve	IVT	8	ND	3 (3 months)	No	No
Gopal et al. (19)	66/M	Mitral valve	IVT	7	ND	6 (3 months)	Yes	Yes
Gopal et al. (19)	25/M	Mitral valve	IVT	3	ND	3 (3 months)	Yes	No
Maeoka et al. (21)	46/M	Aortic valve	IVT + EVT	ND	ND	1 (ND)	Yes	No
Distefano et al. (22)	75/M	Aortic valve	IVT + EVT	16	ND	6 (ND)	Yes	Yes

IE, infective endocarditis; AIS, acute ischemic stroke; IVT, intravenous thrombolysis; NIHSS, National Institutes of Health Stroke Scale; mRS, modified Ranking Scale; sICH, symptomatic intracranial hemorrhage; F, female; M, male; EVT, endovascular therapy; ND, not described.

mitral valve in 78% of these cases and the aortic valve in the remainder. Eight of the nine cases reported preprocedure NIHSS scores, but only one reported postprocedure NIHSS scores, so we could not evaluate the improvement in NIHSS scores. The median modified Ranking Scale (mRS) was 3, and only two patients achieved good functional outcomes (mRS$\leq$2). Of all these reported cases, 56% (5/9) developed symptomatic intracranial hemorrhage (sICH), and the mortality reached 44% (4/9). IE should be considered from the outset to avoid IVT, particularly given the time pressures in acute stroke care.

Endovascular therapy (EVT) may be a choice in ischemic stroke with large vessel occlusion due to cardiac emboli. Routine histopathological analysis of EVT-retrieved clots could have value in confirming clinical diagnoses and supporting early treatment in acute stroke with IE (23, 24). Even though EVT results in highly successful recanalization rates, stroke patients with IE are most likely to have worse clinical and safety outcomes than non-IE patients following reperfusion therapy in the acute phase (25, 26). With the limitation of the available evidence and a lack of consensus, EVT still should be considered seriously as the efficacy and safety have not yet been well established (14).

In many cases of IE, vegetation decreases during treatment with antibiotics. However, in some patients, valvular lesions that form the basis for the development of IE may remain after treatment with antibiotics (27). Surgery is recommended in uncontrolled infections according to the European Society of Cardiology (ESC) guidelines (15). Due to the persistent fever and burdensome BAV vegetations, valve surgery seemed to be an imminent emergency in our patient. However, the benefit of potential valve surgery can be challenging given the risk of bleeding in the setting of high doses of heparin during surgery and worsening neurological deficits attributed to perioperative hypotension in IE patients who have already had a stroke (28). Traditionally, cardiac surgery should be delayed for several months in endocarditis complicated by stroke, while a growing body of available evidence supports that early surgery is beneficial for outcomes (29, 30). In this patient, the surgery was performed 24 days after stroke onset as the infection could not be controlled by antibiotics. Postponing surgery to achieve clinical stabilization and better perioperative circumstances may have worsened the disease process with recurrent embolization and resulted in heart failure. Early surgery for IE with small acute cerebral infarction (<2 cm) was confirmed to be performed safely with good outcomes (31). As the stroke lesions were small with a low risk of hemorrhage, this patient eventually recovered well after the early surgery.

Limitation

Aspirin has negligible or poor effects and shows a heightened risk of hemorrhage in IE-related acute ischemic stroke; therefore, the use of aspirin is not recommended in the early therapy of patients with IE (32). Fortunately, the delay in IE diagnosis and the use of aspirin and clopidogrel did not result in hemorrhage complications in this case. A 5-year prospective study showed that the median time for a recurrent thrombotic event is shorter in patients with a high titer of aCL antibodies and intracardiac thrombus (33). This patient did not receive any immunotherapy, and his aPL level remained high. Furthermore, we still need long-term follow-up to confirm the diagnosis. This literature review may also have lapsed due to publication bias.

CONCLUSION

Bicuspid aortic valve (BAV) vegetation-related cerebral embolism may present as cryptogenic and can be confusing in the acute phase, particularly when APS and IE are diagnosed simultaneously. Early consultation with a multidisciplinary team can be extremely helpful. Timely surgical intervention should always be considered in cases of small cerebral infarction accompanied by large valve vegetations. Going forward, there is a demand for further study within this area to direct future practice.

DATA AVAILABILITY STATEMENT

The original contributions presented in the study are included in the article/supplementary material, further inquiries can be directed to the corresponding author.

ETHICS STATEMENT

The study involving human participants was reviewed and approved by Shanghai Changhai Hosptial Ethics Committee. Written informed consent was obtained from the individual(s) for the publication of any potentially identifiable images or data included in this article.

AUTHOR CONTRIBUTIONS

LC and PZ: conceptualization and writing of the article. XZ and MZ: original case and draft preparation. BD: supervision and reviewing. All authors contributed to the article and approved the submitted version.

REFERENCES

1. Kleindorfer DO, Towfighi A, Chaturvedi S, Cockroft KM, Gutierrez J, Williams LS, et al. 2021 guideline for the prevention of stroke in patients with stroke and transient ischemic attack: a guideline from the AHA/ASA. *Stroke.* (2021) 52:e364–467. doi: 10.1161/STR.0000000000000375
2. Hobohm C, Hagendorff A, Schulz S, Fritzsch D, Budig S, Stöbe S, et al. Clinical presentation and multi-parametric screening surrogates of ischemic stroke patients suffering from infective endocarditis. *Cerebrovasc Dis.* (2016) 41:60–7. doi: 10.1159/000442005
3. Kiran G, Shashivardhan J, Chandrasekhar P. Left ventricular thrombus: an interesting presentation of primary antiphospholipid antibody syndrome with a mini-review of the literature. *J Cardiovasc Echogr.* (2020) 30:217–22. doi: 10.4103/jcecho.jcecho_52_20
4. Basnet S, Stauffer T, Jayswal A, Tharu B. Recurrent nonbacterial thrombotic endocarditis and stroke on anticoagulation. *J Community Hosp Intern Med Perspect.* (2020) 10:466–9. doi: 10.1080/20009666.2020.1791028
5. Arboix A, Alió J. Cardioembolic stroke: clinical features, specific cardiac disorders and prognosis. *Curr Cardiol Rev.* (2010) 6:150–61. doi: 10.2174/157340310791658730
6. Tzemos N, Therrien J, Yip J, Thanassoulis G, Tremblay S, Jamorski MT, et al. Outcomes in adults with bicuspid aortic valves. *JAMA.* (2008) 300:1317–25. doi: 10.1001/jama.300.11.1317
7. Garcia-Cabrera E, Fernandez-Hidalgo N, Almirante B, Ivanova-Georgieva R, Noureddine M, Plata A, et al. Neurological complications of infective endocarditis: risk factors, outcome,and impact of cardiac surgery: a multicenter observational study. *Circulation.* (2013) 127:2272–84. doi: 10.1161/CIRCULATIONAHA.112.000813
8. Naranjo L, Ostos F, Gil-Etayo FJ, Hernandez-Gallego J, Cabrera-Marante O, Pleguezuelo DE, et al. Presence of extra-criteria antiphospholipid antibodies is an independeng risk factor for ischemic stroke. *Front Cardiovasc Med.* (2021) 8:665741. doi: 10.3389/fcvm.2021.665741
9. Yang W, Kang MK, Ha SY, Kang DW, Bae J, Lee EJ, et al. Current status and role of antiphospholipid antibody testing in cryptogenic stroke. *Eur J Neurol.* (2021) 29:753–60. doi: 10.1111/ene.15191
10. Lee JL, Naguwa SM, Cheema GS, Gershwin E. Revisiting Libman–sacks endocarditis: a historical review and update. *Clin Rev Allerg Immunol.* (2009) 36:126–30. doi: 10.1007/s12016-008-8113-y
11. Liu J, Frishman WH. Nonbacterial thrombotic endocarditis: pathogenesis, diagnosis, and management. *Cardiol Rev.* (2016) 24:244–7. doi: 10.1097/CRD.0000000000000106
12. Baddour LM, Wilson WR. Bayer AS, Fowler VG, Tleyjeh IM, Rybak MJ, et al. Infective endocarditis in adults: diagnosis, antimicrobial therapy, and management of complications. *Circulation.* (2015) 132:1435–86. doi: 10.1161/CIR.0000000000000296
13. Asaithambi G, Adil MM, Qureshi AI. Thrombolysis for ischemic stroke associated with infective endocarditis: results from the nationwide inpatient sample. *Stroke.* (2013) 44:2917-9. doi: 10.1161/STROKEAHA.113.001602
14. D'Anna L. Endovascular treatment of ischemic large-vessel stroke due to infective endocarditis: case series and review of the literature. *Neurol Sci.* (2020) 41:3517–25. doi: 10.1007/s10072-020-04599-9
15. Habib G, Lancellotti P, Antunes MJ, Bongiorni MG, Casalta JP, Zotti FD, et al. ESC Guidelines for the management of infective endocarditis: the task force for the management of infective endocarditis of the European Society of Cardiology (ESC) endorsed by: European Association for Cardio-Thoracic Surgery (EACTS), the European Association of Nuclear Medicine (EANM). *Eur Heart J.* (2015) 36:3075–128. doi: 10.1093/eurheartj/ehv319
16. Demaerschalk BM, Kleindorfer DO, Adeoye OM, Demchuk AM, Fugate JE, Grotta JC, et al. Scientific rationale for the inclusion and exclusion criteria for intravenous alteplase in acute ischemic stroke. *Stroke.* (2016) 47:581–641. doi: 10.1161/STR.0000000000000086
17. Ashkanani A, Bitar Z, Maadrani O. Acute stroke thrombolysis in infective endocarditis. *SAGE Open Med Case Rep.* (2018) 6:1–3. doi: 10.1177/2050313X18807629
18. Brownlee WJ, Anderson NE, Barber PA. Intravenous thrombolysis is unsafe in stroke due to infective endocarditis. *Intern Med J.* (2014) 44:195–7. doi: 10.1111/imj.12343
19. Gopal M, Lakhani S, Lee VH. Intravenous thrombolysis in acute ischemic stroke patients with unsuspected infective endocarditis. *J Stroke Cerebrovasc Dis.* (2021) 30:1–5. doi: 10.1016/j.jstrokecerebrovasdis.2020.105502
20. Jennings R, Hammersley D, Hancock J, Blauth C. The diagnostic and therapeutic challenges of infective endocarditis presenting as acute stroke. *BMJ Case Rep.* (2017) 2017. doi: 10.1136/bcr-2017-219762
21. Maeoka R, Nakagawa I, Ohnishi H, Takahashi K, Nakase H, Ohnishi H. Catastrophic multiple microbleeds caused by infective endocarditis following intravenous thrombolysis and endovascular thrombectomy. *J Stroke Cerebrovasc Dis.* (2019) 28:e123–5. doi: 10.1016/j.jstrokecerebrovasdis.2019.06.004
22. Distefano M, Calandrelli R, Arena V, Pedicelli A, Della Marca G, Pilato F, et al. Puzzling case of cryptogenic stroke. *J Stroke Cerebrovasc Dis.* (2019) 28:e33–5. doi: 10.1016/j.jstrokecerebrovasdis.2019.01.001
23. Bhaskar S, Saab J, Cappelen-Smith C, Killingsworth M, Wu XJ, Cheung A, et al. Clot histopathology in ischemic stroke with infective endocarditis. *Can J Neurol Sci.* (2019) 46:331–6. doi: 10.1017/cjn.2019.8
24. Bhaskar S, Cordato D, Cappelen-Smith C, Cheung A, Ledingham D, Celermajer D, et al. Clarion call for histopathological clot analysis in "cryptogenic" ischemic stroke: implications for diagnosis and treatment. *Ann Clin Transl Neurol.* (2017) 4:926–30. doi: 10.1002/acn3.500
25. Maheshwari R, Cordato DJ, Wardman D, Thomas P, Bhaskar SMM. Clinical outcomes following reperfusion therapy in acute ischemic stroke patients with infective endocarditis: a systematic review. *J Cent Nerv Syst Dis.* (2022) 14:1–10. doi: 10.1177/11795735221081597
26. Feil K, Küpper C, Tiedt S, Dimitriadis K, Herzberg M, Dorn F, et al. Safety and efficacy of mechanical thrombectomy in infective endocarditis: a matched case-control analysis from the German Stroke Registry-Endovascular Treatment. *Eur J Neurol.* (2021) 28:861–7. doi: 10.1111/ene.14686
27. Danish N. Propensity Score–Matched Cohort Study. *Clin Infect Dis.* (2020) 70:1186–92. doi: 10.1093/cid/ciz320
28. Chakraborty T, Rabinstein A, Wijdicks AE. Chapter 11: Neurologic complications of infective endocarditis. In: Stone TE, editor. *Handbook of Clinical Neurology. Heart and Neurologic Disease*. Amsterdam, The Netherlands: ELSEVIER B.V. (2021). doi: 10.1016/B978-0-12-819814-8.00008-1
29. Kadam M, Birns J, Bhalla A. The management of infective endocarditis complicated by stroke. *Int J Clin Pract.* (2020) 74:e13469. doi: 10.1111/ijcp.13469
30. Yanagawa B, Pettersson GB, Habib G, Ruel M, Saposnik G, Latter DA, et al. Surgical management of infective endocarditis complicated by embolic stroke. *Circulation.* (2016) 134:1280–92. doi: 10.1161/CIRCULATIONAHA.116.024156
31. Samura T, Yoshioka D, Toda K, Sakaniwa R, Yokoyama J, Suzuki K et al. Emergency valve surgery improves clinical results in patients with

infective endocarditis complicated with acute cerebral infarction: analysis using propensity score matching. *Eur J Cardiothorac Surg*. (2019) 56:942–9. doi: 10.1093/ejcts/ezz100

32. Chan KL, Tam J, Dumesnil JG, Cujec B, Sanfilippo AJ, Jue J, et al. Effect of long-term aspirin use on embolic events in infective endocarditis. *Clin Infect Dis*. (2008) 46:37–41. doi: 10.1086/524021
33. Turiel M, Sarzi-Puttini P, Peretti R, Rossi E, Atzeni F, Parsons W, et al. Thrombotic risk factors in primary antiphospholipid syndrome: a 5-year prospective study. *Stroke*. (2005) 36:1490–4. doi: 10.1161/01.STR.0000170645.40562.09

Conflict of Interest: The authors declare that the research was conducted in the absence of any commercial or financial relationships that could be construed as a potential conflict of interest.

Publisher's Note: All claims expressed in this article are solely those of the authors and do not necessarily represent those of their affiliated organizations, or those of the publisher, the editors and the reviewers. Any product that may be evaluated in this article, or claim that may be made by its manufacturer, is not guaranteed or endorsed by the publisher.

frontiers | Frontiers in Neurology

TYPE Review
PUBLISHED 28 July 2022
DOI 10.3389/fneur.2022.968390

OPEN ACCESS

EDITED BY
Bing Tian,
Naval Medical University, China

REVIEWED BY
QinJian Sun,
Shandong University, China
Ailian Du,
Shanghai Jiao Tong University, China
Kenichi Todo,
Osaka University, Japan

*CORRESPONDENCE
Jae W. Song
jae.song@pennmedicine.upenn.edu

SPECIALTY SECTION
This article was submitted to Stroke, a section of the journal Frontiers in Neurology

RECEIVED 13 June 2022
ACCEPTED 01 July 2022
PUBLISHED 28 July 2022

CITATION
Sakai Y, Lehman VT, Eisenmenger LB, Obusez EC, Kharal GA, Xiao J, Wang GJ, Fan Z, Cucchiara BL and Song JW (2022) Vessel wall MR imaging of aortic arch, cervical carotid and intracranial arteries in patients with embolic stroke of undetermined source: A narrative review. *Front. Neurol.* 13:968390. doi: 10.3389/fneur.2022.968390

Vessel wall MR imaging of aortic arch, cervical carotid and intracranial arteries in patients with embolic stroke of undetermined source: A narrative review

Yu Sakai[1], Vance T. Lehman[2], Laura B. Eisenmenger[3], Emmanuel C. Obusez[4], G. Abbas Kharal[5], Jiayu Xiao[6], Grace J. Wang[7], Zhaoyang Fan[6], Brett L. Cucchiara[8] and Jae W. Song[1]*

[1]Department of Radiology, Hospital of the University of Pennsylvania, Philadelphia, PA, United States, [2]Department of Radiology, The Mayo Clinic, Rochester, MN, United States, [3]Department of Radiology, University of Wisconsin-Madison, Madison, WI, United States, [4]Department of Radiology, Cleveland Clinic, Cleveland, OH, United States, [5]Department of Neurology, Cerebrovascular Center, Neurological Institute, Cleveland, OH, United States, [6]Department of Radiology, Keck School of Medicine, University of Southern California, Los Angeles, CA, United States, [7]Department of Vascular Surgery and Endovascular Therapy, Hospital of the University of Pennsylvania, Philadelphia, PA, United States, [8]Department of Neurology, Hospital of the University of Pennsylvania, Philadelphia, PA, United States

Despite advancements in multi-modal imaging techniques, a substantial portion of ischemic stroke patients today remain without a diagnosed etiology after conventional workup. Based on existing diagnostic criteria, these ischemic stroke patients are subcategorized into having cryptogenic stroke (CS) or embolic stroke of undetermined source (ESUS). There is growing evidence that in these patients, non-cardiogenic embolic sources, in particular non-stenosing atherosclerotic plaque, may have significant contributory roles in their ischemic strokes. Recent advancements in vessel wall MRI (VW-MRI) have enabled imaging of vessel walls beyond the degree of luminal stenosis, and allows further characterization of atherosclerotic plaque components. Using this imaging technique, we are able to identify potential imaging biomarkers of vulnerable atherosclerotic plaques such as intraplaque hemorrhage, lipid rich necrotic core, and thin or ruptured fibrous caps. This review focuses on the existing evidence on the advantages of utilizing VW-MRI in ischemic stroke patients to identify culprit plaques in key anatomical areas, namely the cervical carotid arteries, intracranial arteries, and the aortic arch. For each anatomical area, the literature on potential imaging biomarkers of vulnerable plaques on VW-MRI as well as the VW-MRI literature in ESUS and CS patients are reviewed. Future directions on further elucidating ESUS and CS by the use of VW-MRI as well as exciting emerging techniques are reviewed.

KEYWORDS

vessel wall MRI, atherosclerosis, imaging, cerebrovascular disease/stroke, embolic stroke of undetermined source (ESUS), stroke

10.3389/fneur.2022.968390

Introduction

The term Embolic Stroke of Undetermined Source (ESUS) was introduced in 2014 by the Cryptogenic Stroke/ESUS International Working Group (1). It describes patients with non-lacunar brain infarcts without a high-grade large artery stenosis, a high-risk cardioembolic source, or another determined stroke mechanism. The ESUS population is of clinical importance as it may account for up to 20% of all ischemic strokes (1).

As prior clinical trials with patients initially suspected of cryptogenic stroke (CS) revealed a high prevalence of underlying atrial fibrillation (2, 3), subsequent clinical trials focusing on the ESUS population, namely NAVIGATE ESUS and RE-SPECT ESUS, studied the use of anticoagulant therapy, with the underlying premise that unrecognized paroxysmal atrial fibrillation might be a common ESUS mechanism. However, both of these randomized clinical trials showed no significant reduction in recurrent stroke with anticoagulation compared to antiplatelet therapy (4, 5). Given this result, the prospect that non-cardiogenic embolic sources contribute to a significant proportion of ESUS seems increasingly likely. One such source is non-stenosing plaque, which might be present in the cervical carotid or vertebral arteries (6, 7), the intracranial arteries (8), or the aortic arch (9) (Figure 1). In the carotid arteries, this concept has been recently referred to as "symptomatic non-stenotic carotid disease" (SyNC) (10).

Recent advancements in neuroimaging allow us to better evaluate non-stenotic plaque and characterize its potential embolic risk. Potential plaque imaging biomarkers include wall thickness, intraplaque hemorrhage (IPH), lipid-rich necrotic core (LRNC), fibrous cap status, neovascularization manifested by enhancement, and surface morphologies such as ulcerations (11–13). In particular, vessel wall MRI (VW-MRI) is increasingly being used for evaluation of plaque to identify vulnerable features. VW-MRI protocols commonly include magnetic resonance angiography (MRA) and multi-contrast MRI sequences that suppress the signal from adjacent tissue and flowing blood to highlight vessel wall pathologies of both intracranial and extracranial vessels. VW-MRI complements traditional imaging techniques such as CT angiography, MRA, and Digital Subtraction Angiography (DSA) because it allows evaluation of pathology beyond luminal stenosis, namely vulnerable plaque features such as IPH, LRNC, and fibrous cap status (13).

We review how VW-MRI has been explored for evaluation of disease in the cervical carotid arteries, intracranial arteries, and the aortic arch in ischemic stroke patients and show imaging examples of vulnerable plaque features. We also review the available literature on how VW-MRI has been used to study patients who meet criteria for ESUS (or, in older literature prior to introduction of the ESUS concept, CS).

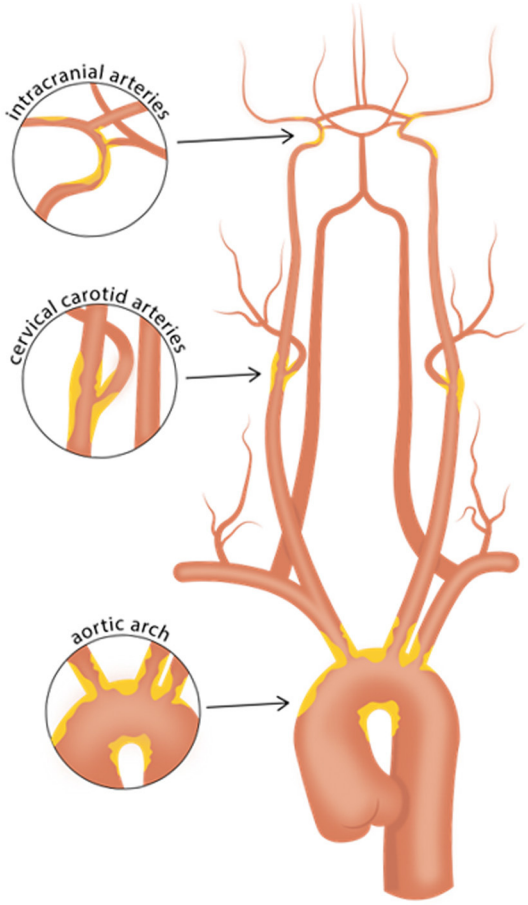

FIGURE 1
Vascular beds commonly affected with atherosclerosis. Careful evaluation of high-risk plaque features using vessel wall MRI of the intracranial arteries, cervical carotid arteries, and aortic arch may aid in identifying culprit plaques in patients with cryptogenic stroke or embolic stroke of undetermined source. Such efforts may help identify causes of stroke that may have been previously overlooked.

Search strategy

We searched PubMed for reports published between January 1980 to March 1st, 2022. Search terms included: "Vessel Wall Imaging," "Vessel Wall MR Imaging," "High Resolution Vessel Wall MRI," "Stroke Etiology," "Cryptogenic Stroke," "Embolic source of undetermined source," "ESUS," "Atherosclerosis," "Atherosclerotic Plaque," "Intraplaque hemorrhage," and "Lipid-rich necrotic core." Furthermore, we reviewed the reference lists of retrieved reports to identify additional relevant articles.

Relevant practice guidelines and their reference lists were also reviewed. We did not restrict our search by language. The final reference list was generated based on relevance to the broad scope of this narrative review with preference given to meta-analyses/systematic reviews and studies with rigorous methodology.

Cervical carotid arteries

Background

Established in 1993, the TOAST classification remains the most widely used system of classifying stroke by etiology. The TOAST classification applies a threshold of ≥50% carotid luminal stenosis as causal of stroke and classifies patients with <50% stenosis and no other identified mechanism as having "stroke of undetermined cause" (14). This is problematic as it may result in an underestimation of the role of carotid atherosclerosis in ischemic stroke since patients with non-stenosing but potentially culprit plaques are not captured. A more recent classification system, the ASCOD Phenotyping of Ischemic Stroke, has expanded the definition of carotid-etiology by classifying the presence of an ipsilateral atherosclerotic stenosis <50% in an intra- or extracranial artery with a luminal thrombus supplying the ischemic field as a potential stroke etiology (15).

The concept of "vulnerable plaque" was initially established with regards to the coronary arteries, where several features of coronary plaques were found to be associated with acute coronary events and sudden cardiac death. These high-risk features include a large lipid rich necrotic core (LRNC), thin/ruptured fibrous cap, and intraplaque hemorrhage (IPH) (16–18).

Advancements in imaging modalities have allowed us to extend the concept of the vulnerable plaque to the evaluation of the carotid arteries beyond assessing the degree of stenosis to explore imaging features and potential biomarkers such as IPH, LRNC, and fibrous cap status (19–21). In particular, MRI has been validated with histology to have high sensitivity and specificity in the evaluation of these vulnerable plaque features (22–24). In recent years, increasing interest in the use of VW-MRI to assess the carotid arteries in ESUS/CS patients has led to investigations on potential imaging biomarkers that may aid us in deciphering ESUS/CS and improve risk stratification. Below we review several plaque features that have been investigated as promising biomarkers.

Carotid plaque features

Studies to date using VW-MRI to evaluate carotid plaque features in the ESUS population have examined one or more of the following imaging biomarkers: IPH, fibrous cap rupture, LRNC, and thrombus. We briefly review how MRI identifies these specific plaque characteristics.

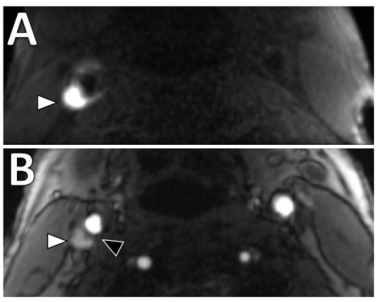

FIGURE 2
Intraplaque hemorrhage in carotid plaque on Magnetization-Prepared Rapid Gradient Echo (MPRAGE) and Time-of-flight MR angiography (TOF MRA). T1 hyperintense IPH at the right carotid bifurcation (white arrowheads) on both **(A)** MPRAGE and **(B)** TOF MRA. The MPRAGE image has fat and blood flow suppression, allowing for the IPH to standout in contrast to the vessel lumen and surrounding soft tissues. The TOF MRA image also demonstrates an intact hypointense fibrous cap at this level (black arrowhead).

Intraplaque hemorrhage

Intraplaque hemorrhage (IPH) is one of the features of a vulnerable plaque (18). Physiologically, it represents the extravasation of red blood cells or iron accumulation in plaque, which may result in plaque instability (25). IPH in carotid plaque has been shown to have significant association with ischemic stroke (26, 27). A meta-analysis on carotid plaque MRI and stroke risk reported patients with carotid IPH on MRI were almost five-times more likely to have subsequent stroke or transient ischemic attack than those without (hazard ratio 4.59, 95% confidence interval 2.91–7.94), although a limitation of the included studies was a considerable range in stenosis degree (28). On imaging, T1-weighted (T1W) sequences are considered the best imaging modality for detection of IPH in the carotid arteries compared to CT or ultrasound due to its ability to detect blood products (11, 13). A variety of T1W sequences can be used, including magnetization-prepared rapid acquisition gradient echo (MPRAGE) and 3D time-of-flight (TOF) sequences (29, 30). An example is shown in Figure 2. MPRAGE is considered to have the highest accuracy given other plaque components such as fibrous tissue and LRNC are suppressed on the inversion-recovery preparation and fat saturation of MPRAGE sequences thereby allowing for the highest tissue contrast between IPH and background structures. Using histology as the gold standard, MPRAGE has the highest specificity (97%) and sensitivity (80%) in detecting carotid IPH (31).

Lipid rich necrotic core

Physiologically, LRNC in carotid plaques represent heterogeneous tissue composed of apoptotic cell debris, calcium particles, and cholesterol crystals (19). A recent meta-analysis showed carotid plaque LRNC is associated with increased risk of ipsilateral ischemic stroke (28). On MRI, LRNC can be seen as focal hypointensity on a T2-weighted sequence. Contrast-enhanced T1-weighted sequences can also help distinguish non-enhancing LRNC from enhancing fibrous plaque tissue (22). LRNC and IPH commonly co-exist and can appear similarly on CT as low-density plaque. While there are efforts to further differentiate the two by Hounsfield units (32, 33), MRI is generally considered superior (19).

Fibrous cap status

Physiologically, the fibrous cap refers to a layer of fibrous connective tissue that contains macrophages and smooth muscle cells, which if ruptured, exposes the adjacent LRNC to luminal blood resulting in activation of the thromboembolic cascade. It has been shown that thin or ruptured fibrous cap is associated with increased risk of ischemic stroke (27, 28, 34). One of the key advantages of MRI is that it can assess fibrous cap status with contrast-enhanced T1W sequences and 3D time-of-flight magnetic resonance angiography (TOF MRA) (11). On contrast-enhanced T1W sequences, normal thick fibrous cap shows smooth linear enhancement overlying the plaque, whereas on TOF MRA, uniform hypointense band between bright lumen and gray plaque core is present (22, 24). An example is shown in Figure 2B. Presence of an irregular and disrupted fibrous cap is associated with ipsilateral ischemic stroke, most commonly due to a thromboembolic mechanism (35). However, this feature can be more difficult to assess than other features in clinical practice.

Surface morphology and ulceration

Luminal surface morphology of carotid plaques can be classified as smooth (no irregularity/ulceration), irregular (surface fluctuates from 0.3 to 0.9 mm), or ulcerated (cavities measuring $\geq$1 mm) (36). Both irregular and ulcerated carotid plaque surfaces are associated with increased risk of stroke (36, 37). An example is shown in Figure 3. On MRI, luminal evaluation is possible with contrast-enhanced MRA (38, 39). MRI can detect carotid plaque ulcerations with similar sensitivity to CTA and the use of contrast-enhanced MRA is preferred over unenhanced TOF MRA due to reduced flow artifacts (38).

Literature on carotid VW-MRI in ESUS patients

Vessel wall-MRI of carotid plaques in the ESUS population suggests a higher prevalence of vulnerable plaque features in the ipsilateral carotid artery compared to the contralateral, regardless of the degree of luminal narrowing (35, 40–45) (Table 1). These observations support the hypothesis that embolization from large artery atherosclerosis may occur even in the absence of hemodynamically significant internal carotid artery stenosis.

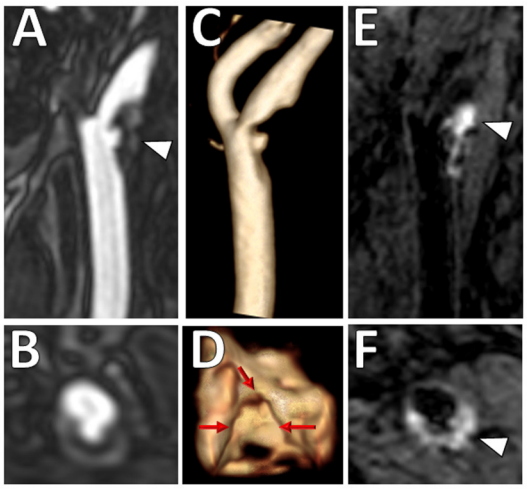

FIGURE 3
Ulcerated plaque with intraplaque hemorrhage on VW-MRI. Male patient presented with clinical and imaging evidence of a 1–2-year history of recurrent left MCA territory infarcts. **(A,B)** Contrast-enhanced MRA neck confirmed a left cervical carotid bifurcation stenosis with an ulcerated plaque (**A**, arrowhead). **(C,D)** 3D surface volume rendering of the left carotid plaque depicts the ulcerated surface morphology with **(D)** axial image through the ulceration showing marked surface irregularity (red arrows). **(E,F)** Carotid VW-MRI showed intraplaque hemorrhage (arrowheads), depicted as T1 hyperintense signal on a fat-suppressed T1W MPRAGE image. Based on the clinical and imaging findings, the patient underwent a left carotid endarterectomy.

Two recent systematic reviews/meta-analyses described the prevalence of carotid artery IPH and other high-risk features in mildly stenotic carotid arteries on VW-MRI in patients meeting ESUS criteria (6, 7). Mark et al., included seven studies from 2012 to 2020 with 354 patients and reported a prevalence estimate of IPH ipsilateral to cerebral ischemia to be 25.8% (95% CI 13.1–38.5) and odds ratio of IPH ipsilateral to ischemia vs. contralateral side to be 6.92 (95% CI 3.04–15.79). Pooled analyses by Kamtchum-Tatuene et al., included eight studies from 2013 to 2018 with 323 patients with unilateral anterior circulation ischemic stroke with plaque imaging performed within 14 days of stroke onset using either VW-MRI, CTA, or US (7). High-risk features assessed included ulceration, IPH, thrombus, fibrous cap rupture, echolucency, or plaque thickness $\geq$3 mm. They reported the prevalence of mild ($\leq$50% luminal narrowing) carotid stenosis with the aforementioned high-risk features in the ipsilateral carotid to be 32.5% (95% CI, 25.3–40.2) compared to 4.6% (95% CI 0.1–13.1) in the contralateral side.

TABLE 1 Select studies using VW-MRI in an ESUS/CS population for evaluation of carotid atherosclerosis.

Study	Imaging technique	Vessel	Key imaging characteristics	Select results
Altaf et al. (26)	1.5 T. 3D T1W GRE	Carotid	IPH	39 (61%) ipsilateral arteries with IPH. During follow-up, 13 ischemic events, of which 5 were strokes, occurred in those with ipsilateral carotid IPH (HR = 9.8, 95% CI 1.3–75.1, $p = 0.03$)
Freilinger et al. (35)	3T. TOF MRA, axial pre-and post-contrast black-blood T1W, PD, T2W	Carotid	IPH, fibrous plaque rupture, luminal thrombus	AHA-LT V1 plaques in 37.5% ipsilateral to the stroke, none in contralateral ($p = 0.001$). Most common diagnostic feature of AHA-LT V1 plaques: IPH (75%), fibrous plaque rupture (50%), luminal thrombus (33%)
Bayer-Karpinska et al. (40)	3T. TOF MRA, axial pre- and post-contrast black-blood T1W, PD, T2W. Additional Dynamic contrast-enhanced MRI series in subgroup	Carotid	Characteristics including fibrous cap rupture, IPH, juxtaluminal hemorrhage/mural thrombus	Initial analysis showed significantly higher prevalence of complicated ipsilateral AHA-LT VI plaques in cryptogenic stroke patients than contralateral (37% vs. 3%, $p < 0.0001$)
Gupta et al. (41)	1.5T/3T. 3D TOF MRA	Carotid	IPH	6 patients (22.2%) with IPH ipsilateral to the side of ischemic stroke, 0 patients with IPH on contralateral side ($p = 0.01$)
Gupta et al. (42)	1.5T/3T. 3D TOF MRA	Carotid	IPH	22 patients (20.2%) with <50% ICA plaque with IPH ipsilateral to stroke, 9 (8.3%) patients with IPH in <50% ICA plaque contralateral to side of stroke ($p = 0.01$)
Hyafil et al. (43)	3T. 3D TOF MRA, axial pre- and post-contrast black-blood T1W, T2W	Carotid	IPH, fibrous cap rupture, luminal thrombus	AHA-LT V1 plaques significantly higher ipsilateral to the stroke side than contralateral (39 vs. 0 %; $p = 0.001$). For all other AHA lesion types, no significant differences between ipsilateral and contralateral sides
Singh et al. (44)	3T. 3D T1W GRE	Carotid	IPH	Significantly higher prevalence of ipsilateral than contralateral IPH (20% vs. 8.6%, $p = 0.005$)

VW-MRI, vessel wall MRI; T1W GRE, T1 weighted gradient-echo; T, Tesla; TOF MRA, Time-of-flight MR angiography; PD, proton density; T2W, T2 weighted; IPH, intraplaque hemorrhage; AHA-LT VI, American heart association lesion type VI; HR, hazard ratio; 95% CI, 95% confidence interval.

Plaque with high-risk features was more than five times more likely to be present in the ipsilateral vs. contralateral carotid artery (OR 5.5, 95% CI, 2.5–12.0). Both studies highlight a role for VW-MRI to detect the presence of morphologic and compositional features in mildly stenotic plaque in patients with ESUS/CS.

Future directions

The use of VW-MRI to evaluate carotid plaque features is a rapidly evolving field. Multi-center prospective studies with larger patient pools to clarify the relationship between vulnerable carotid plaque features on VW-MRI and risk of stroke recurrence are needed. Currently, there are several prospective studies (CAPIAS, CARE II, and the PARISK) intended to examine the value of carotid plaque imaging. These studies are described in more detail in Table 2 (40, 46, 47). How to use diagnostic imaging information from carotid VW-MRI in clinical decision-making to determine stroke mechanism or to choose optimum preventative therapy remains an area of investigation. Some challenges to clinical translation of these VW-MRI protocols include lengthy acquisition times for multiple contrast weightings. Technical efforts to accelerate or simplify protocols include testing different neurovascular vs. surface coils (48) and the use of simultaneous non-contrast angiography and intraplaque hemorrhage (SNAP) (49) and multi-contrast atherosclerosis characterization (MATCH) (50) techniques and remain an active area of investigation.

TABLE 2 Prospective carotid plaque imaging studies.

Study	Study sites, start dates	Patient selection and imaging	Primary outcome	Secondary outcome
The carotid plaque imaging in acute stroke study (CAPIAS) (40)	• Initiated Feb 2011 • 3 Sites: Interdisciplinary Stroke Center in Munich (Ludwig-Maximilians-University), Technical University Munich, University of Freiburg • Observational cohort study; • NCT01284933	• Age >49 years • Stroke or TIA with symptom onset within 7 days • 1 or more acute ischemic lesion(s) on DWI in the territory of a single internal carotid artery • <70% stenosis by NASCET in carotid artery ipsilateral to stroke or TIA defined by US • Carotid artery plaques in the ipsi- or contra-lateral carotid artery as defined by ultrasound (plaque thickness at least 2 mm; located within 1 cm proximal or distal to the carotid bifurcation) • Excluded if history of neck radiation, DWI positive lesions outside territory of a single ICA; surgery within 24 hours prior to MRI • All subjects imaged with VW-MRI at baseline and 12 months follow-up • Subgroup imaged with dynamic CE VW-MRI to visualize neovascularization and inflammation • Subgroup imaged with ^{18}F-FDG PET/MRI at baseline to quantify plaque inflammation	Prevalence of complicated AHA-LT VI plaques	• Association of AHA-LT VI plaques with recurrence rates of ischemic events up to 36 months • Rates of new ischemic lesions on cerebral MRI (including clinically silent lesions) after 12 months • Influence of specific AHA-LT VI plaque features on the progression of atherosclerotic disease burden, infarct patterns, biomarkers and aortic arch plaques
Chinese Atherosclerosis Risk Evaluation (CARE II) (46)	• Sites: 13 medical centers and hospitals in China and University of Washington • Cross-sectional study; • NCT02017756	• Stroke or TIA within 2 weeks • Carotid plaque in at least 1 carotid artery with wall thickness ≥1.5, as defined by US • Exclude cardiogenic stroke, hemorrhagic stroke, neck radiation, unable to undergo MRI • Carotid VW-MRI and routine brain MRI	Prevalence and characteristics of specific VW-MRI features of high-risk atherosclerotic plaque in Chinese patients with stroke or TIA	• Association of carotid plaque features and cerebral infarcts • Differences of carotid plaque patterns among different regions in China • Gender specific characteristics of carotid plaque in Chinese patients with stroke
Plaque At RISK (PARISK) (47)	• Observational cohort study • 4 Sites: Academic Medical Center Amsterdam; Erasmus Medical Center Rotterdam; Maastricht University Medical Center; University Medical Center Utrecht	• TIA, amaurosis fugax or minor stroke (modified Rankin scale ≤3) of the carotid artery territory and an atherosclerotic plaque with <70% stenosis of the ipsilateral ICA • No revascularization procedure • Exclude cardioembolic course, clotting disorder, unable to undergo MRI with contrast • Imaging performed within 5-day window of symptom onset • Baseline: Carotid VW-MRI, MRI brain, CTA, TCD, US, & biomarkers • 2 years: Carotid VW-MRI (subset), CTA, TCD, Carotid US, Brain MRI (all)	Identify whether VW-MRI, multidetector CTA, US and/or transcranial Doppler will predict future ischemic events in symptomatic patients with <70% carotid stenosis Endpoint: ipsilateral recurrent ischemic stroke or TIA and/or ipsilateral ischemic brain lesion on follow-up brain MRI	• Identify determinants for plaque progression • Examine relationship between plaque characteristics, microemboli, and vascular damage on brain MRI • Determine associations between blood biomarkers and plaque parameters

VW-MRI, vessel wall MRI; TIA, transient ischemic attack; US, ultrasound, MRI, magnetic resonance imaging, AHA-LT VI, American Heart Association-Lesion Type VI; CTA, computed tomography angiography; TCD, transcranial doppler; US, ultrasound.

Intracranial arteries

Background

Several structural differences between intracranial and extracranial arteries may contribute to differences in plaque composition and the development of vulnerable plaque features. Intracranial arteries have denser internal elastic lamina, a thinner media, less abundant adventitia with decreased elastic fibers and do not have external elastic lamina (51). In addition, there is a relative paucity of vasa vasorum in the walls of intracranial arteries (52), possibly because intracranial arteries are bathed in nutrient-rich CSF (53). The development and progression of atherosclerotic lesions may therefore be different between intracranial and extracranial arteries (54–56). For example, fibrosis is more prevalent than lipid infiltration of the intima or the adventitia in intracranial plaque compared to extracranial plaque (57). Much of our understanding of imaging features of atherosclerosis stems from extracranial carotid arteries due to the availability of carotid endarterectomy specimens and histologic validation studies (58). Given the lack of readily available specimens for intracranial arteries, intracranial VW-MRI may be a non-invasive imaging modality enabling serial imaging to provide additional insight about intracranial atherosclerosis. Several features of intracranial atherosclerosis on VW-MRI have been described (59, 60) and are detailed below.

VW-MRI of intracranial plaque features

Intraplaque hemorrhage

Presence of intrinsic T1 hyperintensity on T1W imaging of intracranial plaque is thought to reflect IPH (Figure 4). More specifically, IPH has been defined by several authors as having T1 signal intensity of >150% of the adjacent gray matter (61, 62) or adjacent muscle, noting wide variability of referenced tissue (59). In one case report, radiology and pathology findings were indeed histologically validated as such (63). Similar to the cervical carotid arteries, IPH may also be associated with ipsilateral ischemic stroke. A meta-analysis pooling five studies included 521 intracranial vessel wall segments of the circle of Willis and reported an odds ratio of 2.1 (95% CI 1.3, 3.3) for the presence of T1W hyperintensity in a culprit plaque on VW-MRI in patients with acute to subacute ischemia in the territory supplied by that culprit plaque (64). Notably, many of the included studies originated in China and presumably predominantly included Chinese patients. In Chinese studies, the reported prevalence of IPH ranges between 12 and 30% (65, 66) and appears to be higher compared to the Western counterpart. These studies raise the possibility of differences in plaque composition by race for extracranial vs. intracranial plaque (67) and additional studies evaluating ethnic differences would be valuable.

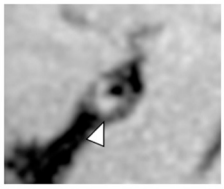

FIGURE 4
Intrinsic T1 hyperintense signal of intracranial plaque on precontrast VW-MRI. Orthogonal view of a precontrast VW-MRI of the middle cerebral artery shows intrinsic T1 hyperintense signal (arrowhead) and positive (outward) wall remodeling (arrowhead).

LRNC

The prevalence of LRNC as part of intracranial atherosclerosis in ischemic stroke patients is unclear. Due to the restraints of spatial resolution, detecting LRNC on intracranial VW-MRI is a challenge. However, several radiology-pathology correlation studies have histologically validated the presence of LRNCs in intracranial plaques indicating a contributory role in plaque progression and a feature of vulnerability (68–71). In these studies, LRNC showed T1W hypointensity on fat-suppressed T1W VW-MRI, Short TI inversion recovery (STIR) hypointensity, T1 iso/hyperintensity and T2 iso/hypointensity.

Vessel wall thickening

Vessel wall thickening due to atherosclerotic plaque, has been described as a common feature of intracranial atherosclerosis on VW-MRI, albeit non-specific, as wall thickening is also seen in other intracranial pathologies such as vasculitis (12, 72).

The pattern of wall thickening can be either concentric or eccentric. Per a recent systematic review, the most common definition of identifying intracranial plaque using VW-MRI was focal/eccentric vessel wall thickening (59). Several authors have defined that vessel wall thickening can be considered concentric if it is circumferential and uniform, with the thinnest segment being at least 50% of the thickest segment. On the other hand, vessel wall thickening is considered eccentric if the wall thickening is clearly focal, or when circumferential wall thickening is noted but the thinnest segment of the wall thickening is <50% of the thickest segment (62, 73). Examples of plaque with both eccentric and concentric wall thickening are shown in Figure 5.

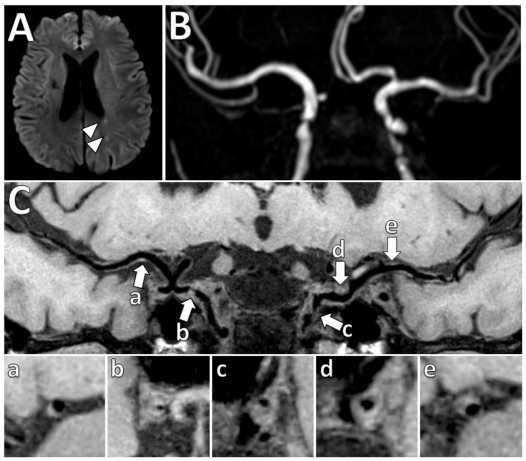

FIGURE 5
Vessel wall thickening and atherosclerosis on VW-MRI in a symptomatic patient. **(A)** A patient with left parietal lobe acute ischemic infarcts (arrowheads) underwent intracranial VW-MRI. **(B)** Time-of-flight MRA and **(C)** intracranial VW-MRI shows multiple intracranial plaques (arrows) that showed both eccentric (a, b, c, e) and concentric (d) vessel wall thickening. The culprit lesion was thought to be the most stenotic lesion (c) in the left internal carotid artery.

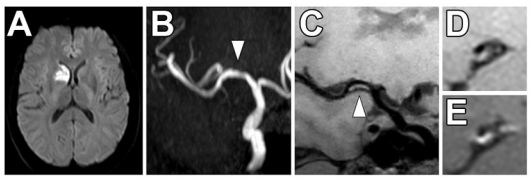

FIGURE 6
Non-stenotic right middle cerebral artery enhancing culprit plaque. **(A)** A patient with a right basal ganglia acute infarct showed **(B)** mild luminal irregularity but no appreciable stenosis of the right middle cerebral artery on time-of-flight MRA imaging (arrowhead). **(C)** Precontrast VW-MRI showed eccentric wall thickening along the right M1 middle cerebral artery (arrowhead). **(D)** Precontrast and **(E)** postcontrast images in the orthogonal plane through the plaque shows eccentric wall thickening and enhancement of the culprit plaque, which likely caused the ischemic infarct.

Contrast enhancement

Multiple VW-MRI studies on intracranial atherosclerosis have shown that there is a higher prevalence of ipsilateral ischemic stroke in patients with contrast enhancing intracranial plaques independent of the degree of luminal stenosis (74–80). Figure 6 shows an example of an enhancing culprit plaque in a non-stenotic vessel that was felt to be the most likely source of a right basal ganglia ischemic stroke after a diagnostic work-up. VW-MRI studies with histological correlation propose contrast enhancement is a marker of inflammation and instability (70, 71). A meta-analysis pooling 990 circle of Willis vessel segments from 11 VW-MRI studies reported that it was more than seven times more likely to observe contrast enhancement of a culprit plaque in association with acute/subacute ischemia in the supplied vascular territory {OR of 7.4 [(95% CI, 3.4–16.4), $p < 0.001$]} (64), indicating this may be one of the stronger imaging biomarkers to detect culprit intracranial plaque. In the literature, definitions of focal/eccentric and circumferential vessel wall thickening detailed above are similar to the definitions of degrees of eccentric and circumferential enhancement.

Vessel wall remodeling

There are two features of vessel wall remodeling, outward and inward, which may be associated with different risks of ischemic events. Arterial walls can accommodate plaque deposition by adapting and remodeling outwardly (81), also known as positive wall remodeling (12). Initial studies in the coronary arteries suggested positive wall remodeling is associated with features of plaque instability (82). A meta-analysis pooling 352 middle cerebral and basilar artery segments from seven VW-MRI studies reported an odds ratio of 5.6 [(95% CI, 2.2–14.0), $p < 0.001$] for presence of positive wall remodeling in culprit plaques supplying the ischemic territory (64). In contrast, fibrotic healing changes may result in arterial wall shrinkage, otherwise known as negative remodeling (81, 83) and hypoperfusion due to stenosis may be a stroke etiology. Additional efforts to understand the role of intracranial vessel wall remodeling in ischemic events are warranted.

Calcifications

The role of calcification in intracranial atherosclerosis is unclear. Atherosclerotic calcification burden is thought to be a marker for cardiovascular events. CT is the gold standard for detecting intracranial calcifications. Detecting calcifications on MRI can be difficult as signal intensities may vary (84, 85), though most often are described to be hypointense on 3D TOF, T1W, T2W, proton density sequences and non-enhancing on gadolinium-enhanced T1W sequence (86). Although CT may be best for calcification detection, distinguishing the type of vascular calcification may be a challenge. For instance, calcifications affecting the arterial intima vs. media may have different clinical consequences. Intimal calcifications are associated with subintimal lipid and cholesterol deposition and macrophage accumulation whereas calcifications of the media are metabolite-induced vascular changes in the absence of lipid deposits and contribute to arterial stiffness (87, 88). Intracranial VW-MRI may play a role to help discriminate intimal calcifications. In a study with 75 patients, non-contrast CT and VW-MRI were used to evaluate intracranial artery calcification and intracranial atherosclerotic plaques, respectively. The study reported 72% of intimal

TABLE 3 Select studies using VW-MRI in an ESUS/CS population for evaluation of intracranial atherosclerosis.

Study	Imaging technique	Vessel	Key imaging characteristics	Select results
Fakih et al. (62)	7T. 3D TOF MRA, 3D T1W fast-spin-echo (CUBE), T2W CUBE, 3D susceptibility-weighted angiogram, post-contrast 3D TIW CUBE	Supraclinoid ICA, MCA, ACA, VA, Basilar, PCA	Contrast enhancement; plaque-to-pituitary stalk contrast enhancement ratio (CR), degree of stenosis, morphology	Culprit plaques ($n = 36$) had higher CR and had concentric morphology than non-culprit plaques ($p \leq 0.001$). CR $\geq$53 ($p = 0.008$), stenosis $\geq$50% ($p < 0.001$), and concentric morphology ($p = 0.030$) as independent predictors of culprit plaques.
Tao et al. (8)	3T. 3D TOF MRA, 3D T1W CUBE, 2D T2W	ICA, MCA, ACA, VA, Basilar artery, PCA	Remodeling index (RI), plaque burden, plaque surface discontinuity, thick fibrous cap, IPH	Higher prevalence of intracranial plaque ipsilateral than contralateral side of ischemic stroke [63.8% vs. 42.8%; odds ratio (OR): 5.25; 95% CI: 2.83–9.73]. RI independently associated with ESUS; model 1 (OR: 2.329; 95% CI: 1.686 −3.217; $p < 0.001$) and model 2 (OR: 2.295; 95% CI: 1.661–3.172; $p < 0.001$).

VW-MRI, vessel wall MRI; T1W GRE, T1 weighted gradient-echo; T, Tesla; TOF MRA, Time-of-flight MR angiography; PD, proton density; T2W, T2 weighted; ICA, internal carotid artery; MCA, middle cerebral artery; ACA, anterior cerebral artery; VA, vertebral artery; PCA, posterior cerebral artery; IPH, intraplaque hemorrhage; CR, plaque-to-pituitary stalk contrast enhancement ratio; RI, remodeling index; 95% CI, 95% confidence interval.

calcifications coexisted with atherosclerotic plaques whereas only 10.2% of medial calcifications coexisted with atherosclerotic plaques (89). The authors also reported intimal calcifications were more common in non-culprit plaques (25.9 vs. 9.4% $P = 0.008$) in their study cohort, raising the possibility that intimal calcifications may indicate a stable form of plaque (89). Additional studies would be of value to understand intracranial calcifications with VW-MRI having a complementary role to CT.

Intracranial VW-MRI in ESUS patients

There are few studies evaluating the use of intracranial VW-MRI specifically in the ESUS/CS population (Table 3). A 7 Tesla (T) VW-MRI study in 2020 by Fakih et al., evaluated 34 patients admitted to the stroke service with acute stroke of cryptogenic origin and unspecific arterial changes on CTA, MRA or DSA that did not meet a diagnosis of a specific vasculopathy. 7T VW-MRI led to the determination of a new stroke etiology in 28 of 34 patients, among which intracranial atherosclerosis was adjudicated as the stroke etiology in 25 of 28 patients. 7T VW-MRI identified culprit plaques as having significantly higher plaque-to-pituitary stalk contrast enhancement ratio, showed concentric morphology compared to non-culprit plaques, showed higher mean signal intensity, and higher contrast ratios compared to non-culprit plaques ($p \leq 0.001$) (62). This study suggests 7T VW-MRI may be used to achieve a more accurate diagnosis of underlying intracranial atherosclerosis as a stroke etiology in a subset of stroke patients meeting criteria for cryptogenic stroke (Figure 7).

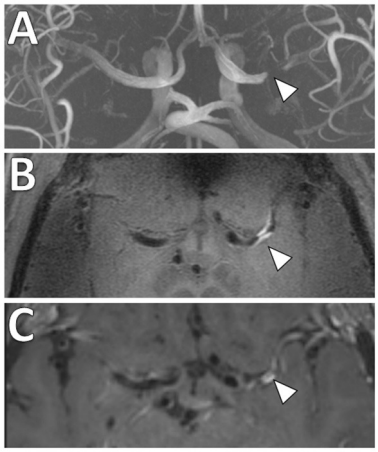

FIGURE 7
Comparison of 3 and 7 Tesla (T) VW-MRI for intracranial atherosclerosis. A patient with history of obesity, hyperlipidemia and hypertension and ischemic stroke underwent a **(A)** 7T TOF-MRA, which showed left M1 middle cerebral artery severe stenosis (arrowhead). **(B)** 7T MRI axial T1 SPACE post-gadolinium (0.5 mm isotropic resolution) image clearly delineates arterial wall thickening and avid vessel wall enhancement in the region of stenosis (arrowhead). **(C)** The same patient was imaged 18 days later on a 3T MRI (T1 SPACE post-gadolinium, 0.8 × 0.8 × 1.0 mm) to assess the stenosis (arrowhead). The 7T VW-MRI shows improved conspicuity and delineation of the margins of the arterial wall compared to the 3T, an advantage of the higher magnet strength due to the higher signal to noise leveraged for higher spatial resolution and soft tissue contrast.

A 3T VW-MRI study by Tao et al. (8) evaluated the morphology and composition of intracranial plaque in the ESUS population compared to patients with small-vessel disease

(SVD). The authors hypothesized a higher prevalence of non-stenotic plaque with positive wall remodeling, which is more prone to vulnerability and rupture, on the ipsilateral side of stroke in ESUS patients. Among 243 patients with ESUS, the prevalence of intracranial plaque ipsilateral to ESUS was significantly higher compared to the contralateral side (63.8% vs. 42.8%; odds ratio 5.25, 95% CI 2.83–9.73). In comparison, among 160 patients with SVD, there was no significant difference in the prevalence of intracranial plaques between the ipsilateral/contralateral sides. Vulnerable plaque features significantly more prevalent on the ipsilateral side of ESUS included positive remodeling and discontinuity of plaque surface (DPS; e.g., surface irregularity suggesting an ulcer, fibrous cap rupture, or formation of overlying mural thrombus), a plaque finding not evident in patients with SVD. The authors concluded that high-risk non-stenotic intracranial plaque may represent a significant but currently underestimated embolic source of ESUS.

Future directions

The use of intracranial VW-MRI to evaluate intracranial atherosclerosis as the culprit source of ischemic stroke is in its early stages. Challenges toward clinical adoption may be related to lengthy acquisition times, variability in VW-MRI protocols and pulse sequence designs, and lack of histologic validation studies (90). Given challenges in obtaining histologic specimens, serial imaging to evaluate the progression of vessel wall changes may be useful to better understand the role of MRI in plaque characterization.

Many patients with vascular risk factors will have systemic atherosclerosis and have disease involving both the intracranial and cervical carotid arteries (91). To address this, investigators have proposed VW-MRI pulse sequences that permit joint intracranial and extracranial artery evaluation (Figure 8). Technical considerations for these pulse sequences include attention to the (1) needed spatial resolution to evaluate the smaller intracranial artery walls compared to the extracranial carotid artery walls, (2) need for adequate cerebrospinal fluid suppression around the circle of Willis compared to fat suppression around the carotid arteries, and (3) head/neck coils that allow adequate coverage. These innovative joint intracranial-extracranial VW-MRI pulse sequences provide promise in identifying the culprit source of stroke in vulnerable patients with systemic atherosclerosis and multiple potential sources of stroke (92–95).

In addition, there is increased interest in characterizing velocity using 4D Flow MRI. This is an advanced phase-contrast MRI technique which allows non-invasive quantifications of blood flow to characterize the hemodynamic impact of intracranial atherosclerosis and identify hemodynamic biomarkers (96) (Figure 9). While studies to date share limitations including long scan duration, low spatial/temporal resolutions and associated tradeoffs (97), this is a promising emerging technique.

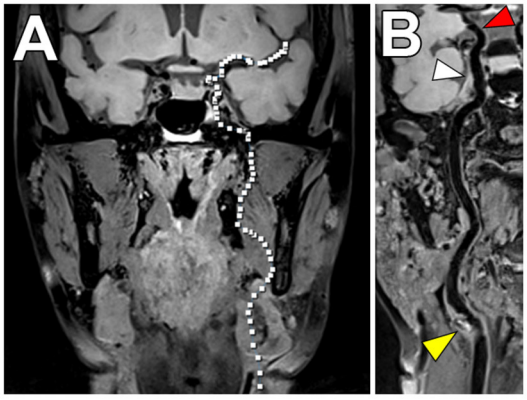

FIGURE 8
Joint VW-MRI of the extracranial and intracranial arteries. **(A)** Coronal precontrast VW-MRI image shows the coverage of the joint intracranial and extracranial VW-MR image. **(B)** A curved reformatted image of the left cervico-cranial carotid artery shows intrinsic T1 hyperintense signal at the carotid bulb (yellow arrowhead), which was favored to be the culprit source of plaque in this patient with ischemic strokes. The intracranial internal carotid artery at the siphon (white arrowhead) and M1 middle cerebral artery segment (red arrowhead) showed no significant wall thickening to suggest intracranial atherosclerosis.

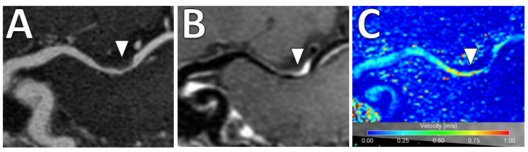

FIGURE 9
4D Flow MRI of intracranial atherosclerosis. **(A)** TOF MRA image demonstrates a focal area of middle cerebral artery narrowing (arrowhead) with **(B)** post-contrast T1-weighted VW-MRI showing a corresponding eccentric, enhancing atherosclerotic plaque (arrowhead). **(C)** On 4D Flow MRI, increased velocities are seen in the area of greatest narrowing (arrowhead).

Aortic arch

Background

Observational studies have identified several morphological features of aortic arch atherosclerosis associated with a high risk of stroke recurrence. Plaque thickness ≥4 mm was observed to be an independent predictor of recurrent stroke and new arterial vascular events (98). Plaque ulcerations and the presence

TABLE 4 Comparison of transesophgeal echocardiogram vs. MR imaging of the aortic arch/proximal aorta evaluating plaque thickness.

Study	Imaging technique	Aortic segment	Key imaging characteristics	Select results
Kutz et al. (108)	1.5T. 3D MRA with T1W vs. TEE; patients imaged with both modalities within 1 month	Asc, Arch, Desc	Plaque size/thickness	$N = 30$ patients; Plaques measuring ≥5 mm, 22 (92%) were seen on TEE and only 13 (54%) on MRA, $p = 0.003$
Fayad et al. (109)	1.5T. T1W, PDW, T2W vs. TEE; patients imaged with both modalities within 39 ± 13 days	Desc	Max plaque thickness, plaque extent, plaque composition	$N = 10$ patients, 25 plaques; Strong correlation or agreement between modalities for max plaque thickness ($r = 0.88$, $n = 25$; 4.56 ± 0.21 mm by MR and 4.62 ± 0.31 mm by TEE), plaque extent [$\chi^2 = 61.77$, $p < 0.0001$; 80% overall agreement] and plaque composition [$\chi^2 = 43.5$, $p < 0.0001$; 80% overall agreement]
Harloff et al. (110)	3T. ECG-synchronized pre- and post-contrast 3D T1W FS, 2D T2W, time resolved (CINE) imaging vs. TEE; patients imaged with both modalities within 5–6 days (median)	Asc, Arch, Desc	Max wall thickness of high risk plaques (≥4 mm or superimposed thrombi)	$N = 74$ patients; No significant difference between MRI and TEE measurements of plaque thickness; Strong agreement in detection of high risk plaques ($0.90 > \kappa > 0.50$); CINE imaging allowed for detection of mobile thrombus
Harloff et al. (111)	3T. 3D contrast-enhanced MRA, ECG-gated 3D T1W RF-spoiled FS bright-blood GRE, 2D T2W TSE, 3D CINE T1W vs. TEE; patients imaged with both modalities within 3 days (median)	Asc, Arch, Desc	Complex plaques (≥4 mm thick, ulcerated, or with mobile thrombus)	$N = 99$ patients. MRI detected more complex plaques than TEE (Asc, 13 vs. 7; Arch, 37 vs. 11; Desc, 101 vs. 70). Image quality was higher for MRI in Asc and Arch and higher for TEE in Desc

Asc, ascending, Desc, descending; FS, fat suppressed; MRA, magnetic resonance angiography; TEE, transesophageal echocardiogram.

of mobile thrombi were also shown to be high-risk features of aortic arch atherosclerosis (99, 100). Given these results, the ASCOD Phenotyping of Ischemic Stroke, which is an etiological classification system for ischemic stroke proposed in 2013, classifies aortic arch atherosclerosis with mobile thrombus and plaque ≥4 mm without a mobile thrombus as possible causes of stroke (15).

Aortic arch atherosclerosis is an often unrecognized stroke mechanism and a potentially important contributor to ESUS (1). In an exploratory analysis of the NAVIGATE ESUS trial, 29% of ESUS patients who underwent evaluation of the aortic arch by transesophageal echocardiography (TEE) had aortic arch atherosclerosis of any severity, 21% had non-complex aortic arch atherosclerosis, and 8% had complex aortic arch atherosclerosis (9). "Complex plaques" included plaques with ulcerations or ≥4 mm in wall thickness or had a mobile thrombus (9). A prospective case-control study by the French Aortic Plaque in Stroke (FAPS) group used TEE to quantify the risk of ischemic stroke with arch atherosclerosis. The authors showed an adjusted odds ratio of 9.1 (3.3–25.2) among 250 cases and 250 controls of a risk of cerebral infarction with arch/proximal plaque thickness ≥4 mm (101).

The dominant imaging modality used to evaluate the aorta in most centers currently is TEE (102). TEE has high sensitivity and specificity for aortic arch atherosclerosis and has sufficient image quality to allow measurement of plaque thickness as well as detection of ulceration and mobile thrombus (103). Limitations of TEE include its invasive nature and operator-dependence. Specifically in regards to aortic plaque imaging, the aortic wall cannot be visualized in its entirety on TEE due to near-field signal losses (104) and limited anatomic evaluations of the ascending aorta due to tracheal and bronchial artifacts (105). Given these limitations, investigations using cross-sectional imaging modalities, such as CT and MRI, have started to emerge (102). Recent advances in 3D-multi-contrast MRI for the detection of aortic atherosclerosis has enabled characterizations of plaque compositions and identification of vulnerable plaques (106, 107).

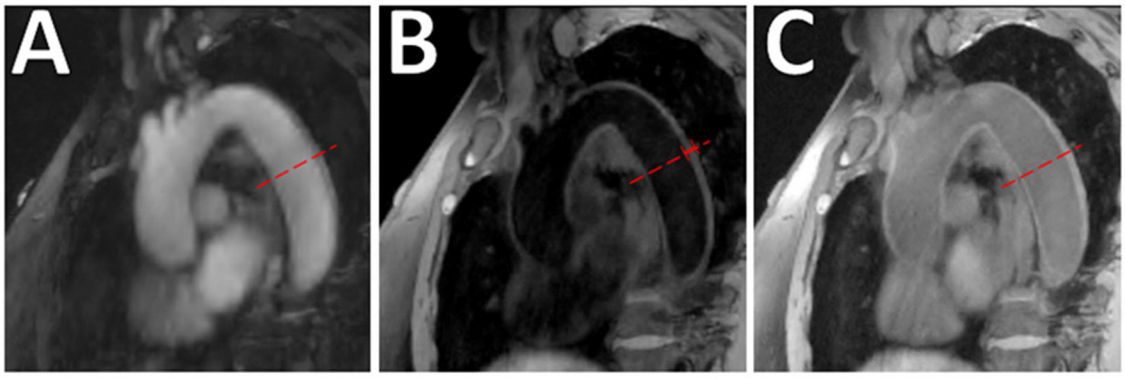

FIGURE 10
Aortic VW-MRI using the MR MultiTasking based 3D Multidimensional Assessment of Cardiovascular System (MT-MACS) Technique. **(A)** In a 71-year-old patient with aortic atherosclerosis, bright-blood lumenography, **(B)** dark-blood (vessel wall imaging), and **(C)** gray-blood (optimized to detect calcium/calcified nodules) images were acquired. In the thoracic aorta (dashed line), increased aortic wall thickness (4.491 mm) was measured and most conspicuous on the dark-blood **(B)** and gray-blood **(C)** images. [These images are re-printed with permission from Zhaoyang Fan, PhD from Magnetic Resonance in Medicine (112).]

MRI of vulnerable aortic arch atherosclerosis features

Plaque thickness

Both 1.5 and 3T MR studies imaging the aortic arch have been compared to TEE with respect to plaque thickness and are summarized in Table 4. Comparing 1.5T MR and TEE, Kutz et al. (108), reported the mean atheroma size in the aortic arch was underestimated on MR compared to TEE (3.4 ± 3.1 mm by TEE, 1.4 ± 3.0 mm by MRA, $P = 0.01$). However, Fayad et al. (109), reported strong correlation and agreement for both 1.5T MR and TEE when measuring maximum plaque thickness and no significant difference in the measurements values (4.62 ± 0.31 mm by TEE, 4.56 ± 0.21 mm by MRI, $r = 0.88$).

Using 3T MR showed more promising results between TEE and MRI and advantages with MRI. Harloff et al. (110), compared the maximum aortic wall thickness measured by TEE against T1W sequence and reported the wall of the aortic arch was not reliably assessed by TEE because of limited visualization in 45 of 74 patients. Among those who were able to be measured, the maximum wall thickness of the aortic arch did not have a statistically significant difference between the modalities (3.36 ± 1.46 mm by TEE, 2.83 ± 1.37 by MRI, p = NS). A subsequent study by Harloff et al. (111), used the same MRI acquisition protocol and showed that MRI detected more complex plaques than TEE at the aortic arch (MRI 37 vs. TEE 11, $p = 0.003$). Notably, the authors reported MRI may potentially overestimate the wall thickness (mean plaque thickness in MRI 5.2 ± 1.1 95% CI 4.1–8.4 vs. TEE 4.7 ± 0.8 95% CI 4.0–6.5).

The long acquisition times for performing multiple acquisitions and the need for ECG-gating and respiratory navigations have resulted in a slow adoption of aortic VW-MRI techniques. Newer innovations in the aortic VW-MRI space show the ability to simultaneously image both the lumen and vessel wall integrity (112, 113). One technique that circumvents the need for these is the MR MultiTasking (MT) based 3D Multi-dimensional Assessment of Cardiovascluar System (MCAS) technique which allows for motion-resolved, isotropic high-spatial resolution, multi-dimensional (multiple contrast weights and cine images) imaging of the thoracic aorta in 6 min (112) (Figure 10). Due to its non-invasive nature, MRI is becoming increasingly used to investigate surveillance imaging for atherosclerosis treatment (114, 115).

Plaque ulceration

An autopsy study showed a higher prevalence of ulcerated aortic plaques with depth and width ≥2 mm in cryptogenic stroke patients (99) and a subsequent study observed that ulcerated plaques were detected by TEE more frequently in patients with cryptogenic stroke than in patients with known-cause strokes or age-matched controls without stroke (116). When directly compared to TEE, 3D MRI has demonstrated mixed results regarding its ability in detecting ulceration. One study using 3D MRI observed limited ability of MRI in detecting ulceration compared to TEE (MRI detected 89% of proximal aorta ulcerations and 64% of distal aorta ulceration) (117). Meanwhile, another 3D MRI study reported MRI detected more plaques with ulcerations compared to TEE (111). These differences may be due to differences in MRI techniques, such as magnet strength (1.5T vs. 3 T MRI) as well as small sample sizes (22 vs. 74) and thus additional explorations are warranted.

Mobile thrombus

Recent advancements in cardiac MRI techniques such as ECG-gated CINE imaging, which is a type of MRI sequence to capture motion, has allowed evaluation of mobile thrombus by

TABLE 5 Select studies using VW-MRI in an ESUS/CS population for evaluation of aortic arch atherosclerosis.

Study	Imaging technique	Vessel	Key imaging characteristics	Select results
Harloff et al. (110)	3T. ECG-synchronized pre- and post-contrast 3D T1W FS, 2D T2W, time resolved (CINE) imaging	Asc, Arch, Desc	Max Wall Thickness of high risk plaques (≥4 mm or superimposed thrombi)	MRI identified high risk pathologies in 8 of 26 (30.8%) CS patients after standard diagnostic work-up including TEE
Harloff et al. (111)	3T. 3D contrast-enhanced MRA, ECG-gated 3D T1W RF-spoiled FS bright blood GRE, 2D T2W TSE, 3D CINE T1W	Asc, Arch, Desc	Complex plaques (≥4 mm thick, ulcerated, or with mobile thrombus)	MRI showed additional complex plaques in 19 of 58 (32.8%) CS patients after diagnostic work-up including TEE
Wehrum et al. (107)	3T. 3D T1W bright-blood, 3D T2W black-blood, 3D PD black-blood. 4D flow used to visualize 3D blood flow within the thoracic aorta	Asc, Arch, Desc	Plaque thickness, surface irregularities, thrombus, IPH, calcification, fibrous tissue	Plaques ≥4 mm more frequent in CS patients than controls [22 (55.0%) vs. 10 (16.7%); $p < 0.001$]. Of those with plaques ≥4 mm, AHA-LT VI plaques higher in stroke patients (17.5% vs. 3.3%, $p < 0.001$). No significant difference between groups for plaques <4 mm thickness [23 (57.5%) vs. 33 (55.0%); $p = 0.81$]
Jarvis et al. (120)	1.5T. 4D flow MRI and 3D T1W black-blood TSE	Mid-Asc, Arch, proximal-Desc, distal-Desc	Aortic wall thickness (3D T1W black-blood), pulse wave velocity (PWV, measure of arterial stiffness) and voxel-wise mapping of flow reversal fraction (FRF)	Aortic PWV and FRF higher in CS patients (8.9 ± 1.7 m/s, 18.4 ± 7.7%) than younger controls (5.3 ± 0.8 m/s, $p < 0.0167$; 8.5 ± 2.9%, $p < 0.0167$), but not age-matched controls (8.2 ± 1.6 m/s, $p = 0.22$; 15.6 ± 5.8%, $p = 0.22$). Maximum aortic wall thickness higher in CS patients (3.1 ± 0.7 mm) than younger controls (2.2 ± 0.2 mm, $p < 0.0167$) and age-matched controls (2.7 ± 0.5 mm) ($p < 0.0167$)

VW-MRI, vessel wall MRI; T1W, T1 weighted; T, Tesla; RF, radiofrequency; FS, fat suppressed; PD, proton density; T2W, T2 weighted; CE MRA, contrast-enhanced magnetic resonance angiography; IPH, intraplaque hemorrhage; AHA-LT VI, American Heart Association lesion type VI; PWV, pulse wave velocity; FRF, flow reversal fraction; 95% CI, 95% confidence interval; Asc, Ascending aorta; Desc, Descending aorta; TSE, turbo spin echo; CS, cryptogenic stroke.

MRI (110, 111). In these studies, structures within the blood stream that were mobile on CINE imaging were defined as mobile thrombus.

Plaque compositions

Similar to investigative aims for VW-MRI of plaque in the cervical carotid and intracranial arteries, aortic VW-MRI has been used to investigate plaque compositions. Yamaguchi et al. (118), performed a retrospective study of 135 patients with ischemic stroke/TIA and imaged on a 3T MRI using a T1W MPRAGE fat suppressed pulse sequence of the aortic arch. Detection of high signal intensity (>200% of sternocleidomastoid muscle signal intensity) on T1W MPRAGE was considered a vulnerable feature and compared to aortic complicated lesions (ACLs) detected by TEE. The results showed that high intensities on MPRAGE were independently associated with ACLs (OR 5.72, 95% CI 2.38–13.70).

Morihara et al. (119), applied a technique called liver-acquisition-with-volume-acceleration-flexible (LAVA-Flex) to assess the relationship between high-intensity plaque lesions in cervical carotid and aortic plaques and plaque thickness on TEE. High-intensity carotid plaque lesions detected on LAVA-Flex were histologically validated on carotid endarterectomy specimens to be large lipid cores and hemorrhage. Hyperintense lesions detected in the thoracic aorta on LAVA-Flex were observed in 24 (51.1%) of 47 CS patients. Twenty-one (87.5%) of these hyperintense aortic lesions also showed a ≥4 mm plaque on TEE, which was considered the gold standard. LAVA-Flex showed a sensitivity of 95.5% and a

specificity of 88.0% in patients with large aortic plaques (≥4 mm thickness).

Literature on aortic arch atherosclerosis VW-MRI in ESUS/CS patients

Literature on the use of MRI to study the prevalence of complex aortic arch atherosclerosis specifically in the ESUS/CS populations is scarce and summarized in Table 5. Harloff et al. (110), reported up to one-third of patients initially to have CS were re-categorized with a high risk aortic plaque after undergoing aortic VW-MRI. In a recent study comparing 40 CS patients to 60 controls, plaques <4 mm thickness were found in similar numbers in CS patients and controls [23 (57.5%) vs. 33 (55.0%); $p = 0.81$] but plaques ≥4 mm were more frequent in CS patients [22 (55.0%) vs. 10 (16.7%); $p < 0.001$] (107).

Future directions

Interest in the use of MRI to evaluate aortic arch atherosclerosis in acute ischemic stroke patients is re-emerging. VW-MRI techniques used for cervical carotid and intracranial arteries may have reignited an interest in characterizing vulnerable aortic plaque features as a potential source for ESUS. Features of aortic arch atherosclerosis that have traditionally been used to define "complex plaques" for risk stratification in acute ischemic stroke patients, such as plaque thickness, ulcerations, and mobile thrombus, are mostly derived from studies using TEE as the main diagnostic imaging modality. However, MR evaluation of the aorta in CS/ESUS patients may be complementary to TEE (110, 111) by offering additional specificity in detecting aortic sources of embolism in patients who would otherwise be labeled as having CS (121, 122).

Advanced MR imaging techniques such as multicontrast VW-MRI, 4D Flow MRI, and CINE imaging are increasingly being explored. 4D Flow MRI allows analysis of hemodynamic flow parameters and can be used to investigate not only aortic wall thickness and stiffness but also flow reversal in the proximal descending aorta in patients with ESUS/CS given retrograde embolic mechanisms during diastole may explain a portion of ESUS/CS (120, 123–125). As technical feasibility is established using these advanced imaging techniques, more studies examining ESUS/CS populations are anticipated to emerge in the future. These advanced imaging techniques may have future applications in the evaluation of aortic arch atherosclerosis in the ESUS population and are promising avenues of research for this vulnerable population.

Conclusion

Despite advancements in stroke diagnostics, a considerable proportion of acute ischemic stroke patients remain without a clear determined mechanism. There has been increased attention to decoding the contributory role of non-stenotic atherosclerosis in the carotid arteries, intracranial arteries, and the aortic arch, in ESUS patients. Non-invasive methods to detect such atherosclerotic plaques and evaluate their morphologies for risk stratification is desirable, and the use of VW-MRI is increasingly becoming investigated.

The preponderance of existing literature on the use of VW-MRI for assessment of vulnerable plaque focuses on the cervical carotid arteries, with increasing translation to the intracranial arteries and the aortic arch. High-risk features of carotid artery atherosclerosis such as IPH, LRNC and fibrous cap status are concepts derived from earlier work in the coronary arteries, and it has been demonstrated that VW-MRI is capable of detecting these features. For intracranial atherosclerosis, additional VW-MRI imaging features have been proposed such as contrast enhancement, vessel wall thickening and vessel wall remodeling; further evaluation in ESUS patients is needed to firmly establish histologic correlation and potential for risk stratification. For aortic arch atherosclerosis, the conventional definitions of "high-risk" features are those derived from earlier non-MRI studies. VW-MRI allows further characterization of aortic arch plaque compositions similar to that seen in carotid studies. Given the rapid advancement of VW-MRI techniques, further studies may demonstrate novel imaging features in aortic arch atherosclerosis.

The use of VW-MRI to detect and characterize carotid, intracranial, and aortic arch atherosclerosis in ESUS patients is an exciting and rapidly evolving field. Additional efforts are warranted to elucidate the contributory role of these atherosclerotic plaques in ESUS.

Author contributions

YS: writing and original draft. VL, LE, EO, and ZF: contributions of images and manuscript review and editing. GK, JX, GW, and BC: manuscript review and editing. JS: conceptualization, contributions of images, and manuscript review and editing. All authors contributed to the article and approved the submitted version.

Funding

The work is supported by the NINDS (L30 NS118632) (JS), Vice Provost for Research University Research Foundation (JS), NHLB (R01 HL147355) (ZF), the Clinical and Translational Science Award program/NIH National Center for Advancing Translational Sciences UL1TR002373 and KL2TR002374 (LE),

and Wisconsin Alzheimer's Disease Research Center grant P30-AG062715 (LE).

Conflict of interest

The authors declare that the research was conducted in the absence of any commercial or financial relationships that could be construed as a potential conflict of interest.

Publisher's note

References

1. Hart RG, Diener HC, Coutts SB, Easton JD, Granger CB, O'Donnell MJ, et al. Embolic strokes of undetermined source: the case for a new clinical construct. *Lancet Neurol.* (2014) 13:429–38. doi: 10.1016/S1474-4422(13)70310-7

2. Gladstone DJ, Spring M, Dorian P, Panzov V, Thorpe KE, Hall J, et al. Atrial fibrillation in patients with cryptogenic stroke. *N Engl J Med.* (2014) 370:2467–77. doi: 10.1056/NEJMoa1311376

3. Sanna T, Diener HC, Passman RS, Di Lazzaro V, Bernstein RA, Morillo CA, et al. Cryptogenic stroke and underlying atrial fibrillation. *N Engl J Med.* (2014) 370:2478–86. doi: 10.1056/NEJMoa1313600

4. Diener HC, Sacco RL, Easton JD, Granger CB, Bernstein RA, Uchiyama S, et al. Dabigatran for prevention of stroke after embolic stroke of undetermined source. *N Engl J Med.* (2019) 380:1906–17. doi: 10.1056/NEJMoa1813959

5. Hart RG, Sharma M, Mundl H, Kasner SE, Bangdiwala SI, Berkowitz SD, et al. Rivaroxaban for stroke prevention after embolic stroke of undetermined source. *N Engl J Med.* (2018) 378:2191–201. doi: 10.1056/NEJMoa1802686

6. Mark IT, Nasr DM, Huston J, de Maria L, de Sanctis P, Lehman VT, et al. Embolic stroke of undetermined source and carotid intraplaque hemorrhage on MRI: a systemic review and meta-analysis. *Clin Neuroradiol.* (2021) 31:307–13. doi: 10.1007/s00062-020-00921-2

7. Kamtchum-Tatuene J, Wilman A, Saqqur M, Shuaib A, Jickling GC. Carotid plaque with high-risk features in embolic stroke of undetermined source: systematic review and meta-analysis. *Stroke.* (2020) 51:311–4. doi: 10.1161/STROKEAHA.119.027272

8. Tao L, Li XQ, Hou XW, Yang BQ, Xia C, Ntaios G, et al. Intracranial atherosclerotic plaque as a potential cause of embolic stroke of undetermined source. *J Am Coll Cardiol.* (2021) 77:680–91. doi: 10.1016/j.jacc.2020.12.015

9. Ntaios G, Pearce LA, Meseguer E, Endres M, Amarenco P, Ozturk S, et al. Aortic arch atherosclerosis in patients with embolic stroke of undetermined source: an exploratory analysis of the NAVIGATE ESUS trial. *Stroke.* (2019) 50:3184–90. doi: 10.1161/STROKEAHA.119.025813

10. Goyal M, Singh N, Marko M, Hill MD, Menon BK, Demchuk A, et al. Embolic stroke of undetermined source and symptomatic nonstenotic carotid disease. *Stroke.* (2020) 51:1321–5. doi: 10.1161/STROKEAHA.119.028853

11. Saba L, Yuan C, Hatsukami TS, Balu N, Qiao Y, DeMarco JK, et al. Carotid artery wall imaging: perspective and guidelines from the ASNR vessel wall imaging study group and expert consensus recommendations of the American Society of Neuroradiology. *AJNR Am J Neuroradiol.* (2018) 39:E9–31. doi: 10.3174/ajnr.A5488

12. Mandell DM, Mossa-Basha M, Qiao Y, Hess CP, Hui F, Matouk C, et al. Intracranial vessel wall MRI: principles and expert consensus recommendations of the American Society of Neuroradiology. *AJNR Am J Neuroradiol.* (2017) 38:218–29. doi: 10.3174/ajnr.A4893

13. Ntaios G, Wintermark M, Michel P. Supracardiac atherosclerosis in embolic stroke of undetermined source: the underestimated source. *Eur Heart J.* (2020) 42:1789–96. doi: 10.1093/eurheartj/ehaa218

14. Adams HP, Jr., Bendixen BH, Kappelle LJ, Biller J, Love BB, Gordon DL, et al. Classification of subtype of acute ischemic stroke. Definitions for use in a multicenter clinical trial. TOAST. Trial of Org 10172 in acute stroke treatment. *Stroke.* (1993) 24:35–41. doi: 10.1161/01.STR.24.1.35

15. Amarenco P, Bogousslavsky J, Caplan LR, Donnan GA, Wolf ME, Hennerici MG. The ASCOD phenotyping of ischemic stroke (updated ASCO phenotyping). *Cerebrovasc Dis.* (2013) 36:1–5. doi: 10.1159/000352050

16. Virmani R, Burke AP, Kolodgie FD, Farb A. Vulnerable plaque: the pathology of unstable coronary lesions. *J Interv Cardiol.* (2002) 15:439–46. doi: 10.1111/j.1540-8183.2002.tb01087.x

17. Naghavi M, Libby P, Falk E, Casscells SW, Litovsky S, Rumberger J, et al. From vulnerable plaque to vulnerable patient: a call for new definitions and risk assessment strategies: Part II. *Circulation.* (2003) 108:1772–8. doi: 10.1161/01.CIR.0000087481.55887.C9

18. Naghavi M, Libby P, Falk E, Casscells SW, Litovsky S, Rumberger J, et al. From vulnerable plaque to vulnerable patient: a call for new definitions and risk assessment strategies: Part I. *Circulation.* (2003) 108:1664–72. doi: 10.1161/01.CIR.0000087480.94275.97

19. Saba L, Saam T, Jäger HR, Yuan C, Hatsukami TS, Saloner D, et al. Imaging biomarkers of vulnerable carotid plaques for stroke risk prediction and their potential clinical implications. *Lancet Neurol.* (2019) 18:559–72. doi: 10.1016/S1474-4422(19)30035-3

20. Saam T, Ferguson MS, Yarnykh VL, Takaya N, Xu D, Polissar NL, et al. Quantitative evaluation of carotid plaque composition by *in vivo* MRI. *Arterioscler Thromb Vasc Biol.* (2005) 25:234–9. doi: 10.1161/01.ATV.0000149867.61851.31

21. Saam T, Hatsukami TS, Takaya N, Chu B, Underhill H, Kerwin WS, et al. The vulnerable, or high-risk, atherosclerotic plaque: noninvasive MR imaging for characterization and assessment. *Radiology.* (2007) 244:64–77. doi: 10.1148/radiol.2441051769

22. Cai J, Hatsukami TS, Ferguson MS, Kerwin WS, Saam T, Chu B, et al. *In vivo* quantitative measurement of intact fibrous cap and lipid-rich necrotic core size in atherosclerotic carotid plaque. *Circulation.* (2005) 112:3437–44. doi: 10.1161/CIRCULATIONAHA.104.528174

23. Puppini G, Furlan F, Cirota N, Veraldi G, Piubello Q, Montemezzi S, et al. Characterisation of carotid atherosclerotic plaque: comparison between magnetic resonance imaging and histology. *Radiol Med.* (2006) 111:921–30. doi: 10.1007/s11547-006-0091-7

24. Hatsukami TS, Ross R, Polissar NL, Yuan C. Visualization of fibrous cap thickness and rupture in human atherosclerotic carotid plaque *in vivo* with high-resolution magnetic resonance imaging. *Circulation.* (2000) 102:959–64. doi: 10.1161/01.CIR.102.9.959

25. Moulton KS. Plaque angiogenesis and atherosclerosis. *Curr Atheroscler Rep.* (2001) 3:225–33. doi: 10.1007/s11883-001-0065-0

26. Altaf N, Daniels L, Morgan PS, Auer D, MacSweeney ST, Moody AR, et al. Detection of intraplaque hemorrhage by magnetic resonance imaging in symptomatic patients with mild to moderate carotid stenosis predicts recurrent neurological events. *J Vasc Surg.* (2008) 47:337–42. doi: 10.1016/j.jvs.2007.09.064

27. Takaya N, Yuan C, Chu B, Saam T, Underhill H, Cai J, et al. Association between carotid plaque characteristics and subsequent ischemic cerebrovascular events. *Stroke.* (2006) 37:818–23. doi: 10.1161/01.STR.0000204638.91099.91

28. Gupta A, Baradaran H, Schweitzer AD, Kamel H, Pandya A, Delgado D, et al. Carotid plaque MRI and stroke risk: a systematic review and meta-analysis. *Stroke.* (2013) 44:3071–7. doi: 10.1161/STROKEAHA.113.002551

29. Qiao Y, Etesami M, Malhotra S, Astor BC, Virmani R, Kolodgie FD, et al. Identification of intraplaque hemorrhage on MR angiography images: a comparison of contrast-enhanced mask and time-of-flight techniques. *AJNR Am J Neuroradiol.* (2011) 32:454–9. doi: 10.3174/ajnr.A2320

30. McNally JS, Kim SE, Mendes J, Hadley JR, Sakata A, De Havenon AH, et al. Magnetic resonance imaging detection of intraplaque hemorrhage. *Magn Reson Insights.* (2017) 10:1–8. doi: 10.1177/1178623X17694150

31. Ota H, Yarnykh VL, Ferguson MS, Underhill HR, Demarco JK, Zhu DC, et al. Carotid intraplaque hemorrhage imaging at 30-T MR imaging: comparison of the diagnostic performance of three T1-weighted sequences. *Radiology.* (2010) 254:551–63. doi: 10.1148/radiol.09090535

32. Saba L, Francone M, Bassareo PP, Lai L, Sanfilippo R, Montisci R, et al. CT Attenuation analysis of carotid intraplaque hemorrhage. *AJNR Am J Neuroradiol.* (2018) 39:131–7. doi: 10.3174/ajnr.A5461

33. Li Z, Cao J, Bai X, Gao P, Zhang D, Lu X, et al. Utility of dual-layer spectral detector CTA to characterize carotid atherosclerotic plaque components: an imaging-histopathology comparison in patients undergoing endarterectomy. *AJR Am J Roentgenol.* (2022) 218:517–25. doi: 10.2214/AJR.21.26540

34. Yuan C, Zhang SX, Polissar NL, Echelard D, Ortiz G, Davis JW, et al. Identification of fibrous cap rupture with magnetic resonance imaging is highly associated with recent transient ischemic attack or stroke. *Circulation.* (2002) 105:181–5. doi: 10.1161/hc0202.102121

35. Freilinger TM, Schindler A, Schmidt C, Grimm J, Cyran C, Schwarz F, et al. Prevalence of nonstenosing, complicated atherosclerotic plaques in cryptogenic stroke. *JACC Cardiovasc Imaging.* (2012) 5:397–405. doi: 10.1016/j.jcmg.2012.01.012

36. Barnett HJ, Taylor DW, Eliasziw M, Fox AJ, Ferguson GG, Haynes RB, et al. Benefit of carotid endarterectomy in patients with symptomatic moderate or severe stenosis. North American Symptomatic Carotid Endarterectomy Trial Collaborators. *N Engl J Med.* (1998) 339:1415–25. doi: 10.1056/NEJM199811123392002

37. Wasserman BA, Smith WI, Trout HH. 3rd, Cannon RO, 3rd, Balaban RS, Arai AE. Carotid artery atherosclerosis: *in vivo* morphologic characterization with gadolinium-enhanced double-oblique MR imaging initial results. *Radiology.* (2002) 223:566–73. doi: 10.1148/radiol.2232010659

38. Etesami M, Hoi Y, Steinman DA, Gujar SK, Nidecker AE, Astor BC, et al. Comparison of carotid plaque ulcer detection using contrast-enhanced and time-of-flight MRA techniques. *AJNR Am J Neuroradiol.* (2013) 34:177–84. doi: 10.3174/ajnr.A3132

39. Demarco JK, Ota H, Underhill HR, Zhu DC, Reeves MJ, Potchen MJ, et al. MR carotid plaque imaging and contrast-enhanced MR angiography identifies lesions associated with recent ipsilateral thromboembolic symptoms: an *in vivo* study at 3T. *AJNR Am J Neuroradiol.* (2010) 31:1395–402. doi: 10.3174/ajnr.A2213

40. Bayer-Karpinska A, Schwarz F, Wollenweber FA, Poppert H, Boeckh-Behrens T, Becker A, et al. The carotid plaque imaging in acute stroke (CAPIAS) study: protocol and initial baseline data. *BMC Neurol.* (2013) 13:1–10. doi: 10.1186/1471-2377-13-201

41. Gupta A, Gialdini G, Lerario MP, Baradaran H, Giambrone A, Navi BB, et al. Magnetic resonance angiography detection of abnormal carotid artery plaque in patients with cryptogenic stroke. *J Am Heart Assoc.* (2015) 4:e002012. doi: 10.1161/JAHA.115.002012

42. Gupta A, Gialdini G, Giambrone AE, Lerario MP, Baradaran H, Navi BB, et al. Association between nonstenosing carotid artery plaque on MR angiography and acute ischemic stroke. *JACC: Cardiovasc Imaging.* (2016) 9:1228–9. doi: 10.1016/j.jcmg.2015.12.004

43. Hyafil F, Schindler A, Sepp D, Obenhuber T, Bayer-Karpinska A, Boeckh-Behrens T, et al. High-risk plaque features can be detected in non-stenotic carotid plaques of patients with ischaemic stroke classified as cryptogenic using combined (18)F-FDG PET/MR imaging. *Eur J Nucl Med Mol Imaging.* (2016) 43:270–9. doi: 10.1007/s00259-015-3201-8

44. Singh N, Moody AR, Panzov V, Gladstone DJ. Carotid intraplaque hemorrhage in patients with embolic stroke of undetermined source. *J Stroke Cerebrovasc Dis.* (2018) 27:1956–9. doi: 10.1016/j.jstrokecerebrovasdis.2018.02.042

45. Zhao H, Zhao X, Liu X, Cao Y, Hippe DS, Sun J, et al. Association of carotid atherosclerotic plaque features with acute ischemic stroke: a magnetic resonance imaging study. *Eur J Radiol.* (2013) 82:e465–70. doi: 10.1016/j.ejrad.2013.04.014

46. Zhao X, Li R, Hippe DS, Hatsukami TS, Yuan C. Chinese Atherosclerosis Risk Evaluation (CARE II) study: a novel cross-sectional, multicentre study of the prevalence of high-risk atherosclerotic carotid plaque in Chinese patients with ischaemic cerebrovascular events-design and rationale. *Stroke Vasc Neurol.* (2017) 2:15–20. doi: 10.1136/svn-2016-000053

47. Truijman MT, Kooi ME, van Dijk AC, de Rotte AA, van der Kolk AG, Liem MI, et al. Plaque At RISK (PARISK): prospective multicenter study to improve diagnosis of high-risk carotid plaques. *Int J Stroke.* (2014) 9:747–54. doi: 10.1111/ijs.12167

48. Brinjikji W, DeMarco JK, Shih R, Lanzino G, Rabinstein AA, Hilditch CA, et al. Diagnostic accuracy of a clinical carotid plaque MR protocol using a neurovascular coil compared to a surface coil protocol. *J Magn Reson Imaging.* (2018) 48:1264–72. doi: 10.1002/jmri.25984

49. Wei H, Zhang M, Li Y, Zhao X, Canton G, Sun J, et al. Evaluation of 3D multi-contrast carotid vessel wall MRI: a comparative study. *Quant Imaging Med Surg.* (2020) 10:269–82. doi: 10.21037/qims.2019.09.11

50. Fan Z, Yu W, Xie Y, Dong L, Yang L, Wang Z, et al. Multi-contrast atherosclerosis characterization (MATCH) of carotid plaque with a single 5-min scan: technical development and clinical feasibility. *J Cardiovasc Magn Reson.* (2014) 16:53. doi: 10.1186/s12968-014-0053-5

51. Ritz K, Denswil NP, Stam OCG. Lieshout JJv, Daemen MJAP. Cause and mechanisms of intracranial atherosclerosis. *Circulation.* (2014) 130:1407–14. doi: 10.1161/CIRCULATIONAHA.114.011147

52. Aydin F. Do human intracranial arteries lack vasa vasorum? A comparative immunohistochemical study of intracranial and systemic arteries. *Acta Neuropathol.* (1998) 96:22–8. doi: 10.1007/s004010050856

53. Zervas NT, Liszczak TM, Mayberg MR, Black PM. Cerebrospinal fluid may nourish cerebral vessels through pathways in the adventitia that may be analogous to systemic vasa vasorum. *J Neurosurg.* (1982) 56:475–81. doi: 10.3171/jns.1982.56.4.0475

54. Ritman EL, Lerman A. The dynamic vasa vasorum. *Cardiovasc Res.* (2007) 75:649–58. doi: 10.1016/j.cardiores.2007.06.020

55. Maiellaro K, Taylor WR. The role of the adventitia in vascular inflammation. *Cardiovasc Res.* (2007) 75:640–8. doi: 10.1016/j.cardiores.2007.06.023

56. Kwon T-G, Lerman Lilach O, Lerman A. The vasa vasorum in atherosclerosis. *J Am Coll Cardiol.* (2015) 65:2478–80. doi: 10.1016/j.jacc.2015.04.032

57. Wang Y, Meng R, Liu G, Cao C, Chen F, Jin K, et al. Intracranial atherosclerotic disease. *Neurobiol Dis.* (2019) 124:118–32. doi: 10.1016/j.nbd.2018.11.008

58. Koo J. The latest information on intracranial atherosclerosis: diagnosis and treatment. *Interv Neurol.* (2015) 4:48–50. doi: 10.1159/000438779

59. Song JW, Pavlou A, Burke MP, Shou H, Atsina KB, Xiao J, et al. Imaging endpoints of intracranial atherosclerosis using vessel wall MR imaging: a systematic review. *Neuroradiology.* (2021) 63:847–56. doi: 10.1007/s00234-020-02575-w

60. Song JW, Wasserman BA. Vessel wall MR imaging of intracranial atherosclerosis. *Cardiovasc Diagn Ther.* (2020) 10:982–93. doi: 10.21037/cdt-20-470

61. Xu WH Li ML, Gao S, Ni J, Yao M, Zhou LX, et al. Middle cerebral artery intraplaque hemorrhage: prevalence and clinical relevance. *Ann Neurol.* (2012) 71:195–8. doi: 10.1002/ana.22626

62. Fakih R, Roa JA, Bathla G, Olalde H, Varon A, Ortega-Gutierrez S, et al. Detection and quantification of symptomatic atherosclerotic plaques with high-resolution imaging in cryptogenic stroke. *Stroke.* (2020) 51:3623–31. doi: 10.1161/STROKEAHA.120.031167

63. Chen XY, Wong KS, Lam WW, Ng HK. High signal on T1 sequence of magnetic resonance imaging confirmed to be intraplaque haemorrhage by histology in middle cerebral artery. *Int J Stroke.* (2014) 9:E19. doi: 10.1111/ijs.12277

64. Song JW, Pavlou A, Xiao J, Kasner SE, Fan Z, Messé SR. Vessel wall magnetic resonance imaging biomarkers of symptomatic intracranial atherosclerosis: a meta-analysis. *Stroke.* (2021) 52:193–202. doi: 10.1161/STROKEAHA.120.031480

65. Yang WJ, Fisher M, Zheng L, Niu CB, Paganini-Hill A, Zhao HL, et al. Histological characteristics of intracranial atherosclerosis in a Chinese population: a postmortem study. *Front Neurol.* (2017) 8:488. doi: 10.3389/fneur.2017.00488

66. Chen XY, Wong KS, Lam WWM, Zhao HL, Ng HK. Middle cerebral artery atherosclerosis: histological comparison between plaques associated with and not associated with infarct in a postmortem study. *Cerebrovasc Dis.* (2008) 25:74–80. doi: 10.1159/000111525

67. Watase H, Shen M, Sui B, Gao P, Zhang D, Sun J, et al. Differences in atheroma between Caucasian and Asian subjects with anterior stroke: a vessel wall MRI study. *Stroke Vasc Neurol.* (2021) 6:25–32. doi: 10.1136/svn-2020-000370

68. Jiang Y, Zhu C, Peng W, Degnan AJ, Chen L, Wang X, et al. *Ex-vivo* imaging and plaque type classification of intracranial atherosclerotic plaque using high resolution MRI. *Atherosclerosis.* (2016) 249:10–6. doi: 10.1016/j.atherosclerosis.2016.03.033

69. Yang WJ, Chen XY, Zhao HL, Niu CB, Zhang B, Xu Y, et al. Postmortem study of validation of low signal on fat-suppressed T1-weighted magnetic resonance imaging as marker of lipid core in middle cerebral artery atherosclerosis. *Stroke.* (2016) 47:2299–304. doi: 10.1161/STROKEAHA.116.013398

70. Turan TN, Rumboldt Z, Granholm AC, Columbo L, Welsh CT, Lopes-Virella MF, et al. Intracranial atherosclerosis: correlation between *in-vivo* 3T high resolution MRI and pathology. *Atherosclerosis.* (2014) 237:460–3. doi: 10.1016/j.atherosclerosis.2014.10.007

71. van der Kolk AG, Zwanenburg JJ, Denswil NP, Vink A, Spliet WG, Daemen MJ, et al. Imaging the intracranial atherosclerotic vessel wall using 7T MRI:

initial comparison with histopathology. *AJNR Am J Neuroradiol.* (2015) 36:694–701. doi: 10.3174/ajnr.A4178

72. Arnett N, Pavlou A, Burke MP, Cucchiara BL, Rhee RL, Song JW. Vessel wall MR imaging of central nervous system vasculitis: a systematic review. *Neuroradiology.* (2022) 64:43–58. doi: 10.1007/s00234-021-02724-9

73. Swartz RH, Bhuta SS, Farb RI, Agid R, Willinsky RA, Terbrugge KG, et al. Intracranial arterial wall imaging using high-resolution 3-tesla contrast-enhanced MRI. *Neurology.* (2009) 72:627–34. doi: 10.1212/01.wnl.0000342470.69739.b3

74. Gupta A, Baradaran H, Al-Dasuqi K, Knight-Greenfield A, Giambrone AE, Delgado D, et al. Gadolinium enhancement in intracranial atherosclerotic plaque and ischemic stroke: a systematic review and meta-analysis. *J Am Heart Assoc.* (2016) 5:e003816. doi: 10.1161/JAHA.116.003816

75. Choi YJ, Jung SC, Lee DH. Vessel wall imaging of the intracranial and cervical carotid arteries. *J Stroke.* (2015) 17:238–55. doi: 10.5853/jos.2015.17.3.238

76. Kim JM, Jung KH, Sohn CH, Moon J, Shin JH, Park J, et al. Intracranial plaque enhancement from high resolution vessel wall magnetic resonance imaging predicts stroke recurrence. *Int J Stroke.* (2016) 11:171–9. doi: 10.1177/1747493015609775

77. Lee HN Ryu CW, Yun SJ. Vessel-wall magnetic resonance imaging of intracranial atherosclerotic plaque and ischemic stroke: a systematic review and meta-analysis. *Front Neurol.* (2018) 9:1032. doi: 10.3389/fneur.2018.01032

78. Kim JM, Jung KH, Sohn CH, Moon J, Han MH, Roh JK. Middle cerebral artery plaque and prediction of the infarction pattern. *Arch Neurol.* (2012) 69:1470–5. doi: 10.1001/archneurol.2012.1018

79. Kwee RM, Qiao Y, Liu L, Zeiler SR, Wasserman BA. Temporal course and implications of intracranial atherosclerotic plaque enhancement on high-resolution vessel wall MRI. *Neuroradiology.* (2019) 61:651–7. doi: 10.1007/s00234-019-02190-4

80. Qiao Y, Zeiler SR, Mirbagheri S, Leigh R, Urrutia V, Wityk R, et al. Intracranial plaque enhancement in patients with cerebrovascular events on high-spatial-resolution MR images. *Radiology.* (2014) 271:534–42. doi: 10.1148/radiol.13122812

81. Glagov S, Weisenberg E, Zarins CK, Stankunavicius R, Kolettis GJ. Compensatory enlargement of human atherosclerotic coronary arteries. *N Engl J Med.* (1987) 316:1371–5. doi: 10.1056/NEJM198705283162204

82. Burke AP, Kolodgie FD, Farb A, Weber D, Virmani R. Morphological predictors of arterial remodeling in coronary atherosclerosis. *Circulation.* (2002) 105:297–303. doi: 10.1161/hc0302.102610

83. Xu WH Li ML, Gao S, Ni J, Zhou LX, Yao M, et al. *In vivo* high-resolution MR imaging of symptomatic and asymptomatic middle cerebral artery atherosclerotic stenosis. *Atherosclerosis.* (2010) 212:507–11. doi: 10.1016/j.atherosclerosis.2010.06.035

84. Sarmiento de la Iglesia MM, Lecumberri Cortés G, Lecumberri Cortés I, Oleaga Zufiria L, Isusi Fontan M, Grande Icaran D. [Intracranial calcifications on MRI]. *Radiologia.* (2006) 48:19–26. doi: 10.1016/S0033-8338(06)73125-3

85. Chen W, Zhu W, Kovanlikaya I, Kovanlikaya A, Liu T, Wang S, et al. Intracranial calcifications and hemorrhages: characterization with quantitative susceptibility mapping. *Radiology.* (2014) 270:496–505. doi: 10.1148/radiol.13122640

86. Mazzacane F, Mazzoleni V, Scola E, Mancini S, Lombardo I, Busto G, et al. Vessel wall magnetic resonance imaging in cerebrovascular diseases. *Diagnostics.* (2022) 12:258. doi: 10.3390/diagnostics12020258

87. Amann K. Media calcification and intima calcification are distinct entities in chronic kidney disease. *Clin J Am Soc Nephrol.* (2008) 3:1599–605. doi: 10.2215/CJN.02120508

88. Kockelkoren R, Vos A, Van Hecke W, Vink A, Bleys RL, Verdoorn D, et al. Computed tomographic distinction of intimal and medial calcification in the intracranial internal carotid artery. *PLoS ONE.* (2017) 12:e0168360. doi: 10.1371/journal.pone.0168360

89. Yang WJ, Wasserman BA, Zheng L, Huang ZQ Li J, Abrigo J, et al. Understanding the clinical implications of intracranial arterial calcification using brain CT and vessel wall imaging. *Front Neurol.* (2021) 12:619233. doi: 10.3389/fneur.2021.619233

90. Song JW, Moon BF, Burke MP, Kamesh Iyer S, Elliott MA, Shou H, et al. MR intracranial vessel wall imaging: a systematic review. *J Neuroimaging.* (2020) 30:428–42. doi: 10.1111/jon.12719

91. Ntaios G, Pearce LA, Veltkamp R, Sharma M, Kasner SE, Korompoki E, et al. Potential embolic sources and outcomes in embolic stroke of undetermined source in the NAVIGATE-ESUS trial. *Stroke.* (2020) 51:1797–804. doi: 10.1161/STROKEAHA.119.028669

92. Zhou Z, Li R, Zhao X, He L, Wang X, Wang J, et al. Evaluation of 3D multi-contrast joint intra- and extracranial vessel wall cardiovascular magnetic resonance. *J Cardiovasc Magn Reson.* (2015) 17:41. doi: 10.1186/s12968-015-0143-z

93. Zhang L, Zhang N, Wu J, Liu X, Chung YC. High resolution simultaneous imaging of intracranial and extracranial arterial wall with improved cerebrospinal fluid suppression. *Magn Reson Imaging.* (2017) 44:65–71. doi: 10.1016/j.mri.2017.08.004

94. Jia S, Zhang L, Ren L, Qi Y, Ly J, Zhang N, et al. Joint intracranial and carotid vessel wall imaging in 5 minutes using compressed sensing accelerated DANTE-SPACE. *Eur Radiol.* (2020) 30:119–27. doi: 10.1007/s00330-019-06366-7

95. Xie Y, Yang Q, Xie G, Pang J, Fan Z, Li D. Improved black-blood imaging using DANTE-SPACE for simultaneous carotid and intracranial vessel wall evaluation. *Magn Reson Med.* (2016) 75:2286–94. doi: 10.1002/mrm.25785

96. Wåhlin A, Eklund A, Malm J. 4D flow MRI hemodynamic biomarkers for cerebrovascular diseases. *J Intern Med.* (2022) 291:115–27. doi: 10.1111/joim.13392

97. Morgan AG, Thrippleton MJ, Wardlaw JM, Marshall I. 4D flow MRI for non-invasive measurement of blood flow in the brain: a systematic review. *J Cereb Blood Flow Metab.* (2021) 41:206–18. doi: 10.1177/0271678X20952014

98. Amarenco P, Cohen A, Hommel M, Moulin T, Leys D, Bousser MG. Atherosclerotic disease of the aortic arch as a risk factor for recurrent ischemic stroke. *N Engl J Med.* (1996) 334:1216–21. doi: 10.1056/NEJM199605093341902

99. Amarenco P, Duyckaerts C, Tzourio C, Hénin D, Bousser MG, Hauw JJ. The prevalence of ulcerated plaques in the aortic arch in patients with stroke. *N Engl J Med.* (1992) 326:221–5. doi: 10.1056/NEJM199201233260402

100. Tunick PA, Rosenzweig BP, Katz ES, Freedberg RS, Perez JL, Kronzon I. High risk for vascular events in patients with protruding aortic atheromas: a prospective study. *J Am Coll Cardiol.* (1994) 23:1085–90. doi: 10.1016/0735-1097(94)90595-9

101. Amarenco P, Cohen A, Tzourio C, Bertrand B, Hommel M, Besson G, et al. Atherosclerotic disease of the aortic arch and the risk of ischemic stroke. *N Engl J Med.* (1994) 331:1474–9. doi: 10.1056/NEJM199412013312202

102. Jansen Klomp WW, Brandon Bravo Bruinsma GJ, van 't Hof AW, Grandjean JG, Nierich AP. Imaging techniques for diagnosis of thoracic aortic atherosclerosis. *Int J Vasc Med.* (2016) 2016:4726094. doi: 10.1155/2016/4726094

103. Viedma-Guiard E, Guidoux C, Amarenco P, Meseguer E. Aortic sources of embolism. *Front Neurol.* (2020) 11:606663. doi: 10.3389/fneur.2020.606663

104. Shunk KA, Garot J, Atalar E, Lima JAC. Transesophageal magnetic resonance imaging of the aortic arch and descending thoracic aorta in patients with aortic atherosclerosis. *J Am Coll Cardiol.* (2001) 37:2031–5. doi: 10.1016/S0735-1097(01)01340-7

105. Krinsky GA, Freedberg R, Lee VS, Rockman C, Tunick PA. Innominate artery atheroma: a lesion seen with gadolinium-enhanced MR angiography and often missed by transesophageal echocardiography. *Clin Imaging.* (2001) 25:251–7. doi: 10.1016/S0899-7071(01)00292-3

106. Wehrum T, Dragonu I, Strecker C, Hennig J, Harloff A. Multi-contrast and three-dimensional assessment of the aortic wall using 3T MRI. *Eur J Radiol.* (2017) 91:148–54. doi: 10.1016/j.ejrad.2017.04.011

107. Wehrum T, Dragonu I, Strecker C, Schuchardt F, Hennemuth A, Drexl J, et al. Aortic atheroma as a source of stroke – assessment of embolization risk using 3D CMR in stroke patients and controls. *J Cardiovasc Magn Reson.* (2017) 19:67. doi: 10.1186/s12968-017-0379-x

108. Kutz SM, Lee VS, Tunick PA, Krinsky GA, Kronzon I. Atheromas of the thoracic aorta: a comparison of transesophageal echocardiography and breath-hold gadolinium-enhanced 3-dimensional magnetic resonance angiography. *J Am Soc Echocardiogr.* (1999) 12:853–8. doi: 10.1016/S0894-7317(99)70191-4

109. Fayad ZA, Nahar T, Fallon JT, Goldman M, Aguinaldo JG, Badimon JJ, et al. *In vivo* magnetic resonance evaluation of atherosclerotic plaques in the human thoracic aorta: a comparison with transesophageal echocardiography. *Circulation.* (2000) 101:2503–9. doi: 10.1161/01.CIR.101.21.2503

110. Harloff A, Dudler P, Frydrychowicz A, Strecker C, Stroh AL, Geibel A, et al. Reliability of aortic MRI at 3 Tesla in patients with acute cryptogenic stroke. *J Neurol Neurosurg Psychiatry.* (2008) 79:540–6. doi: 10.1136/jnnp.2007.125211

111. Harloff A, Brendecke SM, Simon J, Assefa D, Wallis W, Helbing T, et al. 3D MRI provides improved visualization and detection of aortic arch plaques compared to transesophageal echocardiography. *J Magn Reson Imaging.* (2012) 36:604–11. doi: 10.1002/jmri.23679

112. Hu Z, Christodoulou AG, Wang N, Shaw JL, Song SS, Maya MM, et al. Magnetic resonance multitasking for multidimensional assessment of cardiovascular system: development and feasibility study on the thoracic aorta. *Magn Reson Med.* (2020) 84:2376–88. doi: 10.1002/mrm.28275

113. Munoz C, Fotaki A, Hajhosseiny R, Kunze K, Neji R, Botnar R, et al. Simultaneous lumen and vessel wall imaging with iT2Prep-BOOST for an efficient comprehensive assessment of aortic disease. In: *Joint Annual Meeting ISMRM-ESMRMB ISMRT 31st Annual Meeting*. London (2022).

114. Lima JAC, Desai MY, Steen H, Warren WP, Gautam S, Lai S. Statin-induced cholesterol lowering and plaque regression after 6 months of magnetic resonance imaging–monitored therapy. *Circulation.* (2004) 110:2336–41. doi: 10.1161/01.CIR.0000145170.22652.51

115. Corti R, Fuster V, Fayad ZA, Worthley SG, Helft G, Smith D, et al. Lipid lowering by simvastatin induces regression of human atherosclerotic lesions. *Circulation.* (2002) 106:2884–7. doi: 10.1161/01.CIR.0000041255.88750.F0

116. Stone DA, Hawke MW, LaMonte M, Kittner SJ, Acosta J, Corretti M, et al. Ulcerated atherosclerotic plaques in the thoracic aorta are associated with cryptogenic stroke: a multiplane transesophageal echocardiographic study. *Am Heart J.* (1995) 130:105–8. doi: 10.1016/0002-8703(95)90243-0

117. Faber T, Rippy A, Hyslop WB, Hinderliter A, Sen S. Cardiovascular MRI in detection and measurement of aortic atheroma in stroke/TIA patients. *J Neurol Disord.* (2013) 1:139. doi: 10.4172/2329-6895.1000139

118. Yamaguchi Y, Tanaka T, Morita Y, Yoshimura S, Koga M, Ihara M, et al. Associations of high intensities on magnetization-prepared rapid acquisition with gradient echo with aortic complicated lesions in ischemic stroke patients. *Cerebrovasc Dis.* (2019) 47:15–23. doi: 10.1159/000497068

119. Morihara K, Nakano T, Mori K, Fukui I, Nomura M, Suzuki K, et al. Usefulness of rapid MR angiography using two-point Dixon for evaluating carotid and aortic plaques. *Neuroradiology.* (2022) 64:693–702. doi: 10.1007/s00234-021-02812-w

120. Jarvis K, Soulat G, Scott M, Vali A, Pathrose A, Syed AA, et al. Investigation of aortic wall thickness, stiffness and flow reversal in patients with cryptogenic stroke: a 4D flow MRI study. *J Magn Reson Imaging.* (2021) 53:942–52. doi: 10.1002/jmri.27345

121. Baher A, Mowla A, Kodali S, Polsani VR, Nabi F, Nagueh SF, et al. Cardiac MRI improves identification of etiology of acute ischemic stroke. *Cerebrovasc Dis.* (2014) 37:277–84. doi: 10.1159/000360073

122. Haeusler KG, Wollboldt C. Bentheim Lz, Herm J, Jäger S, Kunze C, et al. Feasibility and diagnostic value of cardiovascular magnetic resonance imaging after acute ischemic stroke of undetermined origin. *Stroke.* (2017) 48:1241–7. doi: 10.1161/STROKEAHA.116.016227

123. Markl M, Semaan E, Stromberg L, Carr J, Prabhakaran S, Collins J. Importance of variants in cerebrovascular anatomy for potential retrograde embolization in cryptogenic stroke. *Eur Radiol.* (2017) 27:4145–52. doi: 10.1007/s00330-017-4821-0

124. Harloff A, Strecker C, Dudler P, Nussbaumer A, Frydrychowicz A, Olschewski M, et al. Retrograde embolism from the descending aorta: visualization by multidirectional 3D velocity mapping in cryptogenic stroke. *Stroke.* (2009) 40:1505–8. doi: 10.1161/STROKEAHA.108.530030

125. Harloff A, Simon J, Brendecke S, Assefa D, Helbing T, Frydrychowicz A, et al. Complex plaques in the proximal descending aorta: an underestimated embolic source of stroke. *Stroke.* (2010) 41:1145–50. doi: 10.1161/STROKEAHA.109.577775

frontiers | Frontiers in Neurology

TYPE Review
PUBLISHED 26 August 2022
DOI 10.3389/fneur.2022.982896

OPEN ACCESS

EDITED BY
Chengcheng Zhu,
University of Washington,
United States

REVIEWED BY
Fiona Xiangyan Chen,
Hong Kong Polytechnic University,
Hong Kong SAR, China
Fang Wu,
Capital Medical University, China
Shuang Xia,
Tianjin First Central Hospital, China

*CORRESPONDENCE
Hediyeh Baradaran
hediyeh.baradaran@hsc.utah.edu

SPECIALTY SECTION
This article was submitted to Applied Neuroimaging, a section of the journal Frontiers in Neurology

RECEIVED 30 June 2022
ACCEPTED 10 August 2022
PUBLISHED 26 August 2022

CITATION
Baradaran H, Kamel H and Gupta A (2022) The role of cross-sectional imaging of the extracranial and intracranial vasculature in embolic stroke of undetermined source. *Front. Neurol.* 13:982896. doi: 10.3389/fneur.2022.982896

The role of cross-sectional imaging of the extracranial and intracranial vasculature in embolic stroke of undetermined source

Hediyeh Baradaran[1]*, Hooman Kamel[2,3] and Ajay Gupta[3,4]

[1]Department of Radiology and Imaging Sciences, University of Utah, Salt Lake City, UT, United States, [2]Department of Neurology, Weill Cornell Medicine, New York, NY, United States, [3]Feil Family Brain and Mind Research Institute, Weill Cornell Medicine, New York, NY, United States, [4]Department of Radiology, Weill Cornell Medicine, New York, NY, United States

Despite an extensive workup, nearly one third of ischemic strokes are defined as Embolic Stroke of Undetermined Source (ESUS), indicating that no clear etiologic cause has been identified. Since large vessel atherosclerotic disease is a major cause of ischemic stroke, we focus on imaging of large vessel atherosclerosis to identify further sources of potential emboli which may be contributing to ESUS. For a stroke to be considered ESUS, both the extracranial and intracranial vessels must have <50% stenosis. Given the recent paradigm shift in our understanding of the role of plaque vulnerability in ischemic stroke risk, we evaluate the role of imaging specific high-risk extracranial plaque features in non-stenosing plaque and their potential contributions to ESUS. Further, intracranial vessel-wall MR is another potential tool to identify non-stenosing atherosclerotic plaques which may also contribute to ESUS. In this review, we discuss the role of cross-sectional imaging of the extracranial and intracranial arteries and how imaging may potentially uncover high risk plaque features which may be contributing to ischemic strokes.

KEYWORDS

cerebrovascular disease/stroke, atherosclerosis, carotid artery stenosis, magnetic resonance angiography, carotid artery disease

Introduction

Despite an extensive workup, nearly one-third of ischemic strokes are defined as Embolic Stroke of Undetermined Source (ESUS) meaning that no definite cause of the stroke has been identified (1). ESUS has proven to be a difficult clinical entity to treat with an almost 5% per year stroke recurrence rate (1). Most non-lacunar ischemic strokes are embolic and can originate from cardiac sources, from more proximal arterial structures, such as the carotid arteries or aortic arch, or potentially from a venous source in the setting of paradoxical embolism.

Cardiac sources, specifically atrial fibrillation, were thought to play a major role in ESUS because occult atrial fibrillation was found in many patients with ESUS (2). However, two major randomized clinical trials comparing oral anticoagulants to aspirin in patients with ESUS had neutral results (3, 4), suggesting that other embolic causes for ESUS may play a larger role. A major contributor to ischemic stroke is large artery atherosclerotic disease accounting for approximately 25% of ischemic strokes and most commonly arising from the extracranial carotid artery. According to the most common methods for classifying stroke etiologies, in order to attribute an ischemic stroke to large artery atherosclerosis, there must be associated luminal stenosis of at least 50% (5). These criteria do not take into account the recent paradigm shift in our scientific understanding of the contribution of specific plaque features to ischemic stroke.

In this review article, we will review the role of cross-sectional imaging of the carotid arteries in patients presenting with ESUS. First, we will discuss the current standard of care and typical imaging workup to exclude carotid disease as a potential cause of stroke. We will then discuss the role of computed tomography angiography (CTA) and magnetic resonance angiography (MRA) in evaluating potential causes of ischemic stroke in the extracranial carotid artery. We will also review the role of intracranial vessel wall MR (VW-MR) in assessing intracranial atherosclerosis, another potential contributor to ESUS.

Current paradigm/standard of care

Rather than being a diagnosis of exclusion, ESUS has a standardized, criteria-based definition requiring specific imaging and clinical workup. In order to meet criteria for a diagnosis of ESUS, an ischemic stroke must be a non-lacunar stroke detected on CT or MR imaging, the patient must have $\leq$50% luminal stenosis of the extracranial and intracranial vessels supplying the territory of the brain infarction, and have no major risk of a cardioembolic source or other specific identifiable cause of stroke, such as arteritis, dissection, migraine/vasospasm, or drug misuse. In order to make this diagnosis, suggested diagnostic assessment in evaluating those with ESUS is a brain CT or MR, 12-lead electrocardiogram, precordial echocardiography, cardiac monitoring for 24 h with automated rhythm detection, and imaging of both the extracranial and intracranial arteries supplying the area of brain ischemia with either digital subtraction angiography, MR or CT angiography, or cervical duplex and transcranial Doppler ultrasonography (1). These relatively recent guidelines have allowed for standardization in the identification of those with acute ischemic stroke and have made those with ESUS easier to identify. These more rigid definitions have led to more concentrated effort in mitigating stroke in this population and have paved the way for recent large randomized clinical trials (3, 4).

Limitations of current imaging techniques

While the current diagnostic criteria for ESUS require assessment of both the extracranial and intracranial arterial structures, the primary focus remains on the degree of luminal stenosis. For decades, the degree of stenosis has been the primary indicator of stroke risk in the extracranial and intracranial arteries. Carotid disease is thought to lead to ischemic stroke by two distinctive, but often synergistic factors: flow-limitation in the setting of stenosis leading to hypoperfusion and artery-to-artery embolism from plaque leading to thromboemboli (6). It is likely that hypoperfusion from flow limitation contributes to cerebral ischemia. Further, impaired perfusion in the setting of flow-limitation may lead to a potentially transient embolic event resulting in an infarct. While flow-limiting stenosis is clearly a risk factor for the development of ischemic stroke, there is mounting evidence that the plaque itself, regardless of the degree of accompanying stenosis is likely a contributor to ischemic strokes *via* artery-to-artery embolism (7).

Recent interest in the plaque components have furthered our understanding of the role of plaque features in contributing to embolic strokes. There is strong histopathologic evidence that plaque may have different features conferring higher risk for an embolic phenomenon. The American Heart Association plaque classification describes a spectrum of plaque with certain features, including intraplaque hemorrhage, lipid-rich necrotic core, and surface defects including fibrous cap rupture which are features indicative of more "vulnerable" plaque that is more likely to rupture and lead to emboli (8, 9). With the current recommendations for imaging, specific carotid plaque features are not always appropriately imaged or may not always be identified or treated as important drivers of ischemic stroke. Despite strong scientific evidence supporting the role of vulnerable plaque features in the development of ischemic stroke, specifically in those with non-stenotic carotid atherosclerosis, these plaque features are not always being routinely assessed using the current guidelines. There is strong evidence that specific plaque vulnerable features in non-stenosing plaque are more commonly seen ipsilateral to infarction in ESUS patients (10). By recognizing the importance of non-stenosing plaque in the extracranial and intracranial vasculature, we may potentially be able to reclassify patients originally thought to have ESUS (11).

Extracranial carotid plaque

Extracranial internal carotid artery atherosclerosis has traditionally been the most common source of large vessel

atherosclerotic disease-causing ischemic stroke. The extracranial carotid arteries are always imaged in the setting of acute ischemic stroke to evaluate for a source. The simplest method for imaging extracranial plaque is by duplex ultrasound (US) where the degree of stenosis based on flow measurements can be assessed. US can also evaluate various plaque features which are known to be higher risk, including echolucent plaque (12). Though US certainly plays a major role in the evaluation of stroke etiology and ESUS (13), we will focus on other cross-sectional imaging modalities which can more accurately assess specific plaque features as well as luminal stenosis for a more complete assessment of stroke risk.

When imaging the extracranial carotid artery in the setting of ischemic stroke, there are two major considerations. First, the degree of luminal stenosis must be assessed using a standardized system, most commonly using North American Symptomatic Carotid Endarterectomy Trial (NASCET) criteria (14). This can be accurately ascertained in any of the imaging modalities currently being utilized for the diagnosis of ESUS. In addition to the degree of luminal stenosis, the components of the plaque must also be assessed, even in those with non-stenosing plaque. All imaging modalities for the extracranial carotid arteries can assess plaque features to a certain degree, though some are more well-suited than others.

MR imaging

MR is the most studied method to visualize vulnerable plaque features with considerable evidence supporting its use to evaluate advanced atherosclerotic plaque. Intraplaque hemorrhage (IPH) is the most commonly encountered MR-detected plaque feature considered to be "high-risk" and is strongly associated with infarction (15–17). Other MR-detected vulnerable plaque features including lipid-rich necrotic core, ulceration, or fibrous cap rupture are also strongly associated with ischemic infarction. There is strong histopathologic evidence correlating MR imaging findings to known specific vulnerable plaque features (9, 18). In order to accurately image these plaque features, many utilize dedicated carotid coils or specific high-resolution MR sequences, including T1 and T2 weighted sequences, proton density, and time-of flight sequences to evaluate flow (19). Contrast-enhanced MR sequences can also improve plaque characterization and allow for better characterization of plaque ulceration (20). While using dedicated carotid coils improves imaging by increasing signal-to-noise ratios, some studies have found that even simple MR sequences can accurately identify basic high-risk carotid plaque features (Figure 1) (21).

Multiple studies have specifically evaluated the role of MR imaging of plaque in the setting of ESUS. Several studies have evaluated individuals with ESUS and have found that these MR-detected vulnerable plaque features are more commonly seen

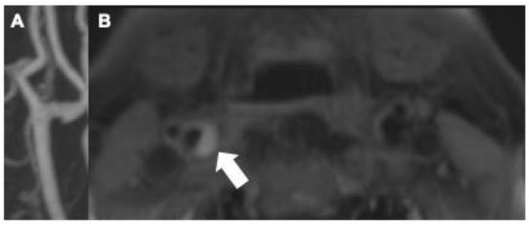

FIGURE 1
Though there is no accompanying significant stenosis [**(A)** maximum intensity projection of contrast-enhanced MRA], this MPRAGE sequence of the proximal right internal carotid artery in a 73-years-old male demonstrates a large T1 hyperintense plaque [**(B)** arrow]. These findings are compatible with intraplaque hemorrhage, a well-established marker of vulnerable plaque and likely contributor to acute ischemic stroke in this patient.

ipsilateral to the side of stroke compared to the contralateral side (22–25). Recent prospective studies have confirmed these findings. The Plaque At RISK study showed that in patients with mild-moderate extracranial carotid stenosis, those with IPH and higher total plaque volume were more likely to experience recurrent ipsilateral ischemic stroke over a 5 years follow-up period, though plaque ulcerations and calcifications were not significantly associated (26). Another recent prospective study of patients with non-stenosing plaque found that patients with complicated plaque, such as IPH or surface defects, were much more likely to experience recurrent ipsilateral infarctions in the 30 months following an initial infarct (27). The findings from these studies suggest that even in the setting of non-stenosing plaque, certain higher-risk plaque features may be responsible for infarcts.

Though MR imaging of the extracranial carotid arteries can be helpful in identifying high risk plaque features, its widespread use is somewhat limited by availability, patient contraindications (e.g., implanted metal), and usually lengthy sequences making it a time-consuming imaging examination.

CTA

CTA is an increasingly commonly used imaging modality in the assessment of etiology of acute ischemic stroke. Because it is relatively cost-effective and quick to obtain, it is most often the first-line examination for those presenting emergently with acute stroke symptoms. While there is more prospective evidence that MR-assessed vulnerable plaque features contribute to future and recurrent ischemic stroke, many of these plaque features can also be assessed using CTA imaging (28). While MR is a superior imaging modality for differentiating histopathologic components of plaque, CTA is able to assess a few specific features which are known to increase risk of

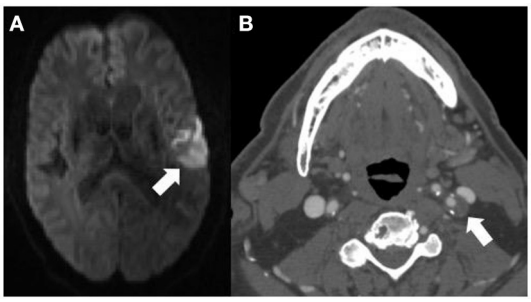

FIGURE 2
This 71-years-old patient presenting with an acute left middle cerebral artery territory infarction [arrow **(A)**] did not have any significant stenosis by North American Symptomatic Carotid Endarterectomy Trial criteria on CT angiography (CTA) and was thought to have an embolic stroke of undetermined source. The CTA **(B)** does however show a large, predominantly non–calcified plaque up to 5 mm in thickness in the proximal left internal carotid artery [**(B)** arrow] compatible with a vulnerable plaque, potentially the embolic source of the infarction.

emboli, including "soft" or predominantly non–calcified plaque which is thought to be a correlate of IPH or lipid-rich necrotic core, plaque ulceration, and plaque thickness (Figure 2). These features are readily visible on routine CTA imaging and are associated with increased likelihood of symptomaticity (28, 29). Similar to studies performed with MR-detected plaque features, several have found that non-stenotic plaques are more commonly seen ipsilateral to the infarcted cerebral hemisphere in patients with ESUS (30, 31). Specifically, several have found that having plaques >3 mm was more common ipsilateral to the side of stroke (30–32). Other studies have found that plaque with spotty calcification and a "rim sign" were also associated with cerebrovascular ischemic symptoms (33, 34). These studies indicate that though there is a paucity of prospective data evaluating the role of CT-plaque features in future ischemic stroke, certain imaging findings may be useful in identifying those at higher risk of ischemic stroke.

Other imaging techniques

Though not frequently used in everyday practice, there may be a role for more advanced imaging to evaluate for higher risk plaque. Positron Emission Tomography (PET) imaging has been studied as a method for assessing the vulnerability of carotid plaque. A recent systematic review and meta-analysis found that carotid arteries ipsilateral to recent ischemic events had more avid uptake of markers of inflammatory activity (e.g., 18-F fluorodeoxyglucose) than asymptomatic arteries (35). Other types of more advanced imaging has been studied to evaluate for plaque vulnerability, including dynamic contrast enhanced perfusion imaging (36). These and other findings point to a potential role for advanced imaging in evaluating plaque vulnerability in the future.

Intracranial atherosclerosis

Intracranial atherosclerosis leads to up to 9–15% of ischemic infarctions in the United States and up to 50% worldwide. Similar to extracranial atherosclerosis, intracranial atherosclerosis must result in at least 50% narrowing in order to be considered causative in the setting of ischemic stroke. Active atherosclerotic plaque can easily be overlooked when using conventional angiographic imaging because plaques do not always produce associated vessel narrowing. Because of this, intracranial vessel wall MR (VW-MR) can be used as an imaging assessment of atherosclerosis, particularly non-stenosing plaque.

Intracranial VW-MR

Intracranial VW-MR is a powerful tool to image beyond the vessel lumen and for evaluating non-stenosing plaque which may lead to ischemic stroke. In order to accurately assess the vessel wall, there are several critical components to intracranial VW-MR imaging (37). First, in order to highlight the wall itself and any potential plaque, it is essential to suppress flowing luminal blood and CSF, which can be done with a variety of different T1-weighted sequences. This is essential to increase conspicuity of any plaque features or enhancement. Further, high spatial resolution is needed in order to see the small vessel wall with most institutions performing approximately 0.5 mm voxels. Multiplanar acquisitions are also essential to assess the vessels en face because of the inherent tortuosity of the intracranial vessels. This is usually achieved by acquiring images using 3D techniques then creating reformats. Lastly, multiple tissue weightings are also performed to evaluate specific T1 and T2 characteristics in order to distinguish different plaque components.

Intracranial VW-MR can more easily detect smaller plaques or plaques with associated positive remodeling which may not produce narrowing on angiographic imaging but may still lead to ischemic stroke. Positive remodeling is an adaptive process where the outer wall of a vessel can outwardly bulge in the setting of an atherosclerotic plaque to preserve cerebral blood flow, leading to a normal, non-stenotic appearance on standard angiographic imaging techniques, including CTA, MRA, and DSA. Positive remodeling is commonly seen in the posterior circulation but can be seen in any intracranial arteries. Because of the common occurrence of positive remodeling, many patients presenting with acute ischemic stroke may have a normal appearing angiographic study without any suspicious findings for a contributing atherosclerotic lesion. When imaged using VW-MR, however, culprit atherosclerotic plaques may be

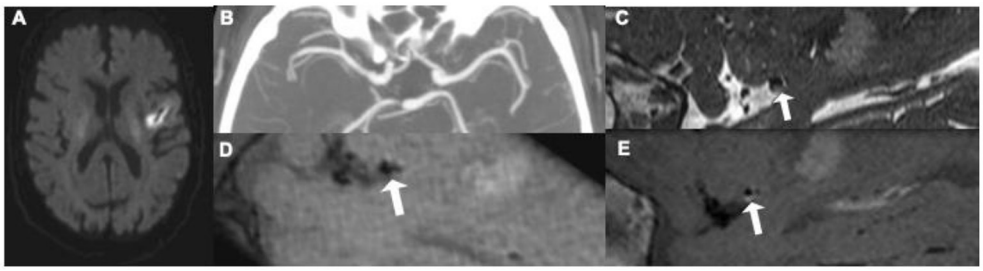

FIGURE 3
This 62-year old patient presenting with an acute left middle cerebral artery (MCA) infarction on MR **(A)** had CT angiography [**(B)** maximum intensity projection] at presentation without evidence of any significant stenosis. Initially thought to have an embolic stroke of undetermined source, he underwent an intracranial vessel wall MR where he was found to have a focal, eccentric T2 hyperintense [**(C)** white arrow] enhancing [**(D)** pre-contrast image, **(E)** post-contrast image, white arrow] plaque, in the distal M1 segment of the left MCA, thought to be the culprit plaque.4.

identified (Figure 3) and are generally assumed to be causative for ischemic stroke.

VW-MR uses a few specific imaging findings to identify active or culprit atherosclerotic plaques. The most important imaging finding for evaluating plaque in the setting of acute ischemic stroke is plaque enhancement. Several meta-analyses show that plaque/vessel wall enhancement is very strongly associated with culprit or symptomatic plaques (38–40). Plaque enhancement is readily assessable on post-contrast MR sequences and is a fundamental aspect of imaging with VW-MR techniques. In addition to plaque enhancement, positive remodeling is another important imaging finding that is strongly associated with symptomatic plaques (39, 40). This strong association of positive remodeling with symptomatic plaque highlights the importance of VW-MR in identifying potential culprit plaques. Similar to extracranial carotid plaque, discontinuities on the plaque surface indicative of fibrous cap rupture are also associated with ischemic stroke and symptomatic plaques (39, 40). Though intraplaque hemorrhage is a very strong marker of high risk plaque in the extracranial carotid artery, the association between IPH or intraplaque high T1 signal in the intracranial artery is not as strong, with a more modest association with ischemic stroke and symptomatic plaque, more commonly seen in the basilar artery (40, 41). Further studies evaluating the role of intracranial IPH in contributing to acute ischemic stroke are warranted.

When used in patients with ESUS, some studies have found that intracranial VW-MR can be a helpful tool. A study with over 240 patients with ESUS found that intracranial plaque was much more common ipsilateral to the side of stroke (42). They also found that there was increased wall remodeling in patients with ESUS, again highlighting the importance of non-stenosing plaque (42). A recent systematic review of 21 studies of patients with non–stenosing atherosclerosis found that intracranial plaque with higher risk features such as plaque enhancement and positive remodeling were more commonly seen in those with acute infarction, again indicating the role of specific plaque features (43). Another study found that using intracranial VW-MR could change the stroke etiology classification as it identified alternate causes of the ischemic stroke (44).

Intracranial VW-MR has become increasingly popular in evaluating ischemic stroke and ESUS patients, with a recent survey suggesting that more than 50% of neuroradiology practices routinely perform this type of study (45). Despite its increasing popularity, intracranial VW-MR imaging is limited by lengthy acquisitions, patient contraindications, and cost. Further, there has been limited histopathologic validation of MR signal characteristics of intracranial vessel wall pathology due to limitations in correlation with vessel samples (46, 47). This inherent limitation in our ability to correlate imaging findings with histopathologic components constrains our understanding of intracranial plaque characteristics.

Conclusion

Given recent randomized clinical trial findings that treating cardiac sources for ESUS may not be as beneficial as originally hoped, more attention is being placed on other potential embolic sources. Since the current ESUS definitions require <50% luminal narrowing, potential culprit plaques could be missed or inadequately treated because they are producing insignificant narrowing. In the extracranial carotid artery, both MR and CTA can be used to identify certain plaque features which indicate more plaque vulnerability including IPH on MR and increased soft plaque thickness on CTA. VW-MR can also be used as a powerful tool to identify non-stenosing but active atherosclerotic plaque in the intracranial arteries by identifying an enhancing plaque with positive remodeling. Though these studies can be helpful in determining the source of potential emboli, there are some Further studies are needed to validate these imaging techniques and pave a path for their routine use in ESUS.

Author contributions

HB, HK, and AG contributed to conception of the manuscript. HB wrote the first draft of the manuscript. HK and AG critically revised and wrote sections of the manuscript. All authors contributed to manuscript revision, read, and approved the submitted version.

Funding

HB is in part supported by National Institutes of Health grant 5U24NS107156-04. AG is in part supported by National Institutes of Health grants R01HL144541 and R01NS123576. HK serves as a PI for the NIH-funded ARCADIA trial (NINDS U01NS095869).

Conflict of interest

HK serves as a PI for the NIH-funded ARCADIA trial (NINDS U01NS095869), which receives in-kind study drug from the BMS-Pfizer Alliance for Eliquis® and ancillary study support from Roche Diagnostics; as Deputy Editor for JAMA Neurology; on clinical trial steering/executive committees for Medtronic, Janssen, and Javelin Medical; and on endpoint adjudication committees for AstraZeneca, Novo Nordisk, and Boehringer Ingelheim. He has an ownership interest in TETMedical, Inc.

The remaining authors declare that the research was conducted in the absence of any commercial or financial relationships that could be construed as a potential conflict of interest.

Publisher's note

References

1. Hart RG, Diener H-C, Coutts SB, Easton JD, Granger CB, O'Donnell MJ, et al. Embolic strokes of undetermined source: the case for a new clinical construct. *Lancet Neurol.* (2014) 13:429–38. doi: 10.1016/S1474-4422(13)70310-7

2. Sanna T, Diener H-C, Passman RS, Di Lazzaro V, Bernstein RA, Morillo CA, et al. Cryptogenic stroke and underlying atrial fibrillation. *N Engl J Med.* (2014) 370:2478–86. doi: 10.1056/NEJMoa1313600

3. Hart RG, Sharma M, Mundl H, Kasner SE, Bangdiwala SI, Berkowitz SD, et al. Rivaroxaban for stroke prevention after embolic stroke of undetermined source. *N Engl J Med.* (2018) 378:2191–201. doi: 10.1056/NEJMoa1802686

4. Diener H-C, Sacco RL, Easton JD, Granger CB, Bernstein RA, Uchiyama S, et al. Dabigatran for prevention of stroke after embolic stroke of undetermined source. *N Engl J Med.* (2019) 380:1906–17. doi: 10.1056/NEJMoa1813959

5. Adams Jr HP, Bendixen BH, Kappelle LJ, Biller J, Love BB, Gordon DL, et al. Classification of subtype of acute ischemic stroke. Definitions for use in a multicenter clinical trial. TOAST. Trial of Org 10172 in acute stroke treatment. *Stroke.* (1993) 24:35–41. doi: 10.1161/01.STR.24.1.35

6. Caplan LR, Hennerici M. Impaired clearance of emboli (washout) is an important link between hypoperfusion, embolism, and ischemic stroke. *Arch Neurol.* (1998) 55:1475–82. doi: 10.1001/archneur.55.11.1475

7. Brinjikji W, Huston J, Rabinstein AA, Kim G-M, Lerman A. Lanzino G. Contemporary carotid imaging: from degree of stenosis to plaque vulnerability. *J Neurosurg.* (2016) 124:27. doi: 10.3171/2015.1.JNS142452

8. Stary HC, Chandler AB, Dinsmore RE, Fuster V, Glagov S, Insull Jr W, et al. A definition of advanced types of atherosclerotic lesions and a histological classification of atherosclerosis: a report from the committee on vascular lesions of the council on arteriosclerosis, american heart association. *Circulation.* (1995) 92:1355–74. doi: 10.1161/01.CIR.92.5.1355

9. Cai J-M, Hatsukami TS, Ferguson MS, Small R, Polissar NL, Yuan C. Classification of human carotid atherosclerotic lesions with in vivo multicontrast magnetic resonance imaging. *Circulation.* (2002) 106:1368–73. doi: 10.1161/01.CIR.0000028591.44554.F9

10. Kamtchum-Tatuene J, Wilman A, Saqqur M, Shuaib A, Jickling GC. Carotid plaque with high-risk features in embolic stroke of undetermined source. *Stroke.* (20200 51:311–14. doi: 10.1161/STROKEAHA.119.027272

11. Kamel H, Navi BB, Merkler AE, Baradaran H, Díaz I, Parikh NS, et al. Reclassification of ischemic stroke etiological subtypes on the basis of high-risk nonstenosing carotid plaque. *Stroke.* (2020) 51:504–10. doi: 10.1161/STROKEAHA.119.027970

12. Gupta A, Kesavabhotla K, Baradaran H, Kamel H, Pandya A, Giambrone AE, et al. Plaque echolucency and stroke risk in asymptomatic carotid stenosis: a systematic review and meta-analysis. *Stroke.* (2015) 46:91–7. doi: 10.1161/STROKEAHA.114.006091

13. Komatsu T, Iguchi Y, Arai A, Sakuta K, Sakai K, Terasawa Y, et al. Large but nonstenotic carotid artery plaque in patients with a history of embolic stroke of undetermined source. *Stroke.* (2018) 49:3054–56. doi: 10.1161/STROKEAHA.118.022986

14. Collaborators* NASCET. Beneficial effect of carotid endarterectomy in symptomatic patients with high-grade carotid stenosis. *N Engl J Med.* (1991) 325:445–53. doi: 10.1056/NEJM199108153250701

15. Gupta A, Baradaran H, Schweitzer AD, Kamel H, Pandya A, Delgado D, et al. Carotid plaque MRI and stroke risk. *Stroke.* (2013) 44:3071–77. doi: 10.1161/STROKEAHA.113.002551

16. Hosseini AA, Kandiyil N, MacSweeney ST, Altaf N, Auer DP. Carotid plaque hemorrhage on magnetic resonance imaging strongly predicts recurrent ischemia and stroke. *Ann Neurol.* (2013) 73:774–84. doi: 10.1002/ana.23876

17. Saam T, Hetterich H, Hoffmann V, Yuan C, Dichgans M, Poppert H, et al. Meta-analysis and systematic review of the predictive value of carotid plaque hemorrhage on cerebrovascular events by magnetic resonance imaging. *J American Coll Cardiol.* (2013) 62:1081–91. doi: 10.1016/j.jacc.2013.06.015

18. Yuan C, Mitsumori LM, Ferguson MS, Polissar NL, Echelard D, Ortiz G, et al. In vivo accuracy of multispectral magnetic resonance imaging for identifying lipid-rich necrotic cores and intraplaque hemorrhage in advanced human carotid plaques. *Circulation.* (2001) 104:2051–56. doi: 10.1161/hc4201.097839

19. Saba L, Yuan C, Hatsukami T, Balu N, Qiao Y, DeMarco J, et al. Carotid artery wall imaging: perspective and guidelines from the ASNR Vessel Wall Imaging Study Group and expert consensus recommendations of the American Society of Neuroradiology. *Am J Neuroradiol.* (2018) 39:E9–31. doi: 10.3174/ajnr.A5488

20. Etesami M, Hoi Y, Steinman D, Gujar SK, Nidecker A, Astor B, et al. Comparison of carotid plaque ulcer detection using contrast-enhanced and time-of-flight MRA techniques. *Am J Neuroradiol.* (2013) 34:177–84. doi: 10.3174/ajnr.A3132

21. Gupta A, Baradaran H, Kamel H, Mangla A, Pandya A, Fodera V, et al. Intraplaque high-intensity signal on 3D time-of-flight MR angiography is strongly associated with symptomatic carotid artery stenosis. *Am J Neuroradiol.* (2014) 35:557–61. doi: 10.3174/ajnr.A3732

22. Freilinger TM, Schindler A, Schmidt C, Grimm J, Cyran C, Schwarz F, et al. Prevalence of nonstenosing, complicated atherosclerotic plaques in cryptogenic stroke. *JACC: Cardiovascul Imag.* (2012) 5:397–405. doi: 10.1016/j.jcmg.2012.01.012

23. Gupta A, Gialdini G, Lerario MP, Baradaran H, Giambrone A, Navi BB, et al. Magnetic resonance angiography detection of abnormal carotid artery plaque in patients with cryptogenic stroke. *J Am Heart Assoc.* (2015) 4:e002012. doi: 10.1161/JAHA.115.002012

24. Gupta A, Gialdini G, Giambrone AE, Lerario MP, Baradaran H, Navi BB, et al. Association between nonstenosing carotid artery plaque on MR angiography and acute ischemic stroke. *JACC: Cardiovascul Imag.* (2016) 9:1228–29. doi: 10.1016/j.jcmg.2015.12.004

25. Singh N, Moody AR, Panzov V, Gladstone DJ. Carotid intraplaque hemorrhage in patients with embolic stroke of undetermined source. *J Stroke Cerebrovascul Dis.* (2018) 27:1956–59. doi: 10.1016/j.jstrokecerebrovasdis.2018.02.042

26. van Dam-Nolen DH, Truijman MT, van der Kolk AG, Liem MI, Schreuder FH, Boersma E, et al. Carotid plaque characteristics predict recurrent ischemic stroke and TIA: the ParisK (Plaque At Risk) study. *JACC: Cardiovascul Imag.* (2022). doi: 10.1016/j.jcmg.2022.04.003. [Epub ahead of print].

27. Kopczak A, Schindler A, Sepp D, Bayer-Karpinska A, Malik R, Koch ML, et al. Complicated carotid artery plaques and risk of recurrent ischemic stroke or TIA. *J Am Coll Cardiol*. (2022): 79:2189–99. doi: 10.1016/j.jacc.2022.03.376

28. Baradaran H, Al-Dasuqi K, Knight-Greenfield A, Giambrone A, Delgado D, Ebani E, et al. Association between carotid plaque features on CTA and cerebrovascular ischemia: a systematic review and meta-analysis. *Am J Neuroradiol.* (2017) 38:2321–6. doi: 10.3174/ajnr.A5436

29. Baradaran H, Eisenmenger LB, Hinckley PJ. Havenon AHd, Stoddard GJ, Treiman LS, et al. Optimal carotid plaque features on computed tomography angiography associated with ischemic stroke. *J Am Heart Assoc.* (2021) 10:e019462. doi: 10.1161/JAHA.120.019462

30. Coutinho JM, Derkatch S, Potvin AR, Tomlinson G, Kiehl T-R, Silver FL, et al. Nonstenotic carotid plaque on CT angiography in patients with cryptogenic stroke. *Neurology*. (2016) 87:665–72. doi: 10.1212/WNL.0000000000002978

31. Ospel JM, Singh N, Marko M, Almekhlafi M, Dowlatshahi D, Puig J, et al. Prevalence of ipsilateral nonstenotic carotid plaques on computed tomography angiography in embolic stroke of undetermined source. *Stroke.* (2020) 51:1743–49. doi: 10.1161/STROKEAHA.120.029404

32. Knight-Greenfield A, Nario JJQ, Vora A, Baradaran H, Merkler A, Navi BB, et al. Associations between features of nonstenosing carotid plaque on computed tomographic angiography and ischemic stroke subtypes. *J Am Heart Assoc.* (2019) 8:e014818. doi: 10.1161/JAHA.119.014818

33. Eisenmenger LB, Aldred BW, Kim S-E, Stoddard GJ, de Havenon A, Treiman GS, et al. Prediction of carotid intraplaque hemorrhage using adventitial calcification and plaque thickness on CTA. *Am J Neuroradiol.* (2016) 37:1496–503. doi: 10.3174/ajnr.A4765

34. Zhang F, Yang L, Gan L, Fan Z, Zhou B, Deng Z, et al. Spotty calcium on cervicocerebral computed tomography angiography associates with increased risk of ischemic stroke. *Stroke.* (2019) 50:859–66. doi: 10.1161/STROKEAHA.118.023273

35. Chaker S, Al-Dasuqi K, Baradaran H, Demetres M, Delgado D, Nehmeh S, et al. Carotid plaque positron emission tomography imaging and cerebral ischemic disease. *Stroke.* (2019) 50:2072–79. doi: 10.1161/STROKEAHA.118.023987

36. Yuan J, Makris G, Patterson A, Usman A, Das T, Priest A, et al. Relationship between carotid plaque surface morphology and perfusion: a 3D DCE-MRI study. *MAGMA.* (2018) 31:191–9. doi: 10.1007/s10334-017-0621-4

37. Mandell D, Mossa-Basha M, Qiao Y, Hess C, Hui F, Matouk C, et al. Intracranial vessel wall MRI: principles and expert consensus recommendations of the American society of neuroradiology. *Am J Neuroradiol.* (2017) 38:218–29. doi: 10.3174/ajnr.A4893

38. Gupta A, Baradaran H, Al-Dasuqi K, Knight-Greenfield A, Giambrone AE, Delgado D, et al. Gadolinium enhancement in intracranial atherosclerotic plaque and ischemic stroke: a systematic review and meta-analysis. *J Am Heart Assoc.* (2016) 5:e003816. doi: 10.1161/JAHA.116.003816

39. Lee HN Ryu C-W, Yun SJ. Vessel-wall magnetic resonance imaging of intracranial atherosclerotic plaque and ischemic stroke: a systematic review and meta-analysis. *Front Neurol.* (2018) 9:1032. doi: 10.3389/fneur.2018.01032

40. Song JW, Pavlou A, Xiao J, Kasner SE, Fan Z, Messé SR. Vessel wall magnetic resonance imaging biomarkers of symptomatic intracranial atherosclerosis: a meta-analysis. *Stroke.* (2021) 52:193–202. doi: 10.1161/STROKEAHA.120.031480

41. Zhu C, Tian X, Degnan AJ, Shi Z, Zhang X, Chen L, et al. Clinical significance of intraplaque hemorrhage in low-and high-grade basilar artery stenosis on high-resolution MRI. *Am J Neuroradiol.* (2018) 39:1286–92. doi: 10.3174/ajnr.A5676

42. Tao L, Li X-Q, Hou X-W, Yang B-Q, Xia C, Ntaios G, et al. Intracranial atherosclerotic plaque as a potential cause of embolic stroke of undetermined source. *J Am Coll Cardiol.* (2021) 77:680–91. doi: 10.1016/j.jacc.2020.12.015

43. Wang Y, Liu X, Wu X, Degnan AJ, Malhotra A, Zhu C. Culprit intracranial plaque without substantial stenosis in acute ischemic stroke on vessel wall MRI: a systematic review. *Atherosclerosis.* (2019) 287:112–21. doi: 10.1016/j.atherosclerosis.2019.06.907

44. Schaafsma JD, Rawal S, Coutinho JM, Rasheedi J, Mikulis DJ, Jaigobin C, et al. Diagnostic impact of intracranial vessel wall MRI in 205 patients with ischemic stroke or TIA. *Am J Neuroradiol.* (2019) 40:1701–06. doi: 10.3174/ajnr.A6202

45. Mossa-Basha M, Zhu C, Yuan C, Saba L, Saloner DA, Edjlali M, et al. Survey of the American society of neuroradiology membership on the use and value of intracranial vessel wall MRI. *Am J Neuroradiol.* (2022) 43:951–57. doi: 10.3174/ajnr.A7541

46. Turan TN, Rumboldt Z, Granholm A-C, Columbo L, Welsh CT, Lopes-Virella MF, et al. Intracranial atherosclerosis: correlation between in-vivo 3T high resolution MRI and pathology. *Atherosclerosis.* (2014) 237:460–63. doi: 10.1016/j.atherosclerosis.2014.10.007

47. Van Der Kolk A, Zwanenburg J, Denswil N, Vink A, Spliet W, Daemen M, et al. Imaging the intracranial atherosclerotic vessel wall using 7T MRI: initial comparison with histopathology. *Am J Neuroradiol.* (2015) 36:694–701. doi: 10.3174/ajnr.A4178

frontiers | Frontiers in Neurology

TYPE Original Research
PUBLISHED 13 September 2022
DOI 10.3389/fneur.2022.952462

OPEN ACCESS

EDITED BY
Chengcheng Zhu,
University of Washington,
United States

REVIEWED BY
Zhen Zhang,
Longgang Central Hospital,
Shenzhen, China
Hans Worthmann,
Hannover Medical School, Germany

*CORRESPONDENCE
Yen-Chu Huang
yenchu.huang@msa.hinet.net

SPECIALTY SECTION
This article was submitted to Stroke,
a section of the journal
Frontiers in Neurology

RECEIVED 25 May 2022
ACCEPTED 25 July 2022
PUBLISHED 13 September 2022

CITATION
Chen C-H, Lee M, Weng H-H, Lee J-D, Yang J-T, Tsai Y-H and Huang Y-C (2022) Identification of magnetic resonance imaging features for the prediction of unrecognized atrial fibrillation in acute ischemic stroke. *Front. Neurol.* 13:952462. doi: 10.3389/fneur.2022.952462

Identification of magnetic resonance imaging features for the prediction of unrecognized atrial fibrillation in acute ischemic stroke

Chao-Hui Chen[1], Meng Lee[1], Hsu-Huei Weng[2], Jiann-Der Lee[1], Jen-Tsung Yang[3], Yuan-Hsiung Tsai[2] and Yen-Chu Huang[1]*

[1]Department of Neurology, Chang Gung Memorial Hospital at Chiayi, Chang-Gung University College of Medicine, Chiayi City, Taiwan, [2]Department of Diagnostic Radiology, Chang Gung Memorial Hospital at Chiayi, Chang-Gung University College of Medicine, Chiayi City, Taiwan, [3]Department of Neurosurgery, Chang Gung Memorial Hospital at Chiayi, Chang-Gung University College of Medicine, Chiayi City, Taiwan

Background and purpose: The early identification of cardioembolic stroke is critical for the early initiation of anticoagulant treatment. However, it can be challenging to identify the major cardiac source, particularly since the predominant source, paroxysmal atrial fibrillation (AF), may not be present at the time of stroke. In this study, we aimed to evaluate imaging predictors for unrecognized AF in patients with acute ischemic stroke.

Methods: We performed a cross-sectional analysis of data and magnetic resonance imaging (MRI) scans from two prospective cohorts of patients who underwent serial 12-lead electrocardiography and 24-h Holter monitoring to detect unrecognized AF. The imaging patterns in diffusion-weighted imaging and imaging characteristics were assessed and classified. A logistic regression model was used to identify predictive factors for newly detected AF in patients with acute ischemic stroke.

Results: A total of 734 patients were recruited for analysis, with a median age of 72 (interquartile range: 65–79) years and a median National Institutes of Health Stroke Scale score of 4 (interquartile range: 2–6). Of these patients, 64 (8.7%) had newly detected AF during the follow-up period. Stepwise multivariate logistic regression revealed that age ≥75 years [adjusted odds ratio (aOR) 5.66, 95% confidence interval (CI) 2.98–10.75], receiving recombinant tissue plasminogen activator treatment (aOR 4.36, 95% CI 1.65–11.54), congestive heart failure (aOR 6.73, 95% CI 1.85–24.48), early hemorrhage in MRI (aOR 3.62, 95% CI 1.52–8.61), single cortical infarct (aOR 6.49, 95% CI 2.35–17.92), and territorial infarcts (aOR 3.54, 95% CI 1.06–11.75) were associated with newly detected AF. The C-statistic of the prediction model for newly detected AF was 0.764.

Conclusion: Initial MRI at the time of stroke may be useful to predict which patients have cardioembolic stroke caused by unrecognized AF. Further studies are warranted to verify these findings and their application to high-risk patients.

KEYWORDS

ischemic stroke, cryptogenic stroke, cardioembolic stroke, MRI, atrial fibrillation

Introduction

Cardioembolic stroke has been reported to account for about one fifth of all cases of ischemic stroke (1), and it is associated with higher stroke severity and recurrence rate (2, 3). Atrial fibrillation (AF) is the leading cause of cardioembolic stroke (4), and oral anticoagulants are the most effective method to prevent cardioembolic stroke recurrence in patients with AF (5, 6). Therefore, the early diagnosis of AF after stroke is critical to allow for the early initiation of anticoagulant treatment. However, it can be challenging to identify AF, particularly as paroxysmal AF may not be present at the time of stroke. In these situations, 24-h Holter monitoring is the standard method to detect AF, however it is still far from satisfactory. Extended electrocardiogram monitoring may improve the detection rate of AF, however it is expensive and inconvenient, limiting its widespread use in clinical practice. Therefore, a method to accurately identify patients with cardioembolism from unrecognized AF is urgently needed.

Previous studies have used several clinical scales to predict new-onset AF, including CHA2DS2-VASc (congestive heart failure, hypertension, age ≥75 years, diabetes mellitus, prior stroke or transient ischemic attack, vascular disease, age 65–74 years, female) (7). Cohorts for Heart and Aging Research in Genomic Epidemiology-AF (CHARGE-AF) (8), and Electronic Health Record–Based AF (EHR-AF) scores (9). These AF scales have also been shown to be highly associated with cardioembolic stroke (10). However, the use of these scales requires a thorough survey and extensive clinical information to enable calculation of the scores, and their sensitivity and specificity are still far from satisfactory, which limits their usage in the clinic.

Magnetic resonance imaging (MRI) is widely used in clinical practice to identify acute ischemic stroke, and it may be useful to identify cardioembolic stroke from unrecognized AF at the time of stroke. Several infarct patterns on MRI support the diagnosis of cardioembolism, including multiple simultaneous infarcts located in one or more major arterial territories of the anterior and/or posterior circulation (11), single cortical infarction or cortical-subcortical infarct without large artery occlusion (12). In addition, the presence of a susceptibility vessel sign (SVS) in a gradient recalled echo (GRE) MR imaging sequence is associated with erythrocyte-rich thrombus and cardioembolism (13).

In this study, we aimed to evaluate the MRI characteristics associated with newly detected AF among two prospective cohorts of patients with acute ischemic stroke who did not have AF at baseline.

Materials and methods

Patients

We analyzed data from two prospective cohorts at Chang Gung Memorial Hospital (14). The first cohort was derived from the Atrial Fibrillation Trial to Evaluate Real-world Procedures for their Utility in helping to Lower Stroke Events (AFTER-PULSE), which compared the detection rate of AF using serial 12-lead electrocardiography vs. 24-h Holter monitoring within 3 months after the index ischemic stroke event, and included elderly patients with no known AF between October 2015 and July 2018 (14). The second cohort was derived from an observational study conducted between January 2014 and September 2017, which evaluated the correlation between left atrial enlargement and new-onset AF among patients with no known AF after their index ischemic stroke event; all patients underwent serial 12-lead electrocardiography and were followed up for 6 months.

Among these two cohorts, we selected patients who had undergone MRI within 5 days after the index stroke event and had a visible acute infarction in diffusion-weighted imaging (DWI). A detailed flow chart of patient selection is shown in Figure 1. In both cohorts, data on sex, age, and a medical history of diabetes mellitus, hypertension, hypercholesterolemia, congestive heart failure, prior cerebrovascular disease and prior coronary artery disease were recorded. Systolic and diastolic blood pressure values, blood cell counts and biochemistry data were collected on admission. Neurological deficits were evaluated using the National Institutes of Health Stroke Scale (NIHSS) when the patient arrived at hospital, and the modified Rankin scale at the 90th day.

MRI protocol and image analysis

All data were collected using a 3 Tesla Siemens Verio MRI system (Siemens Medical System, Erlangen, Germany) or a 1.5-T

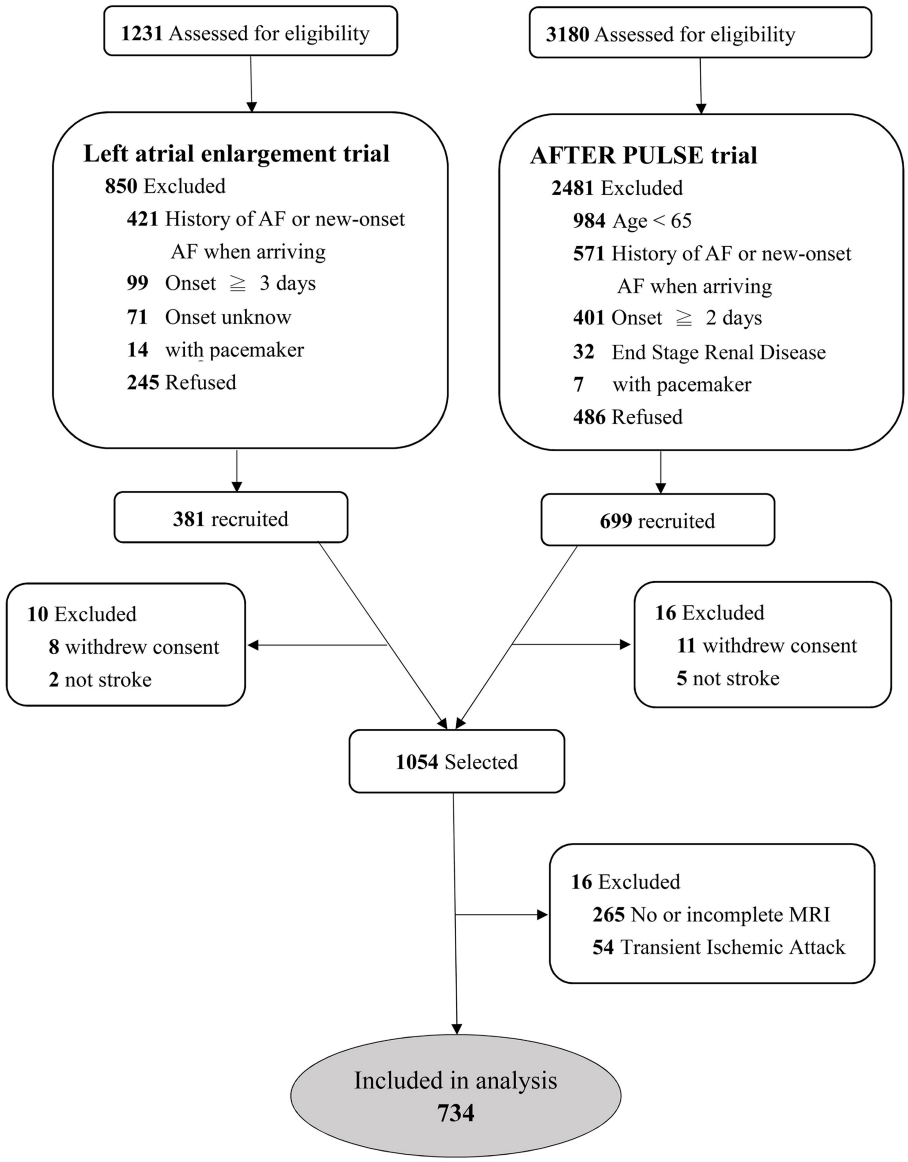

FIGURE 1
Study flowchart of patient selection.

Philips Gyroscan Intera scanner (Philips Medical Systems, Best, The Netherlands).

Standard sequences included axial DWI, fluid-attenuated inversion recovery images, axial T1- and T2-weighted images, and three-dimensional time of flight angiography covering the extracranial carotid artery and circle of Willis. Patients also received either axial T2*-GRE imaging or susceptibility-weighted imaging (SWI). The imaging data were evaluated by two stroke neurologists, who were blinded to the clinical information. If there were any discrepancies in the interpretation of the images, the two readers discussed the data further or consulted a third reader to form a consensus.

Definition of imaging predictors

Classification of DWI patterns

We divided the patients into the following groups based on the observed DWI patterns with reference to previous reports (Supplementary Figure 1) (11, 12, 15, 16), and the illustrated patients are shown in Figure 2 and Supplementary Figure 2.

1. Territorial infarct, involving territories of the internal carotid artery (ICA) or middle cerebral artery (MCA), with at least one division. The DWI pattern should be homogenous, including cortical and subcortical

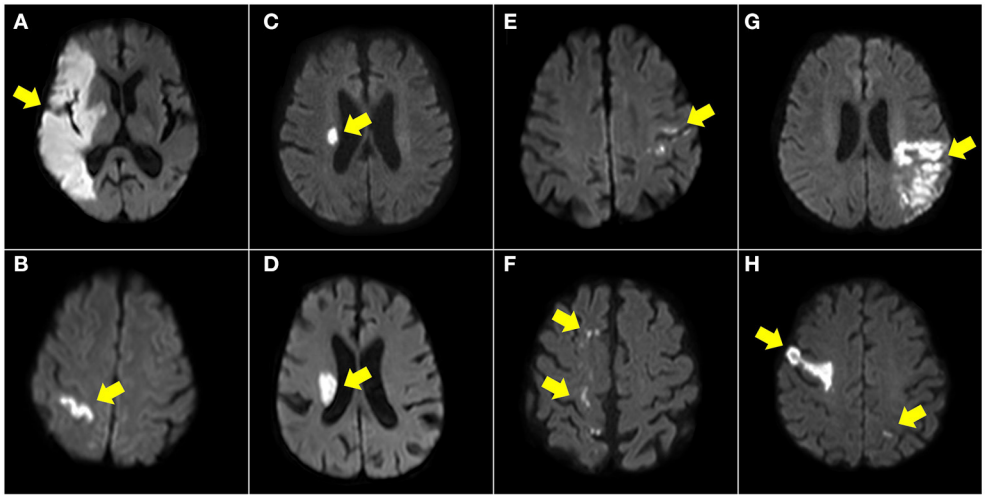

FIGURE 2
Illustration of DWI patterns in anterior circulation. Territory infarct **(A)**, single cortical infarct **(B)**, single subcortical infarct (<20 mm) **(C)**, single subcortical infarct (>20 mm) **(D)**, small scattered cortical or subcortical infarcts **(E)**, border zone infarcts **(F)**, other cortical and subcortical infarcts **(G)**, and multiple territories **(H)**.

areas. Small separate infarctions in the same vascular territory or in different territories were also classified as territorial infarcts.

2. Single cortical infarct, with a length <30 mm and not involving the subcortical area.
3. Single subcortical infarct (diameter ≤20 mm) in the penetrating artery territories.
4. Single subcortical infarct (diameter ≥20 mm) in the penetrating artery territories.
5. Small scattered cortical or subcortical infarcts, defined as small scattered cortical infarctions with a length <30 mm or multiple subcortical lesions but not restricted to the penetrating artery territories.
6. Border zone infarcts, including internal border zone infarction in the MCA territory or infarction at the MCA-anterior cerebral artery or MCA-posterior cerebral artery cortical border zones.
7. Other cortical and subcortical infarcts, defined as lesions ≥30 mm in one vascular territory but not classified in the patterns above.
8. Multiple territories: multiple infarcts in different vascular territories, including in both left and right ICA territories or in both anterior and posterior circulation territories.

Early hemorrhage

Hemorrhagic transformation after ischemic stroke is related to cardioembolism due to a large core infarction and recanalization. The radiologic appearance of hemorrhagic transformation after ischemic stroke was defined according to the European Cooperative Acute Stroke Study II trial, including hemorrhagic infarction and parenchymal infarction (17). These hemorrhages appeared as hypointense signals within or next to the areas of infarction in SWI or GRE imaging (Figures 3C,D), excluding hemorrhage mimics, such as vessels, mineralization, air-bone interfaces, partial volume artifacts, or microbleeds. Early hemorrhage was defined as any hemorrhagic transformation within 5 days of stroke onset.

SVS in SWI and GRE imaging

SVSs from deoxygenated hemoglobin in red clots and imaging markers are highly related to cardioembolism. SVS was defined as a hypointense signal in the symptomatic occlusive vessel on GRE imaging or SWI that was larger than the contralateral arterial diameter (Figures 3A,B).

Statistical analysis

Descriptive statistics were presented as frequencies, means and standard deviations, or medians and interquartile ranges (IQRs), as appropriate. The Kolmogorov-Smirnov test was used to examine the normality of continuous variables, which were then compared using a Student's *t*-test or Mann-Whitney *U*-test, as appropriate. Categorical data were analyzed using a chi-squared test or Fisher's exact test. All tests were two-tailed, and a p-value < 0.05 was considered to indicate a statistically significant difference.

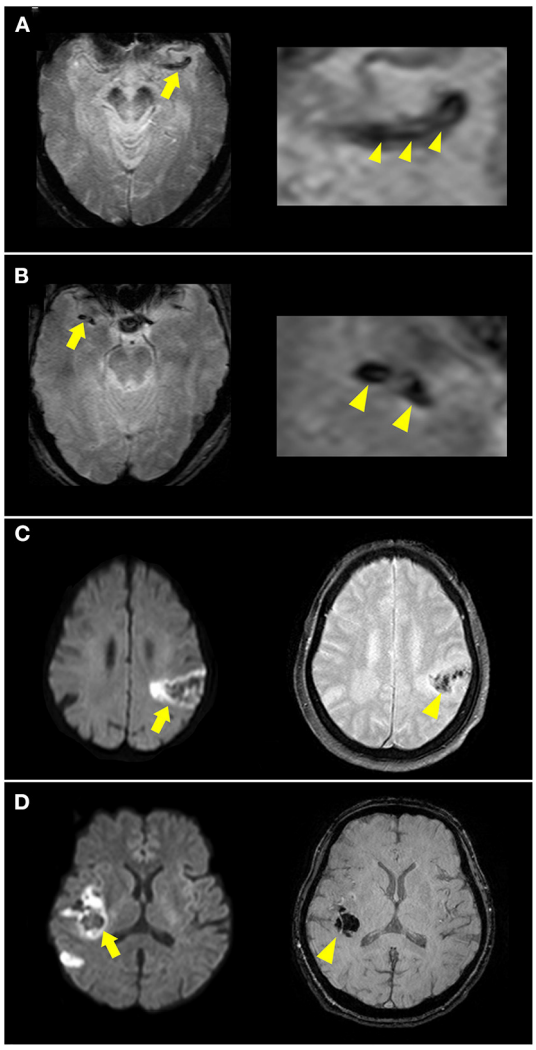

FIGURE 3
Illustration of susceptibility vessel sign (SVS) and early hemorrhage. **(A)** A hypointense signal was noted at the left occluded middle cerebral artery (MCA) [**(A)**, arrow] in T2*-weighted imaging, with a low-intensity core surrounded by a signal of higher intensity [**(A)** arrowheads], suggesting a 2-layered SVS. **(B)** A homogenous hypointense signal was noted at the right occluded MCA [**(B)**, arrow and arrowheads] in T2*-weighted imaging suggesting SVS. **(C)** DWI showed acute infarction in the left MCA territory with restricted diffusion and hypointense lesions inside (arrow). T2*-weighted imaging showed hypointense signal changes (arrowhead) suggesting hemorrhagic infarction. **(D)** DWI showed acute infarction in the right MCA territory (arrow). Susceptibility-weighted imaging showed a hypointense space-occupying lesion (arrowhead) suggesting parenchymal hemorrhage.

Factors potentially associated with newly-detected AF were evaluated using descriptive statistics. Univariable logistic regression models were used to evaluate candidate variables. Odds ratios (ORs) together with 95% confidence intervals (CIs) were reported, and p-values < 0.05 were considered to indicate a statistically significant difference. We built a multivariable regression model based on all potential predictors using forward stepwise selection with $p < 0.05$. Then the "nomolog" package was used to establish a predictive model and generate the nomogram to predict newly detected AF. We also examined discrimination using the C-statistic in our regression model, CHA2DS2-VASc, CHARGE-AF, and EHR-AF scores. Analyses were performed using Stata SE software (version 15.1; StataCorp, College Station, TX).

Results

A total of 1,054 patients were selected from the two previous trials (Figure 1). After excluding 263 patients without MRI or without complete MRI sequences and 54 patients with transient ischemic stroke, a total of 734 patients were recruited for analysis. The median age of the patients was 72 (IQR 65–79) years, and the median NIHSS score was 4 (IQR 2–6). Among them, 64 (8.7%) patients had AF during the follow-up period; 46 (71.9%) within 14 days, 8 (12.5%) within 15–90 days, and 10 (15.6%) within 90–180 days following stroke onset. Among the 179 patients with embolic stroke of an undetermined source (ESUS), 30 (16.8%) were detected as having AF.

According to the classification of DWI patterns, there were 18 (2.3%) territorial infarcts, 27 (3.7%) single cortical infarcts, 289 (39.4%) single subcortical infarcts with a diameter <20 mm, 61 (8.3%) single subcortical infarcts with a diameter ≥20 mm, 96 (13.1%) small scattered cortical or subcortical infarcts, 58 (7.9%) border zone infarcts, 143 (19.5%) other cortical and subcortical infarcts, and 42 (5.7%) infarcts in multiple territories. Among the included patients, 301 had >50% stenosis or occlusion of the relevant vessels, 40 (5.5%) had hemorrhagic infarcts, and 4 (0.5%) had parenchymal hemorrhage.

Compared to the patients without newly detected AF (Table 1), the patients with AF were significantly older (80 vs. 71 years; $p < 0.001$), included more females (48.4 vs. 34.7%; $p = 0.028$), had a higher rate of ESUS (46.9 vs. 22.2%; $p < 0.001$), lower incidence of diabetes mellitus (31.3 vs. 47.8%; $p = 0.011$), higher incidence of receiving recombinant tissue plasminogen activator (rt-PA) treatment (12.5 vs. 4.0%; $p = 0.002$), and higher incidence of congestive heart failure (7.8 vs. 1.3%; $p < 0.001$). The imaging patterns of territorial infarcts, single cortical infarct, and early hemorrhage were more likely to be associated with newly detected AF, whereas single subcortical infarcts (diameter <20 mm) and border zone infarcts were less likely to be associated with newly detected AF.

In multivariate logistic regression analysis (Table 2), age ≥75 years [adjusted odds ratio (aOR) 5.66, 95% CI 2.98–10.75], receiving rt-PA treatment (aOR 4.36, 95% CI 1.65–11.54), congestive heart failure (aOR 6.73, 95% CI 1.85–24.48), early hemorrhage in MRI (aOR 3.62, 95% CI 1.52–8.61), single cortical infarct (aOR 6.49, 95% CI 2.35–17.92), and territorial infarcts (aOR 3.54, 95% CI 1.06–11.75) were associated with

TABLE 1 Baseline characteristics, imaging findings and outcomes, and correlations with newly detected atrial fibrillation.

Characteristics	Patients without newly detected AF	Patients with newly detected AF	*p*
All patients	670	64	
Age	71 (63–79)	79.5 (73.3–85)	<0.001
Female sex	232 (34.7)	31 (48.4)	0.028
Stroke information			
Baseline NIHSS	4 (2–6)	5 (2–8)	0.105
ESUS	149 (22.2)	30 (46.9)	<0.001
Diabetes mellitus	320 (47.8)	20 (31.3)	0.011
Hypertension	519 (77.5)	52(81.3)	0.486
Hypercholesterolemia	259 (38.7)	22 (34.4)	0.501
Coronary artery disease	60 (9.0)	7 (10.9)	0.599
Old stroke	169 (25.2)	11 (17.2)	0.153
Congestive heart failure	9 (1.3)	5 (7.8)	<0.001
Intravenous rt-PA treatment	27 (4.0)	8 (12.5)	0.002
Imaging patterns			
Territorial infarcts	12 (1.8)	6 (9.4)	<0.001
Single cortical infarcts	20 (3.0)	7 (10.9)	0.001
Single subcortical infarcts (diameter <20 mm)	272 (40.6)	17 (26.6)	0.028
Single subcortical infarcts (diameter ≥20 mm)	59 (8.8)	2 (3.1)	0.153
Small scattered cortical or subcortical infarcts	86 (12.8)	10 (15.6)	0.527
Border zone infarcts	57 (8.5)	1 (1.6)	0.050
Other cortical and subcortical infarcts	127 (19.0)	16 (25.0)	0.243
Multiple territories	37 (5.5)	5 (7.8)	0.451
Relevant vessel stenosis >50%	279 (41.6)	22 (34.4)	0.247
Susceptibility vessel sign	26 (3.9)	5 (7.8)	0.128
Early hemorrhage	33 (4.9)	11 (17.2)	<0.001

Values presented as n (%) and median (interquartile range).
AF, atrial fibrillation; ESUS, embolic stroke of undetermined source; IQR, interquartile range; NIHSS, national institutes of health stroke scale; rt-PA, recombinant tissue plasminogen activator.

newly detected AF. A nomogram of the prediction model for newly detected AF is shown in Figure 4. The C-statistic of the prediction model for newly detected AF was 0.764 for all patients, and 0.811 for the patients with ESUS. Using CHA2DS2-VASc, EHR-AF and CHARGE-AF score, the C-statistics for the prediction of newly detected AF were 0.551, 0.690, and 0.702, respectively, for all patients.

Discussion

In this study, we demonstrated that specific infarction patterns, including single cortical infarctions, territorial infarctions, and early hemorrhage in MRI independently predicted newly detected AF in patients with acute ischemic stroke. Our findings also challenge the current imaging definition of ESUS, which includes large single subcortical infarctions, as they were not associated with newly detected AF in the current study. Furthermore, the use of additional imaging parameters improved the predictive accuracy for newly detected AF compared to current scales using clinical characteristics (10). A clinical and imaging prediction model may be useful to determine which high-risk patients should receive extended electrocardiogram monitoring. In keeping with previous studies which reported an association between territorial infarcts and cardioembolic stroke, we also found that territorial infarcts were highly associated with newly detected AF in this study (12, 18–20). For acute stroke caused by large vessel occlusion, cardioembolic stroke tends to have less collateral flow compared with atherosclerotic stroke because of the more abrupt perfusion compromise in cardioembolic occlusion (21, 22). As there are fewer leptomeningeal collaterals in cardioembolic stroke, the infarct pattern is unsurprisingly larger, wedge-shaped and homogenous in both cortical and subcortical areas (18, 23). Single or multiple cortical infarcts in either the cerebral or cerebellar cortex have been reported to be related to cardioembolism or AF, suggesting small or fragmented cardio-emboli (24–26). However, only

TABLE 2 Logistic regression for the predictors of newly detected atrial fibrillation in the patients with acute ischemic stroke.

	Univariate model			Multivariate model		
	Odds ratio	95% CI	*p*	Adjusted odds ratio	95% CI	*p*
Age ≧ 75 years	3.93	2.25–6.87	<0.001	5.66	2.98–10.75	<0.001
Female sex	2.05	1.22–3.43	0.006			
NIHSS score	1.06	1.02–1.10	0.006			
Diabetes mellitus	0.50	0.29–0.86	0.013			
Hypertension	1.25	0.65–2.40	0.503			
Hypercholesterolemia	0.86	0.50–1.46	0.572			
Coronary artery disease	1.23	0.54–2.81	0.629			
Old stroke	0.62	0.31–1.21	0.157			
Congestive heart failure	6.22	2.02–19.18	0.001	6.73	1.85–24.48	0.004
Intravenous rt-PA treatment	3.40	1.48–7.84	0.004	4.36	1.65–11.54	0.003
Imaging patterns						
Territorial infarcts	5.67	2.05–15.7	0.001	3.54	1.06–11.75	0.039
Single cortical infarcts	3.99	1.62–9.84	0.003	6.49	2.35–17.92	<0.001
Single subcortical infarcts (diameter < 20 mm)	0.53	0.30–0.94	0.030			
Single subcortical infarcts (diameter ≧20 mm)	0.33	0.08–1.40	0.134			
Small scattered cortical or subcortical infarcts	1.26	0.62–2.56	0.528			
Border zone infarcts	0.17	0.02–1.25	0.082			
Other cortical and subcortical infarcts	1.43	0.78–2.59	0.245			
Multiple territories	1.45	0.55–3.83	0.453			
Parental vessel stenosis >50%	0.73	0.43–1.25	0.249			
Susceptibility vessel sign	2.13	0.79–5.79	0.137			
Early hemorrhage	4.03	1.92–8.47	<0.001	3.62	1.52–8.61	0.004

CI, confidence interval; NIHSS, national institutes of health stroke scale; rt-PA, recombinant tissue plasminogen activator.

single cortical infarcts were associated with newly detected AF in our study, and multiple cortical infarcts were not. The reason for this finding could be that multiple cortical infarcts are also related to artery-to-artery embolism from atherosclerotic plaques of steno-occlusive vessels, whereas single cortical infarcts are more likely to be related to the cardioembolism (26).

Multiple simultaneous infarcts in multiple territories have been reported to be more prevalent in patients with an acute ischemic stroke of cardioembolic origin (27) and in patients with occult AF in ESUS (28). However, in the current study, there was no significant difference in infarctions in multiple territories between the patients with or without newly detected AF. The reason for this may be that we excluded patients with a documented risk of cardioembolism and included patients with small vessel occlusion. Therefore, only 5.2% of the patients presented with multiple circulation infarcts in our study. The lack of significant correlation between multiple simultaneous infarcts in multiple territories and AF may also be due to the small sample size. In addition, we did not exclude patients with large atherosclerotic occlusion, which may have also led to multiple circulation infarcts, such as in bilateral anterior cerebral arteries from unilateral ICA or a fetal type posterior cerebral artery. Despite these limitations, our findings are close to clinical practice and provide valuable information that the presence of multiple simultaneous infarctions is not as useful as previously assumed for the prediction of unrecognized AF.

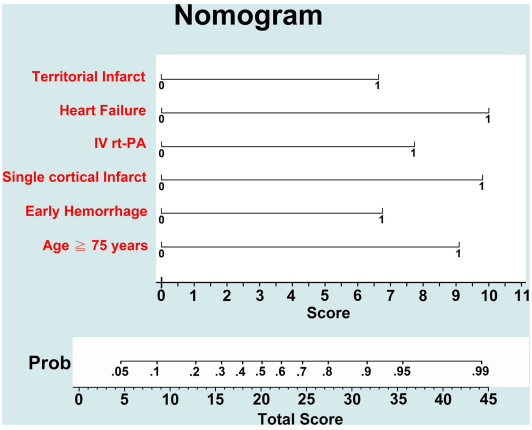

FIGURE 4
Nomogram of the prediction model for newly detected AF.

The infarction pattern of single subcortical infarcts with a diameter <20 mm, commonly called lacunar infarcts, was less likely to be associated with newly detected AF in this study, which is comparable with previous reports (12, 27). A single subcortical infarct with a diameter ≥20 mm still showed a non-significant trend toward identifying the absence of AF. The major reason for this may be that larger single subcortical infarcts are usually attributed to branch atheromatous disease caused by atherosclerotic plaques involving parent artery perforators and less to cardioembolic occlusion (29). Nevertheless, large single subcortical infarcts with a diameter ≥20 mm are classified as ESUS according to imaging criteria. Since their pathologies favor an atherosclerotic origin rather than cardioembolism, our findings provide evidence against the current definition of ESUS, which includes single subcortical infarcts ≥20 mm (30). In the RE-SPECT ESUS and NAVIGATE ESUS trials, rivaroxaban and dabigatran were not shown to be beneficial in preventing recurrent ESUS. A possible reason for this finding may be the heterogeneity of the recruited patients (31). In our study, 34% (64/179) of the patients with ESUS had a single subcortical infarction with a diameter ≥20 mm. Therefore, it may be reasonable to remove single subcortical infarcts with a diameter ≥20 mm from the imaging definition of ESUS, and instead use a new definition involving MRI imaging.

Both internal border zone infarction and cortical border zone infarction are usually associated with hemodynamic failure and microembolization from steno-occlusive disease or sometimes systemic hypotension (32, 33). When border zone infarction is combined with stenosis or occlusion of relevant vessels, it is usually presumed and classified to be a large atherosclerotic artery stroke in clinical practice. Hence, it is no surprise that the pattern of border zone infarction was less likely to be associated with newly detected AF in our study. However, time of flight angiography in MRI could not clearly distinguish between atherosclerotic and cardioembolic occlusion, so that occlusion or stenosis >50% of relevant vessels failed to predict newly detected AF. Although SVS with specific morphologies has been shown to be associated with cardioembolic stroke (34, 35), the trend was not statistically significant in our study, probably due to the low number of patients (4.2%) with SVS. Further studies with a larger sample size and a precise definition of SVS are warranted to test its efficacy for the prediction of newly detected AF.

Cardioembolic stroke, especially that caused by AF, is strongly associated with hemorrhagic transformation after acute ischemic stroke, probably due to the inherent characteristics of large infarction core and early recanalization (36–38). T2*-weighted GRE and SWI are sensitive methods of detecting early hemorrhagic transformation after acute ischemic stroke (39, 40). In our study, early hemorrhagic transformation in MRI was an independent predictor for newly detected AF.

In addition to specific imaging patterns, we also found that certain clinical characteristics, including female sex, age ≥75 years, and heart failure, were associated with an increased risk of newly detected AF. These factors are also included in the CHA_2DS_2-VASc score, which is used to predict the risk of stroke in individuals with AF, and predict the risk of AF in individuals without AF (41, 42). The CHARGE-AF and EHR-AF scores have been used to predict new-onset AF in population-based cohorts and to predict cardioembolic stroke at the time of stroke (9, 10, 43). AF has also been reported to account for ∼25% of patients receiving thrombolytic therapy because of worse stroke severity (44, 45). Therefore, the patients receiving intravenous rt-PA treatment were related to newly detected AF. The prediction model in our study was robustly associated with newly detected AF and could moderately discriminate occult cardioembolism from unknown paroxysmal AF. A prediction model including MRI information may improve the accuracy of predicting newly detected AF at the time of stroke.

Compared with the NAVIGATE and RESPECT ESUS trials, the definition of cardiac embolism in the ATTICUS trial included additional risk factors (46). Despite the higher rate of newly detected AF (23%), the trial still failed to demonstrate the efficacy of apixaban in ESUS patients. Moreover, apixaban treatment was not superior to "aspirin with the switch to apixaban in case of AF detection by mandatory cardiac monitoring" in preventing new ischemic lesions during follow-up. This may emphasize the importance of extended electrocardiogram monitoring in patients with ESUS, and our prediction model may be useful to identify high-risk patients.

There are several limitations to this study. First, we presumed that the specific infarction patterns were related to cardioembolism due to unknown paroxysmal AF, however other etiologies of embolic stroke were not explored, such as patent foramen ovale, valvular heart disease, aortic arch atheroma, cancer-associated coagulopathy, etc. Second, some patients only received serial 12-lead electrocardiography and were followed up for 3 months. The incidence of newly detected AF may therefore be underestimated in our study, even though the AF detection rate of 8.7% in our ESUS patients is comparable to the 8.9% reported in a previous trial using an insertable cardiac monitor for 6 months (47). The small sample size and the fact that we did not use prolonged cardiac monitoring may mean that we missed potential predictors for unknown paroxysmal AF. Third, we did not recruit patients with endovascular thrombectomy, so the imaging patterns cannot be applied in these patients. Fourth, our study has the inherent drawbacks of selection and detection bias, since one selected cohort excluded patients <65 years old and end-stage renal disease, and we only selected patients who underwent MRI and had a milder stroke severity. Despite these limitations, our study still provides valuable information which may improve the prediction of newly detected AF after acute ischemic stroke.

Conclusion

In addition to clinically known risk factors for AF, our study revealed that MRI at stroke onset provides critical clues for the prediction of newly detected AF, including single cortical infarcts, territorial infarcts and early hemorrhage. Future studies are warranted to verify this new prediction model and to assess whether the identification of AF can be enhanced to improve outcomes after acute ischemic stroke.

Data availability statement

The original contributions presented in the study are included in the article/Supplementary material, further inquiries can be directed to the corresponding author.

Ethics statement

The protocols of these studies were approved by the Institutional Review Board of Chang Gung Memorial Hospital (103-7597B and 104-9611C). The patients/participants provided their written informed consent to participate in this study.

Author contributions

Y-CH interpreted data, analyzed imaging, and revised the manuscript. C-HC analyzed imaging and drafted the manuscript. ML designed the study and interpreted data. J-DL and J-TY acquired data. Y-HT analyzed the imaging. H-HW conducted the statistical analyses. All authors reviewed the manuscript and gave final approval to the version to be published.

Funding

This study was supported by Chang Gung Memorial Hospital research grants (CMRPG6J0361, CMRPG6J0362, and CORPG6G0223).

Acknowledgments

We thank Yi-Chen Kuo for assisting us with this study.

Conflict of interest

The authors declare that the research was conducted in the absence of any commercial or financial relationships that could be construed as a potential conflict of interest.

Publisher's note

All claims expressed in this article are solely those of the authors and do not necessarily represent those of their affiliated organizations, or those of the publisher, the editors and the reviewers. Any product that may be evaluated in this article, or claim that may be made by its manufacturer, is not guaranteed or endorsed by the publisher.

Supplementary material

The Supplementary Material for this article can be found online at: https://www.frontiersin.org/articles/10.3389/fneur.2022.952462/full#supplementary-material

References

1. Palacio S, Hart RG. Neurologic manifestations of cardiogenic embolism: an update. *Neurol Clin.* (2002) 20:179–93. doi: 10.1016/S0733-8619(03)00058-6

2. Sage JI, Van Uitert RL. Risk of recurrent stroke in patients with atrial fibrillation and non-valvular heart disease. *Stroke.* (1983) 14:537–40. doi: 10.1161/01.STR.14.4.537

3. Lin HJ, Wolf PA, Kelly-Hayes M, Beiser AS, Kase CS, Benjamin EJ, et al. Stroke severity in atrial fibrillation. The Framingham study. *Stroke.* (1996) 27:1760–4. doi: 10.1161/01.STR.27.10.1760

4. Wolf PA, Abbott RD, Kannel WB. Atrial fibrillation as an independent risk factor for stroke: the Framingham study. *Stroke.* (1991) 22:983–8. doi: 10.1161/01.STR.22.8.983

5. Ntaios G, Papavasileiou V, Makaritsis K, Vemmos K, Michel P, Lip GYH. Real-world setting comparison of nonvitamin-K antagonist oral anticoagulants versus vitamin-K antagonists for stroke prevention in atrial fibrillation: a systematic review and meta-analysis. *Stroke.* (2017) 48:2494–503. doi: 10.1161/STROKEAHA.117.017549

6. Lip GY, Lane DA. Stroke prevention in atrial fibrillation: a systematic review. *J Am Med Assoc.* (2015) 313:1950–62. doi: 10.1001/jama.2015.4369

7. Saliba W, Gronich N, Barnett-Griness O, Rennert G. Usefulness of Chads2 and Cha2ds2-Vasc scores in the prediction of new-onset atrial fibrillation: a population-based study. *Am J Med.* (2016) 129:843–9. doi: 10.1016/j.amjmed.2016.02.029

8. Alonso A, Roetker NS, Soliman EZ, Chen LY, Greenland P, Heckbert SR. Prediction of atrial fibrillation in a racially diverse cohort: the multi-ethnic study of atherosclerosis (mesa). *J Am Heart Assoc.* (2016) 5:e003077. doi: 10.1161/JAHA.115.003077

9. Hulme OL, Khurshid S, Weng L-C, Anderson CD, Wang EY, Ashburner JM, et al. Development and validation of a prediction model for atrial fibrillation using electronic health records. *JACC Clin Electrophysiol.* (2019) 5:1331–41. doi: 10.1016/j.jacep.2019.07.016

10. Khurshid S, Trinquart L, Weng LC, Hulme OL, Guan W, Ko D, et al. Atrial fibrillation risk and discrimination of cardioembolic from noncardioembolic stroke. *Stroke.* (2020) 51:1396–403. doi: 10.1161/STROKEAHA.120.028837

11. Rovira A, Grive E, Rovira A, Alvarez-Sabin J. Distribution territories and causative mechanisms of ischemic stroke. *Eur Radiol.* (2005) 15:416–26. doi: 10.1007/s00330-004-2633-5

12. Kang DW, Chalela JA, Ezzeddine MA, Warach S. Association of ischemic lesion patterns on early diffusion-weighted imaging with toast stroke subtypes. *Arch Neurol.* (2003) 60:1730–4. doi: 10.1001/archneur.60.12.1730

13. Cho KH, Kim JS, Kwon SU, Cho AH, Kang DW. Significance of susceptibility vessel sign on T2*-weighted gradient echo imaging for identification of stroke subtypes. *Stroke.* (2005) 36:2379–83. doi: 10.1161/01.STR.0000185932.73486.7a

14. Huang WY, Lee M, Sung SF, Tang SC, Chang KH, Huang YS, et al. Atrial fibrillation trial to evaluate real-world procedures for their utility in helping to lower stroke events: a randomized clinical trial. *Int J Stroke.* (2021) 16:300–10. doi: 10.1177/1747493020938297

15. Bang OY, Lee PH, Heo KG, Joo US, Yoon SR, Kim SY. Specific Dwi lesion patterns predict prognosis after acute ischaemic stroke within the Mca territory. *J Neurol Neurosurg Psychiatry.* (2005) 76:1222–8. doi: 10.1136/jnnp.2004.059998

16. Lopez-Cancio E, Matheus MG, Romano JG, Liebeskind DS, Prabhakaran S, Turan TN, et al. Infarct patterns, collaterals and likely causative mechanisms of stroke in symptomatic intracranial atherosclerosis. *Cerebrovasc Dis.* (2014) 37:417–22. doi: 10.1159/000362922

17. Hacke W, Kaste M, Fieschi C, von Kummer R, Davalos A, Meier D, et al. Randomised double-blind placebo-controlled trial of thrombolytic therapy with intravenous alteplase in acute ischaemic stroke (Ecass Ii). Second European-Australasian Acute Stroke study. *Investigators Lancet.* (1998) 352:1245–51. doi: 10.1016/S0140-6736(98)08020-9

18. Cho HJ, Yang JH, Jung YH, Kim YD, Choi HY, Nam HS, et al. Cortex-sparing infarctions in patients with occlusion of the middle cerebral artery. *J Neurol Neurosurg Psychiatry.* (2010) 81:859–63. doi: 10.1136/jnnp.2009.195842

19. Jung JM, Kwon SU, Lee JH, Kang DW. Difference in infarct volume and patterns between cardioembolism and internal carotid artery disease: focus on the degree of cardioembolic risk and carotid stenosis. *Cerebrovasc Dis.* (2010) 29:490–6. doi: 10.1159/000297965

20. Wessels T, Wessels C, Ellsiepen A, Reuter I, Trittmacher S, Stolz E, et al. Contribution of diffusion-weighted imaging in determination of stroke etiology. *Am J Neuroradiol.* (2006) 27:35–9.

21. Rebello LC, Bouslama M, Haussen DC, Grossberg JA, Dehkharghani S, Anderson A, et al. Stroke etiology and collaterals: atheroembolic strokes have greater collateral recruitment than cardioembolic strokes. *Eur J Neurol.* (2017) 24:762–7. doi: 10.1111/ene.13287

22. Lin C-H, Tsai Y-H, Lee J-D, Weng H-H, Yang J-T, Lin L-C, et al. Magnetic resonance perfusion imaging provides a significant tool for the identification of cardioembolic stroke. *Curr Neurovasc Res.* (2016) 13:271–6. doi: 10.2174/1567202613666160901143040

23. Helgason CM. Cardioembolic stroke: topography and pathogenesis. *Cerebrovasc Brain Metab Rev.* (1992) 4:28–58.

24. Favilla CG, Ingala E, Jara J, Fessler E, Cucchiara B, Messé SR, et al. Predictors of finding occult atrial fibrillation after cryptogenic stroke. *Stroke.* (2015) 46:1210–5. doi: 10.1161/STROKEAHA.114.007763

25. Ter Schiphorst A, Tatu L, Thijs V, Demattei C, Thouvenot E, Renard D. Small obliquely oriented cortical cerebellar infarctions are associated with cardioembolic stroke. *BMC Neurol.* (2019) 19:1328. doi: 10.1186/s12883-019-1328-0

26. Lee DK, Kim JS, Kwon SU, Yoo SH, Kang DW. Lesion patterns and stroke mechanism in atherosclerotic middle cerebral artery disease: early diffusion-weighted imaging study. *Stroke.* (2005) 36:2583–8. doi: 10.1161/01.STR.0000189999.19948.14

27. Sharobeam A, Churilov L, Parsons M, Donnan GA, Davis SM, Yan B. Patterns of infarction on Mri in patients with acute ischemic stroke and cardio-embolism: a systematic review and meta-analysis. *Front Neurol.* (2020) 11:606521. doi: 10.3389/fneur.2020.606521

28. Yushan B, Tan BYQ, Ngiam NJ, Chan BPL, Luen TH, Sharma VK, et al. Association between bilateral infarcts pattern and detection of occult atrial fibrillation in embolic stroke of undetermined source (Esus) patients with insertable cardiac monitor (Icm). *J Stroke Cerebrovasc Dis.* (2019) 28:2448–52. doi: 10.1016/j.jstrokecerebrovasdis.2019.06.025

29. Petrone L, Nannoni S, Del Bene A, Palumbo V, Inzitari D. Branch atheromatous disease: a clinically meaningful, yet unproven concept. *Cerebrovasc Dis.* (2016) 41:87–95. doi: 10.1159/000442577

30. Kamel H, Navi BB, Parikh NS, Merkler AE, Okin PM, Devereux RB, et al. Machine learning prediction of stroke mechanism in embolic strokes of undetermined source. *Stroke.* (2020) 51:29305. doi: 10.1161/STROKEAHA.120.029305

31. Maier IL, Schregel K, Karch A, Weber-Krueger M, Mikolajczyk RT, Stahrenberg R, et al. Association between embolic stroke patterns, esus etiology, and new diagnosis of atrial fibrillation: a secondary data analysis of the find-Af trial. *Stroke Res Treat.* (2017) 2017:1–6. doi: 10.1155/2017/1391843

32. Forster A, Szabo K, Hennerici MG. Pathophysiological concepts of stroke in hemodynamic risk zones–do hypoperfusion and embolism interact? *Nat Clin Pract Neurol.* (2008) 4:216–25. doi: 10.1038/ncpneuro0752

33. Man BL, Fu YP, Chan YY, Lam W, Hui AC, Leung WH, et al. Lesion patterns and stroke mechanisms in concurrent atherosclerosis of intracranial and extracranial vessels. *Stroke.* (2009) 40:3211–5. doi: 10.1161/STROKEAHA.109.557041

34. Zhang R, Zhou Y, Liu C, Zhang M, Yan S, Liebeskind DS, et al. Overestimation of susceptibility vessel sign: a predictive marker of stroke cause. *Stroke.* (2017) 48:1993–6. doi: 10.1161/STROKEAHA.117.016727

35. Yamamoto N, Satomi J, Tada Y, Harada M, Izumi Y, Nagahiro S, et al. Two-layered susceptibility vessel sign on 3-tesla T2*-weighted imaging is a predictive biomarker of stroke subtype. *Stroke.* (2015) 46:269–71. doi: 10.1161/STROKEAHA.114.007227

36. Paciaroni M, Agnelli G, Corea F, Ageno W, Alberti A, Lanari A, et al. Early hemorrhagic transformation of brain infarction: rate, predictive factors, and influence on clinical outcome. *Stroke.* (2008) 39:2249–56. doi: 10.1161/STROKEAHA.107.510321

37. Álvarez-Sabín J, Maisterra O, Santamarina E, Kase CS. Factors influencing haemorrhagic transformation in ischaemic stroke. *Lancet Neurol.* (2013) 12:689–705. doi: 10.1016/S1474-4422(13)70055-3

38. Molina CA, Montaner J, Abilleira S, Ibarra B, Romero F, Arenillas JF, et al. Timing of spontaneous recanalization and risk of hemorrhagic transformation in acute cardioembolic stroke. *Stroke.* (2001) 32:1079–84. doi: 10.1161/01.STR.32.5.1079

39. Huang P, Chen CH, Lin WC, Lin RT, Khor GT, Liu CK. Clinical applications of susceptibility weighted imaging in patients with major stroke. *J Neurol.* (2012) 259:1426–32. doi: 10.1007/s00415-011-6369-2

40. Liu L, Wu B, Zhao J, Cao Y, Dedhia N, Caplan LR, et al. Computed tomography perfusion alberta stroke program early computed tomography score is associated with hemorrhagic transformation after acute cardioembolic stroke. *Front Neurol.* (2017) 8:591. doi: 10.3389/fneur.2017.00591

41. Zuo M-L, Liu S, Chan K-H, Lau K-K, Chong B-H, Lam K-F, et al. The Chads2 and Cha2ds2–vasc scores predict new occurrence of atrial fibrillation and ischemic stroke. *J Intervention Cardiac Electrophysiol.* (2013) 37:47–54. doi: 10.1007/s10840-012-9776-0

42. Lip GYH, Nieuwlaat R, Pisters R, Lane DA, Crijns HJGM. Refining clinical risk stratification for predicting stroke and thromboembolism in atrial fibrillation using a novel risk factor-based approach. *Chest.* (2010) 137:263–72. doi: 10.1378/chest.09-1584

43. Christophersen IE, Yin X, Larson MG, Lubitz SA, Magnani JW, McManus DD, et al. A comparison of the charge–Af and the Cha2ds2-vasc risk scores for prediction of atrial fibrillation in the Framingham Heart Study. *Am Heart J.* (2016) 178:45–54. doi: 10.1016/j.ahj.2016.05.004

44. Hu Y, Ji C. Efficacy and safety of thrombolysis for acute ischemic stroke with atrial fibrillation: a meta-analysis. *BMC Neurol.* (2021) 21:66. doi: 10.1186/s12883-021-02095-x

45. Saposnik G, Gladstone D, Raptis R, Zhou L, Hart RG, Investigators of the Registry of the Canadian Stroke N, et al. Atrial fibrillation in ischemic stroke: predicting response to thrombolysis and clinical outcomes. *Stroke.* (2013) 44:99–104. doi: 10.1161/STROKEAHA.112.676551

46. Geisler T, Poli S, Meisner C, Schreieck J, Zuern CS, Nagele T, et al. Apixaban for treatment of embolic stroke of undetermined source (atticus randomized trial): rationale and study design. *Int J Stroke.* (2017) 12:985−90. doi: 10.1177/1747493016681019

47. Sanna T, Diener H-C, Passman RS, Di Lazzaro V, Bernstein RA, Morillo CA, et al. Cryptogenic stroke and underlying atrial fibrillation. *N Engl J Med.* (2014) 370:2478–86. doi: 10.1056/NEJMoa1313600

frontiers | Frontiers in Neurology

TYPE Clinical Trial
PUBLISHED 16 September 2022
DOI 10.3389/fneur.2022.968417

OPEN ACCESS

EDITED BY
Bing Tian,
Naval Medical University, China

REVIEWED BY
Yu Luo,
Shanghai Fourth People's Hospital, China
Zhang Shi,
Fudan University, China

*CORRESPONDENCE
Jian-xun Song
songjianxun@126.com

SPECIALTY SECTION
This article was submitted to Stroke, a section of the journal Frontiers in Neurology

RECEIVED 14 June 2022
ACCEPTED 18 August 2022
PUBLISHED 16 September 2022

CITATION
Lin G-h, Song J-x, Huang T-d, Fu N-x and Zhong L-l (2022) Relationship between the stroke mechanism of symptomatic middle cerebral artery atherosclerotic diseases and culprit plaques based on high-resolution vessel wall imaging. *Front. Neurol.* 13:968417. doi: 10.3389/fneur.2022.968417

Relationship between the stroke mechanism of symptomatic middle cerebral artery atherosclerotic diseases and culprit plaques based on high-resolution vessel wall imaging

Guo-hui Lin, Jian-xun Song*, Teng-da Huang, Nian-xia Fu and Li-ling Zhong

Department of Radiology, Shenzhen Baoan People's Hospital, Shenzhen, China

Purpose: For patients with symptomatic middle cerebral artery (MCA) atherosclerotic stenosis, identifying the potential stroke mechanisms may contribute to secondary prevention. The purpose of the study is to explore the relationship between stroke mechanisms and the characteristics of culprit plaques in patients with atherosclerotic ischemic stroke in the M1 segment of the middle cerebral artery (MCA) based on high-resolution vessel wall imaging (HR-VWI).

Methods: We recruited 61 patients with acute ischemic stroke due to MCA atherosclerotic stenosis from Shenzhen Bao'an District People's Hospital. According to prespecified criteria based on infarct topography and magnetic resonance angiography, possible stroke mechanisms were divided into parent artery atherosclerosis occluding penetrating artery (P), artery-to-artery embolism (A), hypoperfusion (H), and mixed mechanisms (M). The correlation between the characteristics of MCA M1 culprit plaque and different stroke mechanisms was analyzed using HR-VWI. The indicators included plaque surface irregularity, T1 hyperintensity, location, plaque burden (PB), remodeling index (RI), enhancement rate, and stenosis rate.

Results: Parental artery atherosclerosis occluding penetrating artery was the most common mechanism (37.7%). The proposed criteria showed substantial to excellent interrater reproducibility (κ, 0.728; 0.593–0.863). Compared with the P group, the surface irregularity, T1 hyperintensity, and obvious enhancement of the culprit plaque in the A group were more common ($p < 0.0125$). Compared with the other stroke mechanisms, positive remodeling of culprit plaques was more common ($p < 0.0125$), the RI was greater ($p < 0.05$), and the PB was the smallest ($p < 0.05$) in the P group. The enhancement ratio (ER) was smaller in the P group ($p < 0.05$). Compared with the A group, T1 hyperintensity of the culprit plaque was more common in the H group ($p < 0.0125$), and the stenosis rate was greater ($p < 0.05$). After adjustment for clinical demographic factors in the binary logistic regression analysis, the

enhancement level (odds ratio [*OR*] 0.213, 95% *CI* (0.05–0.91), $p = 0.037$) and PB of culprit plaque (*OR* 0, 95% *CI* (0–0.477), $p = 0.034$) were negatively associated with P groups.

Conclusion: The culprit plaque characteristics of patients with symptomatic MCA atherosclerotic in different stroke mechanisms may be evaluated using HR-VWI. The plaque characteristics of different stroke mechanisms may have clinical value for the selection of treatment strategies and prevention of stroke recurrence.

Clinical trial registration: Identifier: ChiCTR1900028533.

KEYWORDS

stroke, mechanism, atherosclerosis, middle cerebral artery, high-resolution vessel wall imaging

Introduction

Intracranial large atherosclerosis is one of the most common causes of stroke worldwide (1). The vessel wall evolves from having a slight thickening to the development of a nonstenotic plaque, which gradually develops into lumen stenosis with significant hemodynamic changes and occlusion (2–4). This process often involves multiple arterial beds, and the middle cerebral artery is the most common. The incidence of the population is highest in Asia (5). The incidence rate of the intracranial large atherosclerotic disease has gradually increased in recent years with changes in the social environment, and it is affecting a younger population (6). Therefore, effective methods are needed to clarify the mechanism of ischemic stroke because these mechanisms have potential significance for the clinical treatment and prevention of secondary stroke (7).

The pathological changes of intracranial large artery atherosclerosis indicate that ischemic stroke may involve a variety of pathogeneses, including perforating artery occlusion due to maternal atherosclerosis, artery–artery embolism, hypoperfusion, and mixed mechanisms (8). There are differences in treatment options for these specific mechanisms. For example, single subcortical infarcts are treated with dual antithrombotic therapy, but the intravascular treatment of large atherosclerosis with significantly narrowed lumens remains controversial (9, 10). A recent study found that more patients with the baseline stroke mechanism of an artery–artery embolism + hypoperfusion had a history of dyslipidemia and hypertension than those with other stroke mechanisms (11). Dyslipidemia is a risk factor for the presence of vulnerable plaques, which may increase the risk of plaque rupture and subsequent A-A embolism. It has been reported that hypertension is associated with poor pial collateral circulation in patients with acute ischemic stroke (12), which may be a risk factor for the subtype mechanism of hypoperfusion stroke. On the other hand, current evidence suggests that enhanced contrast, positive remodeling, and plaque irregularity of intracranial plaques are associated with an increased risk of stroke (13). Therefore, clarifying the potential relationship between the stroke mechanism and plaque characteristics of large artery atherosclerosis may be valuable for individualized clinical treatment and patient management. The present study aimed to explore the relationship between stroke mechanisms and the characteristics of culprit plaques in patients with atherosclerotic ischemic stroke in the M1 segment of the middle cerebral artery (MCA) based on high-resolution vessel wall imaging (HR-VWI).

Methods

Patients

The local ethics committee approved this study. From January 2019 to January 2022, we retrospectively recruited patients admitted to Shenzhen Bao'an District People's Hospital because of acute ischemic stroke caused by atherosclerosis of the M1 segment of the MCA. Acute ischemic stroke was determined based on high-signal lesions on diffusion-weighted imaging and the corresponding central nervous dysfunction in 1 week (14). The hyperintense lesions on diffusion-weighted images (DWIs) were located in the blood supply area of the middle cerebral artery. All patients underwent head magnetic resonance imaging (MRI), magnetic resonance angiography (MRA), and HR-VWI examinations within 1 week from the onset of the disease to assess intracranial atherosclerosis. We retrospectively analyzed 154 patients with acute ischemic stroke and recruited 61 patients. The specific process is shown in Figure 1. All patients satisfied the following criteria: (1) atherosclerotic plaque found on the MCA M1 vessel wall image (when there were ≥2 plaques, the plaque leading to the narrowest lumen was evaluated); and (2) the patient had at least one atherosclerotic risk factor. Patients with an ipsilateral internal carotid artery stenosis rate

≥50% and MCA M1 segment occlusion were excluded. Patients with ischemic stroke caused by nonatherosclerotic factors were also excluded.

Classification of the probable stroke mechanisms in patients with ischemic stroke

According to the China Ischemic Stroke Subclassification (CISS) and other previous studies on the mechanism of intracranial arterial stenosis (ICAS) stroke, we evaluated the distribution pattern of ischemic lesions on diffusion-weighted images (DWIs) and the location and severity of ICAS in combination with MRA. All images were analyzed with the Picture Archiving Communication System. The evidence of ischemic lesions is high-signal lesions in DWI. The possible stroke mechanisms in patients with symptomatic MCA atherosclerosis were divided into four categories (11, 15) (Figure 2). (1) Parent artery atherosclerosis occluding penetrating artery (P): the M1 segment of the MCA had any degree of stenosis, and isolated acute infarction occurred in an area adjacent to the blood supply of the perforating artery. (2) Artery-to-artery embolism (A): the presence of single or multiple small cortical infarctions, with or without subcortical infarction, or wedge-shaped infarcts, and cortical and subcortical areas that were completely located in the blood supply area of the M1 segment of the MCA but did not involve border zone areas. (3) Hypoperfusion (H): the presence of single or multiple infarcts in the watershed area, including the cortical type and the subcortical type. The cortical type refers to the area between the supplying territories of the anterior cerebral artery (ACA) and the MCA or between the MCA and the posterior cerebral artery. Infarctions in these areas are generally wedge-shaped or oval. The subcortical type refers to the white matter along and above the lateral ventricles between the deep and superficial supplying territories of the MCA or between the superficial territories of the MCA and ACA. These infarctions are linearly distributed in the centrum semiovale and the corona radiata and are present as fusion infarctions with large cigar shapes. (4) Mixed mechanisms (M): the coexistence of 2 or 3 of the mechanisms described above.

High-resolution vessel wall imaging

A 3.0-T MRI scanner (Magnetom Skyra; Siemens, Munich, Germany) with a 20-channel phased-array head coil was used. High-resolution vessel wall scanning was performed by 3D T1-sampling perfection with application-optimized contrasts using different flip angle evolutions (SPACE), such as pre- and postcontrast scanning. This imaging sequence was applied using the following parameters: for diffusion-weighted imaging: repetition time (TR) = 4,100 ms, echo time (TE) = 64 ms, field of view (FOV) = 230 mm × 230 mm, matrix size = 160 × 160, and slice thickness = 5 mm; for time of flight: TR = 20 ms, TE = 3.69 ms, FOV = 200 × 172 mm, matrix size = 235 × 320, and slice thickness = 0.6 mm; and for 3D-T1 SPACE: TR = 980 ms, TE = 27 ms, FOV = 200 mm × 178 mm, acquired resolution = 0.78 × 0.78 × 0.78, reconstruction resolution = 0.39 × 0.39 × 0.39, and slice thickness = 0.39. Before the acquisition of the contrast-enhanced 3D-T1 SPACE sequence, 0.1 ml/kg of gadolinium-containing contrast agent (gadobutrol [Gadovist]; Bayer Pharma, Berlin, Germany) was administered to the patient (16).

Image analysis

Plaque was defined as thickening >50% of adjacent or contralateral vessel wall thickness on both pre- and post-contrast HR-VWI (17). The plaque causing the narrowest lumen on the M1 segment of the symptomatic MCA was defined as the culprit plaque (16, 18). The HR-VWI was processed using vessel mass software (Leiden University Medical Centre, Leiden, the Netherlands), which was used to reconstruct multiple cross-sections of continuous vertical vessels with a thickness of 1 mm. Each cross-section was magnified 4-fold, and the vessel and lumen boundaries were semiautomatically tracked. These steps were repeated with the proximal end of the plaque as the reference. Four quadrants (ventral, dorsal, superior, and inferior walls) were selected at the maximal lumen narrowing (MLN) cross-section of the blood vessels. When ≥2 quadrants were involved in the plaque, the quadrant with the thickest plaque was selected. Intraplaque hemorrhage was defined as a bright T1 signal ≥ 150% of the T1 signal of the adjacent muscle or pons (19). Plaque irregularity was defined as surface underfinishing. Plaque enhancement was graded as follows: no enhancement means that in the same individual, the enhancement was similar to or smaller than the intracranial artery wall without plaque; mild enhancement means that the enhancement degree was greater than the grade intracranial artery wall but smaller than pituitary funnel; and the obvious enhancement is similar to or larger than the funnel (20). The parameters were evaluated by the MLN cross-section of blood vessels, such as the maximum wall thickness (WT_{max}), lumen area (LA), outer area (OA), wall area (WA), and signals of the precontrast (Signal $_{pre}$) and postcontrast (Signal $_{post}$) scans of the plaque. The following formulas were used (16): plaque burden (PB) = (WA_{MLN}/OA_{MLN} × 100%); enhancement ratio (ER) = (Signal $_{post}$ − Signal $_{pre}$)/Signal $_{pre}$ × 100%; remodeling index (RI) = OA_{MLN}/OA_{ref} (the remodeling mode is classified according to the RI value: RI ≥ 1.05 is positive remodeling (PR), RI ≤ 0.95 is negative remodeling (NR), and 0.95< RI <1.05 is no reconstruction); and stenosis degree = (1 − LA_{MLN}/LA_{ref}) ×

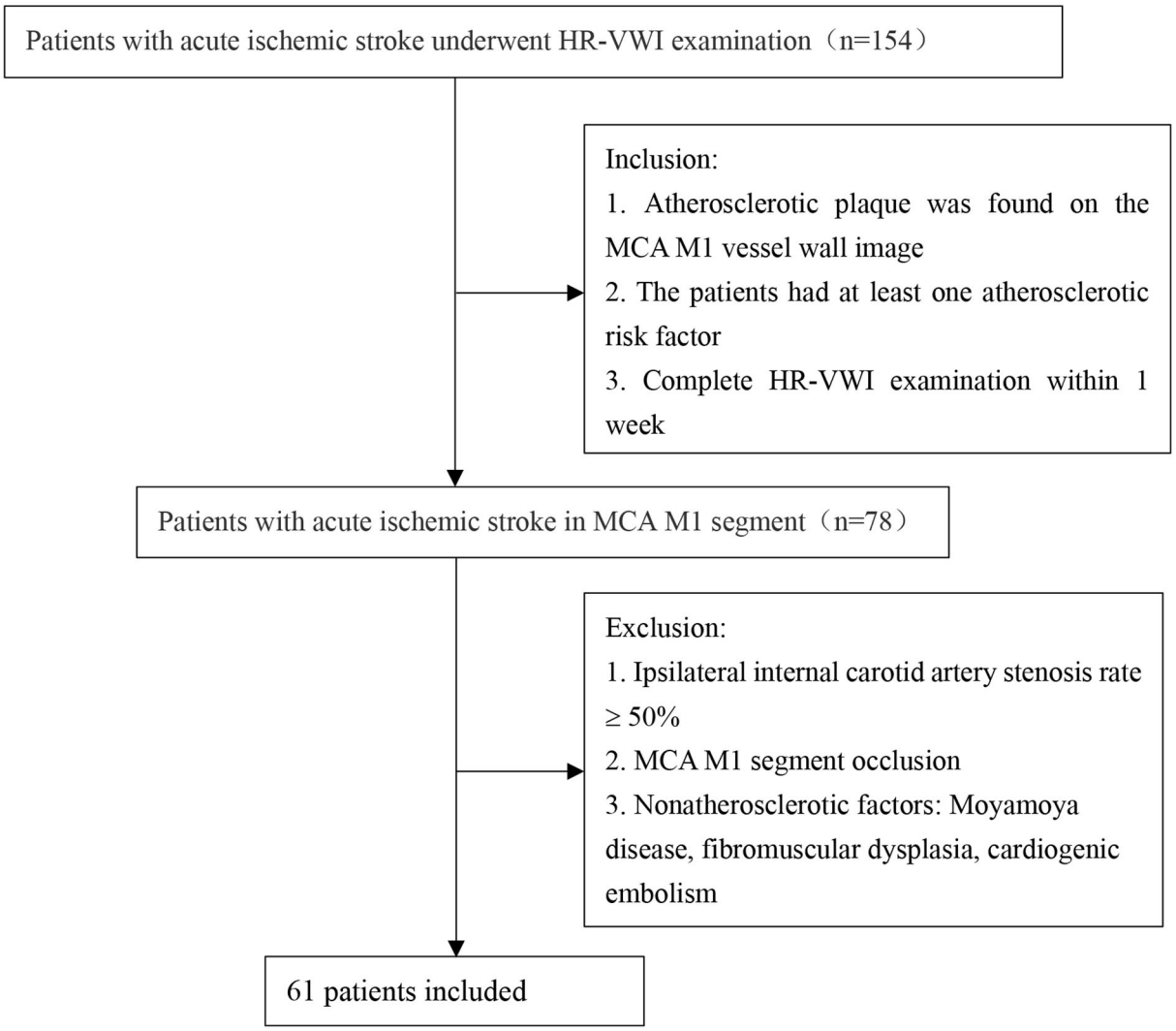

FIGURE 1
A flowchart of patient recruitment. HR-VWI: high-resolution vessel wall imaging.

100%. All of these data were measured two times, 1 month apart, by a neuroradiologist who was unaware of the clinical details, and the averages were calculated and applied.

Statistical analysis

This study used IBM SPSS Statistics 23.0 software for all statistical analyses. The intraobserver reliability for the measurement and evaluation of the vessel wall was determined using the intraclass correlation coefficient (ICC). Cohen's κ value was used to determine the intraobserver reproducibility. Measurement data are presented as the means ± standard deviation (SD), and counting data are presented as a percentage or frequency. Count data were analyzed using the χ^2 test or Fisher's exact probability method. A value of $p < 0.05$ was considered statistically significant. Measurement data were analyzed using analysis of variance (ANOVA) to test differences between groups. A value of $p < 0.05$ was considered statistically significant. For the binary logistic regression analysis, we selected adjusted variables that were statistically significant in the univariate analysis.

Results

Clinical characteristics

In this study, 61 patients with ischemic stroke caused by atherosclerosis in the M1 segment of the MCA were included.

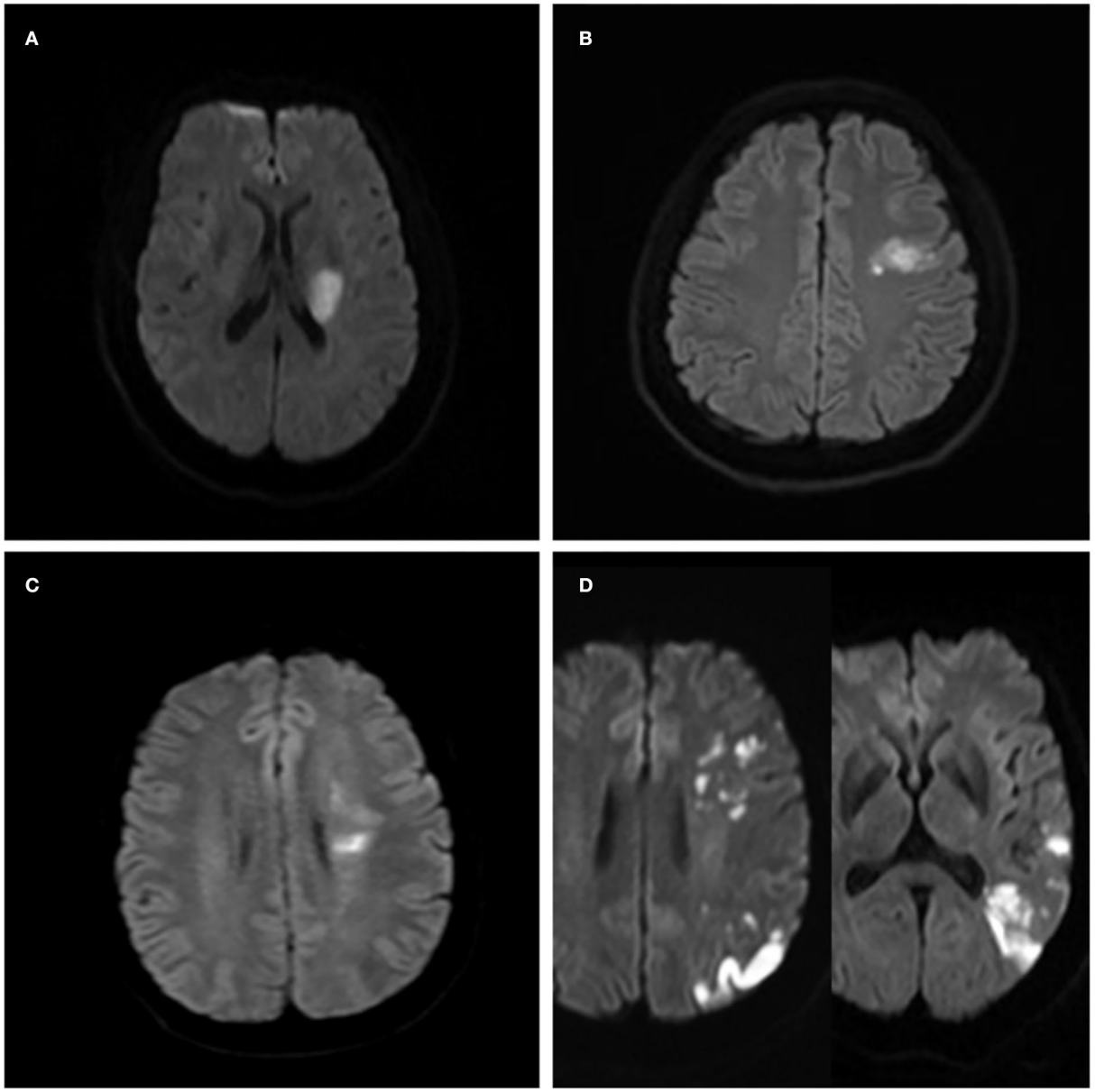

FIGURE 2
Ischemic lesion patterns indicating the different stroke mechanisms in four patients with the symptomatic middle cerebral artery (MCA) atherosclerotic stenosis. **(A)** A case of isolated acute infarction in the area of the perforating artery suggests parent artery atherosclerosis occluding a penetrating artery. **(B)** Local infarction indicating a probable artery-to-artery embolism. **(C)** Internal watershed infarctions indicating probable hypoperfusion. **(D)** Multiple cortical and wedge-shaped infarctions indicating a probable mixed mechanism of artery-to-artery embolism and hypoperfusion.

The average age of the patients was 48.9 ± 8.4 years, and there were 47 men and 14 women. These patients were divided into different stroke mechanism subtypes. There were 23 patients in the P group, 16 patients in the A group, 12 patients in the H group, and 10 patients in the M group. Table 1 shows the baseline characteristics of the patients. There was no significant difference in the stroke risk factors between the different stroke mechanism subtypes.

Reproducibility of the stroke mechanism classification criteria and consistency of vessel wall measurements

The intra-reader reproducibility was substantial (κ, 0.728; 95% *CI*, 0.593–0.863) for the classification of the stroke mechanisms into four categories (Table 2). When the three mechanisms existed independently without

TABLE 1 Baseline demographics of the patients.

Characteristics	P ($n = 23$)	A ($n = 16$)	H ($n = 12$)	M ($n = 10$)	*P*-values
Male	19(82.6)	12(75.0)	9(75.0)	7(70.0)	0.841
Age, y	48.0 ± 8.0	49.3 ± 8.9	50.1 ± 7.4	48.6 ± 10.0	0.904
Cardiovascular risk factors (%)					
Hypertension	17(73.9)	12(75.0)	7(58.3)	6(60.0)	0.673
DM	7(30.4)	2(12.5)	4(33.3)	6(60.0)	0.089
Hyperlipidemia	17(73.9)	11(68.8)	9(75.0)	7(70.0)	0.978
Smoker	17(73.9)	12(75.0)	7(58.3)	6(60.0)	0.673
Laboratory test results (mmol/L)					
FG	6.4 ± 2.1	5.9 ± 1.6	6.2 ± 1.8	7.4 ± 1.9	0.297
TC	4.7 ± 1.2	4.8±1.2	5.0 ± 1.0	4.9 ± 1.4	0.953
Triglyceride	1.6 ± 0.7	1.6 ± 1.0	1.6 ± 1.1	2.0 ± 1.2	0.720
HDL	1.1 ± 0.4	1.0 ± 0.2	1.1 ± 0.3	1.0 ± 0.2	0.724
LDL	3.0 ± 1.2	3.2 ± 0.9	3.3 ± 0.7	3.3 ± 0.9	0.748
Cysteine	14.6 ± 10.8	16.0 ± 8.6	9.9 ± 2.8	13.1 ± 4.2	0.263

DM, diabetes mellitus; FG, fasting glucose; TC, total cholesterol; HDL, high-density lipoprotein cholesterol; LDL, low-density lipoprotein cholesterol; p-values were calculated using ANOVA or the chi-squared/Fisher's exact test between the four groups, as appropriate.

TABLE 2 Intraobserver reproducibility of stroke mechanism classification.

	κ (95% CI)
Overall (4 categories)	0.728(0.593–0.863)
Existence of each mechanism	
P	0.827(0.972–0.682)
A	0.684(0.468–0.899)
H	0.610(0.365–0.855)

A indicates artery-to-artery embolism; H, hypoperfusion; and P, parent artery atherosclerosis occluding a penetrating artery.

considering any other accompanying mechanisms, the intra-reader reproducibility was substantial for each mechanism. The consistencies of OA_{MLN}, LA_{MLN}, WA_{MLN}, $Signal_{pre}$, and $Signal_{post}$ were excellent on a 3.0-T HR-VWI (ICC >0.75), and WT_{max}, OA_{ref}, and LA_{ref} were fair-to-good (0.40< ICC <0.75).

Qualitative analysis of the correlation between culprit plaque characteristics and stroke mechanism

There was a significant difference in the surface irregularity of the culprit plaques of the different subtypes of stroke mechanism ($p = 0.001$). Further pairwise comparison showed that plaque surface irregularity in the A group was more common than in the P group and the M group ($p < 0.0125$), and plaque surface irregularity in the P group was more common than in the H group ($p < 0.0125$). The difference in the T1 high signal in the culprit plaques of the different stroke mechanisms was statistically significant (p =0.004). Further pairwise comparison showed that a high T1 signal in the plaques of the A group was more common than in the P group ($p < 0.0125$), and a high T1 signal in the plaques of the H group was more common than in the A group and the M group ($p < 0.0125$). There was a significant difference in the pattern of culprit plaque remodeling between the different stroke subtypes (p =0.004). Further pairwise comparison showed that the positive remodeling in the P group was more common than in the other groups ($p < 0.0125$). There was no significant difference in the location of the culprit plaques between the different stroke subtypes ($p = 0.061$) (Table 3).

Quantitative analysis of the correlation between culprit plaque characteristics and stroke mechanism

There was no significant difference in the maximum thickness of the vessel wall between the plaques of the different stroke mechanism subtypes ($p = 0.548$). There was a significant difference in the RI between the different stroke subtypes ($p = 0.016$), and the RI in the P group was greater than in the H group and the M group ($p < 0.0125$). There was a significant difference in the PB between the different mechanisms ($p = 0.000$), and the PB in the culprit plaques was the smallest in the P group. There was a significant difference in the plaque enhancement

TABLE 3 Culprit plaque characteristics of the different stroke mechanism subtypes of patients with symptomatic middle cerebral artery (MCA) M1.

Measurement	P ($n = 23$)	A ($n = 16$)	H ($n = 12$)	M ($n = 10$)	*P*-values
Plaque location					0.061
Superior	14 (60.9)	6 (37.5)	3 (25.0)	3 (30.0)	-
Ventral	3 (13.0)	6 (37.5)	3 (25.0)	49 (40.0)	-
Inferior	3 (13.0)	2 (12.5)	5 (41.7)	2 (20.0)	-
Dorsal	3 (13.0)	2 (12.5)	1 (8.30)	1 (10.0)	-
Irregularity [a]	11 (47.8)	13 (81.3)	10 (83.3)	10 (100)	0.001
T1 hyperintensity[b]	1 (4.3)	4 (25.0)	6 (50.0)	4 (40.0)	0.004
Remodeling mode					0.004
PR[c]	12 (60.0)	5 (25.0)	2 (10.0)	1 (5.0)	-
NR	9 (25.7)	8 (22.9)	9 (25.7)	9 (25.7)	-
RI	1.04±0.17	0.97±0.16	0.86±0.17	0.88±0.20	0.016
Enhancement level					0.001
Mild	16 (72.7)	3 (13.6)	1 (4.5)	2 (9.1)	-
Obvious[d]	7 (17.9)	13 (33.3)	11 (28.2)	8 (20.5)	-
ER	0.38 ± 0.34	0.52 ± 0.26	0.62 ± 0.40	0.71 ± 0.43	0.066
WT_{max}, mm	1.32 ± 0.24	1.41 ± 0.33	1.42 ± 0.21	1.44 ± 0.32	0.548
LA_{MLN}, mm^2	0.05 ± 0.02	0.03 ± 0.02	0.02 ± 0.01	0.02 ± 0.01	0.000
OA_{MLN}, mm^2	0.14 ± 0.05	0.12 ± 0.04	0.09 ± 0.03	0.09 ± 0.03	0.002
WA_{MLN}, mm^2	0.09 ± 0.03	0.08 ± 0.03	0.07 ± 0.02	0.07 ± 0.03	0.097
PB	0.65 ± 0.08	0.72 ± 0.09	0.78 ± 0.12	0.79 ± 0.06	0.000
Stenosis	0.36 ± 0.24	0.37 ± 0.24	0.58 ± 0.31	0.66 ± 0.22	0.003

The p-values were calculated using ANOVA or the chi-squared/Fisher's exact test between the four groups, as appropriate; RI indicates the remodeling index; PB, plaque burden; ER, enhancement ratio; PR, Positive remodeling; NR, Negative remodeling. (a) The A group was statistically significant compared with the other groups; (b) the A group was statistically significant compared with the P group; (c) the P group was statistically significant compared with the other groups; and (d) the A and M groups were statistically significant compared with the other groups.

grade between the different mechanisms ($p = 0.001$). Obvious plaque enhancement was more common in the A and M groups than in the other groups ($p < 0.0125$). The ER of the culprit plaque in the M group was higher than in the P group ($p < 0.05$). There was a significant difference in the stenosis rate of the M1 segment of the MCA between the different mechanisms ($p = 0.003$). The stenosis rate of the MCA in the H group and the M group was higher than in the P group and the A group ($p < 0.05$) (Figures 3,4).

Association between culprit plaque characteristics and different stroke subtypes

Figure 5 shows the binary logistic regression analysis results for the parameters associated with the P group compared with the other groups. After adjustment for clinical demographic factors, the enhancement level (odds ratio [*OR*] 0.213, 95% *CI* (0.05–0.91), $p = 0.037$) and the PB of culprit plaques (*OR* 0, 95% *CI* (0–0.477), $p = 0.034$) were negatively associated with the P group.

Discussion

The present study classified the possible stroke mechanisms of MCA M1 atherosclerosis using conventional imaging (DWI and MRA). We demonstrated that there was inter-rater reproducibility of the classification criteria and correlations between the culprit plaque characteristics and different stroke mechanisms. Compared with the parent artery atherosclerosis occluding penetrating artery mechanism, ischemic stroke caused by the artery-to-artery embolism mechanism was more common and exhibited an irregular surface, high T1 signal, and obvious enhancement of the culprit plaque. Compared with the other stroke mechanisms, the PR of the culprit plaques in the P group was more common, the RI was greater, and the PB was minimal. The ER of the plaques in the P group was less than the mixed mechanism group. Compared with the artery-to-artery embolic mechanism, the T1 hyperintensity of the culprit plaque was more common in the hypoperfusion group, and the stenosis rate was greater. The binary logistic regression analysis revealed that the enhancement level (*OR* 0.213, 95% *CI* (0.05–0.91), $p = 0.037$) and PB of culprit plaque (*OR* 0, 95% *CI* (0–0.477), $p = 0.034$) were negatively associated with the P group.

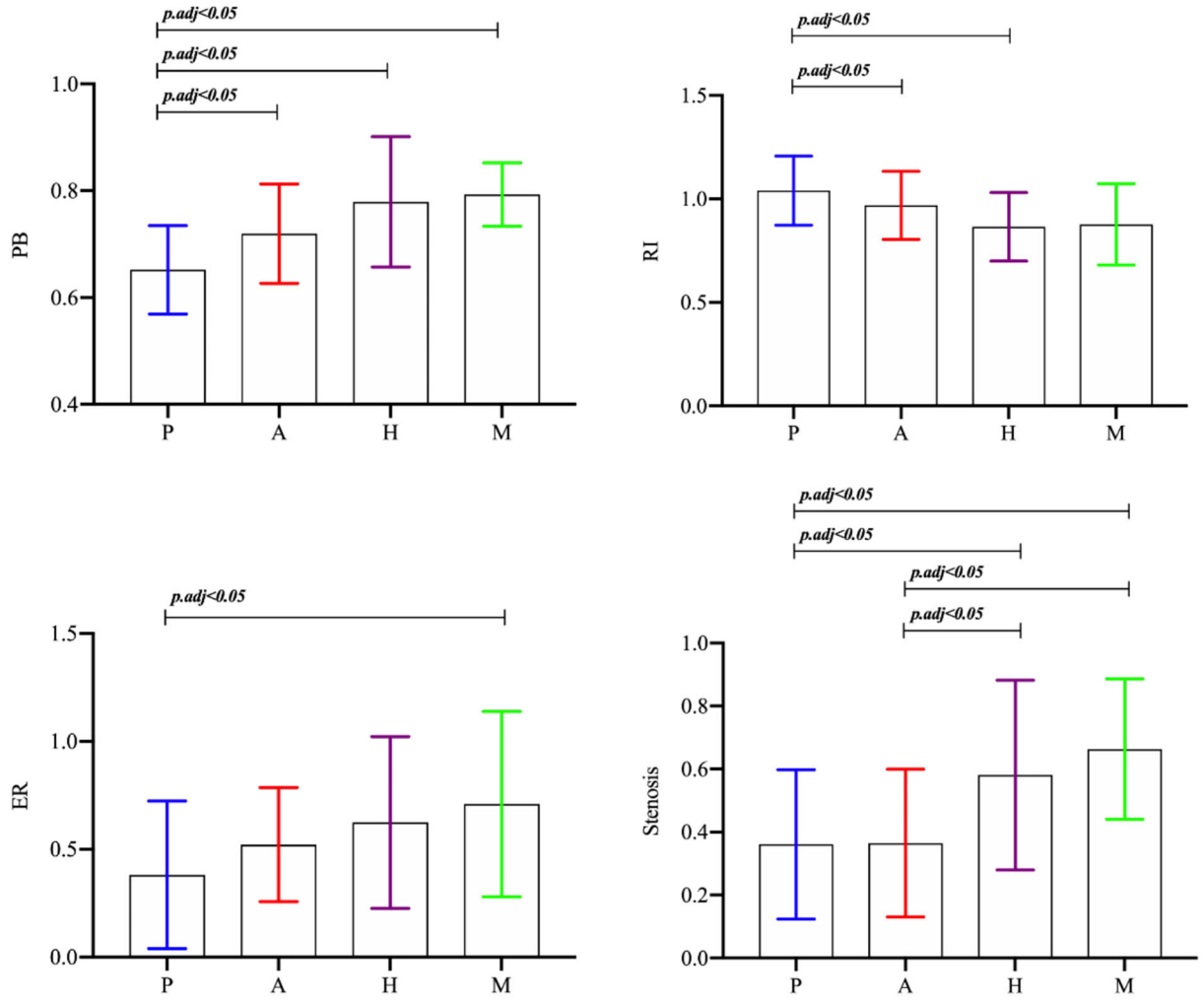

FIGURE 3
The *p*-values were calculated using ANOVA.

Plaque enhancement may be due to gadolinium leakage caused by neovascularization, inflammation, and endothelial dysfunction. Recent studies agree that plaque enhancement is a good biomarker for intracranial atherosclerotic diseases (13), and this enhancement reflects the predictive value of ischemic stroke and may also be used as an evaluation index of curative effect. The present study showed that enhancement of the culprit plaque was more common in the artery-to-artery embolic mechanism, which indicates that the inflammatory reaction was more severe. The neovascularization in the plaque easily ruptures and bleeds, which shows a T1 high signal (21) that better indicates the instability of the plaque, and this association was confirmed by relevant pathology (22). The plaque protrudes into the lumen and causes hemodynamic changes. The low wall shear stress on the plaque surface easily induces endothelial dysfunction (23). The weakening of the fiber cap on the plaque surface increases the vulnerability of the plaque and eventually leads to plaque fragmentation. The embolus dislodges and forms an irregular shape on the surface of the plaque. The instability of plaques may affect the decision-making for clinical treatment. A study of symptomatic carotid stenosis suggested that patients treated with intravascular therapy within 2 weeks after ischemic events had a significantly higher risk of stroke or death within 30 days (26.1 vs. 1.9%) than patients treated after 2 weeks (24). The embolus is easily dislodged and may cause a distal embolism during surgery. The present study suggests that the inflammatory response to responsible plaques in the artery-to-artery embolism may be serious and should be considered. Chung et al. (25) found that high-dose statin treatment significantly reduced plaque enhancement in patients with acute stroke ($p = 0.002$). Chung et al. subsequently performed a

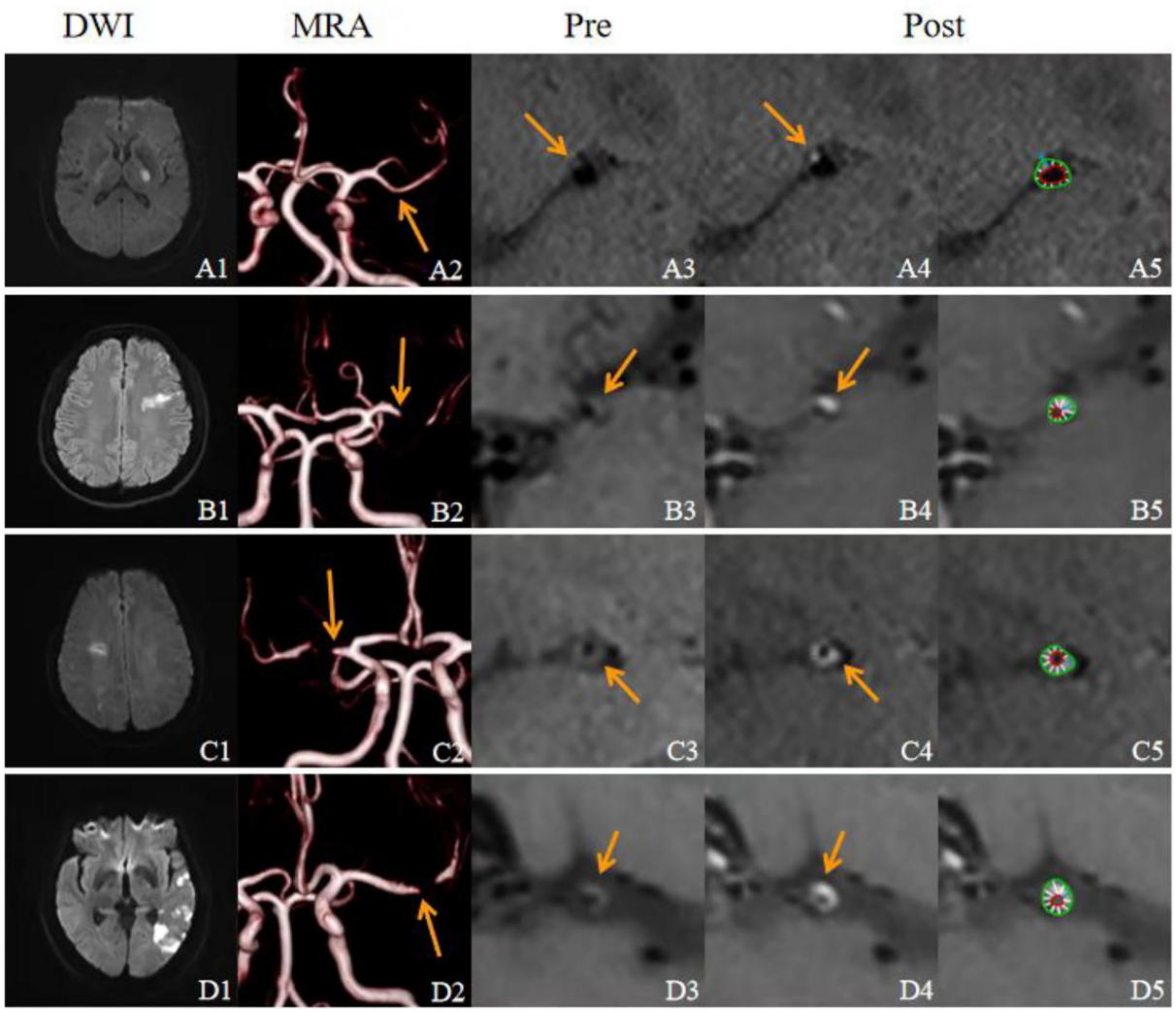

FIGURE 4
Characteristics of the culprit plaque in the M1 segment of the MCA in four patients with acute stroke with different mechanisms. **(A1–A5)**, A 39-year-old male, diffusion-weighted images (DWIs) **(A1)** showed high signal intensity in the left basal ganglia, and the stroke mechanism was parent artery atherosclerosis occluding penetrating artery by MCA atherosclerosis. Magnetic resonance angiography MRA_ **(A2)** showed that the left MCA M1 lumen was normal (arrow). Sagittal images of the precontrast **(A3)** and postcontrast **(A4)** HR-VWI showed that the plaque was located in the upper wall (arrow), showed mild enhancement, and the inner and outer walls of vessels were semiautomatically delineated on postcontrast HR-VWI **(A5)**. **(B1–B5)** A 48-year-old male, DWI **(B1)** showed multiple hypersignals in the left frontal cortex and the subcortical area, and an artery-to-artery embolism was considered the mechanism of stroke; MRA **(B2)** showed that the left MCA M1 lumen was severely stenotic (arrow); **(B3,B4)** HR-VWI showed that the plaque was located in the upper wall, which showed obvious enhancement (arrow). **(C1–C5)**, A 53-year-old male, DWI **(C1)** showed multiple hypersignals in the right subcortical watershed, and the mechanism of stroke was considered when evaluating the mechanism of hypoperfusion. MRA **(C2)** showed that the right MCA M1 lumen was severely stenotic (arrow). **(C3,C4)** HR-VWI showed that the plaque was located in the posterior wall, which showed obvious enhancement (arrow). **(D1–D5)**, A 60-year-old male, DWI **(D1)** showed multiple hypersignals in the left temporal lobe and the left posterior cortical watershed area; MRA **(D2)** showed that the left MCA M1 lumen was severely stenotic (arrow); **(D3,D4)** HR-VWI showed that the plaque was located in the posterior wall, which showed obvious enhancement (arrow).

study on statin treatment for patients with acute ischemic stroke and found that statin treatment significantly decreased the enhancement of play volume after 6 months ($p = 0.013$) (26). These studies show that high-dose statins effectively stabilize symptomatic ICAS plaques. However, the study population of Chung et al. did not include patients with artery-to-artery embolism. The Clopidogrel in High-Risk Patients with Acute Nondisabling Cerebrovascular Events (CHANCE) trial showed that the dual antiplatelet therapy of clopidogrel and aspirin effectively reduced microemboli in ischemic stroke caused by an artery-to-artery embolism (27). For patients with artery-to-artery embolic stroke, reducing the inflammatory response to

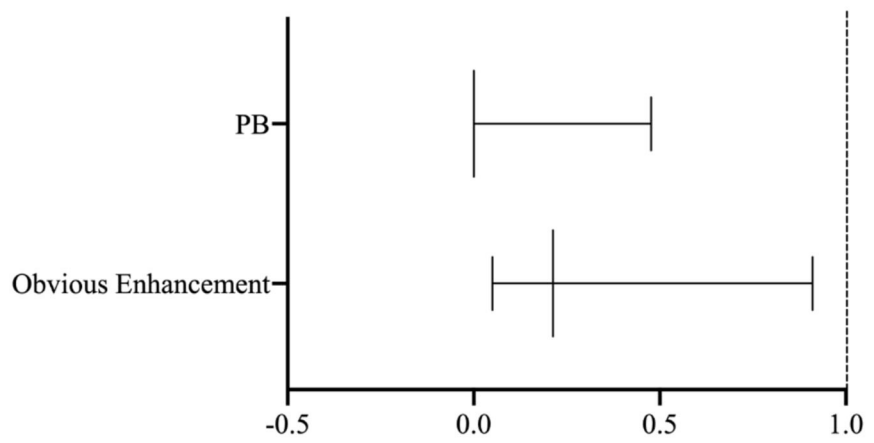

FIGURE 5
A binary logistic regression analysis results for the parameters associated with the P group compared with the other groups.

the culprit plaques and the shedding of emboli may be more beneficial to patients.

In this study, we found that the PR of the culprit plaque was more common in the parent artery atherosclerosis occluding penetrating artery mechanism, the lumen stenosis rate and PB were the smallest, and the ER was lower than the mixed mechanism. Penetrating artery occlusions due to parent artery atherosclerosis are more likely associated with early neurological deterioration and recurrent stroke (28) and are classified as large artery atherosclerosis rather than small vessel occlusion (8, 29). Recent studies showed that the single subcortical infarction was primarily related to plaques of the M1 segment of the MCA located in the upper wall, and the lumen had mild stenosis or was normal (30, 31). This result is similar to the result that the culprit plaque in the perforator artery group was primarily located in the upper wall. Jiang et al. found that the plaque of a single subcortical infarct was located in the upper wall, which was related to the fewer lenticulostriate arteries (LSA) branches on the symptomatic side ($p = 0.011$) and the shorter average length ($p = 0.025$) (32). Therefore, the involved vessel wall may grow outward in the early stage of the atherosclerotic disease to compensate for the stenosis of the lumen, which results in positive remodeling and a certain degree of inflammatory response. Although the stenosis of the carrier artery lumen and the plaque burden are relatively insignificant at this time, the plaque is more likely to occlude the opening of the perforator artery, which results in a high-risk transient ischemic attack or mild ischemic stroke. Patients with minor ischemic stroke or high-risk TIA who received a combination of clopidogrel and aspirin had a lower risk of major ischemic events but a higher risk of major hemorrhage at 90 days than patients who received aspirin alone (33). The dual antiplatelet therapy of cilostazol and clopidogrel may also be better than single antiplatelet therapy (34). Cilostazol has an anti-platelet aggregation effect and dilates arterioles, which may compensate for the involvement of perforator artery openings. High-dose statin therapy improves the short-term functional prognosis (33, 35). However, the therapeutic effect on perforator artery disease must be confirmed in further randomized controlled studies. Therefore, a prospective study using statins and dual antiplatelet therapy to prevent early neurological deterioration and recurrent stroke caused by perforator atherosclerosis should be performed (10) because its efficacy is not certain.

The present study observed that a high T1 signal of the plaque with hypoperfusion mechanism was most common, and the degree of stenosis was most severe. As mentioned above, a high T1 signal reflects the inflammatory progress of plaques. However, obvious stenosis of the lumen reduces the antegrade flow to the relevant area. If the collateral circulation compensation is insufficient, the downstream perfusion may be prolonged or damaged and result in the occurrence of infarction (11, 36). Therefore, focusing only on intensive blood pressure control may increase the risk of recurrent stroke in patients with symptomatic intracranial artery stenosis with impaired perfusion (37). A *post-hoc* analysis of the Stenting and Aggressive Medical Management for Preventing Recurrent Stroke in Intracranial Stenosis (SAMMPRIS) trial also showed that among stroke patients with a stenosis rate of 70–99%, a subgroup with marginal zone infarction and collateral circulation damage had a particularly high risk of recurrent stroke despite drug treatment (38). For the stroke mechanism of hypoperfusion perfusion, the degree of inflammation of the culprit plaque and the stenosis rate of the mechanism should also be considered.

A binary logistic regression analysis revealed that the plaque enhancement level and PB were negatively associated with the

parent artery atherosclerosis occluding a penetrating artery. In other words, when the enhancement of the culprit plaque and the greater plaque burden are obvious, the more likely it is to be the result of other stroke mechanisms. A recent study is similar to our results. The plaque in the branch occlusive disease group was less enhancing plaque than in the artery-to-artery group ($p = 0.030$) (39). However, there are few studies on plaque burden as an indicator of treatment evaluation. One study showed that the total volume of the carotid artery wall was significantly reduced in patients with carotid atherosclerosis with type 2 diabetes after receiving hypoglycemic drugs compared with a control group without diabetes after 2 years of treatment (40). However, the evaluation of HR-VWI related to the therapeutic effect of hypoglycemic drugs on intracranial artery atherosclerosis plaques must be further studied.

Our study has some limitations. First, it was a single-center study with relatively small sample size. Second, the study performed a retrospective analysis, and there may be a selection bias. Third, statistical analysis lacked the evaluation of normal distribution and the consistency analysis of plaque morphological characteristics. Finally, this study only recruited patients with anterior circulation stroke, and further research is needed to evaluate patients with posterior circulation stroke.

Conclusion

Evaluations of the culprit plaque characteristics of patients with symptomatic MCA atherosclerotic in different stroke mechanisms based on HR-VWI are feasible. The plaque characteristics of different stroke mechanisms may have clinical value for the selection of treatment strategies and prevention of stroke recurrence.

Data availability statement

The raw data supporting the conclusions of this article will be made available by the authors, without undue reservation.

Author contributions

Conceptualization and supervision: G-hL and J-xS. Data curation: G-hL, N-xF, and T-dH. Formal analysis and writing—original draft: G-hL. Methodology: G-hL, N-xF, T-dH, and J-xS. Resources and software: J-xS. Validation: N-xF and L-lZ. Writing—review and editing: G-hL and J-xS. All authors contributed to the article and approved the submitted version.

Acknowledgments

We would like to thank Mr. Rui Jiao for his help in this research.

Conflict of interest

The authors declare that the research was conducted in the absence of any commercial or financial relationships that could be construed as a potential conflict of interest.

Publisher's note

References

1. Ko Y, Lee S, Chung JW, Han MK, Park JM, Kang K, et al. MRI-based algorithm for acute ischemic stroke subtype classification. *J Stroke.* (2014) 16:161–72. doi: 10.5853/jos.2014.16.3.161

2. Makowski MR, Botnar RM. MRI imaging of the arterial vessel wall: molecular imaging from bench to bedside. *Radiology.* (2013) 269:34–51. doi: 10.1148/radiol.13102336

3. Sato Y, Hatakeyama K, Marutsuka K, Asada Y. Incidence of asymptomatic coronary thrombosis and plaque disruption: comparison of non-cardiac and cardiac deaths among autopsy cases. *Thromb Res.* (2009) 124:19–23. doi: 10.1016/j.thromres.2008.08.026

4. Lan L, Liu H, Ip V, Soo Y, Abrigo J, Fan F, et al. Regional high wall shear stress associated with stenosis regression in symptomatic intracranial atherosclerotic disease. *Stroke.* (2020) 51:3064–73. doi: 10.1161/strokeaha.120.030615

5. Collaborators GN. Global, regional, and national burden of neurological disorders, 1990–2016: a systematic analysis for the global burden of disease study 2016. *Lancet Neurol.* (2019) 18:459–80. doi: 10.1016/s1474-4422(18)30499-x

6. Hathidara MY, Saini V, Malik AM. Stroke in the young: a global update. *Curr Neurol Neurosci Rep.* (2019) 19:91. doi: 10.1007/s11910-019-1004-1

7. Chen CY, Lin PT, Wang YH, Syu RW, Hsu SL, Chang LH, et al. Etiology and risk factors of intracranial hemorrhage and ischemic stroke in young adults. *J Chin Med Assoc.* (2021) 84:930–6. doi: 10.1097/jcma.0000000000000598

8. Chen PH, Gao S, Wang YJ, Xu AD, Li YS, Wang D. Classifying ischemic stroke, from TOAST to CISS. *CNS Neurosci Ther.* (2012) 18:452–6. doi: 10.1111/j.1755-5949.2011.00292.x

9. Flusty B, De Havenon A, Prabhakaran S, Liebeskind DS, Yaghi S. Intracranial atherosclerosis treatment: past, present, and future. *Stroke.* (2020) 51:e49–53. doi: 10.1161/strokeaha.119.028528

10. Huang YC, Lee JD, Weng HH, Lin LC, Tsai YH, Yang JT. Statin and dual antiplatelet therapy for the prevention of early neurological deterioration and recurrent stroke in branch atheromatous disease: a protocol for a prospective single-arm study using a historical control for comparison. *BMJ Open.* (2021) 11:e054381. doi: 10.1136/bmjopen-2021-054381

11. Feng X, Chan KL, Lan L, Abrigo J, Liu J, Fang H, et al. Stroke mechanisms in symptomatic intracranial atherosclerotic disease: classification and clinical implications. *Stroke.* (2019) 50:2692–9. doi: 10.1161/strokeaha.119.025732

12. Menon BK, Smith EE, Coutts SB, Welsh DG, Faber JE, Goyal M, et al. Leptomeningeal collaterals are associated with modifiable metabolic risk factors *Ann Neurol.* (2013) 74:241–8. doi: 10.1002/ana.23906

13. Song JW, Pavlou A, Xiao J, Kasner SE, Fan Z, Messé SR. Vessel wall magnetic resonance imaging biomarkers of symptomatic intracranial atherosclerosis: a meta-analysis. *Stroke.* (2021) 52:193–202. doi: 10.1161/strokeaha.120.031480

14. Mendelson SJ, Prabhakaran S. Diagnosis and management of transient ischemic attack and acute ischemic stroke: a review. *Jama.* (2021) 325:1088–98. doi: 10.1001/jama.2020.26867

15. Al Kasab S, Derdeyn CP, Guerrero WR, Limaye K, Shaban A, Adams HP Jr. Intracranial large and medium artery atherosclerotic disease and stroke. *J Stroke Cerebrovasc Dis.* (2018) 27:1723–32. doi: 10.1016/j.jstrokecerebrovasdis.2018.02.050

16. Lin GH, Song JX, Fu NX, Huang X, Lu HX. Quantitative and qualitative analysis of atherosclerotic stenosis in the middle cerebral artery using high-resolution magnetic resonance imaging. *Can Assoc Radiol J.* (2021) 72:783–8. doi: 10.1177/0846537120961312

17. Lindenholz A, Van Der Kolk AG, Van Der Schaaf IC, Van Der Worp HB, Harteveld AA, Dieleman N, et al. Intracranial atherosclerosis assessed with 7-T MRI: evaluation of patients with ischemic stroke or transient ischemic attack. *Radiology.* (2020) 295:162–70. doi: 10.1148/radiol.2020190643

18. Xu WH, Li ML, Gao S, Ni J, Zhou LX, Yao M, et al. Plaque distribution of stenotic middle cerebral artery and its clinical relevance. Stroke, (2011, 42(10): 2957-9. doi: 10.1161/strokeaha.111.618132

19. Tao L, Li XQ, Hou X W, Yang BQ, Xia C, Ntaios G, et al. Intracranial atherosclerotic plaque as a potential cause of embolic stroke of undetermined source. *J Am Coll Cardiol.* (2021) 77:680–91. doi: 10.1016/j.jacc.2020.12.015

20. Qiao Y, Zeiler SR, Mirbagheri S, Leigh R, Urrutia V, Wityk R, et al. Intracranial plaque enhancement in patients with cerebrovascular events on high-spatial-resolution MR images. *Radiology.* (2014) 271:534–42. doi: 10.1148/radiol.13122812

21. Derksen WJ, Peeters W, Van Lammeren GW, Tersteeg C, De Vries JP, De Kleijn DP, et al. Different stages of intraplaque hemorrhage are associated with different plaque phenotypes: a large histopathological study in 794 carotid and 276 femoral endarterectomy specimens. *Atherosclerosis.* (2011) 218:369–77. doi: 10.1016/j.atherosclerosis.2011.07.104

22. Chen XY, Wong KS, Lam WW, Ng HK. High signal on T1 sequence of magnetic resonance imaging confirmed to be intraplaque haemorrhage by histology in middle cerebral artery. *Int J Stroke.* (2014) 9:E19. doi: 10.1111/ijs.12277

23. Leng X, Lan L, Ip H, Abrigo J, Scalzo F, Liu H, et al. Hemodynamics and stroke risk in intracranial atherosclerotic disease. *Ann Neurol.* (2019) 85:752–64. doi: 10.1002/ana.25456

24. Topakian R, Strasak AM, Sonnberger M, Haring HP, Nussbaumer K, Trenkler J, et al. Timing of stenting of symptomatic carotid stenosis is predictive of 30-day outcome. *Eur J Neurol.* (2007) 14:672–8. doi: 10.1111/j.1468-1331.2007.01815.x

25. Chung JW, Hwang J, Lee MJ, Cha J, Bang OY. Previous statin use and high-resolution magnetic resonance imaging characteristics of intracranial atherosclerotic plaque: the intensive statin treatment in acute ischemic stroke patients with intracranial atherosclerosis study. *Stroke.* (2016) 47:1789–96. doi: 10.1161/strokeaha.116.013495

26. Chung JW, Cha J, Lee MJ, Yu IW, Park MS, Seo WK, et al. Intensive statin treatment in acute ischaemic stroke patients with intracranial atherosclerosis: a high-resolution magnetic resonance imaging study (STAMINA-MRI study). *J Neurol Neurosurg Psychiatry.* (2020) 91:204–11. doi: 10.1136/jnnp-2019-320893

27. Jing J, Meng X, Zhao X, Liu L, Wang A, Pan Y, et al. Dual antiplatelet therapy in transient ischemic attack and minor stroke with different infarction patterns: subgroup analysis of the chance randomized clinical trial. *JAMA Neurol.* (2018) 75:711–9. doi: 10.1001/jamaneurol.2018.0247

28. Petrone L, Nannoni S, Del Bene A, Palumbo V, Inzitari D. Branch atheromatous disease: a clinically meaningful, yet unproven concept. *Cerebrovasc Dis.* (2016) 41:87–95. doi: 10.1159/000442577

29. Gao S, Wang YJ, Xu AD, Li YS, Wang DZ. Chinese ischemic stroke subclassification. *Front Neurol.* (2011) 2:6. doi: 10.3389/fneur.2011.00006

30. Sun LL, Li ZH, Tang WX, Liu L, Chang FY, Zhang XB, et al. High resolution magnetic resonance imaging in pathogenesis diagnosis of single lenticulostriate infarction with nonstenotic middle cerebral artery, a retrospective study. *BMC Neurol.* (2018) 18:51. doi: 10.1186/s12883-018-1054-z

31. Shen M, Gao P, Zhang Q, Jing L, Yan H, Li H. Middle cerebral artery atherosclerosis and deep subcortical infarction: a 3T magnetic resonance vessel wall imaging study. *J Stroke Cerebrovasc Dis.* (2018) 27:3387–92. doi: 10.1016/j.jstrokecerebrovasdis.2018.08.013

32. Jiang S, Yan Y, Yang T, Zhu Q, Wang C, Bai X, et al. Plaque distribution correlates with morphology of lenticulostriate arteries in single subcortical infarctions. *Stroke.* (2020) 51:2801–9. doi: 10.1161/strokeaha.120.030215

33. Johnston SC, Easton JD, Farrant M, Barsan W, Conwit RA, Elm JJ, et al. Clopidogrel and aspirin in acute ischemic stroke and high-risk TIA. *N Engl J Med.* (2018) 379:215–25. doi: 10.1056/NEJMoa1800410

34. Kamo H, Miyamoto N, Otani H, Kurita N, Nakajima S, Ueno Y, et al. The importance of combined antithrombotic treatment for capsular warning syndrome. *J Stroke Cerebrovasc Dis.* (2018) 27:3095–9. doi: 10.1016/j.jstrokecerebrovasdis.2018.06.038

35. Fang JX, Wang EQ, Wang W, Liu Y, Cheng G. The efficacy and safety of high-dose statins in acute phase of ischemic stroke and transient ischemic attack: a systematic review. *Intern Emerg Med.* (2017) 12:679–87. doi: 10.1007/s11739-017-1650-8

36. Nannoni S, Sirimarco G, Cereda C W, Lambrou D, Strambo D, Eskandari A, et al. Determining factors of better leptomeningeal collaterals: a study of 857 consecutive acute ischemic stroke patients. *J Neurol.* (2019) 266:582–8. doi: 10.1007/s00415-018-09170-3

37. Yamauchi H, Higashi T, Kagawa S, Kishibe Y, Takahashi M. Impaired perfusion modifies the relationship between blood pressure and stroke risk in major cerebral artery disease. *J Neurol Neurosurg Psychiatry.* (2013) 84:1226–32. doi: 10.1136/jnnp-2013-305159

38. Wabnitz AM, Derdeyn CP, Fiorella DJ, Lynn MJ, Cotsonis GA, Liebeskind DS, et al. Hemodynamic markers in the anterior circulation as predictors of recurrent stroke in patients with intracranial stenosis. *Stroke.* (2018) 56:20840. doi: 10.1161/strokeaha.118.020840

39. Won SY, Cha J, Choi HS, Kim YD, Nam H S, Heo JH, et al. High-resolution intracranial vessel wall MRI findings among different middle cerebral artery territory infarction types. *Korean J Radiol.* (2022) 23:333–42. doi: 10.3348/kjr.2021.0615

40. Strang AC, Van Wijk DF, Mutsaerts HJ, Stroes ES, Nederveen AJ, Rotmans JI, et al. Guideline treatment results in regression of atherosclerosis in type 2 diabetes mellitus. *Diab Vasc Dis Res.* (2015) 12:126–32. doi: 10.1177/1479164114559511

Frontiers in Neurology

Explores neurological illness to improve patient care

The third most-cited clinical neurology journal explores the diagnosis, causes, treatment, and public health aspects of neurological illnesses. Its ultimate aim is to inform improvements in patient care.

Discover the latest Research Topics

See more →

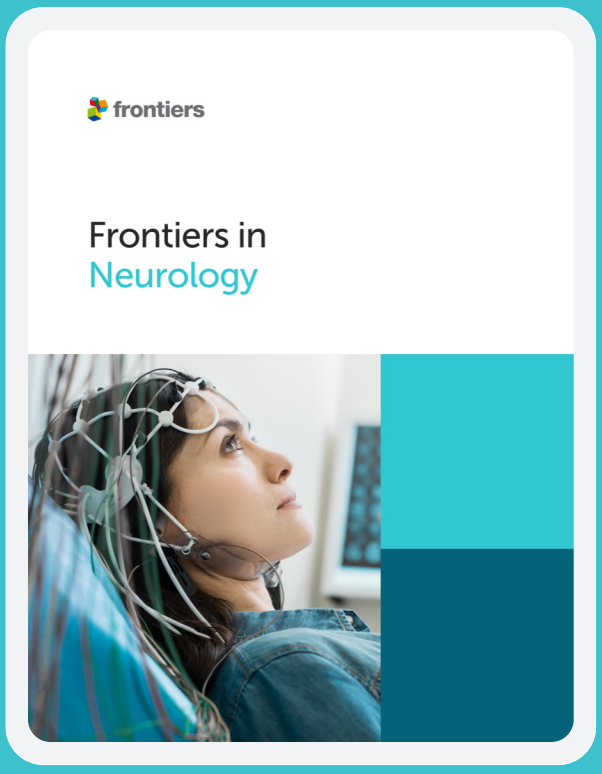

Frontiers

Avenue du Tribunal-Fédéral 34
1005 Lausanne, Switzerland
frontiersin.org

Contact us

+41 (0)21 510 17 00
frontiersin.org/about/contact